

Copyright  
by  
Hyunho Jung  
2017

**The Thesis Committee for Hyunho Jung  
Certifies that this is the approved version of the following thesis:**

**Map / Envelope Based Design Process of the Planetary Roller Screw**

**Approved by  
Supervising Committee:**

Supervisor:

---

Delbert Tesar

---

Richard H. Crawford

# **Map / Envelope Based Design Process of the Planetary Roller Screw**

By

**HYUNHO JUNG**

**THESIS**

Presented to the Faculty of the Graduate School of  
The University of Texas at Austin  
in Partial Fulfillment  
of the Requirements  
for the Degree of

**Master of Science in Engineering**

**The University of Texas at Austin**

**August, 2017**

## ACKNOWLEDGEMENTS

First and foremost, I would like to give my thanks to my savior, Jesus Christ, for giving me the wisdom, endurance, and intelligence to fulfill this research, for as it says in Philippians 4:13, “I can do all things through Christ which strengtheneth me.” And I thank to my supervisor Dr. Delbert Tesar for his encouragement, technical guidance, and friendship. Without your assistance, I would not be able to pursue this advanced degree. You have always motivated me with my best interest and you genuinely want me to be a professional in the world. I also would like to thank to Republic of Korea Air Force that they give me a chance to learn advanced knowledge from one of the best world leader in the area of actuators. And I would like to thank to Dr. Richard Crawford for being on my thesis committees. To Mrs. Betty Wilson, I would also like to thank her assistance while I was one of members of the Robotics Research.

Last, I give all my thanks to my lovers – my wife Mijung and my son Heesung – for being with me and supporting everything that I need for two years. Thank you for encouraging me and thank you for always loving me even though I didn’t have time with you. Your unchanging encouragement and love made me be possible to pursue this long and difficult accomplishment.

# ABSTRACT

## **Map / Envelope Based Design Process of the Planetary Roller Screw**

Hyunho Jung, M.S.E

The University of Texas at Austin, 2017

Supervisor: Delbert Tesar

Electro-Mechanical linear actuators have received recent attention for the aircraft control surface systems to eliminate hydraulic systems from aircraft. This approach is intended to improve reliability, safety, efficiency, and maintainability. For linear actuators, one of the most important components is the planetary roller screws (PRSs). The planetary roller screw (also called the satellite roller screw) is a mechanical transmission device, which converts rotational motion to linear motion or vice versa. The mechanism of planetary screw is similar in principle to the conventional ball screw mechanism (BSM). PRS has been receiving attention in lots research and industry, however, it is hard to produce high-quality PRS transmissions, because it is difficult to determine the PRS parameter relationship among all its components and hard to build visual maps for rapid design.

The main objective of this research is to provide the parametric relationship between components to build design maps. Developing a visual design process for PRSs is the primary goal. In order to understand contact geometry and relative motions in the PRS, an exact PRSs structure is presented, as well as its parameter analysis. Then the parameters are tested to identify how the parameters affect the PRSs requirements such as load distribution, stiffness, dynamic load capacity, and force density as key measures for the visual design process. One of the key impacts of this research is the utilization of design procedures to build sets of 3-D design maps. These maps and design

procedures are helpful to manage parameters to quickly build optimal PRSs dimensions for designers. Each measure has its own parameters. Some of these parameters are fixed constants and others can be set by designer. As variables, the parameters are classified into two types. Ones are primary parameters that have large impact on the mapping and design process and others are secondary parameters that have minor impact. Any set of parameters is given in accordance with each set of 3-D maps and they can be adjusted to generate new visual 3-D maps by designer. Then the designer can reviews the 3-D mapping results, he or she can then quickly decide the effect of first design decision and adjust updated parameter choices to get new maps. This helps the designer to optimize dimensions of PRSs and determine the best solution for application requirements by this design process. Overall, the whole design process accelerates quickly reaching the design goal for the designer.

# TABLE OF CONTENTS

<b>ACKNOWLEDGEMENTS.....</b>	<b>iv</b>
<b>ABSTRACT.....</b>	<b>v</b>
<b>LIST OF TABLES.....</b>	<b>xiii</b>
<b>LIST OF FIGURES.....</b>	<b>xv</b>
<b>NOMENCLATURE.....</b>	<b>xviii</b>
<b>CHAPTER 1. INTRODUCTION.....</b>	<b>1</b>
1.1 Transmission Screw Mechanism Comparison.....	4
1.2 Motivation .....	6
1.3 Chapter Conclusion.....	11
<b>CHAPTER 2. KINEMATICS OF PLANETARY ROLLER SCREW.....</b>	<b>13</b>
2.1 PRS Structure and Terminology.....	13
2.2 Motion Analysis.....	16
2.2.1 PRS Angular Motion Analysis.....	17
2.2.2 Axial Motion Analysis.....	19
2.2.2.1 Relative Motion between the Roller and the Nut.....	19
2.2.2.2 Relative Motion between the Roller and the Screw Shaft.....	20
2.2.2.3 Concentricity of the PRS components.....	22
2.2.2.4 PRS Component Configuration Example.....	23
2.3 Chapter Conclusion.....	24
<b>CHAPTER 3. DEFORMATION AND STIFFNESS ANALYSIS.....</b>	<b>25</b>
3.1 Shaft Section Stiffness.....	26
3.2 Thread Stiffness.....	27
3.3 Hertzian Contact Stiffness.....	30
3.4 Total Deformation and Total Stiffness.....	36
3.5 Total Deformation and Total Stiffness Analysis.....	36

3.5.1 Parameters.....	36
3.5.2 Resulting Maps and Analysis.....	37
3.5.2.1 Nut Outer Diameter Change.....	37
3.5.2.1.1 Parameter Values.....	37
3.5.2.1.2 Resulting maps.....	38
3.5.2.2 Effective Nut Inner Diameter Change.....	39
3.5.2.2.1 Parameter Values.....	39
3.5.2.2.2 Resulting maps.....	39
3.5.2.3 Effective Screw Diameter Change.....	41
3.5.2.3.1 Parameter Values.....	41
3.5.2.3.2 Resulting maps.....	41
3.5.2.4 Effective Roller Diameter Change.....	43
3.5.2.4.1 Parameter Values.....	43
3.5.2.4.2 Resulting maps.....	43
3.5.2.5 Number of Rollers Change.....	45
3.5.2.5.1 Parameter Values.....	45
3.5.2.5.2 Resulting maps.....	45
3.5.2.6 Pitch Change.....	47
3.5.2.6.1 Parameter Values.....	47
3.5.2.6.2 Resulting maps.....	47
3.5.2.7 Number of Start Change.....	49
3.5.2.7.1 Parameter Values.....	49
3.5.2.7.2 Resulting maps.....	49
3.5.2.8 Helix Angle Change.....	51
3.5.2.8.1 Parameter Values.....	51
3.5.2.8.2 Resulting maps.....	51



3.6 Chapter Conclusion.....	53
<b>CHAPTER 4. LOAD DISTRIBUTION ANALYSIS.....</b>	<b>56</b>
4.1 Load Distribution.....	56
4.2 Load Distribution Analysis.....	59
4.2.1 Parameters.....	59
4.3 Resulting Maps and Analysis.....	59
4.3.1 Nut Outer Diameter Change.....	60
4.3.1.1 Parameter Values.....	60
4.3.1.2 Resulting Map.....	60
4.3.2 Nut Inner Diameter Change.....	61
4.3.2.1 Parameter Values.....	61
4.3.2.2 Resulting Map.....	61
4.3.3 Screw Diameter Change.....	62
4.3.3.1 Parameter Values.....	62
4.3.3.2 Resulting Map.....	63
4.3.4 Roller Diameter Change.....	64
4.3.4.1 Parameter Values.....	64
4.3.4.2 Resulting Map.....	64
4.3.5 Number of Rollers Change.....	65
4.3.5.1 Parameter Values.....	65
4.3.5.2 Resulting Map.....	66
4.3.6 Pitch Change.....	66
4.3.6.1 Parameter Values.....	66
4.3.6.2 Resulting Map.....	67
4.3.7 Number of Start Change.....	68
4.3.7.1 Parameter Values.....	68

4.3.7.2 Resulting Map.....	68
4.3.8 Helix Angle Change.....	69
4.3.8.1 Parameter Values.....	69
4.3.8.2 Resulting Map.....	70
4.4 Chapter Conclusion.....	70
<b>CHAPTER 5. LOAD CAPACITY ANALYSIS.....</b>	<b>74</b>
5.1 Dynamic Load Capacity.....	75
5.2 Load Capacity Analysis.....	78
5.2.1 Parameters.....	78
5.2.2 Resulting Maps and Analysis.....	78
5.2.2.1 Dominant Parameter: Nut Inner Diameter ( $d_n$ ).....	78
5.2.2.2 Dominant Parameter: Screw Diameter ( $d_s$ ).....	82
5.2.2.3 Dominant Parameter: Roller Diameter ( $d_r$ ).....	84
5.2.2.4 Dominant Parameter: Length ( $L$ ).....	87
5.2.2.5 Dominant Parameter: Pitch ( $p$ ).....	89
5.2.2.6 Dominant Parameter: Number of Rollers.....	90
5.3 Chapter Conclusion.....	91
<b>CHAPTER 6. WEIGHT AND FORCE DENSITY ANALYSIS.....</b>	<b>94</b>
6.1 Weight of Rollers.....	94
6.2 Weight of Nut.....	95
6.3 Total Weight.....	96
6.4 Force Density.....	96
6.5 Force Density Analysis.....	97
6.5.1 Parameters.....	97
6.5.2 Resulting Maps and Analysis.....	98
6.5.2.1 Dominant Parameter: Nut Inner Diameter ( $d_n$ ).....	98

6.5.2.2 Dominant Parameter: Screw Diameter ( $d_s$ ).....	102
6.5.2.3 Dominant Parameter: Roller Diameter ( $d_r$ ).....	104
6.5.2.4 Dominant Parameter: Length ( $L$ ).....	107
6.5.2.5 Dominant Parameter: Pitch ( $p$ ).....	108
6.5.2.6 Dominant Parameter: Number of Rollers ( $N_r$ ).....	110
6.6 Chapter Conclusion.....	111
<b>CHAPTER 7. MAP/ENVELOPE DESIGN PROCESS: Part 1 – Groundwork Formulation for a Planetary Roller Screw.....</b>	<b>114</b>
7.1 Volume and Measures Comparison Analysis.....	118
7.2 Dominant Parameter Relationship Analysis.....	129
7.2.1 Total Stiffness on Thread.....	130
7.2.2 Load Capacity.....	131
7.2.3 Force Density.....	133
7.3 Combined Measures Analysis.....	134
7.3.1 Adding Measure Values.....	134
7.3.2 Multiplying Measure Values.....	136
7.4 Chapter Conclusion.....	138
<b>CHAPTER 8. MAP / ENVELOPE DESIGN PROCESS: Part 2 – Parametric Management Using Combined Measure Envelopes.....</b>	<b>142</b>
8.1 Envelopes of PRS Performance Measures.....	144
8.1.1 Envelope of Total Stiffness on Thread.....	145
8.1.2 Envelope of Load Capacity.....	147
8.1.3 Envelope of Force Density.....	149
8.1.4 Envelope of Total Weight.....	150
8.2 Design Process Analysis by Combined Envelope.....	152

8.2.1 Comparison between Adding and Multiplying Envelopes.....	152
8.2.2 Design Process Analysis of Combined Envelope.....	153
8.3 Design Process Analysis by Weighted Combined Envelope.....	155
8.4 Analysis of Other Significant Performance Measures.....	156
8.4.1 Contact Pressure.....	157
8.4.2 Load Distribution.....	160
8.4.3 Theoretical Life of PRS.....	162
8.4.4 Efficiency.....	164
8.4.5 Velocity Ratio of the PRS.....	164
8.4.6 Equivalent Inertia of the PRS.....	165
8.5 Chapter Conclusion.....	166
<b>CHAPTER 9. CONCLUSIONS AND RECOMMENDATIONS.....</b>	<b>170</b>
<b>APPENDIX A. DIMENSIONLESS CONTACT PARAMETERS TABLE.....</b>	<b>175</b>
<b>REFERENCES.....</b>	<b>177</b>
<b>VITA .....</b>	<b>180</b>

## LIST OF TABLES

Table 1.1 Linear Transmission Devices Characteristics Comparison Chart.....	5
Table 1.2 Load Rating Comparison Chart between Roller Screw and Ball Screw.....	6
Table 1.3 Result for 1.97 in Case for reaching above 120,000 lbf.....	7
Table 1.4 Chosen Four Samples for Parameter Relationship.....	8
Table 1.5 Planetary Roller Screw Configurations (mm and kN).....	10
Table 1.6 Planetary Roller Screw Configurations (in and lbf).....	10
Table 3.1 Parameters.....	37
Table 3.2 Nut Outer Diameter ( $D_n$ ) Change Case Parameter Values.....	37
Table 3.3 Nut Inner Diameter ( $d_n$ ) Change Case Parameter Values.....	39
Table 3.4 Screw Diameter ( $d_s$ ) Change Case Parameter Values.....	41
Table 3.5 Roller Diameter ( $d_r$ ) Change Case Parameter Values.....	43
Table 3.6 Number of Rollers ( $N_r$ ) Change Case Parameter Values.....	45
Table 3.7 Pitch ( $p$ ) Change Case Parameter Values.....	47
Table 3.8 Number of Start ( $N_s$ ) Change Case Parameter Values.....	49
Table 3.9 Helix Angle ( $\beta_0$ ) Change Case Parameter Values.....	51
Table 3.10 Parameter Effect on PRS for Total Stiffness on Thread.....	54
Table 3.11 Parameter Classification for Total Stiffness on Thread.....	55
Table 4.1 Parameters.....	59
Table 4.2 Nut Outer Diameter ( $D_n$ ) Change Case Parameter Values.....	60
Table 4.3 Nut Inner Diameter ( $d_n$ ) Change Case Parameter Values.....	61
Table 4.4 Screw Diameter ( $d_s$ ) Change Case Parameter Values.....	62
Table 4.5 Roller Diameter ( $d_r$ ) Change Case Parameter Values.....	64
Table 4.6 Number of Rollers ( $N_r$ ) Change Case Parameter Values.....	65
Table 4.7 Pitch ( $p$ ) Change Case Parameter Values.....	66
Table 4.8 Number of Start ( $N_s$ ) Change Case Parameter Values.....	68
Table 4.9 Helix Angle ( $\beta_0$ ) Change Case Parameter Values.....	69

Table 4.10 Parameter Effect on PRS for Load Distribution.....	72
Table 4.11 Parameter Classification for Load Distribution.....	73
Table 5.1 Geometric Factor graph and Table Chart.....	76
Table 5.2 Parameters.....	78
Table 5.3 Parameter Effect on PRS for Load Capacity.....	92
Table 5.4 Parameter Classification for Load Capacity.....	93
Table 6.1 Parameters.....	97
Table 6.2 Parameter Effect on PRS for Force Density.....	112
Table 6.3 Parameter Classification for Force Density.....	113
Table 7.1 1 <sup>st</sup> Case of Volume and Values of Measures Comparison.....	122
Table 7.2 2 <sup>nd</sup> Case of Volume and Values of Measures Comparison.....	125
Table 7.3 Adding /Multiplying Method Comparison.....	139
Table 8.1 Scale Range Chart Comparison Chart.....	145
Table 8.2 Parameter Comparison Table for Total Stiffness on Thread.....	147
Table 8.3 Parameter Comparison Table for Load Capacity.....	148
Table 8.4 Parameter Comparison Table for Force Density.....	150
Table 8.5 Parameter Comparison Table for Total Weight.....	151
Table 8.6 Performance Measures.....	166
Table 8.7 Design Parameters.....	167
Table A1. Dimensionless Contact Parameters (Extracted from Harris (2006)).....	176

## LIST OF FIGURES

Figure 1.1 Planetary Roller Screw and Component.....	2
Figure 1.2 Number of Contact Comparison between Roller Screw and Ball Screw.....	4
Figure 1.3 Lifetime Comparison between Roller Screw and Ball Screw.....	6
Figure 1.4 Volume ( $in^3$ ) and Static Load Capacity ( $lbf$ ).....	8
Figure 1.5 Static Load Capacity Map.....	9
Figure 2.1 Planetary Roller Screw Configuration.....	13
Figure 2.2 Lead, Start, and Pitch.....	14
Figure 2.3 PRS Cross Section View for Helix Angle and Contact Angle.....	15
Figure 2.4 PRS Kinematic Principle.....	15
Figure 2.5 PRS Axial View and Angular Motion Parameters.....	16
Figure 2.6 PRS Component Configuration Examples.....	23
Figure 3.1 Broken Thread View of the PRS Components.....	25
Figure 3.2 Thread Deformation Factors of PRS.....	27
Figure 3.3 Theoretical Contact Ellipse of the Nut and the Screw.....	32
Figure 3.4 Total Deformation and Stiffness ( $D_n$ Change).....	38
Figure 3.5 Total Deformation and Stiffness ( $d_n$ Change).....	40
Figure 3.6 Total Deformation and Stiffness ( $d_s$ Change).....	42
Figure 3.7 Total Deformation and Stiffness ( $d_r$ Change).....	44
Figure 3.8 Total Deformation and Stiffness ( $N_r$ Change).....	46
Figure 3.9 Total Deformation and Stiffness ( $p$ Change).....	48
Figure 3.10 Total Deformation and Stiffness ( $N_s$ Change).....	50
Figure 3.11 Total Deformation and Stiffness ( $\beta_0$ Change).....	52
Figure 4.1 Load Distribution ( $D_n$ Change).....	60
Figure 4.2 Load Distribution ( $d_n$ Change).....	61
Figure 4.3 Load Distribution ( $d_s$ Change).....	63
Figure 4.4 Load Distribution ( $d_r$ Change).....	64

Figure 4.5 Load Distribution ( $N_r$ Change).....	66
Figure 4.6 Load Distribution ( $p$ Change).....	67
Figure 4.7 Load Distribution ( $N_s$ Change).....	68
Figure 4.8 Load Distribution ( $\beta_0$ Change).....	70
Figure 5.1 Number of Contact Comparison between Roller Screw and Ball Screw.....	74
Figure 5.2 Load Capacity ( $d_n$ as dominant parameter).....	78
Figure 5.3 Load Capacity ( $d_s$ as dominant parameter).....	82
Figure 5.4 Load Capacity ( $d_r$ as dominant parameter).....	85
Figure 5.5 Load Capacity ( $L$ as dominant parameter).....	87
Figure 5.6 Load Capacity ( $p$ as dominant parameter).....	89
Figure 5.7 Load Capacity ( $N_r$ as dominant parameter).....	90
Figure 6.1 Force Density ( $d_n$ as dominant parameter).....	98
Figure 6.2 Force Density ( $d_s$ as dominant parameter).....	102
Figure 6.3 Force Density ( $d_r$ as dominant parameter).....	105
Figure 6.4 Force Density ( $L$ as dominant parameter).....	107
Figure 6.5 Force Density ( $p$ as dominant parameter).....	109
Figure 6.6 Force Density ( $N_r$ as dominant parameter).....	110
Figure 7.1 1 <sup>st</sup> Case of Volume and Total Thread Stiffness Comparison.....	122
Figure 7.2 1 <sup>st</sup> Case of Volume and Load Capacity Comparison.....	123
Figure 7.3 1 <sup>st</sup> Case of Volume and Weight Comparison.....	124
Figure 7.4 2 <sup>nd</sup> Case of Volume and Total Thread Stiffness Comparison.....	126
Figure 7.5 2 <sup>nd</sup> Case of Volume and Load Capacity Comparison.....	127
Figure 7.6 2 <sup>nd</sup> Case of Volume and Weight Comparison.....	128
Figure 7.7 Comparison of Total Stiffness on Thread.....	130
Figure 7.8 Comparison of Load Capacity.....	132
Figure 7.9 Comparison of Force Density.....	133
Figure 7.10 Adding Measures.....	135



Figure 7.11 Multiplying Measures.....	137
Figure 8.1 Normalized Total Stiffness Envelope.....	145
Figure 8.2 Parameter Comparison Chart for Total Stiffness on Thread.....	146
Figure 8.3 Normalized Load Capacity Envelope.....	148
Figure 8.4 Normalized Force Density Envelope.....	149
Figure 8.5 Normalized Total Weight Envelope.....	151
Figure 8.6 Comparison of Adding and Multiplying Envelopes.....	152
Figure 8.7 Measure and Parameter Analysis on Final Envelope.....	153
Figure 8.8 Measure and Parameter Analysis on Final Envelope Using Weight Factor.....	155
Figure A.1 Function of $F(\rho)$ and $a^*, b^*, \delta^*$ Graph 1 (Extracted from Harris (2006)).....	175
Figure A.2 Function of $F(\rho)$ and $a^*, b^*, \delta^*$ Graph 2 (Extracted from Harris (2006)).....	175
Figure A.3 Function of $F(\rho)$ and $a^*, b^*, \delta^*$ Graph 3 (Extracted from Harris (2006)).....	176

## NOMENCLATURE

- $A_n$ : Effective Cross Section Area of the Nut  
 $A_s$ : Effective Cross Section Area of the Screw  
 $A_r$ : Effective Cross Section Area of the Roller  
 $C_a$ : Dynamic Load Capacity  
 $C_{eff}$ : Weight Coefficient  
 $C_{nr}$ : Distance of the Centers between the Nut and the Roller  
 $C_{sr}$ : Distance of the Centers between the Roller and the Screw  
 $D_c$ : Diameter of Rolling Element at the Contact Point  
 $D_n$ : Nut Outer Diameter  
 $F_{axial}$ : Axial Load on the Thread  
 $F_D$ : Force Density  
 $F_{load}$ : Calculated Load on Each Thread in the Axial Direction  
 $F_{mc}$ : Equivalent Cubic Mean Load  
 $F_n$ : Output Load on the Nut  
 $F_{normal}$ : Normal Load on the Thread  
 $F_{radial}$ : Radial Load in the Thread  
 $F(\rho)$ : Contact Surface Curvature Function  
 $F_n(\rho)$ : Contact Surface Curvature Function of the Nut  
 $F_s(\rho)$ : Contact Surface Curvature Function of the Screw  
 $F_{s1}, F_{s2}, F_{s3}$ : Stroke Force Component  
 $H_n$ : Functions of Contact Body's Curvature Formula and the Elastic Modulus of the Nut  
 $H_s$ : Function of Contact Body's Curvature Formula and the Elastic Modulus of the Screw  
 $\bar{I}_{n,r}$ : Equivalent Inertia between the Nut and the Roller  
 $\bar{I}_r$ : Inertia of Rotating Rollers  
 $I_r$ : Inertia of Single Rotating Roller  
 $\bar{I}_s$ : Rotary Inertia of The Screw  
 $L$ : Length of the PRS  
 $L_r$ : Length of Roller

$L_n$ : Length of Nut  
 $L_{s1}, L_{s2}, L_{s3}$ : Each Stroke Related to Each Load  
 $L_{10}$ : Theoretical Life of PRS  
 $M_A^*$ : Added Measures of Root Mean Square Value  
 $M_M^*$ : Multiplied Measures of Root Mean Square Value  
 $M_N$ : Mass of the Nut  
 $M_R$ : Mass of the Roller  
 $M_{lc1}, M_{lc2}, M_{lc3}, M_{lc4}$ : Root Mean Square Values of Normalized Load Capacity Envelopes  
 $M_{ts1}, M_{ts2}, M_{ts3}, M_{ts4}$ : Root Mean Square Values of Normalized Total Stiffness Envelopes  
 $M_{fd1}, M_{fd2}, M_{fd3}, M_{fd4}$ : Root Mean Square Values of Normalized Force Density Envelopes  
 $N_c$ : Total Number of Contact Point  
 $N_{dc}$ : Geometric Factor Decision Number  
 $N_r$ : Number of Rollers  
 $N_{sn}$ : Number of the Nut starts  
 $N_{sr}$ : Number of the Roller Starts  
 $N_{ss}$ : Number of the Screw Starts  
 $N_s$ : Number of Starts  
 $R$ : Effective Ball Radius  
 $R_{PRS}$ : Reduction Ratio of the PRS  
 $R_{r11}, R_{r12}$ : Radius of Effective Ball for both Nut and Screw Side Contact Curvatures  
 $R_{n21}, R_{r11}, R_{s21}$ : Contact Radius of Curvatures  
 $R_{n21}, R_{n22}$ : Nut Side Radius Curvature Factors  
 $R_{s21}, R_{s22}$ : Screw Side Radius Curvature Factors  
 $T_n$ : Thickness of the Nut  
 $T_s$ : Input Torque  
 $V_n$ : Linear Velocity of the Nut  
 $V_r$ : Linear Velocity at the Contact Point between the Roller and the Screw  
 $V_s$ : Linear Velocity of the Center of the Roller  
 $V_{total}$ : Total Volume  
 $W_r$ : Weight of Rollers

$W_n$ : Weight of Nut  
 $W_t$ : Total Weight  
 $Y_n$ : Young's Modulus of the Nut  
 $Y_r$ : Young's Modulus of the Roller  
 $Y_s$ : Young's Modulus of the Screw  
 $Y_n^*$ : Effective Modulus of Elastic Nut Body  
 $Y_s^*$ : Effective Modulus of Elastic Screw Body  
 $a, b$ : Semi-axis of the Ellipse of Contact  
 $d_n$ : Nut Inner Diameter  
 $d_r$ : Roller Diameter  
 $d_s$ : Screw Diameter  
 $f_c$ : Geometric Factor of PRS  
 $k_{ts}$ : Total Screw Thread Deformation  
 $k_{tn}$ : Total Nut Thread Deformation  
 $k_{sn}$ : Nut Stiffness  
 $k_{sr}$ : Roller Stiffness  
 $k_{ss}$ : Screw Stiffness  
 $k_{total}$ : Total Stiffness on the Thread  
 $l$ : Lead of the PRS  
 $l_r$ : Displacement between the Roller and the Nut  
 $l_s$ : Axial Movement between the Roller and the Screw  
 $m_a, m_b$ : Hertz Coefficient  
 $p$ : Pitch  
 $p_c$ : Contact Pressure  
 $t_{cw}$ : Crest Width of the Thread  
 $t_{rw}$ : Root Width of the Thread  
 $t_t$ : Thread Thickness  
 $\alpha_0$ : Contact Angle  
 $\beta_0$ : Helix Angle  
 $\delta_{1n}, \delta_{1s}$ : Bending Deformation of the Nut and Screw  
 $\delta_{2n}, \delta_{2c}$ : Shear Force Deformation of the Nut and Screw

$\delta_{3n}, \delta_{3s}$ : Thread Root Inclination Moment Deformation  
 $\delta_{4n}, \delta_{4s}$ : Thread Tooth Root Shear Deformation  
 $\delta_{5n}$ : Radial Expansion on the Nut Thread Deformation  
 $\delta_{5s}$ : Radial Shrinkage on the Screw Thread Deformation  
 $\delta_{hn}$ : Nut Hertzian Contact Deformation  
 $\delta_{hs}$ : Screw Hertzian Contact Deformation  
 $\delta^*$ : Function of the Contact Surface Curvature Function  
 $\delta_{tn}$ : Total Nut Thread Deformation  
 $\delta_{ts}$ : Total Screw Thread Deformation  
 $\delta_{total}$ : Total Deformation on the Thread  
 $\eta$ : Theoretical Efficiency  
 $\nu_n$ : Poisson's Ratio of the Nut  
 $\nu_r$ : Poisson's Ratio of the Roller  
 $\nu_s$ : Poisson's Ratio of the Screw  
 $\mu$ : Friction Coefficient  
 $\rho_{r11}, \rho_{r12}, \rho_{n21}, \rho_{n22}$ : Principal Curvatures of the Nut Side  
 $\rho_{r11}, \rho_{r12}, \rho_{s21}, \rho_{s22}$ : Principal Curvatures of the Screw Side  
 $\Sigma\rho_n, \Sigma\rho_s$ : Sum of each of the Four Principal Curvatures for the Nut and the Screw  
 $\omega_r$ : Angular Velocity of the Roller  
 $\omega_{rev}$ : Angular Velocity where the Roller Revolving the Screw  
 $\omega_s$ : Angular Velocity of the Screw Shaft

## CHAPTER 1. INTRODUCTION

For several decades, the planetary roller screw (PRS) has been being developed since it was invented in 1954 by Strandgren [1] in his patent and PRS is considered as a key component of electro-mechanical linear actuators (EMA). Recently, the electro-mechanical actuator (EMA) is receiving more attention as a significant component for future intelligent mechanical devices because of its advantages compared to traditional pneumatic or hydraulic actuators and ball screw. EMAs provide better performance by integrated design, extended reliability and easy set up and installation. In addition, EMAs are also profitable in the perspective of precision and efficiency because EMA's produce more accurate motion control and reducing maintenance, operation cost, and energy consumption. And the most important advantage is that there are no leaks, which is the weakest characteristic of hydraulic systems. Because of these advantages, EMAs are considered to be able to replace hydraulic and pneumatic actuators and are studied for concrete application such as aircraft surface control [2] and modern ship operation [3].

As the EMA receive more attention, study about the PRS is also emphasized for good design to enhance the EMA's efficiency and performance. The PRS is a mechanical device with low friction precision which is also called the planetary roller screw mechanism (PRSM). This mechanism converts rotational motion to linear motion or vice versa (see Figure 1.1). The principle of the planetary roller is similar to the ball screw. The difference is that the PRS uses threaded rollers to transfer the load between the nut and screw. Figure 1.1 shows the PRS configuration. The PRS is typically composed of three main components. The main components are the nut, the screw shaft, and the planetary rollers. As screw shaft turns, its helical raceway makes turns to the rollers that radially surround the screw shaft and the rollers roll around the screw shaft. During this operation, the rollers engage with both the screw shaft and the nut. The PRS mechanism has many advantages compared to ball screws such as carrying higher load, high load capacity, better kinematics, and higher transmission precision. As will be mentioned and provided, the PRS is

receiving more interest in both research and industry and expanding its application to further areas such as medical, machine tools, aircraft, and military platforms.

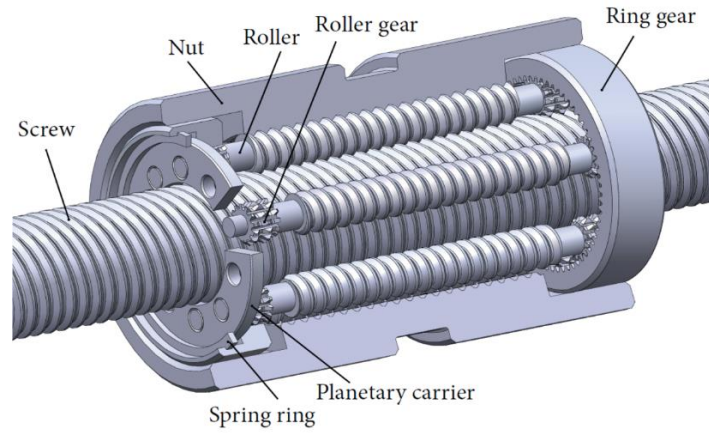


**Figure 1.1 Planetary Roller Screw and Component [4]**

As mentioned above, the planetary roller screw (PRS) is a mechanical transmission device, which converts rotary motion to linear motion, or vice versa. Because of many benefits compared to conventional transmission devices, it receives increasing attention. Those benefits are large load carrying capability, better kinematics, less vibration, and higher precision in working conditions. Because of these advantages, the PRS is applied to many areas such as aerospace, precision machine, robotics, and modern ships. Previous work on the PRS focused on its kinematics and applications. Otsuka et al. [5] investigate operating principles and provide angular factor relationships and structural configuration factor relationships such as the number of thread starts and each component diameter. Research on kinematics of the PRS was done by Velinsky et al. [6]. They focus on the relationship of each component's angular motion analysis and linear motion velocity. Jones et al. [7] derive the nature of the contact kinematics between the load carrying surfaces and provide several geometric relationships. Jones [8] discusses kinematics of the PRS and develops a new approach to calculate stiffness and thread load distribution based on a direct stiffness method in his dissertation. In addition, he analyzes each component's stiffness and provides stiffness matrix as a result. He does some parameter study, however, it is not be applied

to all parameters of PRS. Lemor [9] discusses efficiency of the planetary roller screw and analyzes its advantages in terms of load capacity, life time, and efficiency. A formula is proposed to calculate the dynamic load carrying capacity of the PRS compared to conventional ball screws. However, he doesn't focus much on parameter relationships and each parameter's effect on the PRS system. Otsuka et al. [10] examines theoretical load capacity and displacement result by comparison with experimental values. First, they compare the load distribution between planetary roller screw and the ball screw. And they also compare the values between theoretical and experimental values. Zhang et al. [11] analyze Hertzian contact deformation and thread deformation and provide related formulas to calculate both of them based on contact mechanics. However, they provide limited analysis of parameter relationships and the effect of those parameters, which are an important part of the PRS design. Yang et al. [12] develop a load distribution formula. This equation is used for further research as developed by Ma et al. [13]. They analyze the rolling condition of the PRS and continue previous research conditions and formulas. In addition, they investigate deformations on the thread and load distribution is calculated based on the effective ball concept of contact points. They conduct several cases of parameter relationship analysis; however, the cases are limited. Recently, Zhang et al. [14] discuss stiffness based on the assumption that considers contact points as springs and suggests an improved approach to load distribution by adjusting thread related factors. In addition, they provide formulas to calculate thread stiffness, which is an important element for total screw thread stiffness. However, they doesn't provide relationships between parameters and their impact on the PRS that are the fundamental. Lisowski [15] investigate a computational model of the load distribution on the thread of PRS. They consider the deformation of the component of the PRS as deformation of rectangular volumes and verify the result with a finite element model. They provide results for comparison between the analytical model and numerical results; however, they focus less on the design process, which is a critical part of PRS as pursued in this paper.



Overall, the listed literature does investigate numerous detailed topics to develop the planetary roller screw. However, most of them do not focus on parameter effects on PRS overall design. Even though several papers investigate formulas such as thread stiffness and load distribution - Ma [13] and Zhang [14] - and provide formula for dynamic load capacity - Lemor [9]; however, there is not much analysis about the parameter relationships and the effect of parameters on PRS. For better understanding of the PRS analysis and application in real world, it is important to investigate how many related parameters exist for the PRS design and to determine the effect of these parameters on each other. In addition, it is also critical to analyze the parameter effect on the PRS. The intent in this work is to extend previous work to further understand impact of parameters and develop a useful design process.

### 1.1 Transmission Screw Mechanism Comparison

This research primarily focuses on development of formal a design process of the PRS, which is the key component of linear EMAs. The PRS is most comparable to the ball screw because of its geometric similarity but the PRS has many advantages including durability and load capacity. This is because the number of contact points is far greater for the PRS and the ball screw.

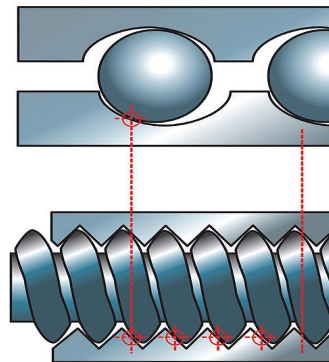


**Figure 1.2 Number of Contact Comparison between Roller Screw and Ball Screw [16]**

Figure 1.2 represents the difference of the number of contact points between two screw mechanisms. As shown in Figure 1.2, the PRS has many more contacts in the same length compared to the ball screw and this results in higher load capacity and longer lifetime.

Table 1.1 represents the characteristics of linear transmission devices and proves that PRS has many advantages. When it compared to the ball screw, the PRS also has better capability in terms of speed and acceleration.

	<b>Exlar Roller Screws</b>	<b>Acme Screws</b>	<b>Ball Screws</b>	<b>Hydraulic cylinders</b>	<b>Pneumatic cylinders</b>
<b>Load ratings</b>	Very High	High	High	Very High	High
<b>Lifetime</b>	Very long, many times greater than ball screw	Very low, due to high friction and wear	Moderate	Can be long with proper maintenance	Can be long with proper maintenance
<b>Speed</b>	Very high	Low	Moderate	Moderate	Very high
<b>Acceleration</b>	Very high	Low	Moderate	Very high	Very high
<b>Electronic Positioning</b>	Easy	Moderate	Easy	Difficult	Very Difficult
<b>Stiffness</b>	Very high	Very high	Moderate	Very high	Very low
<b>Shock Loads</b>	Very high	Very high	Moderate	Very high	High
<b>Relative Space Requirements</b>	Minimum	Moderate	Moderate	High	High
<b>Friction</b>	Low	High	Low	High	Moderate
<b>Efficiency</b>	>90%	approx 40%	>90%	<50%	<50%
<b>Installation</b>	Compatible with standard servo electronic controls	User may have to engineer a motion/ actuator interface	Compatible with standard servo electronic controls	Complex, requires servo-valves, high pressure plumbing, filtering pumps, linear positioning and sensing	Very complex, requires servo-valves, plumbing, filtering, compressors, linear positioning and sensing
<b>Maintenance</b>	Very low	High due to poor wear characteristics	Moderate	Very high	High
<b>Environmental</b>	Minimal	Minimal	Minimal	Hydraulic fluid leaks & disposal	High noise levels

**Table 1.1 Linear Transmission Devices Characteristics Comparison Chart [16]**

In the perspective of load capacity and lifetime, Table 1.2 and Figure 1.3 shows the exact value of the PRS load capacity and lifetime advantage compared to the ball screw. According to Table 1.2 and Figure 1.3, the PRS is capable of higher load capacity by three to five times and longer lifetime up to 10 times that of the ball screw. Therefore, the PRS can be used where the application requires high load and longer life including high speed and acceleration.

ROLLER SCREW		BALL SCREW	
Dia x Lead (mm)	Load Rating (N)	Dia x Lead (mm)	Load Rating (N)
25x5	51,700	25x5	15,600
39x5	105,600	40x5	19,500
48x10	189,300	50x10	66,100
75x20	485,200	80x20	164,700

**Table 1.2 Load Rating Comparison Chart between Roller Screw and Ball Screw [9]**

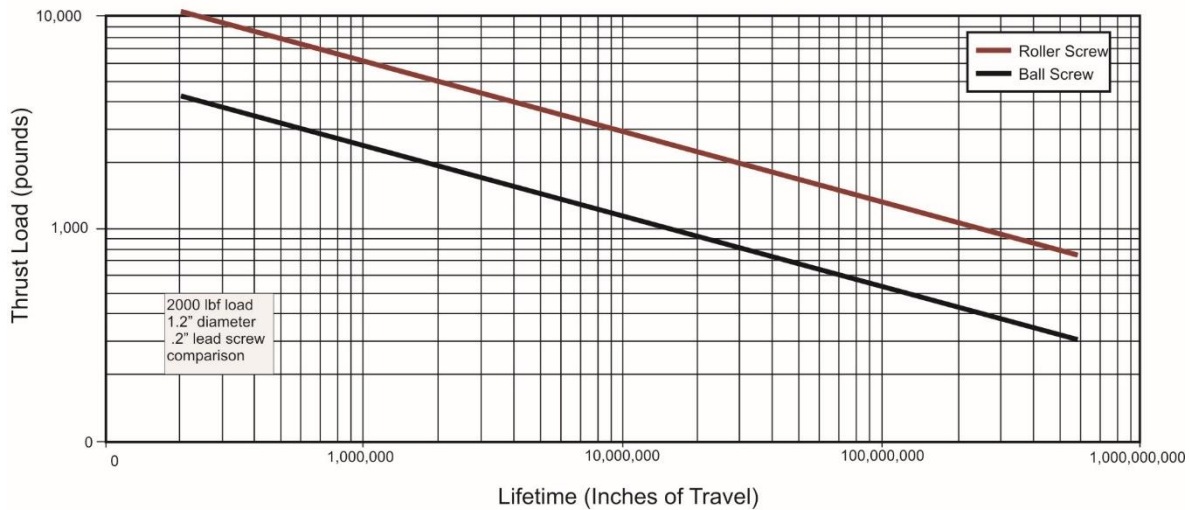


**Figure 1.3 Lifetime Comparison between Roller Screw and Ball Screw [16]**

## 1.2 Motivation

As shown, the PRS has a higher capability to carry load with low weight. We pursued a design with a thrust load peak force of 120,000 lbf. The designed weight was less than 88 lb which required specialized variations of the planetary roller screw (PRS) fully integrated structurally to minimize weight. Three companies (SKF, Rollvis, and Creative Motion Control, CMC) produce the PRS. We used the CMC catalogs [17] for their parametric listing to determine most likely dimensional requirements for the PRS to best meet the needs of the PRS load capacity and weight. We chose four samples from catalog and calculated volume to calculate weight. Then, we analyzed the relationship between volume and static load capacity. With this relationship analysis,

we could re-design dimensions of the PRS components. As given, the required static load capacity is 120,000 lbf for a linear actuator. This load capacity requirement is satisfied when the planetary roller screw volume is 53.73 in<sup>3</sup> for the lead screw diameter of 50 mm (1.97 in) is the proper diameter for this linear actuator, which can carry a load over 120,000 lbf with outer length 4.85 inch and diameter 4.25 inch for the planetary roller screw (see Table 1.3). The static load capacity is 120,655 lbf and volume is 54.02 in<sup>3</sup>. This static load capacity and volume satisfy the required linear actuator load capacity. In comparison, original dimensions are presented with changed dimensional result as shown on Table 1.3. The outer diameter decrease causes the static load capacity decrease, however, length increase makes up the loss of static load capacity.

Case		Screw Diameter	Outer Diameter	Length	Volume	Static Load
		SD (mm)	OD (mm)	L (mm)	mm <sup>3</sup>	SL (kN)
50 mm	Original	50	101.875	127.25	786994.77	480.17
	Result	50	107.95	123.19	885152.67	536.72
Case		Screw Diameter	Outer Diameter	Length	Volume	Static Load
		SD (in)	OD (in)	L (in)	in <sup>3</sup>	SL (lbf)
50 mm	Original	1.97	4.01	5.01	48.03	107942.40
	Result	1.97	4.25	4.85	54.02	120655.10

**Table 1.3 Result for 1.97 in Case for reaching above 120,000 lbf**

In order to calculate load capacity, four samples are chosen from the planetary roller screw catalog. Samples are “39 mm X 10 mm”, “48 mm X 10 mm”, “60 mm X 15 mm”, and “75 mm X 10 mm” cases. Each number indicates screw diameter and lead in mm. As commonly known, lead means that linear movement of lead screw for one revolution. With four samples, volumes were calculated and arranged as Table 1.4. As provided, case No. 3 has more 120,000 lbf static load capacity value. However, the static load capacity gap is large between case 2 and case 3. In other words, there will be dimensions that can reach 120,000 lbf between the two cases. In order to find out exact dimensions reaching in 120,000 lbf, the chosen four original values - volume and static load capacity – are shown in Figure 1.4

Case #	Original Model	Screw Diameter		Outer Diameter		Length		Volume		Static Load Capacity	
		B (mm)	B (in)	OD (mm)	OD (in)	L (mm)	L (in)	mm <sup>3</sup>	in <sup>3</sup>	SL (kN)	SL (lbf)
1	39X10	39.60	1.56	80.00	3.15	100.00	3.94	379299.44	23.15	339.70	76364.56
2	48X10	48.60	1.91	100.00	3.94	127.00	5.00	761474.40	46.47	466.60	104891.68
3	60X15	60.90	2.40	122.00	4.80	166.00	6.54	1456239.01	88.87	947.30	212953.04
4	75X10	75.60	2.98	150.00	5.91	191.00	7.52	2516605.00	153.57	1400.60	314854.88

**Table 1.4 Chosen Four Samples for Parameter Relationship**

In order to find out exact dimensions reaching for 120,000 lbf, four original values - volume and static load capacity – are shown graphically in Figure 1.4.

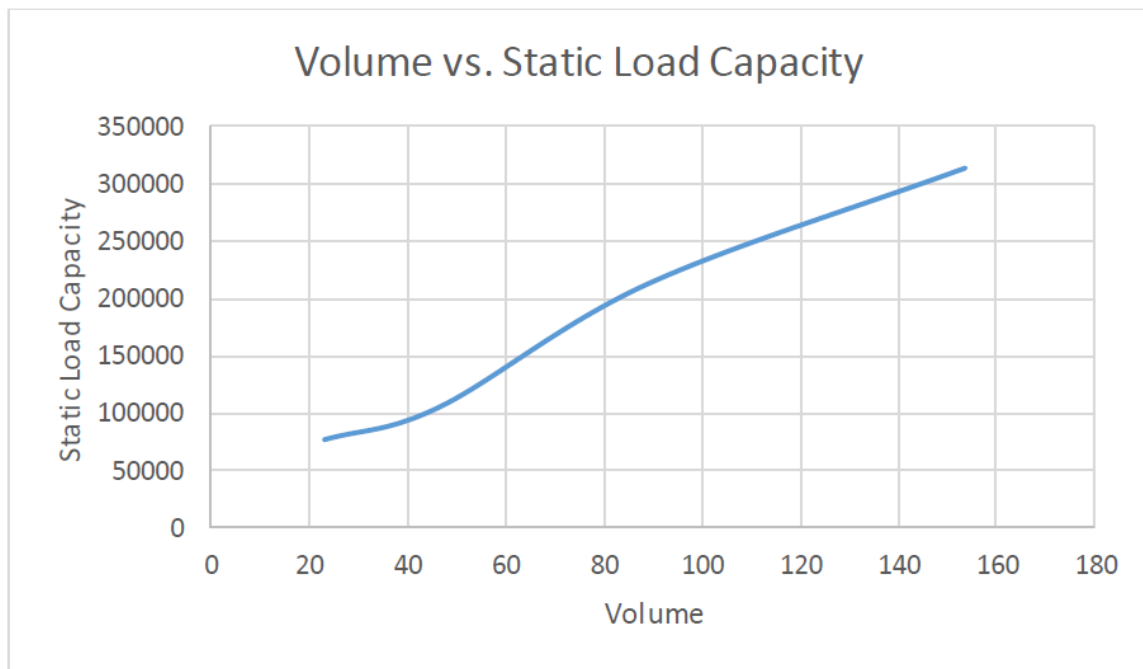


**Figure 1.4 Volume (in<sup>3</sup>) and Static Load Capacity (lbf)**

As shown in Figure 1.4, when volume increases, static load capacity increases proportionally. Using a polynomial approximation program, four data points are transformed to a three order equation as follows:

$$y = -0.2243745572x^3 + 55.72937783x^2 - 1810.33882x + 91192.52799$$

where,

x = volume

y = static load capacity

This equation helps calculate static load capacity with specific dimensions within a specific lead screw range from 39 mm to 75 mm. Furthermore, this equation can be expanded to a 3D map with an increase of screw diameter and nut outer diameter as shown in Figure 1.5. In this Figure 1.5, length was extended to 5 inch.

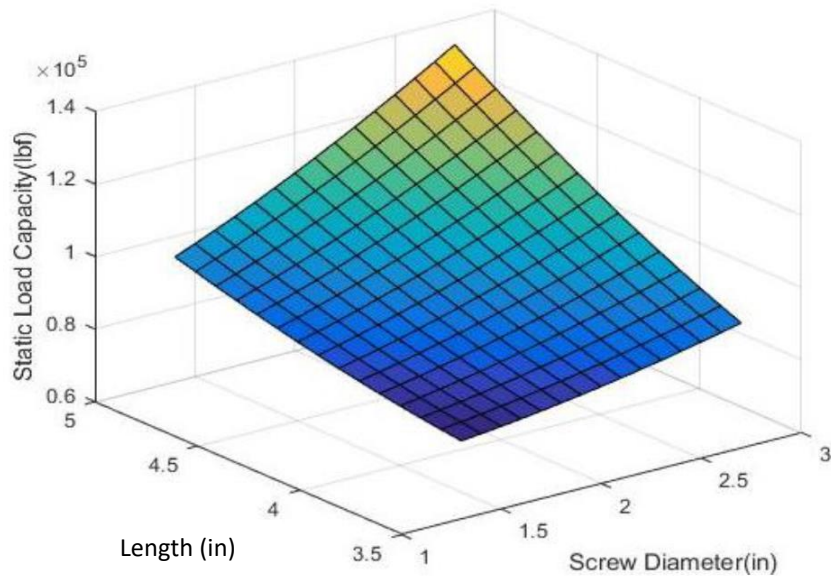


**Figure 1.5 Static Load Capacity Map**

Considering this map, two lead screw diameter cases were chosen to find the best solution to satisfy the planned dimensions and to correspond with grooved roller bearing dimensions. In addition, the recommended lead screw diameter is at least 1.85 inch to carry load. This requirement helps to choose the 48 mm (1.91 inch) and 50 mm (1.97 inch) lead screw cases. Screw diameter and nut length were fixed and the outer diameter was changed for each case in this analysis. However, length is different for each case. In other words, length decreases when outer diameter increases





given outer diameter. Let's assume that the length of the planetary roller screw is acceptable only up to a 3.5 inch maximum because of the requirement for a grooved roller bearing length within limited space in the whole length of the linear actuator as 7.2 inch. When every case has the same length as 3.5 inch, outer diameter should be at least 4.8 inch for 48 mm sample and 4.85 inch for 50 mm sample to reach 120,000 lbf. Hence, we need more diameter increase for achieving 120,000 lbf. In the whole linear actuator system, outer diameter planetary roller screw can accept up to 4.25 inch. This outer diameter requires more length to fulfill 120,000 lbf load capacity. Then this planetary roller screw dimensions satisfy load capacity requirement 120,000 lbf.

### 1.3 Chapter Conclusion

In this chapter, the benefit of the planetary roller screw and its motion was discussed and analyzed. As mentioned previously, there is considerable fundamental research about the PRS; however, not much research about the design of the PRS in terms of parametric effect on the whole PRS system. There are four measures to understand how many parameters related to the design objective of the PRS mechanism. The four measures are load distribution, total thread deformation and stiffness, dynamic load capacity, and force density. These performance measures will be analyzed and investigated in the later chapters. Before these four design objectives were investigated, the motion of the PRS is analyzed in Chapter 2 for understanding fundamental parameter relationships. After this fundamental analysis of the PRS, thread total deformation and stiffness are investigated in Chapter 3. As known, stiffness is calculated based on deformation. This is the reason why two factors are dealt in the same chapter. Parameter effect on load distribution is analyzed in Chapter 4. Load distribution is one of the most necessary condition for the design process. When load is applied to the PRS, each thread of each component has its own amount of divided load. Commonly, first several threads are allotted more load and load on the following threads decreases. Under this condition, we examine how related parameters affect the load distribution curve of the PRS. In Chapter 5, dynamic load capacity is investigated based on



the formula from Lemor [9]. The general meaning of the dynamic load capacity is the load that results in a life of one million revolutions of the inner race. This dynamic load capacity is expressed as a force unit such as N or lbf. Based on this definition and the given formula, we interpret how many parameters are related to load capacity and investigate the effect of each parameter to the PRS. Chapter 6 discusses force density based on weight and load capacity. Force density is a dimensionless value and easy to understand. It shows how much load can be carried per unit weight. As known, weight is a critical factor for most systems. Especially, if there is also small space allowed in the system and a small weight increase can cause large impact on the whole system such as flight control surface or landing gear operation space. However, those systems need higher load carrying capacity. Thus, force density is a critical element for PRS design.

After analysis of the four measures, all four measures are combined and analyzed based on parameter change for the total design of PRS. Then, all of the maps are combined to one final envelope. In this final process, load distribution is excluded because it only presents the load difference on each thread. Hence, this can't be combined with the other three elements. Instead of load distribution, weight is analyzed. Overall, design consideration and total conclusions are discussed in Chapter 7 and Chapter 8.

## CHAPTER 2. KINEMATICS OF PLANETARY ROLLER SCREW

This chapter describes the necessary kinematic conditions of the PRS in order to figure out what parameters exist and to understand parameter relationships among the PRS components. As briefly mentioned in Chapter 1, when the screw shaft starts to turn, rollers surrounded the screw shaft starts to turn around the screw shaft. This motion causes the nut rotation. Even though the nut is fixed, screw shaft and the rollers are rolling on each other. The nut is also affected by the roller motion in contact stiffness and load on the threads, which are presented in the next Chapters. In order to realize the movement among component of the PRS, the necessary conditions have to be recognized for further analysis. The analysis of the motion is based on the rolling characteristics of engaged components and movement conditions of the screw shaft, the rollers, and the nut.

### 2.1 PRS Structure and Terminology

In order to analyze the motion and the kinematics of the PRS, the structure of the PRS must be discussed first. Figure 2.1 and Figure 2.2 show the structure of the PRS and its cross section. Figure 2.1 is presented in Chapter 1, which discussed the operation of the PRS briefly.

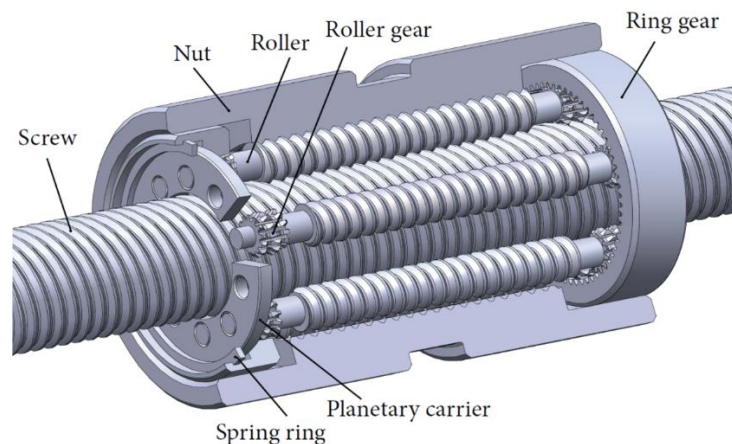


**Figure 2.1 Planetary Roller Screw Configuration [4]**

Figure 2.1 shows the characteristics of each component. In this figure, the screw shaft is formed with threads and the threads make contact with the rollers that are arrayed around the screw shaft. The nut encapsulates the rollers and the screw shaft and the nut has its own threads, which match with the screw shaft. Rollers also have threads on their body, however, rollers threads are single start, which is different from the nut and the screw shaft. The term of thread start is a factor of the lead, which is calculated by multiplication of pitch and starts. Lead is the distance that moves due to one complete turn of the screw shaft. Pitch is the distance from the crest of one thread to the next.

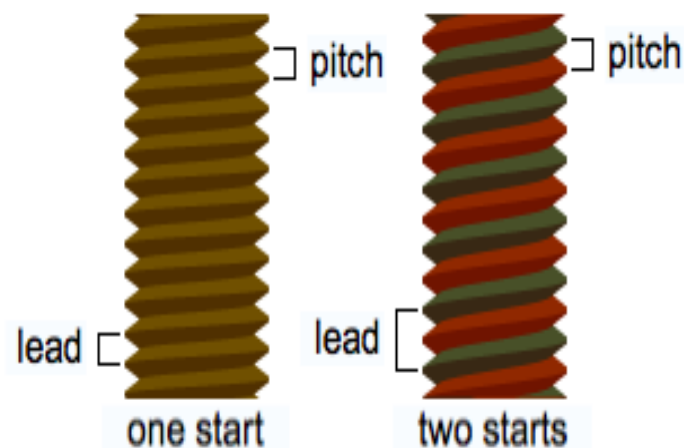


**Figure 2.2 Lead, Start, and Pitch [18]**

As mentioned, lead and pitch are closely related. Because of this relationship, lead and pitch are of the same nature and can be confused when the screw shaft and the nut are single start thread form. They have the same value only in this case. Single start means that there is only one ridge wrap like the first picture of the Figure 2.2. Their values are different and they are distinguished by multiple starts. The rollers have single start thread form and the screw shaft and the nut have multiple starts thread form in the PRS mechanism. The nut and screw have identical starts. In other words, the lead of the screw and nut are the same to operate properly in the PRS. In terms of the design process, it is necessary to understand the meaning of the pitch, the thread start, and the lead.

Figure 2.3 presents the cross section view of a section of the PRS. It shows two important parameters such as contact angle ( $\alpha_0$ ) and helix angle ( $\beta_0$ ) and how they are measured. Angle between helix and a radial line on its right circular cylinder is the helix angle  $\beta_0$ . Contact angle  $\alpha_0$  is the angle between the thread face and an axial line inside the PRS. The helix angle on the rollers must be equal to that on the nut thread to ensure appropriate PRS operation because there can be no relative axial migration between the rollers and the nut.

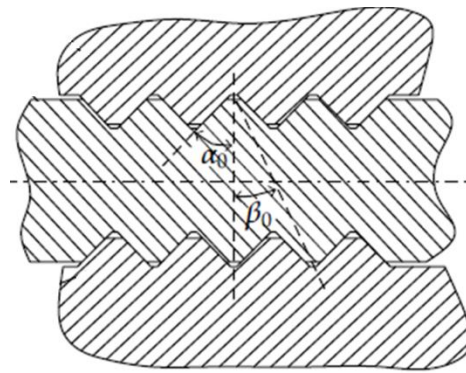


**Figure 2.3 PRS Cross Section View for Helix Angle and Contact Angle [13]**

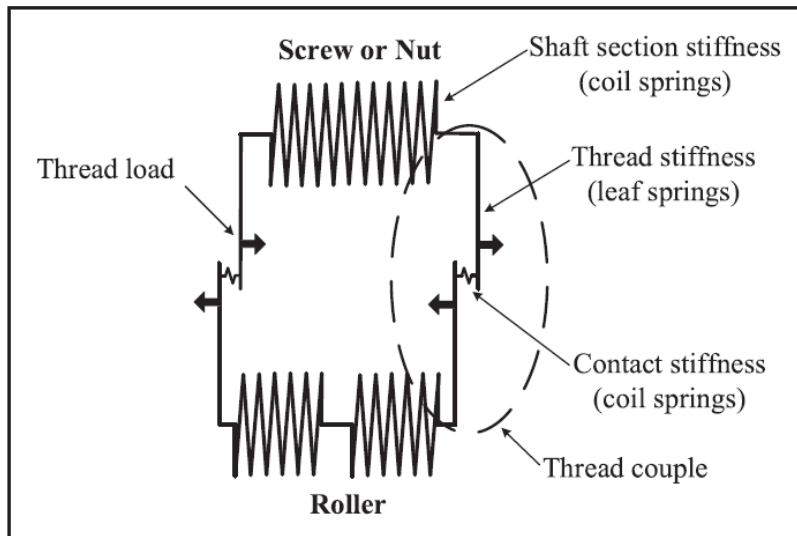


**Figure 2.4 PRS Kinematic Principle [14]**

Figure 2.4 shows the kinematic principle of the PRS mechanism. Zhang et al. consider the PRS mechanism as a combination of springs associated with the screw shaft section, contact area, and thread contact point. This consideration and conditions are important to understand and analyze for further study about decomposed deformation and stiffness and will be discussed in the deformation and stiffness chapter in detail.

2.2 Motion Analysis

The PRS has rolling motion among each of its elements. Basically, rollers and screw rotate relative each other and rollers revolve on the screw shaft while they rotate.

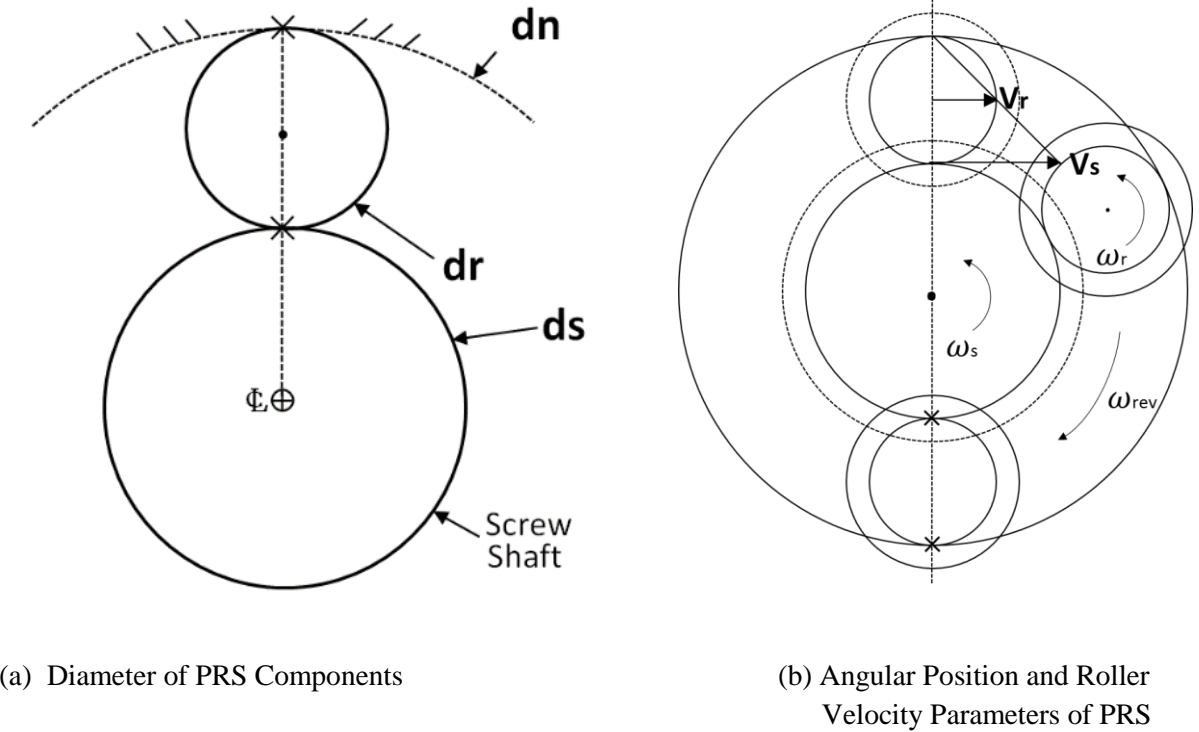


Figure 2.5 PRS Axial View and Angular Motion Parameters

Figure 2.5 shows existing parameters related to the angular motion among the components and it presents how the PRS components work in the system. Figure 2.5 (b) is modified from Ma's paper [13] in order to emphasize angular motion analysis. The dimension  $d_n$  is the effective nut diameter where nut thread and roller thread have contact with each other. Also  $d_r$  is the effective roller diameter where roller thread and nut thread or screw shaft threads have contact with each other. Finally,  $d_s$  is the effective screw shaft diameter where the screw thread and the roller threads have contact with each other. The meaning of  $V_s$  is the linear velocity at the contact point between the roller and the screw. Also  $V_r$  is the linear velocity of center of the roller, which is half of  $V_s$ . Where  $\omega_r$  is the angular velocity of the roller and  $\omega_s$  is the angular velocity of the screw shaft. Note that  $\omega_{rev}$  is the angular velocity where the roller revolves along the screw. All effective diameters are based on the contact point among components where the contact point is shown as 'x' in Figure 2.5 (b).

### 2.2.1 PRS Angular Motion Analysis

In order to analyze angular motion, there is a necessary assumption that there is no slip between the rollers and the screw shaft. Under this assumption,  $V_s$  is twice of the roller linear velocity,  $V_r$  when the nut is stationary. In other words, velocity of the contact point between the nut and the roller is zero under the condition that the nut has no rotational movement.

According to the relationship of each component, two analyses can be expressed first. The PRS is the mechanism that converts rotary motion into linear motion or vice versa. Linear velocity of the screw and the roller contact point ( $V_s$ ) and velocity of the roller center ( $V_r$ ) can be expressed as

$$V_s = \frac{\omega_s d_s}{2} \quad (2.1)$$

$$V_r = \frac{\omega_r d_r}{2} \quad (2.2)$$

As stated above,

$$V_s = 2V_r \quad (2.3)$$

Then,  $V_r$  Can be expressed as:

$$V_r = \frac{\omega_r d_r}{2} = \frac{\omega_s d_s}{4} \quad (2.4)$$

Linear velocities also can be expressed by  $\omega_{rev}$ .

$$V_r = \frac{\omega_{rev} (d_s + d_r)}{2} \quad (2.5)$$

$$V_s = 2V_r = \omega_{rev} (d_s + d_r) \quad (2.6)$$

The relationships among the angular velocities is proportional by diameters of the PRS components and those are expressed as:

$$\frac{\omega_r}{\omega_s} = \frac{\frac{2V_r}{d_r}}{\frac{2V_s}{d_s}} = \frac{\frac{2V_r}{d_r}}{\frac{4V_r}{d_s}} = \frac{d_s}{2d_r} \quad (2.7)$$

$$\frac{\omega_{rev}}{\omega_s} = \frac{\frac{2V_r}{(d_r + d_s)}}{\frac{2V_s}{d_s}} = \frac{\frac{2V_r}{(d_r + d_s)}}{\frac{4V_r}{d_s}} = \frac{d_s}{2(d_r + d_s)} = \frac{d_s}{d_n + d_s} \quad (2.8)$$

and

$$\frac{\omega_{rev}}{\omega_r} = \frac{\frac{2V_r}{(d_r + d_s)}}{\frac{2V_r}{d_r}} = \frac{d_r}{(d_r + d_s)} \quad (2.9)$$

As shown in equation (2.7) – (2.9), each angular velocity ratio is a function of each component's diameters.

## 2.2.2 Axial Motion Analysis

### 2.2.2.1 Relative Motion between the Roller and the Nut

Based on the equations and results from angular motion analysis, axial motion can be analyzed by displacement characteristics among PRS components. As known, there is no relative axial motion between the roller and the nut. And this condition is guaranteed under the requirement, which the helix angle of the roller and the nut is the same as mentioned above. The relative axial displacement ( $l_r$ ) between the roller and the nut is expressed by Ma [13].

$$l_r = \frac{\omega_{rev}}{\omega_s} N_{sn} p - \frac{\omega_r}{\omega_s} N_{sr} p \quad (2.10)$$

where,

$N_{sn}$  = Number of the nut start

$N_{sr}$  = Number of the roller

$p$  = Pitch

All component's pitch values are equal and number of start of the roller ( $N_{sr}$ ) is generally one.

Then, equation (2.10) can be expressed again as:

$$l_r = \frac{\omega_{rev}}{\omega_s} N_{sn} p - \frac{\omega_r}{\omega_s} p \quad (2.11)$$

As mentioned above, there is no relative axial motion between the roller and the nut. In other words,  $l_r$  will be zero. Then, equation (2.11) can be described as:

$$\frac{\omega_{rev}}{\omega_s} N_{sn} - \frac{\omega_r}{\omega_s} = 0 \quad (2.12)$$



And equation (2.12) can be rearranged as:

$$N_{sn} = \frac{\omega_r}{\omega_s} \frac{\omega_s}{\omega_{rev}} = \frac{\omega_r}{\omega_{rev}} \quad (2.13)$$

The number of thread starts of the nut ( $N_{sn}$ ) can be expressed by the diameters of the PRS component as given in Ma's paper [13] as:

$$N_{sn} = \frac{d_s + 2d_r}{d_r} = \frac{d_n}{d_r} \quad (2.14)$$

or

$$N_{sn} = \frac{d_s}{d_r} + 2 \quad (2.15)$$

Then, equations (2.13) and (2.14) gives the result of the gear ratio between the roller and the nut. The gear ratio of the roller to the nut ratio is 1 to the number of starts of the nut and expressed as:

$$d_r : d_n = 1 : N_{sn} \quad (2.16)$$

This ratio is an important condition in the design process in order to calculate and match component dimensions to each other in the PRS mechanism.

#### 2.2.2.2 Relative Motion between the Roller and the Screw Shaft

There are three elements that cause the relative axial motion between the roller and the screw shaft. Those are axial movement from the roller rotation, roller revolution around the screw shaft, and leads of the screw shaft calculated by multiplication of the number of the starts of the screw shaft and the pitch. Adding all three elements gives the result of relative axial motion between the roller and the screw shaft. In this paper, the axial movement between the roller and the screw shaft named as  $l_s$ . And  $l_s$  is defined from Ma's paper [13] as:

$$l_s = \frac{\omega_r}{\omega_s} N_{sr} p_r - \frac{\omega_{rev}}{\omega_s} N_{ss} p_s + N_{ss} p_s \quad (2.17)$$

As mentioned above, if  $N_{sr} = 1$  then all components' pitch value are equal. Then, equation (2.16) can be rearranged as:

$$l_s = \left( \frac{\omega_r}{\omega_s} - \frac{\omega_{rev}}{\omega_s} N_{ss} + N_{ss} \right) p \quad (2.18)$$

The lead  $l_s$  is an absolute constant under the condition of no slip on the screw when the rollers revolve around the screw shaft. In other words, part of the equation is due to the axial movement by the roller rotation and roller revolution on the screw to be zero. This condition is written as:

$$\frac{\omega_r}{\omega_s} p - \frac{\omega_{rev}}{\omega_s} N_{ss} p = 0 \quad (2.19)$$

Then, equation (2.19) can be rearranged after eliminating the pitch ( $p$ ) and angular velocity of the screw shaft ( $\omega_s$ ) as:

$$N_{ss} = \frac{\omega_r}{\omega_{rev}} \quad (2.20)$$

The value for  $N_s$  yields the same result as compared to equation (2.13). Thus, equation (2.20) also can be expressed equal to equation (2.14) and then  $N_s$  and  $N_n$  are same as a result. This result can be expressed as:

$$N_{ss} = \frac{d_s + 2d_r}{d_r} = \frac{d_n}{d_r} = N_{sn} \quad (2.21)$$

or

$$N_{ss} = \frac{d_s}{d_r} + 2 = N_{sn} \quad (2.21)$$

Result from equation (2.21) is already mentioned earlier and proven under these given conditions. This result will be used for the design process in order to find optimal dimensions of the PRS components.

### 2.2.2.3 Concentricity of the PRS components

One more important condition of the axial motion in the PRS is concentricity among the components. Concentricity is represented by dimensions of the rollers that revolve on the screw between the nut and the screw shaft. The rollers are concentric in this condition with other two components. First, the distance of the centers between the nut and the roller is the subtraction half of the effective roller diameter from half of the nut effective diameter and presented as:

$$C_{nr} = \frac{d_n - d_r}{2} \quad (2.22)$$

And the distance of the centers between the roller and the screw shaft is adding half of the effective roller diameter to half of the screw shaft effective diameter and calculated as:

$$C_{sr} = \frac{d_s + d_r}{2} \quad (2.23)$$

As known, each concentricity has equal value ( $C_{nr} = C_{sr}$ ). This condition can be easily proven and the result is zero since  $d_n = d_s + 2d_r$ . An equation is given as:

$$C_{nr} - C_{sr} = \frac{d_n - d_r}{2} - \frac{d_s + d_r}{2} = 0 \quad (2.24)$$

Equation (2.15) and (2.21) are combined due to concentricity conditions and rearranged. The result is written as:

$$\frac{d_s}{d_r} = N_{sn} - 2 = N_{ss} - 2 \quad (2.25)$$

Equation (2.24) helps to define the gear ratio from the roller to the screw shaft. It is written as:

$$d_r : d_s = 1 : N_{sn} - 2 = N_{ss} - 2 \quad (2.26)$$

In addition to the nut-roller gear ratio and screw-roller gear ratio, the nut-screw gear ratio also can be calculated by combining equation (2.21) and (2.25). When equation (2.25) divides equation (2.21), the result is simplified as  $\frac{d_n}{d_s}$ . The overall result is written as:

$$\frac{d_n}{d_s} = \frac{N_{sn}}{N_{sn} - 2} \quad (2.27)$$

And the gear ratio from the nut to the screw is expressed as:

$$d_n : d_s = 1 : \frac{N_{sn}}{N_{sn} - 2} = \frac{N_{ss}}{N_{ss} - 2} \quad (2.27)$$

#### 2.2.2.4 PRS Component Configuration Example

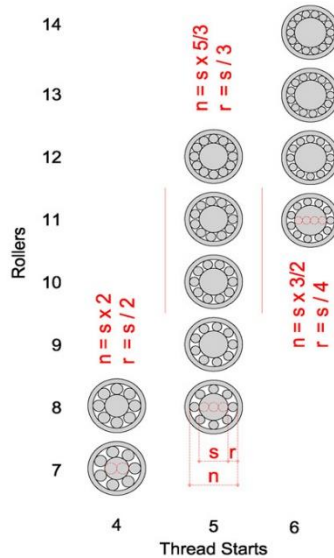


**Figure 2.6 PRS Component Configuration Examples [19]**

Figure 2.6 shows examples of the PRS component configuration by using the motion analysis equation above and based on the Strandgren Patent [1]. In order to not be confused between Figure 2.6 notations and this paper's notation, extra explanation is needed. Here,  $n$  is the nut inner

diameter and  $s$  is screw diameter with  $r$  the roller diameter. As presented, thread starts and the number of the rollers are given in the figure and the effective nut diameter, roller diameter, or screw diameter can be calculated when any one of the two diameters are given. Other values such as pitch length also can be calculated as a result. For example, when the screw shaft effective diameter, screw thread start, and lead are given, then, other related values such as roller diameter, pitch, and the nut effective diameter can be calculated by using the above equations and relationships.

If the screw shaft effective diameter is 50 mm, screw thread starts is seven, and lead is 21 mm, the roller effective diameter will be 10 mm by inserting the given values into equation (2.25). Then, the given parameters help to calculate screw shaft thread pitch by using the definition of the lead, which is mentioned earlier. Pitch is the result of dividing lead by thread starts. Then, pitch is 3 mm as a result. Lastly, nut diameter will be 70 mm by inserting values into the equation (2.21).

### 2.3 Chapter Conclusion

This chapter investigates the structure and the geometric motion of the each part of the PRS. As mentioned above, the PRS has three major components, which are nut, screw, and rollers. Each component is relative to each other. Because of this relationship, analysis of each part is important to design the PRS. As presented in above motion analysis the nut, screw, and roller have their relationships for optimal design of the PRS and this will be considered in later Chapters. Especially, Figure 2.6 is very useful to construct the inner space of the PRS when we investigate parameter effects such as nut inner diameter, screw diameter, and roller diameter. In addition, the relationship between the number of starts and three components diameters is very useful in the analysis of parameter relationships later. Based on this Chapter's motion and configuration analysis, parameter relationships and their effect on load distribution, thread deformation, thread stiffness, load capacity, and force density will be investigated and analyzed in later Chapters.

## CHAPTER 3. DEFORMATION AND STIFFNESS ANALYSIS

In this chapter, axial stiffness of the PRS will be analyzed and discussed in order to set up the design process. As a dominant part for understanding the dynamic operation of the PRS, analyzing the parameters and their effect of axial stiffness is necessary. There are three types of stiffness in the PRS. One is the stiffness on the body section, which is generally called as shaft section stiffness or body stiffness. Shaft section stiffness is defined as the axial stiffness of PRS components such as the nut, screw, or roller. The next type is Hertzian contact stiffness. Hertzian contact stiffness is based on the Hertz contact theory. The last type is thread stiffness. Thread stiffness is the axial deformation, which occurs on each thread when load is applied to the PRS. In order to obtain all three kinds of the axial stiffness, related axial deformations must be solved first. Figure 3.1 shows the basic concept of the PRS mentioned above. Zhang et al. consider that the PRS mechanism is as a combination of the springs including each component's body, threads of each component, and thread contact points as shown in Figure 3.1. Deformation and stiffness will be discussed in more detail with to design process based on the deformation and stiffness analysis.

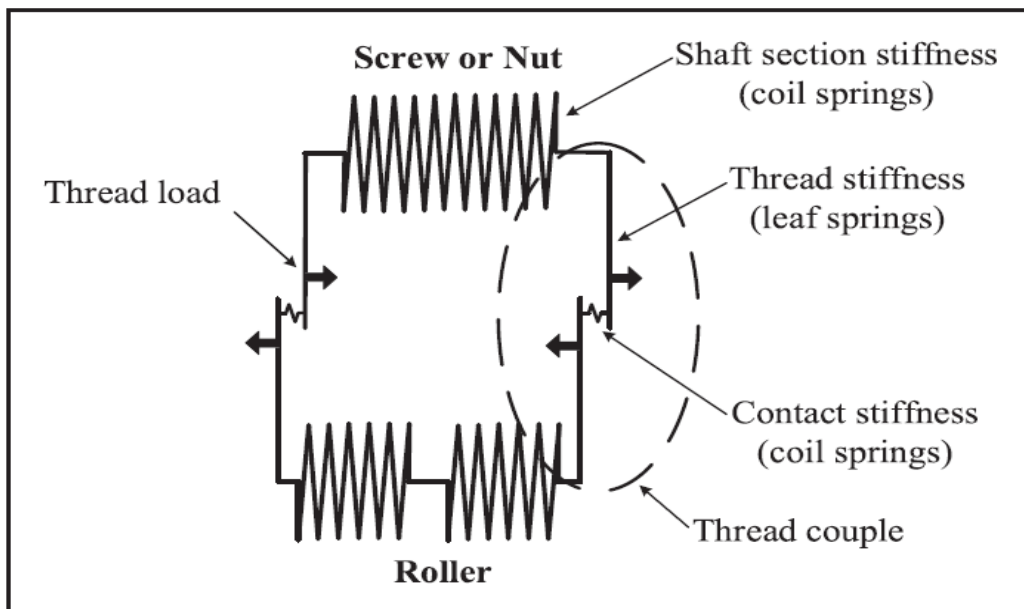


Figure 3.1 Broken Thread View of the PRS Components [14]

### 3.1 Shaft Section Stiffness

As mentioned above, shaft section stiffness is the axial stiffness on the bodies of the roller, the screw, and the nut. Shaft section stiffness of each component is simple relative to the other two stiffnesses. Shaft section stiffness can be determined between two coupled threads of PRS components.

For the nut and the screw body's stiffness values, the required formulas are:

$$k_{sn} = \frac{Y_n A_n}{p} \quad (3.1)$$

$$k_{ss} = \frac{Y_s A_s}{p} \quad (3.2)$$

where,

$k_{sn}$  = Nut Body Section Stiffness

$k_{ss}$  = Screw Shaft Section Stiffness

$Y_n$  = Young's Modulus of the Nut

$Y_s$  = Young's Modulus of the Screw

$A_n$  = Effective Cross Section Area of the Nut

$A_s$  = Effective Cross Section Area of the Screw

$p$  = Pitch of the Nut and the Screw

Effective cross section area of the nut and the screw shaft can be calculated using each diameter. The equation for roller body stiffness is somewhat different compared to the nut and the screw shaft section stiffness. The roller body stiffness equation is expressed as:

$$k_{sr} = \frac{Y_r A_r}{2p} \quad (3.3)$$

where,

$Y_r$  = Young's Modulus of the Roller

$A_r$  = Effective Cross Section Area of the Roller

### 3.2 Thread Stiffness

Thread stiffness is also a main part of the stiffness analysis, which can be calculated where the load is applied. When load is applied on the PRS, this causes axial thread deformation on each component's thread. Thread deformation calculation was started decades ago. Yamamoto [20] developed formulas to predict the deformation of the PRS component's thread and Zhang [14] adapted and proved Yamamoto's formula in his research. Yamamoto's formulas are used to calculate each component's thread deformation and stiffness in this chapter. According to Yamamoto [20] and Zhang [11], five types of elastic deformation exist on the thread. Four of them result in the same formulas for thread of the nut and the screw shaft but parameter values are different because diameters of the nut and the screw are not same as known. The last fifth deformation factor uses a different formula to the nut and the screw shaft. And one more difference between fifth deformation factor and other four factors is that the last deformation is caused by radial load on the thread not like the other four deformation factors, which are due to axial load on the thread.

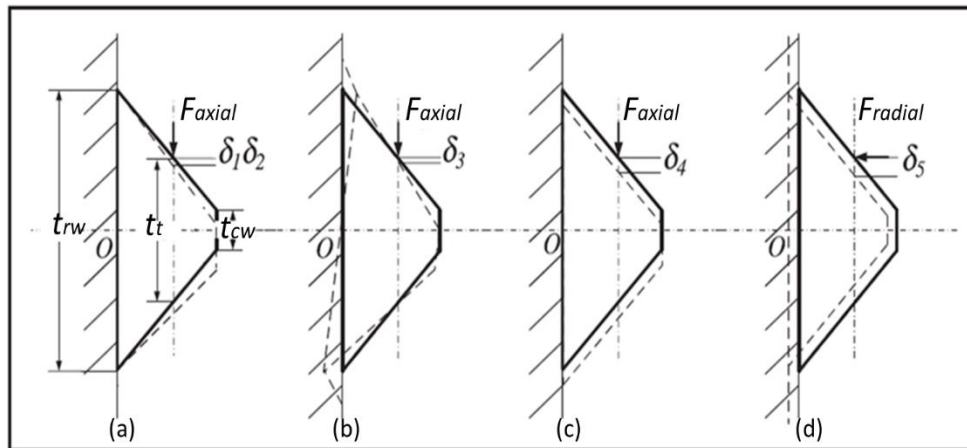


Figure 3.2 Thread Deformation Factors of PRS [14]



Figure 3.2 shows the thread deformation factors of the PRS. Here  $t_{rw}$  is root width of the thread.  $t_t$  is the thread thickness and  $t_{cw}$  is the crest width of the thread. Figure 3.2 (a) presents two of the thread deformation factors, which are the bending deformation ( $\delta_{1n}, \delta_{1s}$ ) and the shear force deformation ( $\delta_{2n}, \delta_{2c}$ ). Figure 3.2 (b) shows the thread deformation that is caused by thread root inclination moment ( $\delta_{3n}, \delta_{3s}$ ). Figure 3.2 (c) is the deformation that occurs due to thread tooth root shear ( $\delta_{4n}, \delta_{4s}$ ). Figure 3.2 (d) indicates the deformation caused by radial load on the thread ( $\delta_{5n}, \delta_{5s}$ ). In detail, radial expansion on the nut thread tooth makes the deformation  $\delta_{5n}$  and radial shrinkage on the screw shaft thread cause the deformation  $\delta_{5s}$ .

First, deformation formulas for the screw thread are provided from Yamamoto [20] as:

$$\delta_{1s} = (1 - \nu_s^2) \frac{3 F_{axial}}{4 Y_s} \left\{ \left[ 1 - \left( 2 - \frac{t_t}{t_{rw}} \right)^2 + 2 \ln \left( \frac{t_{rw}}{t_t} \right) \cot^3(\beta_0) - 4 \left( \frac{t_{cw}}{t_{rw}} \right)^2 \tan(\beta_0) \right] \right\} \quad (3.4)$$

$$\delta_{2s} = (1 + \nu_s) \frac{6 F_{axial}}{5 Y_s} \cot^3(\beta_0) \ln \left( \frac{t_{rw}}{t_t} \right) \quad (3.5)$$

$$\delta_{3s} = (1 - \nu_s^2) \frac{12 t_{cw}}{\pi Y_s t_{rw}^2} F_{axial} \left( t_{cw} - \frac{t_t}{2} \tan(\beta_0) \right) \quad (3.6)$$

$$\delta_{4s} = (1 - \nu_s^2) \frac{2 F_{axial}}{\pi Y_s} \left\{ \frac{p}{t_{rw}} \ln \left( \frac{p + \frac{t_{rw}}{2}}{p - \frac{t_{rw}}{2}} \right) + \frac{1}{2} \ln \left( \frac{4p^2}{t_{rw}^2} \right) - 1 \right\} \quad (3.7)$$

$$\delta_{5s} = (1 - \nu_s) \frac{\tan^2(\beta_0)}{2} \frac{d_s}{p} \frac{F_{radial}}{Y_s} \quad (3.8)$$

Where  $\beta_0$  is thread's helix angle of the screw thread and  $d_s$  is effective diameter of the screw shaft. In addition,  $\nu_s$  is Poisson's ratio and  $Y_s$  is the Young's modulus of the screw shaft material.

$F_{radial}$  is the radial load on the thread and has the following relationship with axial load on the thread as

$$F_{axial} = \frac{F_{radial}}{\tan(\beta_0)} \quad (3.9)$$

Then, equation (3.8) can be expressed as:

$$\delta_{5s} = (1 - \nu_s) \frac{\tan^3(\beta_0) d_s}{2} \frac{F_{axial}}{p Y_s} \quad (3.10)$$

In order to obtain the total deformation on the screw thread, all five equations from (3.4) to (3.8) are added. Then, the total screw thread deformation ( $\delta_{ts}$ ) will be expressed as:

$$\delta_{ts} = \delta_{1s} + \delta_{2s} + \delta_{3s} + \delta_{4s} + \delta_{5s} \quad (3.11)$$

And the screw shaft thread stiffness can be calculated with the applied axial load and equation (3.11). Then, stiffness on each thread will be expressed as:

$$k_{ts} = \frac{F_{axial}}{\delta_{1s} + \delta_{2s} + \delta_{3s} + \delta_{4s} + \delta_{5s}} = \frac{F_{axial}}{\delta_{ts}} \quad (3.12)$$

Next, deformation formulas for the nut thread are also provided from Yamamoto [20] as:

$$\delta_{1n} = (1 - \nu_n^2) \frac{3 F_{axial}}{4 Y_n} \left\{ \left[ 1 - \left( 2 - \frac{t_t}{t_{rw}} \right)^2 + 2 \ln \left( \frac{t_{rw}}{t_t} \right) \cot^3(\beta_0) - 4 \left( \frac{t_{cw}}{t_{rw}} \right)^2 \tan(\beta_0) \right] \right\} \quad (3.13)$$

$$\delta_{2n} = (1 + \nu_n) \frac{6 F_{axial}}{5 Y_n} \cot^3(\beta_0) \ln\left(\frac{t_{rw}}{t_t}\right) \quad (3.14)$$

$$\delta_{3n} = (1 - \nu_n^2) \frac{12 t_{cw}}{\pi Y_n t_{rw}^2} F_{axial} \left( t_{cw} - \frac{t_t}{2} \tan(\beta_0) \right) \quad (3.15)$$

$$\delta_{4n} = (1 - \nu_n^2) \frac{2 F_{axial}}{\pi Y_n} \left\{ \frac{p}{t_{rw}} \ln\left(\frac{p + \frac{t_{rw}}{2}}{p - \frac{t_{rw}}{2}}\right) + \frac{1}{2} \ln\left(\frac{4p^2}{t_{rw}^2}\right) - 1 \right\} \quad (3.16)$$

$$\delta_{5n} = \left( \frac{D_n^2 + d_n^2}{D_n^2 - d_n^2} + \nu_n \right) \frac{\tan^2(\beta_0) d_n}{2} \frac{F_{radial}}{p Y_n} \quad (3.17)$$

Where  $D_n$  is nut outer diameter and  $d_n$  is nut inner diameter. Total deformation on the nut thread can be obtained by adding all five equations from (3.13) to (3.17) in the same manner as the total screw thread deformation. Then, the total screw thread deformation ( $k_{tn}$ ) will be expressed as:

$$\delta_{tn} = \delta_{1n} + \delta_{2n} + \delta_{3n} + \delta_{4n} + \delta_{5n} \quad (3.18)$$

and the nut thread stiffness can be calculated with the applied axial load and equation (3.18). Then, the total stiffness can be expressed as:

$$k_{tn} = \frac{F_{axial}}{\delta_{1n} + \delta_{2n} + \delta_{3n} + \delta_{4n} + \delta_{5n}} = \frac{F_{axial}}{\delta_{tn}} \quad (3.19)$$

### 3.3 Hertzian Contact Stiffness

Hertzian contact stiffness formulas can be derived from Hertzian contact theory [21] and Harris [22]. Hertzian contact theory describes the environment and nature of bodies where two surfaces are in contact under following conditions [23] as:

- The strains are small and within the contact bodies' elastic limit

- The area of the contact is small compared to the size of the bodies. In other words, dimension of the contact is much smaller than dimension of the bodies.
- Each contact body is considered as an elastic half-space
- The body surfaces are non-conforming and continuous
- The surfaces are frictionless

According to the Hertzian contact theory [21] and Harris [22], the contact deformation of two general bodies in contact is expressed as follows in the normal direction where the load is applied.

$$\delta_{hn} = \delta^* \left( \frac{3 F_{normal}}{2 Y_n^* \Sigma \rho_n} \right)^{\frac{2}{3}} \left( \frac{\Sigma \rho_n}{2} \right) \quad (3.20)$$

such that

$$\delta_{hs} = \delta^* \left( \frac{3 F_{normal}}{2 Y_s^* \Sigma \rho_s} \right)^{\frac{2}{3}} \left( \frac{\Sigma \rho_s}{2} \right) \quad (3.21)$$

where,

$\delta_{hn}$  = Nut Hertzian contact deformation

$\delta_{hs}$  = Screw Hertzian contact deformation

$F_{normal}$  = the normal load on the thread

$\delta^*$  = Function of the contact surface curvature function  $F(\rho)$

$Y_n^*$  = Effective modulus of elastic nut body

$Y_s^*$  = Effective modulus of elastic screw body ( $Y_n^* = Y_s^* = \frac{1-\nu_s^2}{Y_s} + \frac{1-\nu_n^2}{Y_n}$ )

Contact between the two bodies have different radii of curvature. This curvature is defined as  $\rho$  where it is the inverse term of the radii of contact surface curvature.  $F(\rho)$  is a function of  $\rho$ . There are two curvature factors on each surface. Thus, there are four curvature factors in the PRS as shown in Figure 3.3. Figure 3.3 presents the fundamental basis for contact stiffness analysis. There are two radii of curvature for each two contacts on the effective ball, which is the dashed circle in Figure 3.3. Lisowski [24] expresses contact radius of curvatures as  $R_{n21}$ ,  $R_{r11}$ , and  $R_{s21}$ . Nut side radius curvature factors are  $R_{n21}$ ,  $R_{r11}$  and screw side curvature factors are  $R_{s21}$ ,  $R_{r11}$ . In order to calculate the radii of curvature, the effective ball radius is necessary. The effective ball radius is expressed following Ma's paper [13], Zhang's paper [14], and Lisowski [24] paper:

$$R = \frac{d_r}{2 \sin(\alpha_0)} \quad (3.22)$$

where,

$d_r$  = effective roller diameter

$\alpha_0$  = contact angle

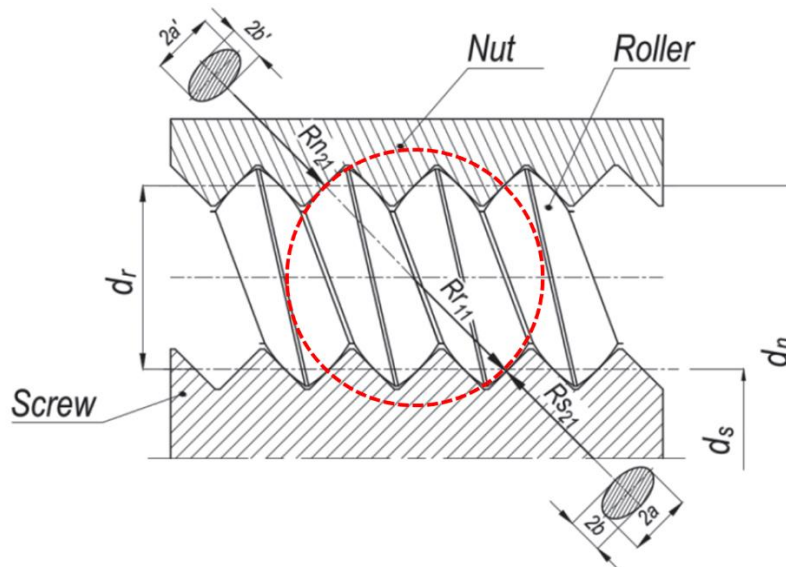


Figure 3.3 Theoretical Contact Ellipse of the Nut and the Screw [24]

According to the Hertz theory, the nut side radii of curvature and screw side radii of curvature are expressed as  $R_{r11}$ ,  $R_{r12}$ ,  $R_{n21}$ ,  $R_{n22}$  for the nut side and  $R_{r11}$ ,  $R_{r12}$ ,  $R_{s21}$ ,  $R_{s22}$  for the screw side.  $R_{r11}$  and  $R_{r12}$  are the radius of effective ball for both nut and screw side contact curvatures and,  $R_{n21}$ ,  $R_{n22}$ ,  $R_{s21}$ ,  $R_{s22}$  are the radii of nut and screw contact thread surface curvature in detail. Firstly, radii of curvature in the nut side are listed as:

$$R_{r11} = \frac{d_r}{2 \sin(\alpha_0)} = R \quad (3.23)$$

$$R_{r12} = \frac{d_r}{2 \sin(\alpha_0)} = R \quad (3.24)$$

$$R_{n21} = \infty \quad (3.25)$$

$$R_{n22} = \frac{d_r + d_s + 2R \cos(\alpha_0)}{-2 \cos(\alpha_0)} \quad (3.26)$$

Then, principal curvatures are expressed as:

$$\rho_{r11} = \frac{2 \sin(\alpha_0)}{d_r} = \frac{1}{R} \quad (3.27)$$

$$\rho_{r12} = \frac{2 \sin(\alpha_0)}{d_r} = \frac{1}{R} \quad (3.28)$$

$$\rho_{n21} = \frac{1}{\infty} = 0 \quad (3.29)$$

$$\rho_{n22} = \frac{-2 \cos(\alpha_0)}{d_r + d_s + 2R \cos(\alpha_0)} \quad (3.30)$$

Next, the radii of curvature in the screw side can be expressed as:

$$R_{r11} = \frac{d_r}{2 \sin(\alpha_0)} = R \quad (3.31)$$

$$R_{r12} = \frac{d_r}{2 \sin(\alpha_0)} = R \quad (3.32)$$

$$R_{s21} = \infty \quad (3.33)$$

$$R_{s22} = \frac{d_r + d_s - 2R \cos(\alpha_0)}{2 \cos(\alpha_0)} \quad (3.34)$$

Then, principal curvatures can be expressed as:

$$\rho_{r11} = \frac{2 \sin(\alpha_0)}{d_r} = \frac{1}{R} \quad (3.35)$$

$$\rho_{r12} = \frac{2 \sin(\alpha_0)}{d_r} = \frac{1}{R} \quad (3.36)$$

$$\rho_{s21} = \frac{1}{\infty} = 0 \quad (3.37)$$

$$\rho_{s22} = \frac{2 \cos(\alpha_0)}{d_r + d_s - 2R \cos(\alpha_0)} \quad (3.38)$$

As mentioned earlier, the contact deformation formula includes  $F(\rho)$  as a parameter.  $F(\rho)$  can be written as curvature function as follows:

$$F_n(\rho) = \frac{|(\rho_{r11} - \rho_{r12}) + (\rho_{n21} - \rho_{n22})|}{\Sigma \rho_n} \quad (3.39)$$

and

$$F_s(\rho) = \frac{|(\rho_{r11} - \rho_{r12}) + (\rho_{s21} - \rho_{s22})|}{\Sigma\rho_s} \quad (3.40)$$

Here,  $\Sigma\rho_n$  and  $\Sigma\rho_s$  are the sum of each of the four principal curvatures for the nut and the screw shaft.  $F_n(\rho)$  and  $F_s(\rho)$  are the key values to determine the dimensionless quantity ( $\delta^*$ ) as mentioned above. In other words,  $\delta^*$  is presented as a function of  $F(\rho)$  with results are given by Harris [22] which is presented in Appendix A.

The Hertzian contact deformation formula eq. (3.20) and (3.21) can be expressed differently because the thread surface has an elliptical contact area. And different formula can be presented as following Ma's paper [13]:

$$\delta_{hn} = H_n F_{normal}^{\frac{2}{3}} \quad (3.41)$$

and in the screw

$$\delta_{hs} = H_s F_{normal}^{\frac{2}{3}} \quad (3.42)$$

As known,  $F_{normal}$  is the load on the each thread in the normal direction that is perpendicular to the thread face. The contact area is elliptical. Then,  $H_n$  and  $H_s$  can be defined as the elastic modulus of the nut and the screw where there is an elliptical contact point, respectively. Then,  $H_n$  and  $H_s$  can be expressed following Yang's analysis [12] as:

$$H_n = \delta^* \left( \frac{3}{2Y_n^* \Sigma\rho_n} \right)^{\frac{2}{3}} \left( \frac{\Sigma\rho_n}{2} \right) \quad (3.43)$$

and

$$H_s = \delta^* \left( \frac{3}{2Y_s^* \Sigma\rho_s} \right)^{\frac{2}{3}} \left( \frac{\Sigma\rho_s}{2} \right) \quad (3.44)$$



As shown above,  $H_n$  and  $H_s$  are the functions of contact bodies' curvature formula and the elastic modulus.  $H_n$  and  $H_s$  will be used to calculate load distribution in Chapter 4.

### 3.4 Total Deformation and Total Stiffness

Total Deformation on each thread is a summation of thread deformation and Hertzian deformation of the nut and the screw. It can be described as:

$$\delta_{total} = \delta_{hn} + \delta_{hs} + \delta_{tn} + \delta_{ts} \quad (3.45)$$

Then, total stiffness can be expressed as:

$$k_{total} = \frac{F_{axial}}{\delta_{total}} \quad (3.46)$$

In order to calculate and make 3D plots, all parameters are considered. Effective and variable parameters are chosen for analysis of effect on total deformation and total stiffness on the thread. There are 13 parameters that are related to calculation of the total deformation and total stiffness. Eight parameters are separated as variables, which are used for calculation and to make plots. The other five parameters are designated as fixed parameters that don't change their values such as Young's modulus and Poisson's ratio. Recall that effective Young's Modulus is a combination of Young's Modulus and the Poisson's ratio. Then, it also doesn't change its value. Dimensionless quantity ( $\delta^*$ ) has near 0.98 in the case of PRS. Thus, it is fixed as 0.98 in the calculation process.

### 3.5 Total Deformation and Total Stiffness Analysis

#### 3.5.1 Parameters

As mentioned, there are 13 parameters and eight parameters are used to analyze effect of these parameters on the total deformation and stiffness. It is expected that 4 or 5 parameters have significant influence on total deformation and total stiffness such as diameters and pitch because those parameters change PRS' geometry when they change their values. Each parameter is used in

the calculation process and analyzed for its impact on the total deformation and stiffness. And x-axis is fixed as thread number. In this analysis, we fixed thread number as 20. In other words, PRS components have 20 thread teeth and we investigated the difference of value on each thread.

Variable Parameters	Fixed Parameters
Nut Outer Diameter: 54 – 75 mm	Young’s Modulus: $2.1 \times 10^{11}$ Pa
Effective Nut Inner Diameter: 50 mm	Poisson’s Ratio: 0.3
Effective Screw Diameter: 30 mm	Effective Young’s Modulus: $4.333 \times 10^{-12}$ Pa
Effective Roller Diameter: 10 mm	Dimensionless Quantity: 0.98
Pitch: 2 mm	Contact Angle: $45^\circ$
Number of Start: 5	
Number of Rollers: 10	
Helix Angle: $6.056^\circ$	

**Table 3.1 Parameters**

### 3.5.2 Resulting Maps and Analysis

#### 3.5.2.1 Nut Outer Diameter Change

##### 3.5.2.1.1 Parameter Values

Variable Parameters (8)	Fixed Parameters (5)
$D_n$ : Nut Outer Diameter	$Y_x$ : Young’s Modulus
$d_n$ : Nut Inner Diameter	$\nu$ : Poisson’s Ratio
$d_s$ : Screw Diameter	$Y_x^*$ : Effective Young’s Modulus
$d_r$ : Roller Diameter	$\delta^*$ : Dimensionless Quantity
$p$ : Pitch	$\alpha_0$ : Contact Angle
$N_s$ : Number of Start	
$N_r$ : Number of Rollers	
$\beta_0$ : Helix Angle	

**Table 3.2 Nut Outer Diameter ( $D_n$ ) Change Case Parameter Values**

3.5.2.1.2 Resulting maps

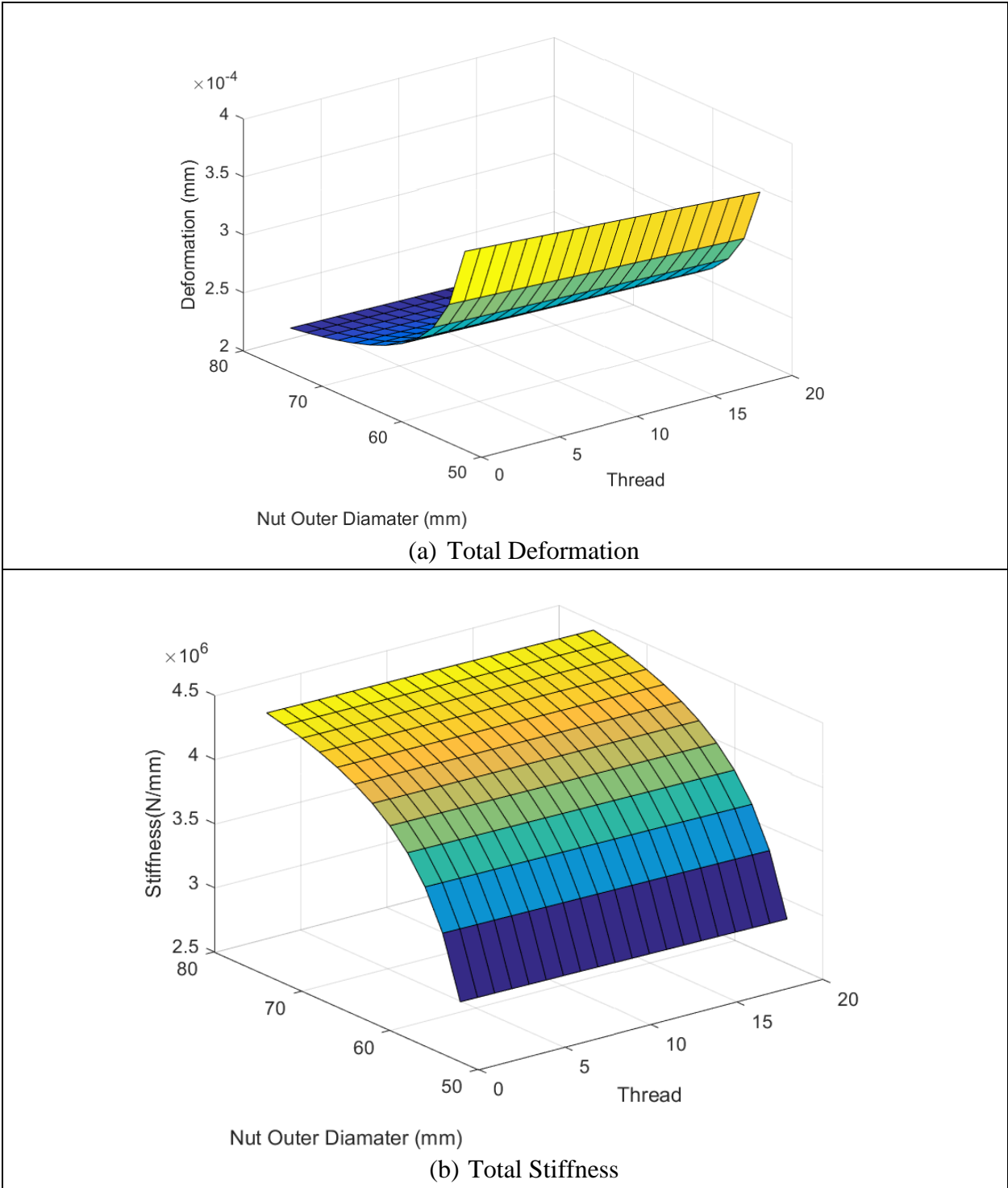


Figure 3.4 Total Deformation and Stiffness ( $D_n$  Change)

Figure 3.4 shows that total deformation and total stiffness changes where nut outer diameter ( $D_n$ ) changes from 54 mm to 75 mm. When nut outer diameter increases, total deformation value

decreases sharply. And it shows non-linear change of total deformation and total stiffness. A useful outer diameter point is about 68 mm. According to the parameter value table, effective nut inner and other parameter values are fixed and only the nut outer diameter changes. This indicates that the thickness of the nut is one of dominant parameter to the total deformation and total stiffness.

### 3.5.2.2 Effective Nut Inner Diameter Change

#### 3.5.2.2.1 Parameter Values

Variable Parameters	Fixed Parameters
Nut Inner Diameter: 50 – 70 mm	Young’s Modulus: $2.1 \times 10^{11}$ Pa
Nut Outer Diameter: 75 mm	Poisson’s Ratio: 0.3
Screw Diameter: 30 - 42 mm	Effective Young’s Modulus: $4.333 \times 10^{-12}$ Pa
Roller Diameter: 10 - 14 mm	Dimensionless Quantity: 0.98
Pitch: 2 mm	Contact Angle: $45^\circ$
Number of Start: 5	
Number of Rollers: 10	
Helix Angle: $6.056^\circ$	

**Table 3.3 Nut Inner Diameter ( $d_n$ ) Change Case Parameter Values**

#### 3.5.2.2.2 Resulting maps

Screw diameter and roller diameter must change when the nut inner diameter changes because of the inside PRS geometry. In other words, inside dimension of the PRS is determined by the nut inner diameter and screw diameter such that the roller diameter changes to match the inside dimension when the nut inner diameter changes. In this condition, Figure 3.5 shows the opposite result when it is compared to the nut outer diameter changes. As presented above, total deformation increases smoothly at first, however, it increases sharply at some point as the nut inner diameter increases.

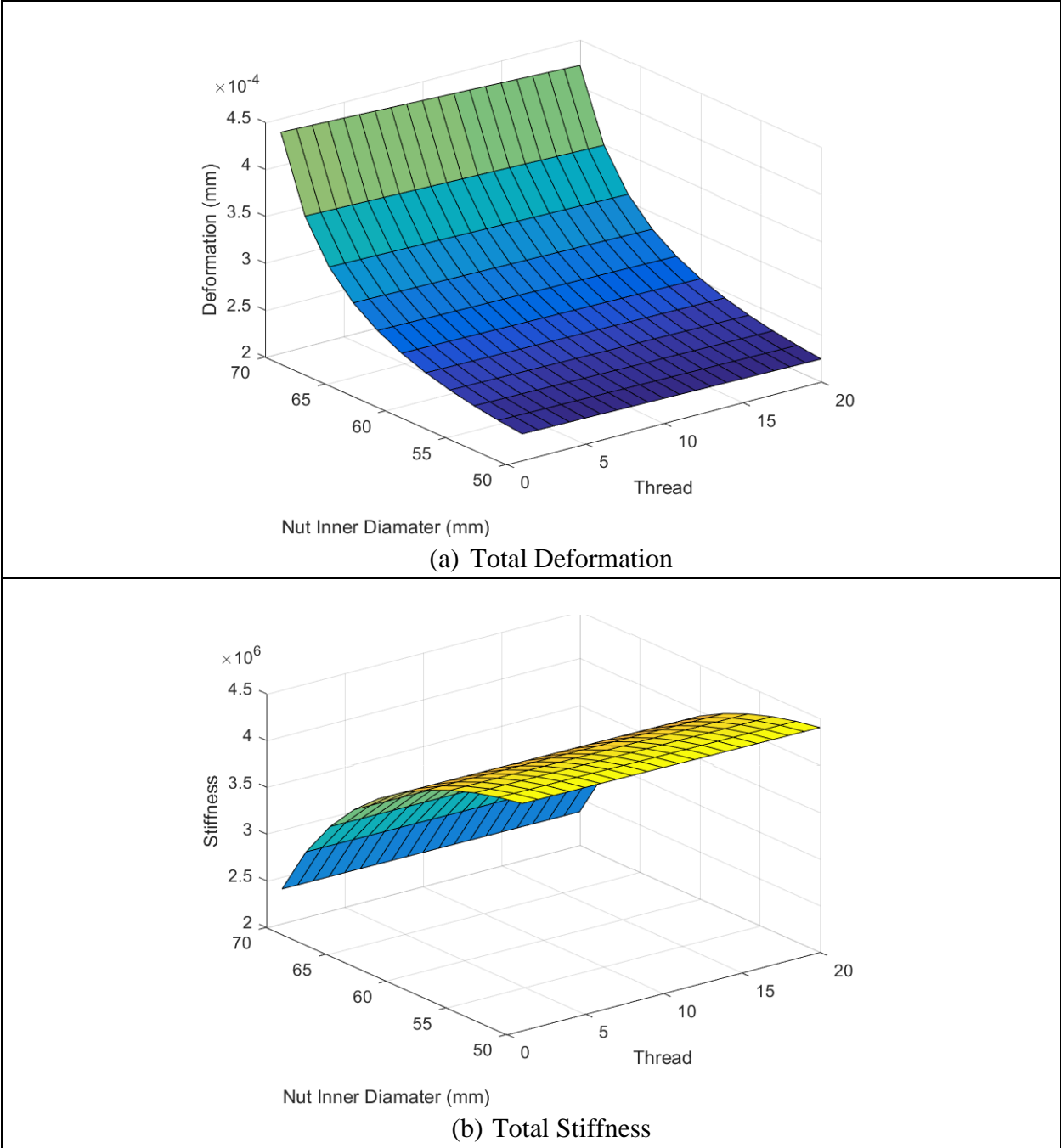


**Figure 3.5 Total Deformation and Stiffness ( $d_n$  Change)**

Figure 3.5 (b) represents the total stiffness change when the nut inner diameter increases. Stiffness is the value that is achieved after dividing force by deformation. This relationship makes stiffness as the universe plot of the total deformation plot. The two plots prove that the nut inner diameter has a great effect on the PRS total tooth deformation and total stiffness.

### 3.5.2.3 Effective Screw Diameter Change

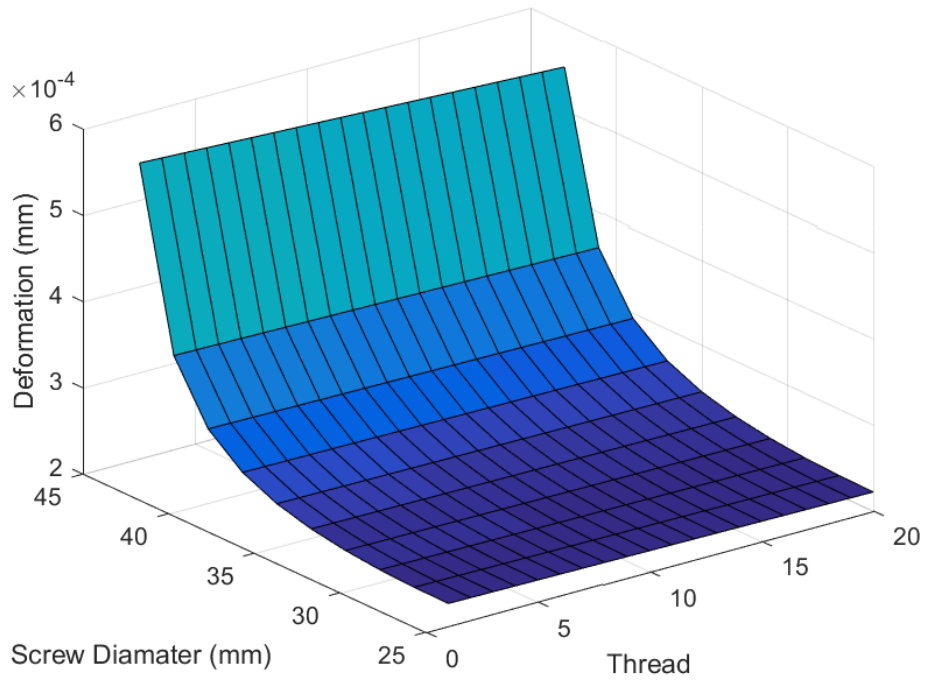
#### 3.5.2.3.1 Parameter Values

Variable Parameters	Fixed Parameters
Screw Diameter: 25 - 45 mm	Young's Modulus: $2.1 \times 10^{11}$ Pa
Nut Outer Diameter: 75 mm	Poisson's Ratio: 0.3
Nut Inner Diameter: 41.6 – 71.6 mm	Effective Young's Modulus: $4.333 \times 10^{-12}$ Pa
Roller Diameter: 8.3 – 14.3 mm	Dimensionless Quantity: 0.98
Pitch: 2 mm	Contact Angle: $45^\circ$
Number of Start: 5	
Number of Rollers: 10	
Helix Angle: $6.056^\circ$	

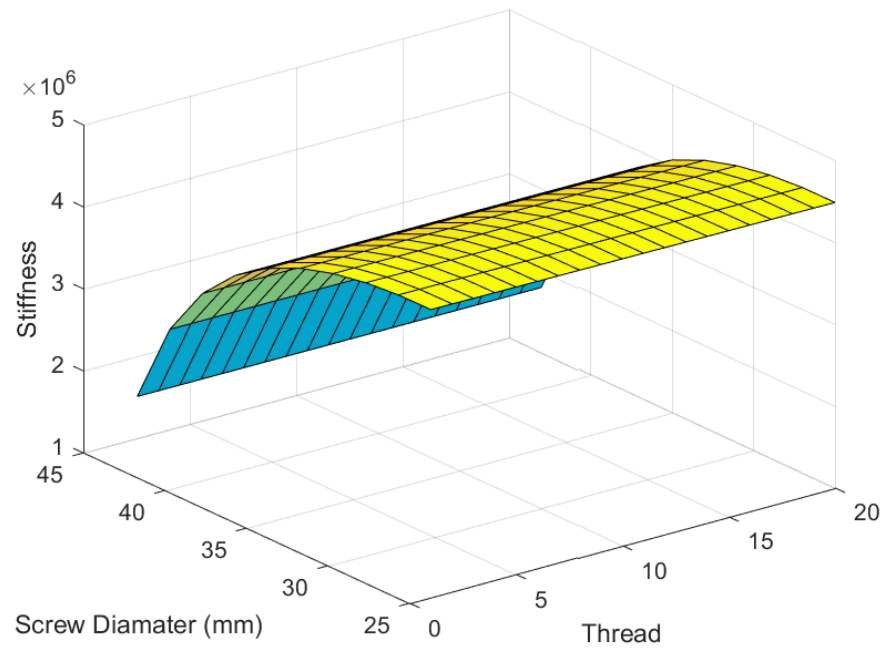
**Table 3.4 Screw Diameter ( $d_s$ ) Change Case Parameter Values**

#### 3.5.2.3.2 Resulting maps

As shown in Figure 3.6, deformation increases as screw diameter increases because the screw diameter increase causes the nut inner diameter and roller diameter to increase. This diameter change relates to decrease of the nut thickness. As proved from below two cases, decrease of nut thickness has a huge influence on the total deformation as shown in Figure 3.6 (a). And total stiffness reflects the total deformation change because of these related factors. Similar to the nut outer diameter and nut inner diameter change cases, screw diameter change case has specific diameter range where the total deformation and total stiffness changes sharply. That point is where the screw diameter is 33 mm in this analysis. And this may change when range is different. This indicates that there is the point, which makes a large change of total deformation and total stiffness. This specific point can be found and recognized by design process motivated by maps like below.



(a) Total Deformation



(b) Total Stiffness

**Figure 3.6 Total Deformation and Stiffness ( $d_s$  Change)**

### 3.5.2.4 Effective Roller Diameter Change

#### 3.5.2.4.1 Parameter Values

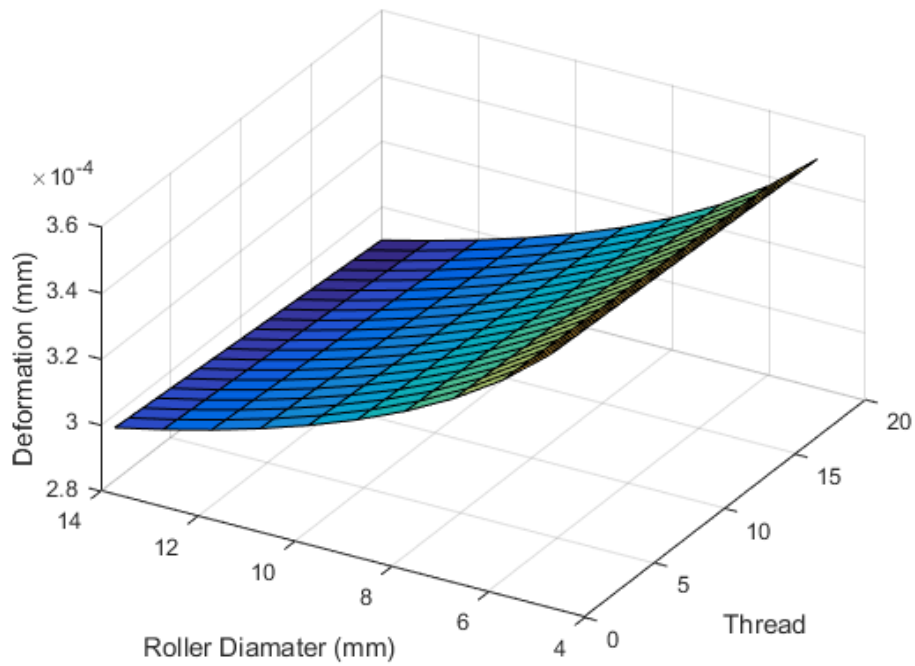
Variable Parameters	Fixed Parameters
Roller Diameter: 5 – 14 mm	Young's Modulus: $2.1 \times 10^{11}$ Pa
Screw Diameter: 15 – 42 mm	Poisson's Ratio: 0.3
Nut Inner Diameter: 70 mm	Effective Young's Modulus: $4.333 \times 10^{-12}$ Pa
Nut Outer Diameter: 75 mm	Dimensionless Quantity: 0.98
Pitch: 2 mm	Contact Angle: $45^\circ$
Number of Start: 5	
Number of Rollers: 10	
Helix Angle: $6.056^\circ$	

**Table 3.5 Roller Diameter ( $d_r$ ) Change Case Parameter Values**

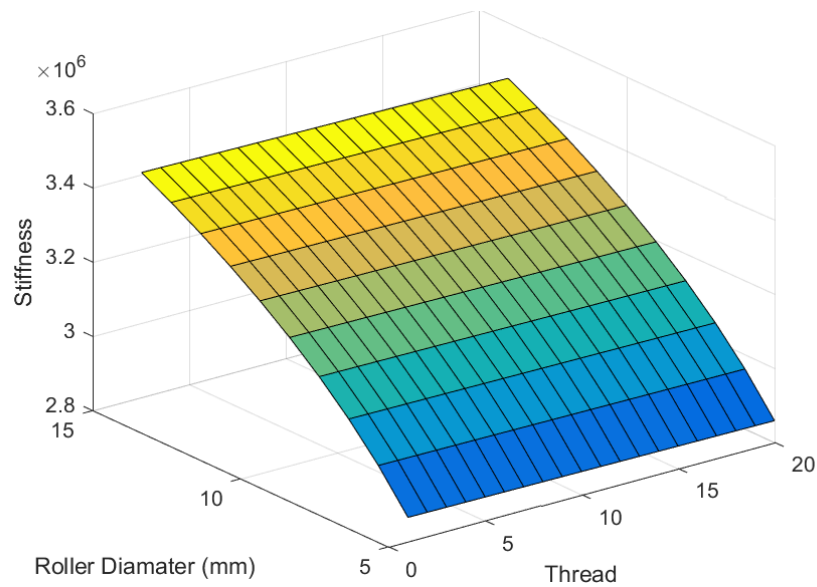
#### 3.5.2.4.2 Resulting maps

Figure 3.7 shows total deformation and total stiffness of roller diameter change. In order to find out the relationship between roller diameter and total deformation and stiffness, nut inner diameter and nut outer diameter are fixed simultaneously. In other words, nut thickness is fixed and this helps to recognize the effect of roller diameter change to the PRS total deformation and total stiffness. As mentioned, PRS inner geometry factors such as screw diameter and roller diameter are coupled to each other. Thus, screw diameter changes as roller diameter changes to fit inner geometry of PRS. With a larger roller diameter, the screw diameter becomes smaller. Roller and screw diameter changes cause a sharp change of total deformation and total stiffness. However, changes of total deformation and total stiffness are smaller than previous cases such as nut outer diameter, nut inner diameter, and screw diameter change cases. It is because the range of the roller diameter change is more restricted than other larger diameter elements. The total stiffness difference on each thread is not large because the axial force on each thread is different as presented in Chapter 4. A load distribution analysis, interesting feature is shown in Figure 3.7 (a) the total deformation plot.





(a) Total Deformation



(b) Total Stiffness

**Figure 3.7 Total Deformation and Stiffness ( $d_r$  Change)**

The small roller diameter can cause large amount of deformation. As shown in Figure 3.7(a), total deformation on each thread is much smoother when roller diameter is larger. From this case, roller

diameter is also a dominant factor of PRS design in the perspective of total deformation and total stiffness.

### 3.5.2.5 Number of Rollers Change

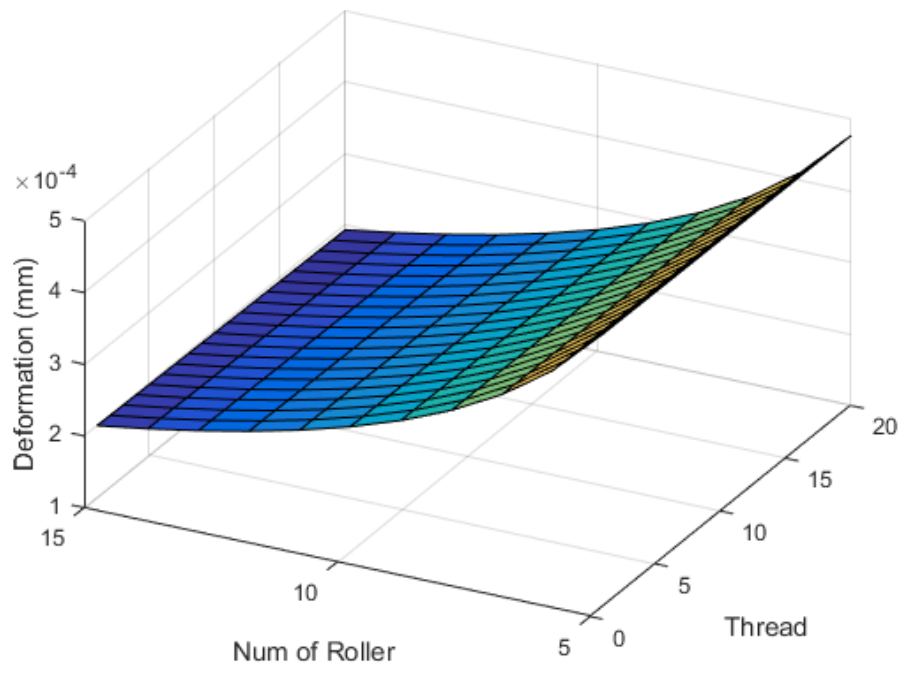
#### 3.5.2.5.1 Parameter Values

Variable Parameters	Fixed Parameters
Number of Rollers: 5 - 15	Young's Modulus: $2.1 \times 10^{11}$ Pa
Roller Diameter: 12.5 mm	Poisson's Ratio: 0.3
Screw Diameter: 37.5 mm	Effective Young's Modulus: $4.333 \times 10^{-12}$ Pa
Nut Inner Diameter: 62.5 mm	Dimensionless Quantity: 0.98
Nut Outer Diameter: 75 mm	Contact Angle: $45^\circ$
Pitch: 2 mm	
Number of Start: 5	
Helix Angle: $6.056^\circ$	

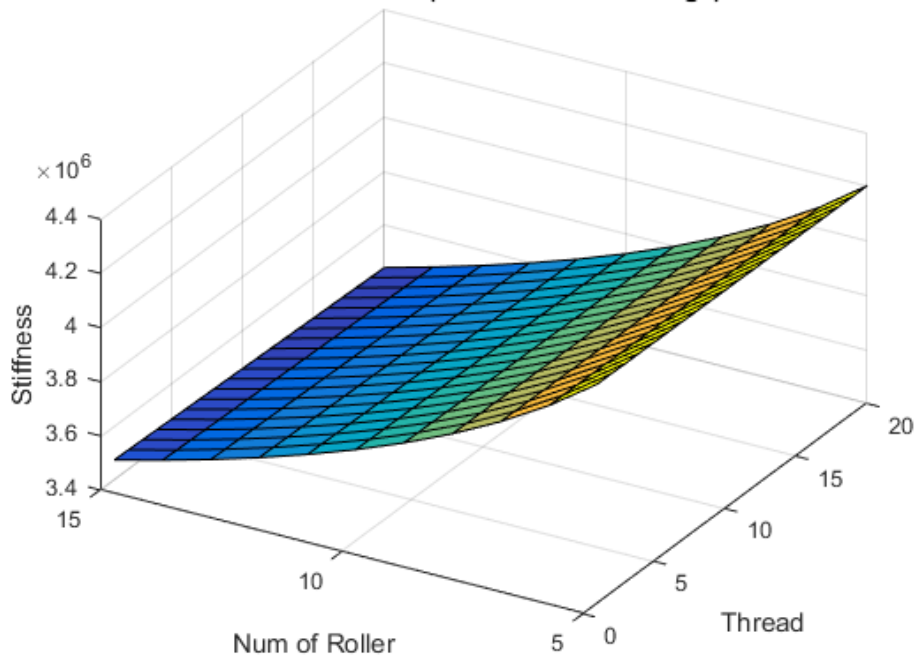
**Table 3.6 Number of Rollers ( $N_r$ ) Change Case Parameter Values**

#### 3.5.2.5.2 Resulting maps

Figure 3.8 shows the total deformation and total stiffness due to the number of rollers. The number of rollers change case differs from other previous cases such as diameters changes. Shape of plots for total deformation and total stiffness are similar because number of rollers is directly related to the load distribution, which is the force applied to each thread and not related to total deformation. In addition, distributed load on each thread is applied to each deformation factor in order to calculate total deformation. Then, total stiffness is achieved by the distributed load and total deformation. Thus, it gives similar plots between total deformation and total stiffness. This will be discussed in Chapter 4. For load distribution analysis, the number of rollers doesn't have an effect in load distribution. And it also doesn't have a distinct effect in the total deformation and total stiffness.



(a) Total Deformation



(b) Total Stiffness

**Figure 3.8 Total Deformation and Stiffness ( $N_r$  Change)**

### 3.5.2.6 Pitch Change

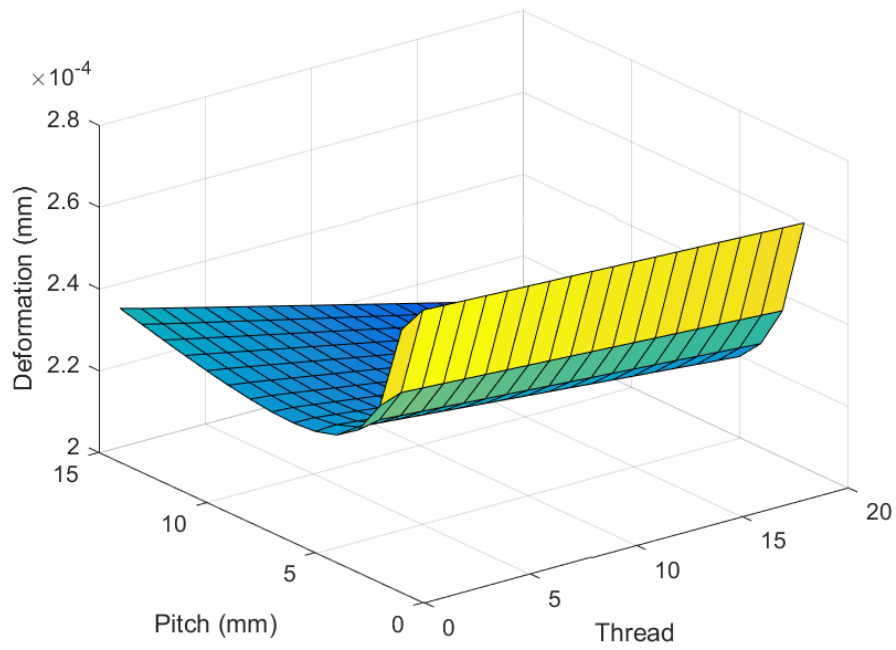
#### 3.5.2.6.1 Parameter Values

Variable Parameters	Fixed Parameters
Pitch: 2 - 15 mm	Young's Modulus: $2.1 \times 10^{11}$ Pa
Number of Rollers: 10	Poisson's Ratio: 0.3
Roller Diameter: 12.5 mm	Effective Young's Modulus: $4.333 \times 10^{-12}$ Pa
Screw Diameter: 37.5 mm	Dimensionless Quantity: 0.98
Nut Inner Diameter: 62.5 mm	Contact Angle: $45^\circ$
Nut Outer Diameter: 75 mm	
Number of Start: 5	
Helix Angle: $6.056^\circ$	

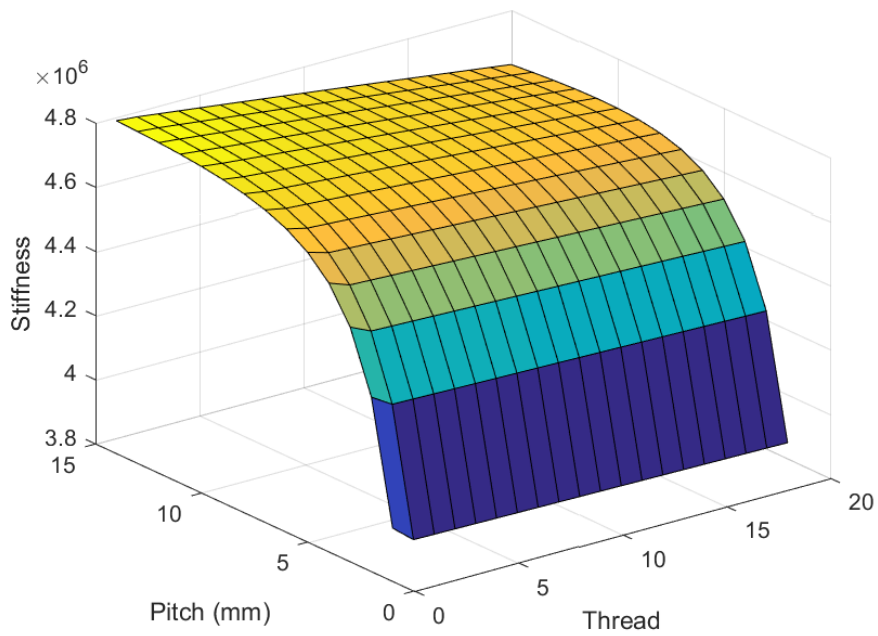
**Table 3.7 Pitch (*p*) Change Case Parameter Values**

#### 3.5.2.6.2 Resulting maps

Figure 3.9 shows the results of total deformation and total stiffness when pitch changes. The pitch change case gives the most sudden change of plots in terms of total deformation and total stiffness. Figure 3.9 (a) shows that a small pitch change can cause a large amount of total deformation change and the total deformation reduces as pitch becomes larger. According to the relationship between total deformation and total stiffness, total stiffness increases as the pitch becomes larger. If total stiffness is only considered in the pitch change case, larger pitch is a proper option in PRS design. However, pitch increase causes severe slope in load distribution as presented in Chapter 4. Load Distribution Analysis. Overall, the pitch is a dominant and sensitive parameter of the PRS and needs to be dealt carefully.



(a) Total Deformation



(b) Total Stiffness

**Figure 3.9 Total Deformation and Stiffness ( $p$  Change)**

### 3.5.2.7 Number of Start Change

#### 3.5.2.7.1 Parameter Values

Variable Parameters	Fixed Parameters
Number of Start: 1 - 15	Young's Modulus: $2.1 \times 10^{11}$ Pa
Roller Diameter: 12.5 mm	Poisson's Ratio: 0.3
Screw Diameter: 37.5 mm	Effective Young's Modulus: $4.333 \times 10^{-12}$ Pa
Nut Inner Diameter: 62.5 mm	Dimensionless Quantity: 0.98
Nut Outer Diameter: 75 mm	Contact Angle: $45^\circ$
Pitch: 2 mm	
Number of Rollers: 10	
Helix Angle: $6.056^\circ$	

**Table 3.8 Number of Start ( $N_s$ ) Change Case Parameter Values**

#### 3.5.2.7.2 Resulting maps

Figure 3.10 presents total deformation and total stiffness when number of thread starts changes. Similar to the pitch change case, total deformation decreases sharply as the number of starts increases. It is applied to total stiffness. However, the number of starts has a similar effect on the load distribution due to pitch change. When the number of starts increases, the load distribution change is sharp. In other words, there is more load on the front few threads as shown in Chapter 4. (Load Distribution Analysis). Because both thread deformation and Hertzian deformation are calculated based on the load distribution, the number of starts also has the effect on total stiffness. Recall, lead is the product of pitch and number of starts. This is the reason why similar change is shown compared to pitch change even though the number of start changes. Even though the total deformation value is a little bit different, the total difference is not large when it is compared to the pitch change case. This can summarized that pitch and number of starts have similar effects on the total deformation and total stiffness, including load distribution. Furthermore, pitch and the number of start are both factor of the lead in the deformation

formulas and results can be interpreted that lead is a dominant parameter in the perspective of total deformation and total stiffness.

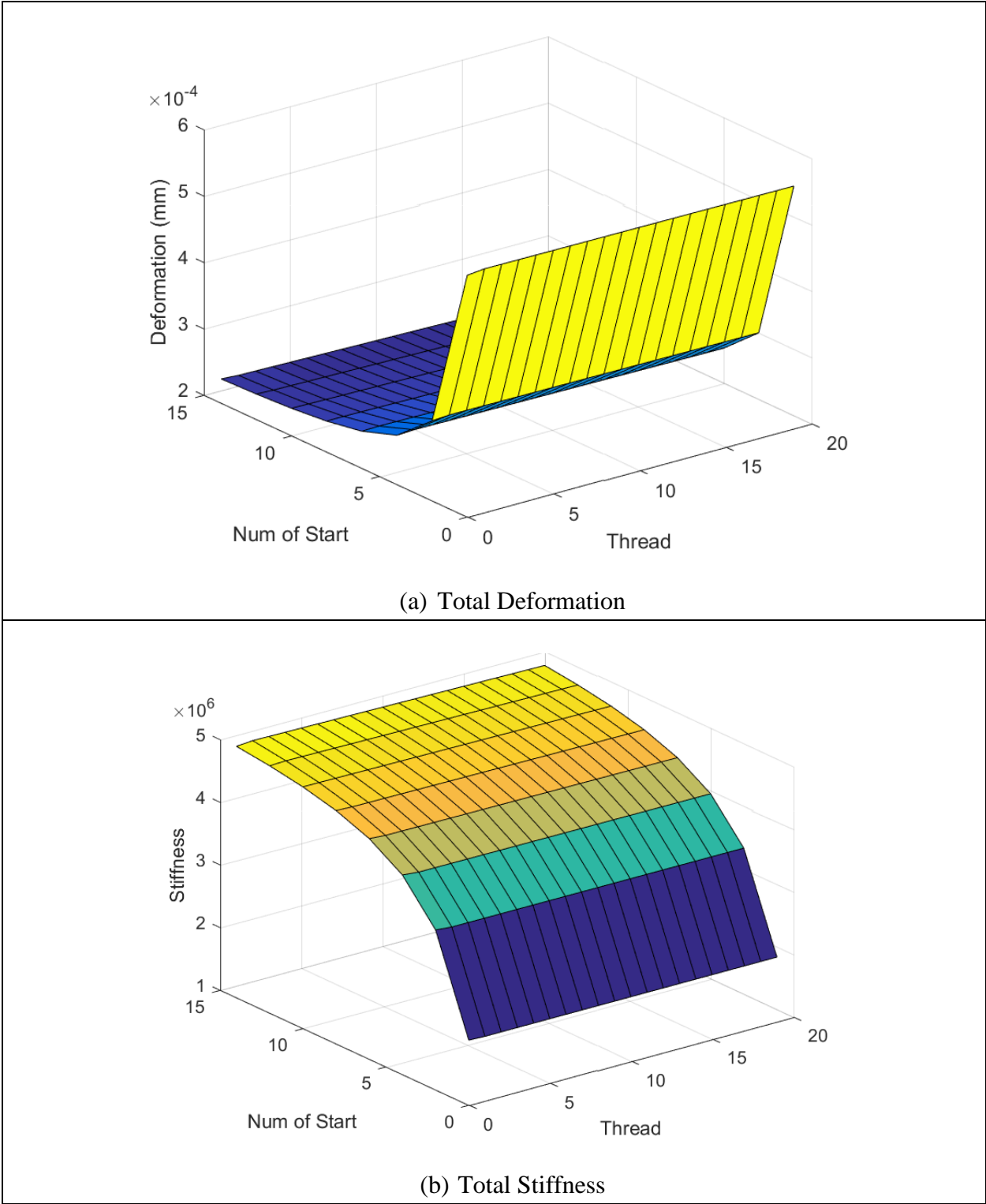


Figure 3.10 Total Deformation and Stiffness ( $N_s$  Change)

### 3.5.2.8 Helix Angle Change

#### 3.5.2.8.1 Parameter Values

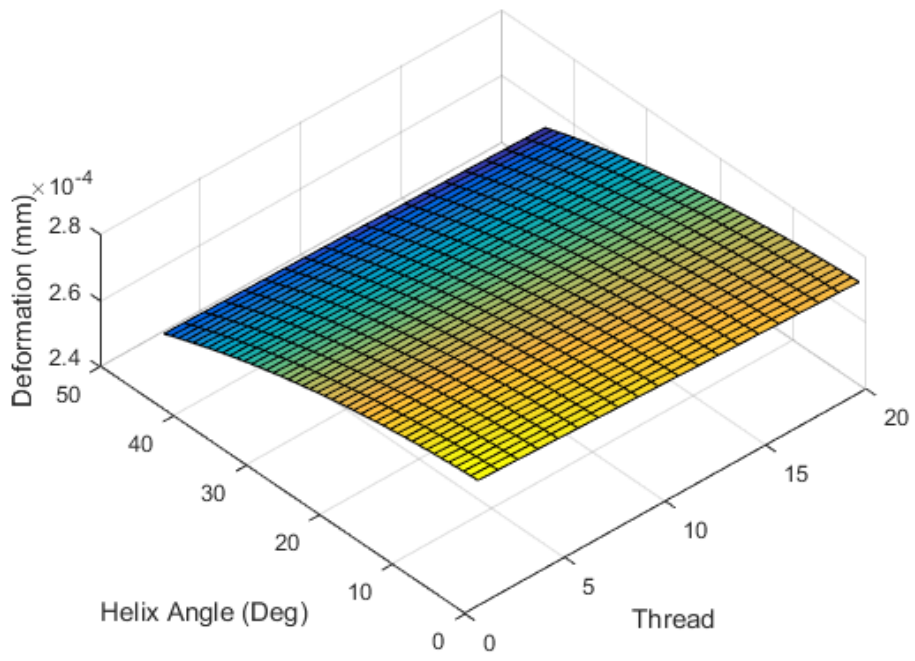
Variable Parameters	Fixed Parameters
Helix Angle: 1° - 45°	Young's Modulus: $2.1 \times 10^{11}$ Pa
Roller Diameter: 12.5 mm	Poisson's Ratio: 0.3
Screw Diameter: 37.5 mm	Effective Young's Modulus: $4.333 \times 10^{-12}$ Pa
Nut Inner Diameter: 62.5 mm	Dimensionless Quantity: 0.98
Nut Outer Diameter: 75 mm	Contact Angle: 45 °
Pitch: 2 mm	
Number of Start: 5	
Number of Rollers: 10	

**Table 3.9 Helix Angle ( $\beta_0$ ) Change Case Parameter Values**

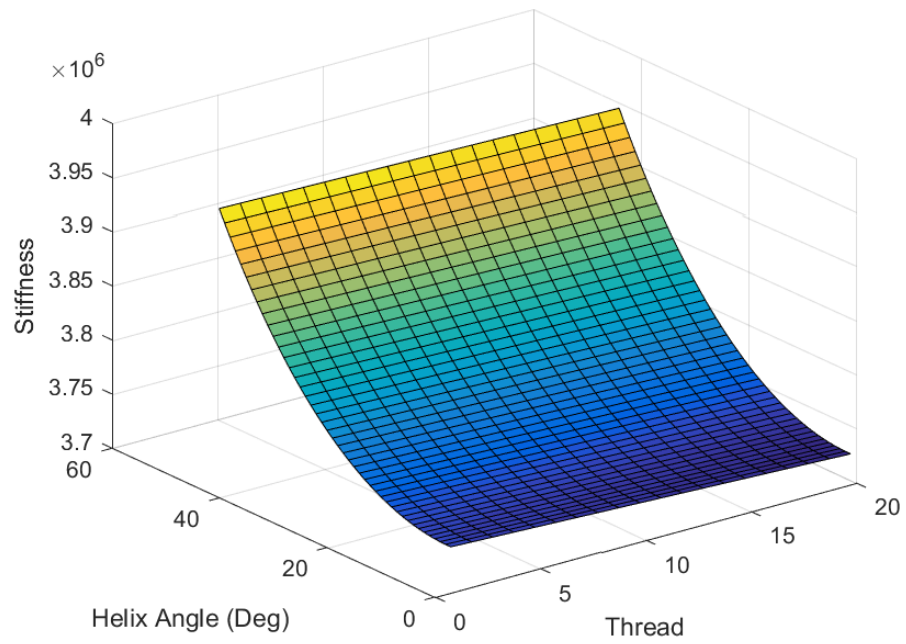
#### 3.5.2.8.2 Resulting maps

Figure 3.11 presents total deformation and total stiffness when the helix angle changes. Total deformation and total stiffness plots show curves, however, that the difference between maximum value and minimum value is not large. The load distribution also has a similar result in the case of helix angle change. This will be discussed more in the load distribution analysis. The biggest difference between maximum value and minimum value is  $1.2153 \times 10^{-5}$  mm in terms of the total deformation. This indicates that the helix angle can't be considered a dominant parameter for total deformation including load distribution.





(a) Total Deformation



(b) Total Stiffness

**Figure 3.11 Total Deformation and Stiffness ( $\beta_0$  Change)**

### 3.6 Chapter Conclusion

This chapter has investigated the effect of each parameter to the total deformation and total stiffness of the planetary roller screw (PRS) and classified the dominant parameters and supporting parameters. The analysis applies to both the total deformation and total stiffness, which are inverses of each other. Parameters are nut outer diameter, nut inner diameter, screw diameter, roller diameter, number of rollers, pitch, number of start, and helix angle. The nut outer diameter and nut inner diameter show a great influence to the total deformation and total stiffness. Total deformation decreases as nut outer diameter increases and nut inner diameter decreases when other diameter is fixed. Results from nut outer diameter and nut inner diameter change cases indicate that nut thickness is interesting factor in terms of total deformation and total stiffness when we design the planetary roller screw. Screw diameter and roller diameter tightly interact each other. If screw diameter increases, roller diameter decreases. On the contrary, roller diameter increases if screw diameter decreases. Both conditions are satisfied under fixed nut outer diameter and the nut inner diameter condition. Screw diameter and roller diameter change cases show that total deformation and total stiffness change rapidly in specific location. In current development, sudden change is shown near 35 mm of screw diameter and near 10 mm of roller screw diameter point. This result suggests that the designer needs to consider proper screw diameter and roller diameter, which minimize total deformation and protect sudden change. The number of rollers has minor effect on the total deformation and total stiffness. The 3D total deformation and total stiffness maps show curves following the number of rollers change, however, each deformation and stiffness value is the value on the each thread and contact point. Then, total deformation and total stiffness on each thread is not much different regardless of the number of rollers. Helix angle change is also a minor parameter relative to the total deformation and total stiffness. When the result is compared to other parameters, total deformation and total stiffness difference is not large enough to be considered as a useful parameter. Pitch and number of starts is considered a dominant parameter to total deformation and total stiffness because those parameter changes cause irregular increase or decrease of values such as total deformation and total stiffness. Both parameters have similar shape

and difference of values from each plot is not large because pitch and number of starts are factor of the lead. This indicates that lead is a distinct factor in the perspective of total deformation and total stiffness. Increase of pitch and number of starts helps to reduce total deformation and increase total stiffness on each thread, however, those parameters have opposite effects in terms of load distribution. Because of this, pitch and number of starts will be further discussed and investigated in other chapters later.

The work here is the first step to classify dominant parameters. It is necessary to classify these dominant parameters for further investigation and analysis such as load distribution, load capacity, and force density. These are other important elements to understand and decide which parameters has significant effect on planetary roller screw design. Six parameters are classified as dominant parameter and two other parameters are separated as supporting parameter in this analysis. This parameter classification is expected to be more developed after other three investigation.

Overall, effect of each parameter on load capacity can be arranged as:

Parameter	Effect
Nut Outer Diameter $D_n$	It affects the thickness of the nut and inner space of the PRS. It makes a non-linear decrease as it increases in terms of the total thread deformation. And it has the opposite effect in terms of the total thread stiffness.
Nut Inner Diameter $d_n$	It affects the inner space of the PRS. It makes a non-linear curve as it changes. Total thread deformation increases when it increases because of nut thickness decrease.
Screw Diameter $d_s$	It affects the roller diameter and nut inner diameter under the condition of fixed nut outer diameter. It makes a non-linear total thread deformation and stiffness curve. When it increases, total deformation increases. And total thread stiffness shows the opposite result compared to the total thread deformation. These results are mainly caused by a nut thickness decrease.

**Table 3.10 Parameter Effect on PRS for Total Stiffness on Thread**

Roller Diameter $d_r$	It affects the inner space of the PRS and provides a non-linear curve in terms of the total thread deformation and total thread stiffness. When it increases, total thread deformation decreases under the condition of fixed nut thickness. Total thread stiffness shows the opposite result compared to total thread deformation when roller diameter changes. Because change of the roller diameter causes the screw diameter decrease, total thread deformation and total thread stiffness value change is not higher than other parameter cases.
Number of Rollers $N_r$	It gives a non-linear curve as it changes. However, each thread of the roller has similar deformation because the number of rollers are different for each line in map. Therefore, the number of rollers doesn't have much effect.
Pitch $p$	It affects the lead of the PRS movement. And it gives a non-linear curve. The curve is slope steep when its value is low. It shows that high pitch value causes low thread deformation and high thread stiffness.
Number of Starts $N_s$	It affects the lead of the PRS movement. It gives a similar non-linear curve compared to the pitch case. As it increases, it gives low thread deformation and high thread stiffness.
Helix Angle $\beta_0$	It has less effect on total thread deformation and total thread stiffness.

Table 3.10 Continued

And each parameter can be classified as:

Primary Parameters	Support Parameters	Fixed Parameters
$D_n$ : Nut Outer Diameter	$N_r$ : Number of Rollers	$\alpha_0$ : Contact Angle
$d_n$ : Nut Inner Diameter	$\beta_0$ : Helix angle	$L$ : Length
$d_s$ : Screw Diameter		
$d_r$ : Roller Diameter		
$p$ : Pitch		
$N_s$ : Number of starts		

**Table 3.11 Parameter Classification for Total Stiffness on Thread**

## CHAPTER 4. LOAD DISTRIBUTION ANALYSIS

This chapter investigates load distribution characteristics of the PRS, which is one of the most necessary condition for the design process. When the load is applied to the PRS, each thread of each component has its own amount of divided load. The feature of the load on each thread is that first several threads are allotted more load and load on the following threads decreases. This tendency of decreasing load on the thread is studied in prior research and proven in the previous research. However, most of the previous work focuses on the distribution of the load on the threads for a set of parameter values and compares each result due to load changes. In addition, some work done previously also compared theoretical and experimental load distributions. The result from this comparison between theoretical load changes and experimental load changes gives the fact that there are differences between theoretical world and real world. However, this result also unvalued large range of parameter changes. In order to calculate the load distribution, many individual or combined parameters must be considered. Because each parameter has a different effect on the PRS load distribution, figuring out which parameters are mainly effective and less effective is necessary. Then, separating parameters based on their effect is helpful to get useful maps and set up the design process. In order to calculate load distribution on the PRS, analysis of Ma [13] and Yang [14] is considered. Both of them regard the roller thread as a number of effective intermediate balls in order to analyze the load distribution on the threads. Based on this assumption, the load distribution is calculated and examined. Then, 3D maps are printed to build the design process after the preliminary choice of governing parameters.

### 4.1 Load Distribution

As mentioned above, there are loads on each thread and each load on each thread is different. And the difference among threads is changed by design parameter selective. There are 13 parameters in the load distribution formula. Nine parameters are variables. However, the

effective diameter of the screw, roller and the nut inner diameter are not independent. This relationship will be presented by formulas, which are cited from Strandgren' patent [1]. Because of this relationship, the effective screw diameter ( $d_s$ ) is excluded in the parameter adjustment process. Three of the 13 parameters are fixed because of chosen material's inherent characteristics. Then the load distribution formula can be obtained from Yang's [12] as:

$$F_{load_i} = F_{load_{i-1}} - \frac{Nr l}{4(H_n + H_s)} \left( \frac{1}{Y_n A_n} + \frac{1}{Y_s A_s} \right) \sum_{k=1}^n F_{axial_j} \sin(\alpha_0) \cos(\beta_0) \quad (4.1)$$

where,

$F_{load}$  = Load on each thread in the axial direction

$H_n$  = Elastic modulus of elliptical contact points in the nut side

$H_s$  = Elastic modulus of elliptical contact points in the screw side

$N_r$  = Number of Roller

$l$  = Lead of the screw and the nut

$Y_n$  = Young's modulus of the nut

$Y_s$  = Young's modulus of the screw

$A_n$  = Effective cross section area of the nut

$A_s$  = Effective cross section area of the screw

$\alpha_0$  = Contact angle

$\beta_0$  = Helix angle

Recall that  $H_n$  and  $H_s$  are functions of the contact bodies' curvature formula, which is mentioned in Chapter 3. Deformation and Stiffness Analysis. Those formulas are expressed as:

$$H_n = \delta^* \left( \frac{3}{2Y_n^* \Sigma \rho_n} \right)^{\frac{2}{3}} \left( \frac{\Sigma \rho_n}{2} \right) \quad (3.43)$$

and

$$H_s = \delta^* \left( \frac{3}{2Y_s^* \Sigma \rho_s} \right)^{\frac{2}{3}} \left( \frac{\Sigma \rho_s}{2} \right) \quad (3.44)$$

As presented, the dimensionless quantity ( $\delta^*$ ) is one of the key components in order to calculate  $H_n$  and  $H_s$ . In the PRS load distribution, this dimensionless quantity has a range from 0.95 to 0.98. In other words, the effect of this dimensionless quantity is not dominant for the elastic modulus of elliptical contact points. Here, we fix the values as 0.98 for the convenient calculation of the elastic modulus of elliptical contact points. Another important parameter for calculating the elastic modulus of the elliptical contact point is the contact bodies' curvature formula. This formula has several parameters such as effective roller diameter, effective screw diameter, and contact angle. All these parameters will be handled carefully in the next section where the parameter selection process is established. The contact angle is fixed at  $45^\circ$  and where the diameters are determinant factors. This indicates that the elastic modulus of elliptical contact points is the result governed by diameter change. Then, the elastic modulus of elliptical contact points in the nut side and the screw side are diameter change dependent. Because of this, the elastic modulus of the elliptical contact points are separated as fixed parameters. Note that effective Young's modulus is classified as fixed parameter. The effective Young's modulus is a combination formula of Young's modulus and Poison's ratio. The material of each part of the PRS such as the nut, screw and roller is considered as steel. Thus, the effective Young's Modulus depends on fixed values.

## 4.2 Load Distribution Analysis

### 4.2.1 Parameters

Variable Parameters	Fixed Parameters
$D_n$ : Nut Outer Diameter	$H_n$ : Elastic Modulus of Elliptical Contact Points in the Nut Side
$d_n$ : Effective Nut Inner Diameter	
$d_s$ : Effective Screw Shaft Diameter	$H_s$ : Elastic Modulus of Elliptical Contact Points in the Screw Side
$d_r$ : Effective Roller Diameter	
$p$ : Pitch	$Y_x$ : Young's Modulus
$N_s$ : Number of Start	$\nu$ : Poisson's Ratio
$N_r$ : Number of Rollers	$Y_x^*$ : Effective Young's Modulus
$\beta_0$ : Helix Angle	$\delta^*$ : Dimensionless Quantity
	$\alpha_0$ : Contact Angle

**Table 4.1 Parameters**

There are 15 interrelated parameters, which are used to calculate the load distribution. Eight of them are variable parameters and those parameters are used to investigate the effect on the load distribution and analyze how they affect the load distribution. Some of those parameters such as the number of rollers, pitch, number of starts and helix angle are discussed in Chapter 3. Deformation and Stiffness. In this chapter, those parameters are analyzed and discussed in more detail by comparing with the total deformation and total stiffness cases. Five parameters such as Young's modulus, Poisson's ratio, effective Young's modulus, dimensionless quantity, and contact angle are fixed and exact values of these parameters will be presented in detail. As mentioned above, elastic modulus of elliptical contact points in the nut side and screw side values are also considered as fixed parameters.

### 4.3 Resulting Maps and Analysis



### 4.3.1 Nut Outer Diameter Change

#### 4.3.1.1 Parameter Values

Variable Parameters	Fixed Parameters
Nut Outer Diameter: 54 – 75 mm	Young's Modulus: $2.1 \times 10^{11}$ Pa
Nut Inner Diameter: 50 mm	Poisson's Ratio: 0.3
Screw Shaft Diameter: 30 mm	Effective Young's Modulus: $4.333 \times 10^{-12}$ Pa
Roller Diameter: 10 mm	Dimensionless Quantity: 0.98
Pitch: 2 mm	Contact Angle: $45^\circ$
Number of Start: 5	
Number of Rollers: 10	
Helix Angle: $6.056^\circ$	

**Table 4.2 Nut Outer Diameter ( $D_n$ ) Change Case Parameter Values**

#### 4.3.1.2 Resulting Map

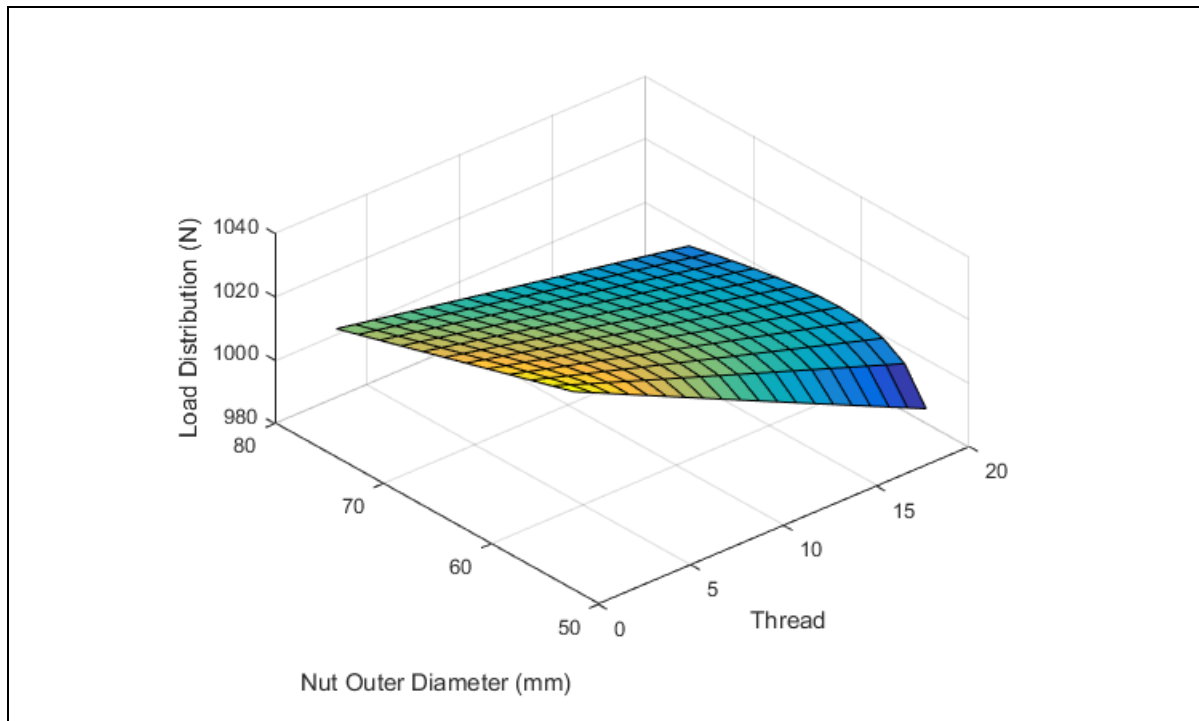


**Figure 4.1 Load Distribution ( $D_n$  Change)**

Nut outer diameter change shows a remarkable effect in the perspective of load distribution. Figure 4.1 presents plot of the load on each thread. As shown, a small nut outer diameter causes a steep

load change. This means that the first few threads bear the larger portion of the load and can harm planetary roller screw operation and decrease life expectancy. As the nut outer diameter increases, the load on each thread becomes more equally distributed even though the difference still exists. From this result, the nut outer diameter is recognized as critical parameter for the load distribution.

4.3.2 Nut Inner Diameter Change

4.3.2.1 Parameter Values

Variable Parameters	Fixed Parameters
Nut Inner Diameter: 50 – 70 mm	Young’s Modulus: $2.1 \times 10^{11}$ Pa
Nut Outer Diameter: 75 mm	Poisson’s Ratio: 0.3
Screw Shaft Diameter: 30 - 42 mm	Effective Young’s Modulus: $4.333 \times 10^{-12}$ Pa
Roller Diameter: 10 - 14 mm	Dimensionless Quantity: 0.98
Pitch: 2 mm	Contact Angle: $45^\circ$
Number of Start: 5	
Number of Rollers: 10	
Helix Angle: $6.056^\circ$	

Table 4.3 Nut Inner Diameter ( $d_n$ ) Change Case Parameter Values

4.3.2.2 Resulting Map

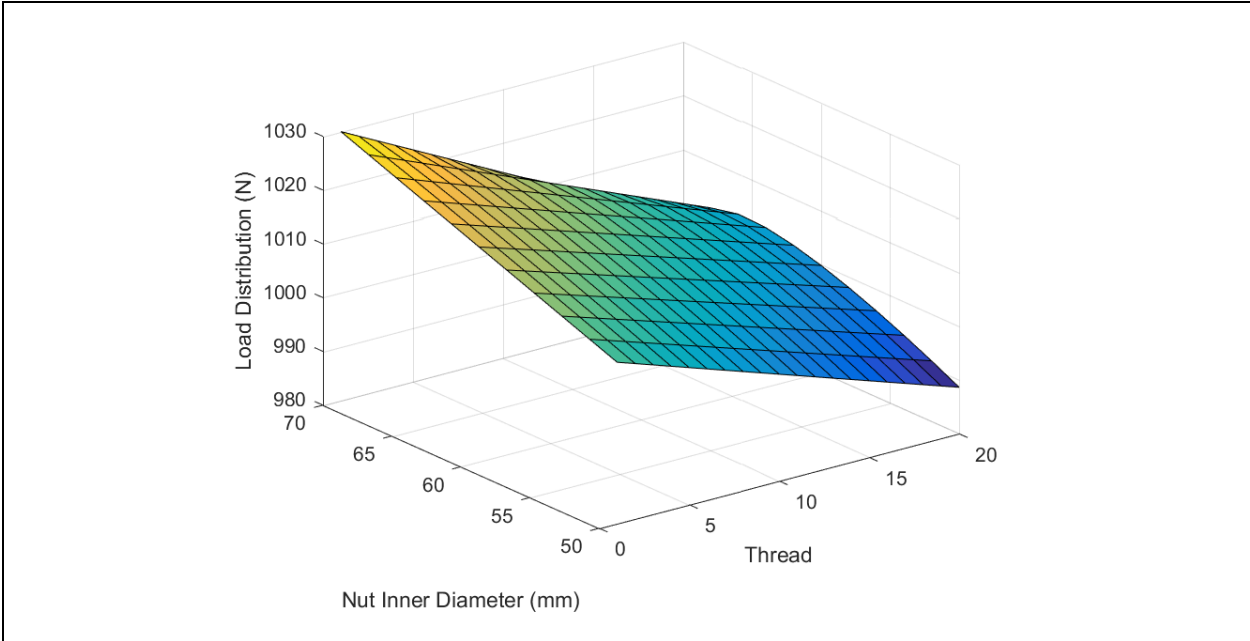


Figure 4.2 Load Distribution ( $d_n$  Change)

Figure 4.2 shows the resulting plot of the load distribution on each thread when the nut inner diameter changes. Load distribution doesn't change much until the nut inner diameter reaches about 60 mm. In this case, the nut inner diameter corresponds to the screw diameter and the roller diameter. Then, the screw diameter and roller diameter increase as the nut inner diameter increases. This inner dimension increase keeps the variable change of load distribution down. In other words, screw diameter and roller diameter expansion compensates for the load distribution originated due to the nut thickness decrease. However, the load distribution curve experiences sudden value change when nut inner diameter passes over the critical point, which starts to make a large difference. This result indicates that there is a critical nut inner diameter point that the screw diameter and roller expansion can't compensate for the slope change and makes the load distribution curve steep. Then, this shows that the nut inner diameter is a dominant parameter to describe the load distribution.

### 4.3.3 Screw Diameter Change

#### 4.3.3.1 Parameter Values

Variable Parameters	Fixed Parameters
Screw Shaft Diameter: 25 - 45 mm	Young's Modulus: $2.1 \times 10^{11}$ Pa
Nut Outer Diameter: 75 mm	Poisson's Ratio: 0.3
Nut Inner Diameter: 41.6 – 71.6 mm	Effective Young's Modulus: $4.333 \times 10^{-12}$ Pa
Roller Diameter: 8.3 – 14.3 mm	Dimensionless Quantity: 0.98
Pitch: 2 mm	Contact Angle: $45^\circ$
Number of Start: 5	
Number of Rollers: 10	
Helix Angle: $6.056^\circ$	

**Table 4.4 Screw Diameter ( $d_s$ ) Change Case Parameter Values**

### 4.3.3.2 Resulting Map

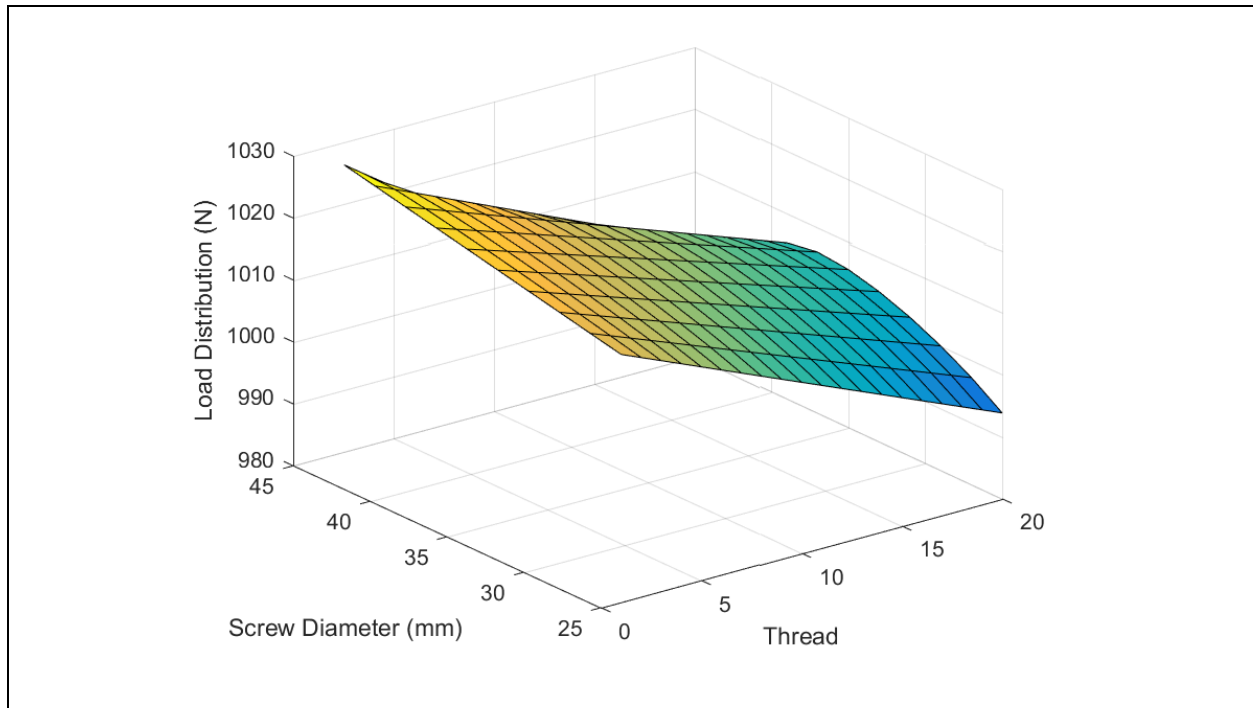


**Figure 4.3 Load Distribution ( $d_s$  Change)**

Figure 4.3 shows load distribution plot when the screw diameter changes. As presented, large screw diameter causes steeper change. As the screw diameter becomes smaller, values of the load distribution on each thread make a smoother curve. At about 43 mm and the nut inner diameter is about 71 mm the map turns down quickly. Each load distribution curve becomes stable as screw diameter increases because the roller diameter increases. In other words, combination of the screw diameter and roller diameter increase makes the load distribution stable. However, stability of the load distribution decreases from the point where screw diameter is about 37 mm. At this point, the nut inner diameter is about 62 mm. Then, nut thickness is small enough to decrease load distribution stability. And of course instability is maximized where the nut thickness becomes near zero. Overall, the screw diameter is an important parameter for the planetary roller screw (PRS) design process because of the relationship with other diameters such as the nut inner diameter and roller diameter.

#### 4.3.4 Roller Diameter Change

##### 4.3.4.1 Parameter Values

Variable Parameters	Fixed Parameters
Roller Diameter: 5 – 14 mm	Young's Modulus: $2.1 \times 10^{11}$ Pa
Screw Shaft Diameter: 15 – 42 mm	Poisson's Ratio: 0.3
Nut Inner Diameter: 70 mm	Effective Young's Modulus: $4.333 \times 10^{-12}$ Pa
Nut Outer Diameter: 75 mm	Dimensionless Quantity: 0.98
Pitch: 2 mm	Contact Angle: $45^\circ$
Number of Start: 5	
Number of Rollers: 10	
Helix Angle: $6.056^\circ$	

**Table 4.5 Roller Diameter ( $d_r$ ) Change Case Parameter Values**

##### 4.3.4.2 Resulting Map

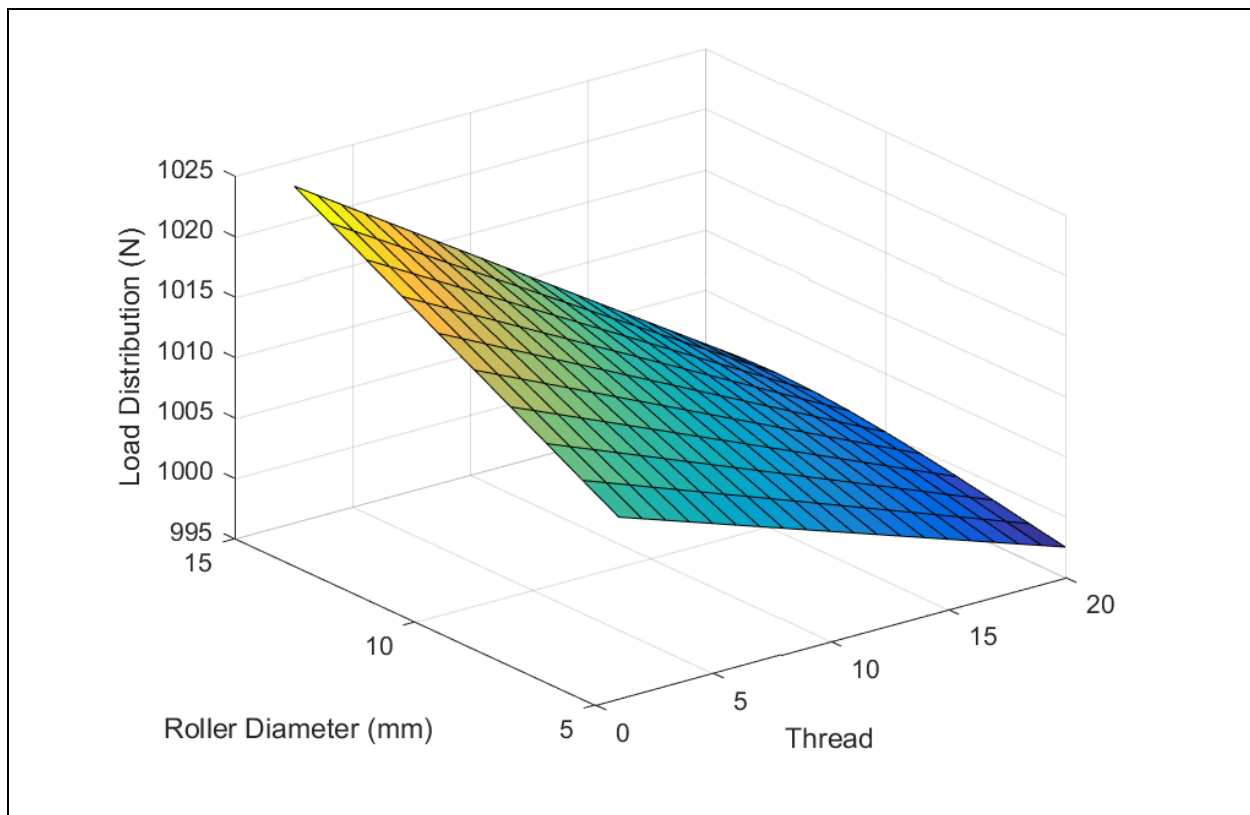


**Figure 4.4 Load Distribution ( $d_r$  Change)**

Figure 4.4 shows the load distribution when the roller diameter changes. In this case, the nut outer diameter and nut inner diameter are fixed to show the effect of the diameter change of roller and screw. As known, roller diameter and screw diameter are relative with each other. It means that the screw diameter decreases when roller diameter increases, or vice versa. The resulting 3D plot presents that the load distribution slope to become unstable as the roller diameter increases and there is the point that the load distribution curve increases much faster. That is at about the 10 mm roller diameter point. Load distribution curve stability decreases smoothly as roller diameter increases until about 10 mm, however, the value change of load distribution on each thread becomes higher after this diameter point. This is because screw diameter decreases as roller diameter increases. In other words, load distribution stability depends very much on roller diameter and screw diameter change. An interesting feature of the roller diameter change is that the result of roller diameter change to load distribution is completely opposite to the result of total deformation and total stiffness. Because the two decision factors give opposite results, the roller diameter change case needs to be carefully managed. This will be discussed more when the factor combination results are presented between total stiffness and load distribution.

#### 4.3.5 Number of Rollers Change

##### 4.3.5.1 Parameter Values

Variable Parameters	Fixed Parameters
Number of Rollers: 5 - 15	Young's Modulus: $2.1 \times 10^{11}$ Pa
Roller Diameter: 12.5 mm	Poisson's Ratio: 0.3
Screw Shaft Diameter: 37.5 mm	Effective Young's Modulus: $4.333 \times 10^{-12}$ Pa
Nut Inner Diameter: 62.5 mm	Dimensionless Quantity: 0.98
Nut Outer Diameter: 75 mm	Contact Angle: $45^\circ$
Pitch: 2 mm	
Number of Start: 5	
Helix Angle: $6.056^\circ$	

**Table 4.6 Number of Rollers ( $N_r$ ) Change Case Parameter Values**

### 4.3.5.2 Resulting Map

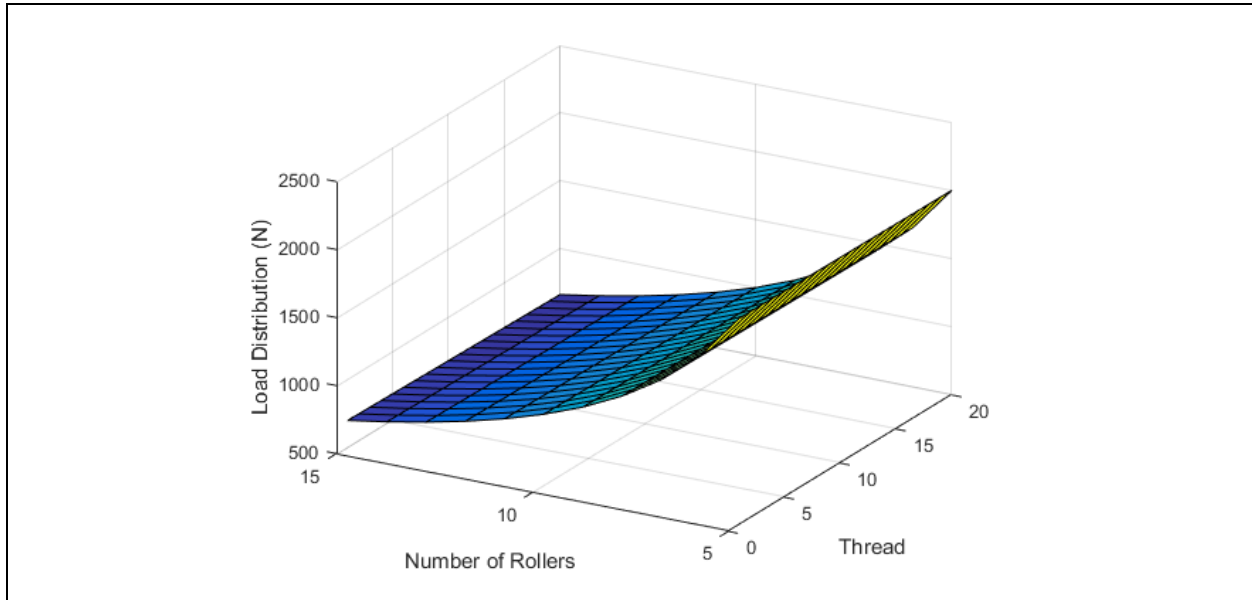


**Figure 4.5 Load Distribution ( $N_r$  Change)**

Figure 4.5 presents the 3D map of load distribution when the number of rollers changes. As shown, the slope of each load distribution curve on the thread doesn't change. The difference of load distribution value on the thread is governed solely by the number of rollers. In other words, load on each roller becomes smaller as number of rollers increases. Then, there is much more load on the roller thread itself when the number of rollers is large. Overall, the number of rollers cannot be considered as a dominant parameter that makes a critical change.

### 4.3.6 Pitch Change

#### 4.3.6.1 Parameter Values

Variable Parameters	Fixed Parameters
Pitch: 2 - 15 mm	Young's Modulus: $2.1 \times 10^{11}$ Pa
Number of Rollers: 10	Poisson's Ratio: 0.3
Roller Diameter: 12.5 mm	Effective Young's Modulus: $4.333 \times 10^{-12}$ Pa
Screw Shaft Diameter: 37.5 mm	Dimensionless Quantity: 0.98
Nut Inner Diameter: 62.5 mm	Contact Angle: $45^\circ$
Nut Outer Diameter: 75 mm	
Number of Start: 5	
Helix Angle: $6.056^\circ$	

**Table 4.7 Pitch ( $p$ ) Change Case Parameter Values**

#### 4.3.6.2 Resulting Map

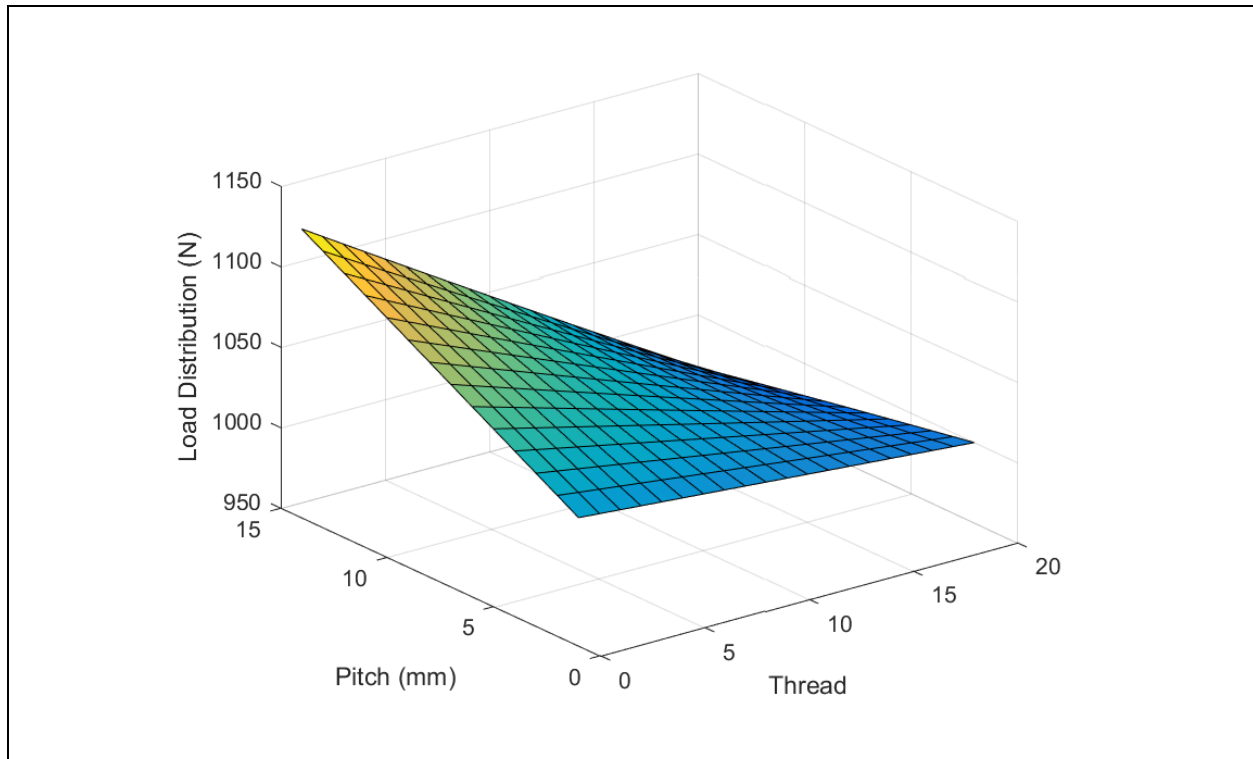


**Figure 4.6 Load Distribution ( $p$  Change)**

Figure 4.6 is the plot of load distribution when the pitch changes. As pitch increases, load distribution value change becomes steeper. There is no big change until about 5 mm pitch. However, the slope of load distribution on the thread decreases rapidly as the pitch increases. The slope of the load distribution is the exact opposite when it is compared to total deformation and total stiffness in roller diameter change case. In other words, total deformation decreases as pitch increases and total stiffness increases as pitch increases near 5 mm pitch length. This means that pitch must be carefully managed to find its proper value for design of the PRS. We note that pitch is a dominant parameter in the PRS design process. Because of these different results between load distribution and total deformation and total stiffness, this will be discussed further in the chapter of factor combinations.



### 4.3.7 Number of Start Change

#### 4.3.7.1 Parameter Values

Variable Parameters	Fixed Parameters
Number of Start: 1 - 15	Young's Modulus: $2.1 \times 10^{11}$ Pa
Roller Diameter: 12.5 mm	Poisson's Ratio: 0.3
Screw Shaft Diameter: 37.5 mm	Effective Young's Modulus: $4.333 \times 10^{-12}$ Pa
Nut Inner Diameter: 62.5 mm	Dimensionless Quantity: 0.98
Nut Outer Diameter: 75 mm	Contact Angle: $45^\circ$
Pitch: 2 mm	
Number of Rollers: 10	
Helix Angle: $6.056^\circ$	

**Table 4.8 Number of Start ( $N_s$ ) Change Case Parameter Values**

#### 4.3.7.2 Resulting Map

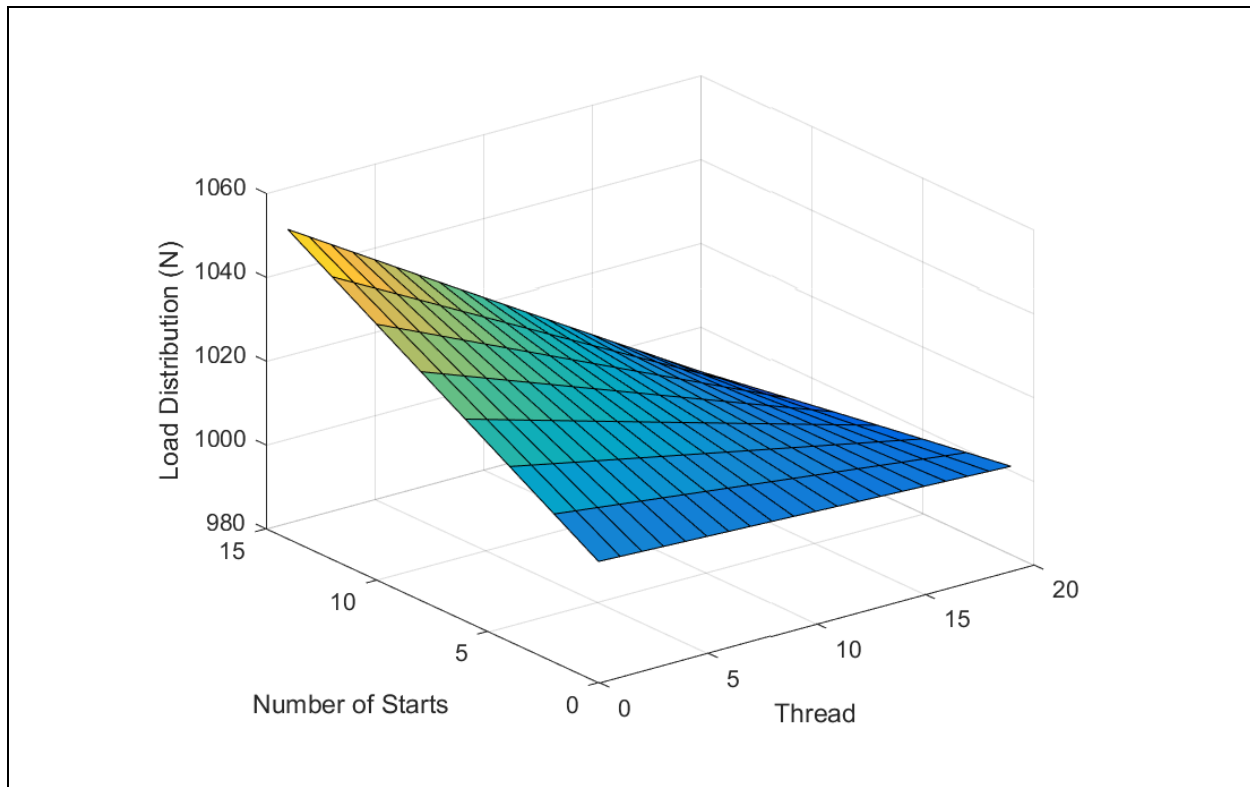


**Figure 4.7 Load Distribution ( $N_s$  Change)**

Figure 4.7 shows the result of load distribution when number of start changes. This shows a similar result as that with the pitch change case. When number of starts is one, the load distribution is almost linear and the load on each thread changes very little. However, the load distribution becomes non-linear as the number of starts increases. The number of starts is a factor in calculating the lead and the lead is linear the movement per one rotation. Then, an increase of number of starts makes more axial movement per rotation. This causes a steeper load distribution slope and it is similar to the effect when pitch increases. Thus, the number of starts is also a dominant parameter to design the PRS properly. Moreover, the number of starts also has the opposite result to that for the total deformation and total stiffness. As a result, the number of starts must be carefully managed to find the proper value when load distribution, total deformation and total stiffness are considered simultaneously.

#### 4.3.8 Helix Angle Change

##### 4.3.8.1 Parameter Values

Variable Parameters	Fixed Parameters
Helix Angle: 1° - 45°	Young's Modulus: 2.1 x 10 <sup>11</sup> Pa
Roller Diameter: 12.5 mm	Poisson's Ratio: 0.3
Screw Shaft Diameter: 37.5 mm	Effective Young's Modulus: 4.333 x 10 <sup>-12</sup> Pa
Nut Inner Diameter: 62.5 mm	Dimensionless Quantity: 0.98
Nut Outer Diameter: 75 mm	Contact Angle: 45 °
Pitch: 2 mm	
Number of Start: 5	
Number of Rollers: 10	

**Table 4.9 Helix Angle ( $\beta_0$ ) Change Case Parameter Values**

#### 4.3.8.2 Resulting Map

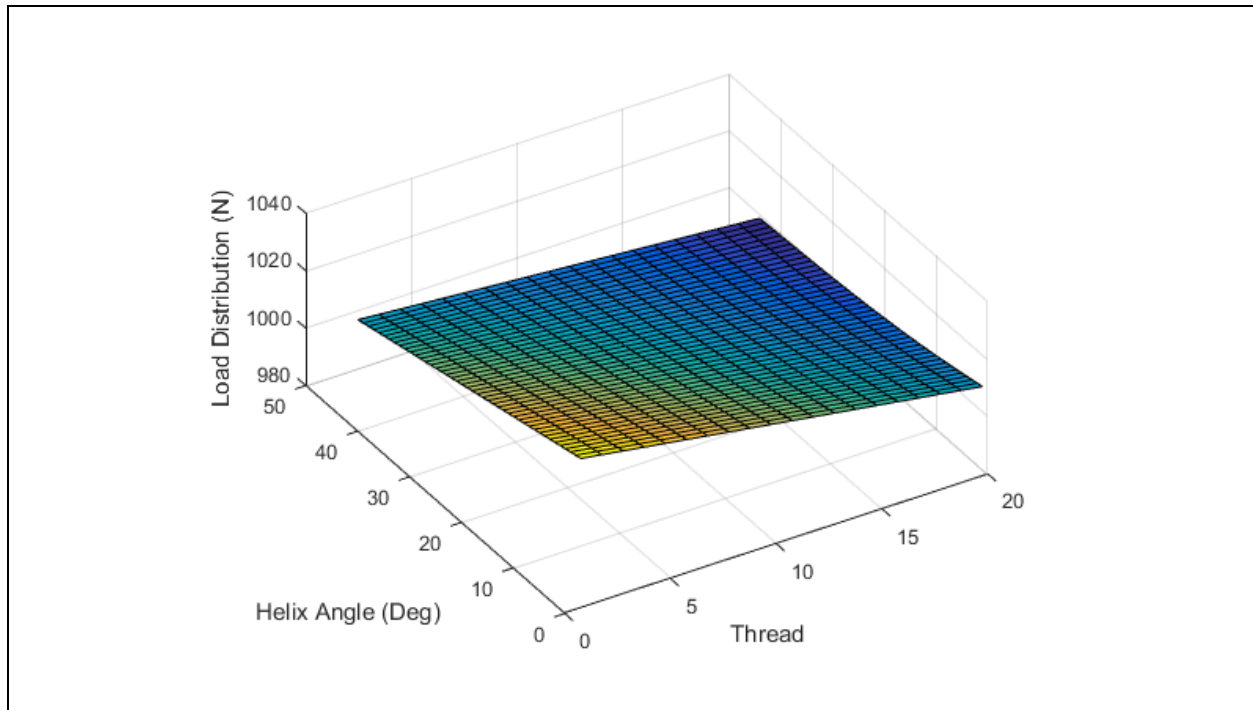


**Figure 4.8 Load Distribution ( $\beta_0$  Change)**

Figure 4.8 is the 3D map of load distribution related to the helix angle change. Helix angle changes from  $0^\circ$  to  $45^\circ$ . Figure 4.8 shows the load distribution curve as while becomes flatter as the helix angle increases. Similar to the total deformation and total stiffness case, there is not much changes through the whole ranges of helix angle. This result indicates that helix angle is less important parameter when it is compared to other parameters such as nut outer diameter, nut inner diameter, screw diameter, roller diameter, and pitch. This result will be reflected later when all categories are combined and interpreted.

#### 4.4 Chapter Conclusion

In this chapter, several key parameters are investigated in terms of the load distribution in the planetary roller screw (PRS). Several parameters have a major effect that changes the curve of load distribution values. Those parameters are regarded as dominant design parameters such as the

nut outer diameter, nut inner diameter, screw diameter, roller diameter, pitch, and number of starts. As shown, the number of rollers and helix angle don't have much impact on the load distribution, total deformation, and total stiffness analysis. Nut outer diameter and nut inner diameter are related to the thickness of the nut. This thickness can be considered as an important factor in the perspective of load distribution. In addition, pitch and number of starts describe the lead. Those two factors can be combined as a basic lead parameter which can be deemed as another dominant parameter for load distribution. Overall, six parameters can be classified as important parameters in this analysis. Some parameters need to be dealt with carefully in the design process such as screw diameter, roller diameter, pitch, and number of starts. Screw diameter and roller diameter are coupled because of limited inner geometry space when nut outer diameter and nut inner diameter are fixed. Then, each diameter change affects the other parameter's diameter change to fit the available inner space. This interaction between screw diameter and roller diameter decides the load distribution curve stability. Pitch and number of starts have together a similar effect on the load distribution. Even though pitch and number of starts are not connected each other when those parameters are applied individually. As mentioned above, however, pitch and number of starts describe the lead of the system. These two parameters have a similar effect on the load distribution because lead is included in the formula of load distribution calculation. Moreover, both the screw diameter and roller diameter condition and pitch and number of starts condition have different results in terms of total deformation and total stiffness. In other words, those two cases cause completely opposite results between load distribution analysis, total deformation, and total stiffness analysis. This means that those parameters are critical to satisfy two different categories. Thus, those parameters need to be carefully managed. This is the reason why combined analysis and envelopes are important. Combined analysis and envelopes will be discussed in later chapter.

Overall, effect of each parameter on load capacity can be arranged as:

Parameter	Effect
Nut Outer Diameter $D_n$	It affects the thickness of the nut and inner space of the PRS. It makes a non-linear change as it changes in terms of load distribution when it is low. When it increases, load distribution line on each nut outer diameter becomes uniform.
Nut Inner Diameter $d_n$	It affects the inner space of the PRS and thickness of the nut. It makes a non-linear curve as it changes. When it has a high value, the load distribution line becomes steeper because of the nut thickness decrease.
Screw Diameter $d_s$	It affects the roller diameter and nut inner diameter under the condition of a fixed nut outer diameter. It makes a non-linear total load distribution curve. As it increases, load distribution line becomes stable. However, the load distribution line becomes steeper after a specific point because of the associated nut thickness decrease.
Roller Diameter $d_r$	It affects the inner space of the PRS and provides a non-linear curve in terms of the load distribution. As it increases, a load distribution line becomes steeper because it decreases the screw diameter under the condition of a fixed nut thickness.
Number of Rollers $N_r$	It gives a non-linear curve as it changes. However, each thread of the roller has a similar load distribution because the number of rollers are different for each line in map. Therefore, the number of rollers doesn't have much effect on the load distribution.
Pitch $p$	It affects the lead of the PRS movement. And it gives a non-linear curve. The curve slope is steeper when its value is high. It shows that a low pitch value provides more flat load distribution as a result.
Number of Starts $N_s$	It affects the lead of the PRS movement. It gives a similar non-linear curve compared to pitch case. As it increases, it gives a steeper load distribution curve.
Helix Angle $\beta_0$	It has a low effect on load distribution.

**Table 4.10 Parameter Effect on PRS for Load Distribution**

And each parameter can be classified as:

Primary Parameters	Support Parameters	Fixed Parameters
$D_n$ : Nut Outer Diameter $d_n$ : Nut Inner Diameter $d_s$ : Screw Diameter $d_r$ : Roller Diameter $p$ : Pitch $N_s$ : Number of starts	$N_r$ : Number of Rollers $\beta_0$ : Helix angle	$\alpha_0$ : Contact Angle $L$ : Length

**Table 4.11 Parameter Classification for Total Stiffness on Thread**

## CHAPTER 5. LOAD CAPACITY ANALYSIS

In this chapter, dynamic load capacity will be dealt and analyzed as a dominant factor for the PRS design process. Dynamic load capacity is a value that is expressed as a force unit such as N or lbf, as the name hints. The general meaning of the dynamic load capacity is the load that allows a life of one million revolutions of the inner race. Because of this definition, dynamic load capacity is a critical factor for PRS design and life calculation. As mentioned in Chapter 1, dynamic load capacity of the PRS is about three times larger compared to conventional ball screw because of PRS' geometry. As presented in Chapter 1, the PRS has more contact points than the ball screw.

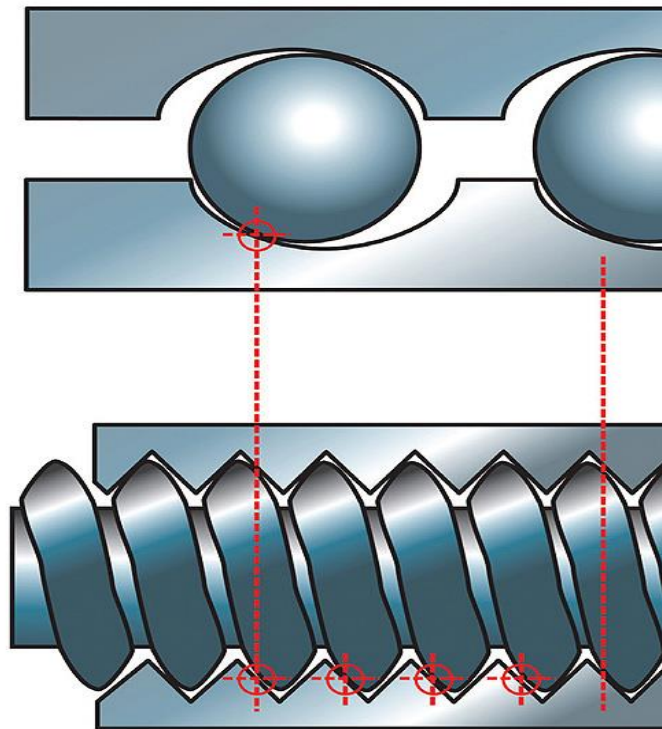


**Figure 5.1 Number of Contact Comparison between Roller Screw and Ball Screw [16]**

Figure 5. 1 shows that difference of the number of contact points between the PRS and the ball screw. This unique shape of PRS and its contact distribution helps to provide higher load carrying capability.

## 5.1 Dynamic Load Capacity

When the load is applied on the PRS system, the nut transfers the load to the screw shaft through the rollers, which are located between the nut and the screw shaft. And this transferred dynamic load capacity can be obtained by Lemor [9] as:

$$C_a = f_c (\cos(\alpha_0))^{0.86} N_c^{\frac{2}{3}} D_c^{1.8} \tan(\alpha_0) (\cos(\beta_0))^{\frac{1}{3}} \quad (6.1)$$

where,

$C_a$  = Dynamic load capacity

$f_c$  = Geometric factor of PRS

$\alpha_0$  = Contact angle between contact bodies ( $45^\circ$ )

$N_c$  = Total number of contact point

$D_c$  = Diameter of rolling element at the contact point

$\beta_0$  = Helix Angle of the Thread

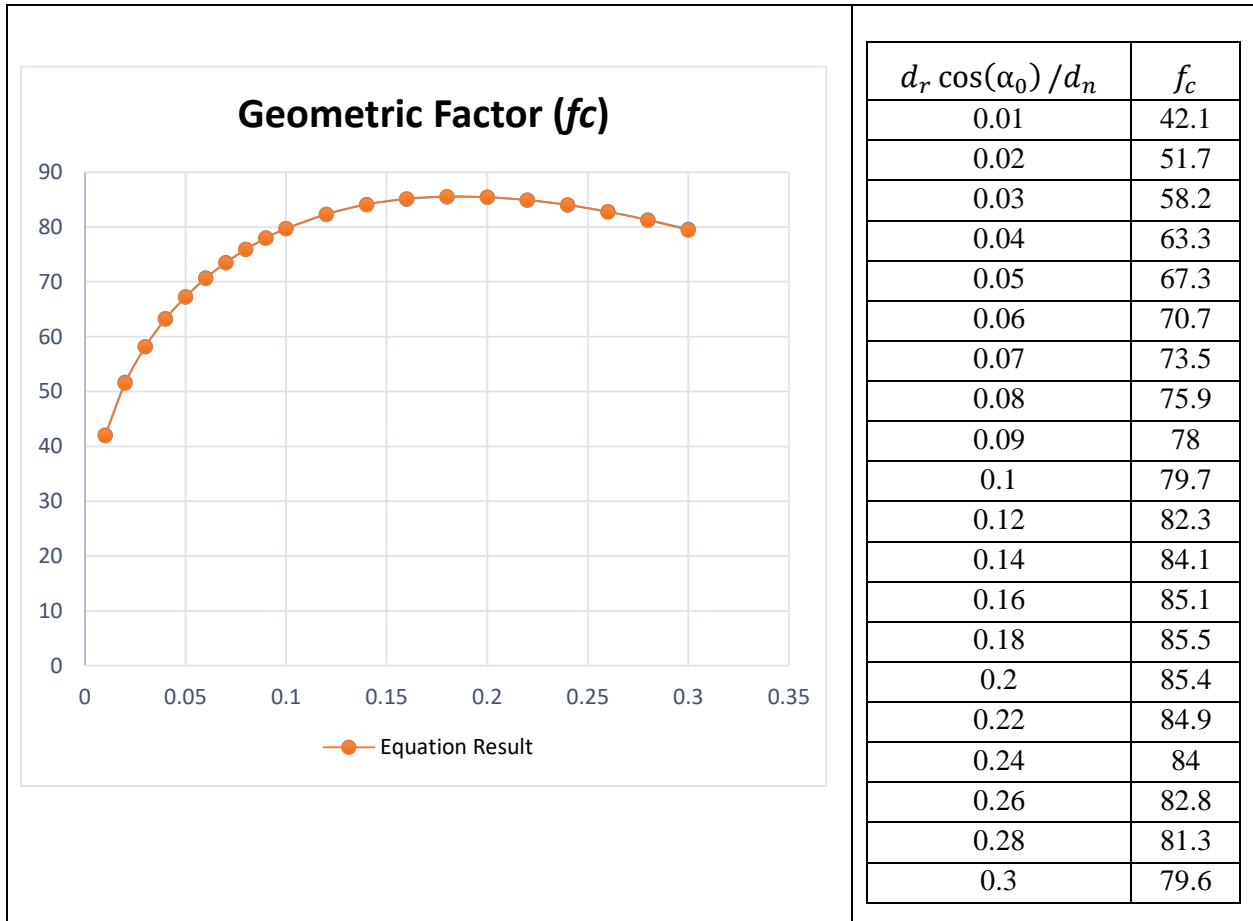
The diameter of rolling element at the contact point is defined by Lemor [9] as:

$$D_c = \left( (2.5p) d_r 2^{\frac{1}{2}} \right)^{\frac{1}{2}} \quad (6.2)$$

where  $p$  is the pitch of the thread and  $d_r$  is the effective roller diameter. This formula is modeled after the dynamic load capacity of rolling element bearings and transformed to calculate the PRS dynamic load capacity. Here,  $N_c$  is the total number of contact points depends on the number of rollers and the number of threads to define the total contact points in the PRS system. All parameters necessary to calculate the load capacity are the nut effective inner diameter ( $d_n$ ),



effective screw shaft diameter ( $d_s$ ), effective roller diameter ( $d_r$ ), pitch ( $p$ ), length ( $L$ ), helix angle ( $\beta_0$ ), number of rollers ( $N_r$ ), and the geometric factor ( $f_c$ ). Length is not directly included in the formula, however, it with pitch is related to the number of roller threads. Generally, number of roller threads can be obtained by dividing the length with the value of the pitch. The geometric factor is a dimensionless value and determined by the rate of  $\left(\frac{d_r \cos(\alpha_0)}{d_n}\right)$ . Lemor [9] and Ma [13] define contact angle as a fixed value such as  $45^\circ$ . And the geometric factor ( $f_c$ ) value can be obtained by Brandlein et al. [25] Geometric factors are presented in Table 5.1.



(a) Geometric Factor Graph

(b) Geometric Factor Table

**Table 5.1 Geometric Factor graph and Table Chart**

Table 5.1 presents a geometric factor graph with Table 5.1 (a), as the geometric factor graph that is drawn based on the geometric factor values. For convenience, let's define its rate

$\left(\frac{d_r \cos(\alpha_0)}{d_n}\right)$  as the geometric factor decision number ( $N_{dc}$ ). The geometric factor values in Table

5.1 (b) can be expressed by the formula as:

$$\begin{aligned}
 f_c = & -5394384948 N_{dc}^{10} + 8851856787 N_{dc}^9 - 6308725579 N_{dc}^8 + 2564041511 N_{dc}^7 - \\
 & 656422710.5 N_{dc}^6 + 110470028.7 N_{dc}^5 - 12407228.47 N_{dc}^4 + 931488.7454 N_{dc}^3 - \\
 & 47724.95951 N_{dc}^2 + 1892.829727 N_{dc} + 26.98514873
 \end{aligned} \tag{6.3}$$

Then, the total number of parameters for the dynamic load capacity calculation including the fixed contact angle and dimensionless geometric factor. The dimensionless geometric factor values varies from 42.1 to 85.5 following the rate of  $\left(\frac{d_r \cos(\alpha_0)}{d_n}\right)$ . However, the geometric factor values are distinguished as fixed parameters because these values are determined by a specific rate, which is related to effective roller diameter and nut effective inner diameter. In addition, effective screw diameter or effective roller diameter are related to nut effective inner diameter. Because of this, one of these diameters must be excluded in the parameter analysis process when nut effective inner diameter is considered at the same time. In other words, effective roller diameter is defined by the formula  $(d_r = \frac{d_n - d_s}{2})$ , only one parameter analysis is enough in the case of nut effective inner diameter and effective screw diameter or effective roller diameter. For parameter analysis based on the diameter relationship, effective screw diameter is only used with nut effective inner diameter in this chapter. The effective screw diameter and the effective roller diameter are used individually with other parameters except for above mentioned case. Overall, eight parameters are used for the analysis with the fixed parameters for the calculation of the dynamic load capacity.

5.2 Load Capacity Analysis

5.2.1 Parameters

Variable Parameters	Fixed Parameters
$d_n$ : Nut Inner Diameter	$D_n$ : Nut Outer Diameter
$d_s$ : Screw Diameter	$f_c$ : Dimensionless Geometric Factor
$d_r$ : Roller Diameter	$\alpha_0$ : Contact Angle
$L$ : Length	$N_s$ : Number of Start
$p$ : Pitch	
$N_r$ : Number of Rollers	

Table 5.2 Parameters

5.2.2 Resulting Maps and Analysis

5.2.2.1 Dominant Parameter: Nut Inner Diameter ( $d_n$ )

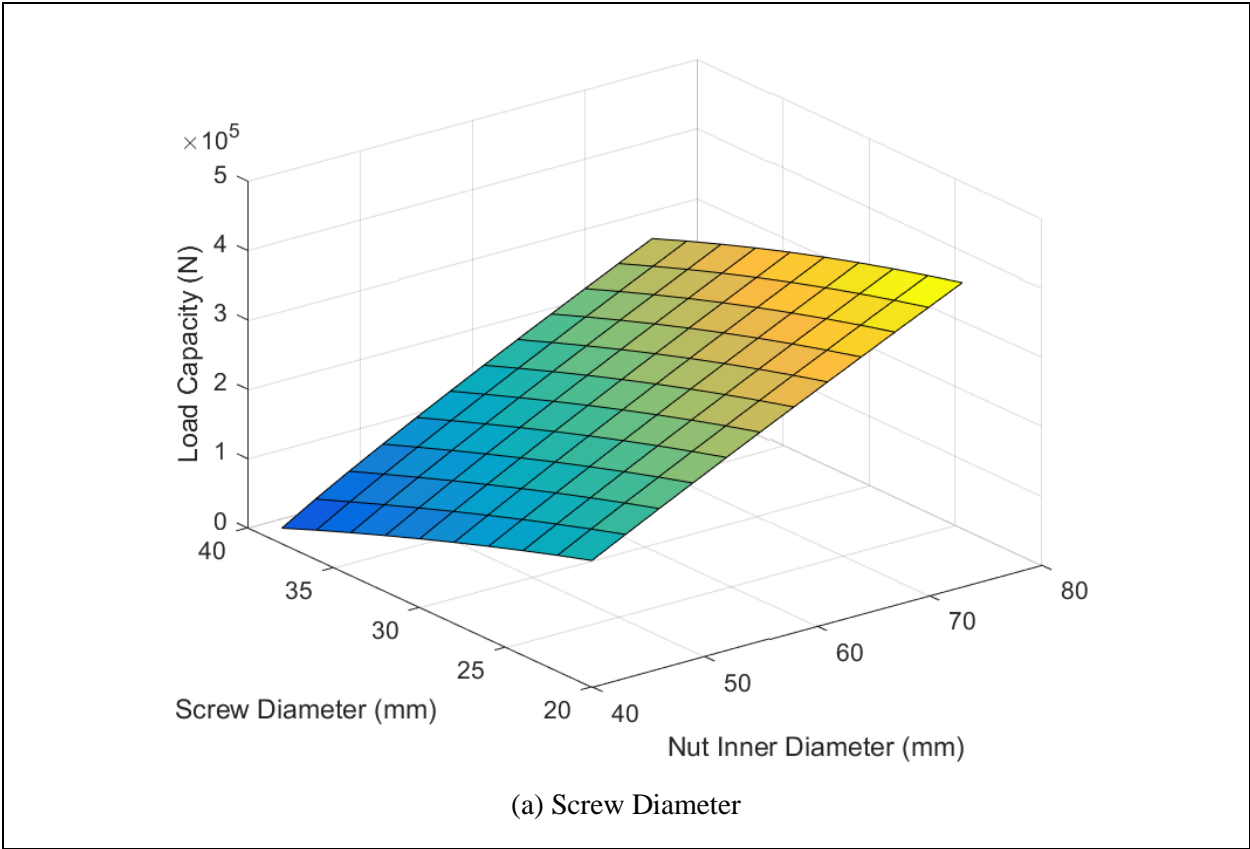
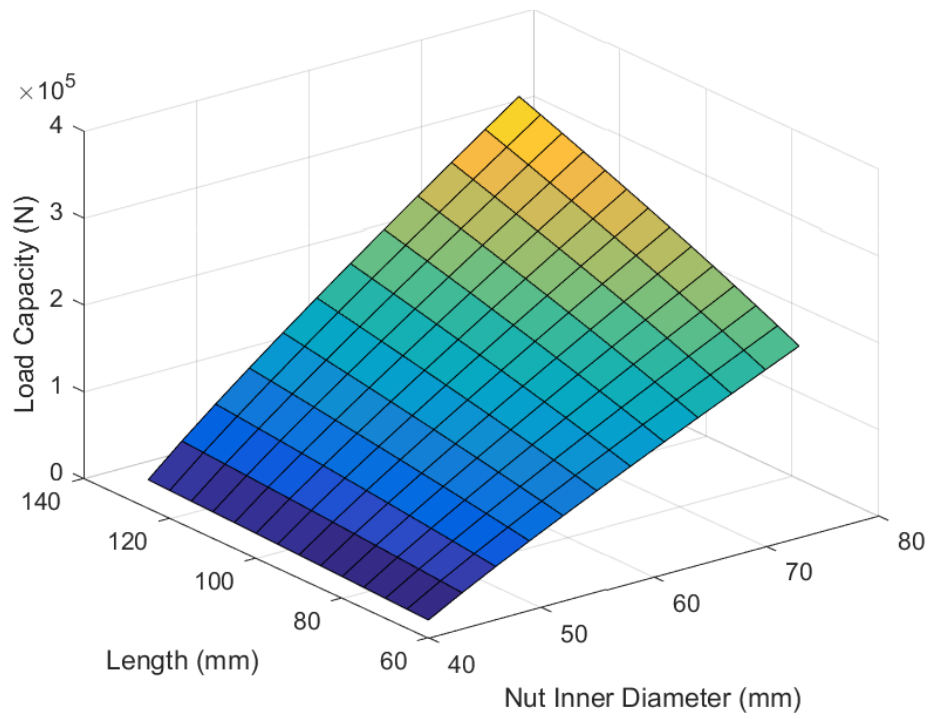
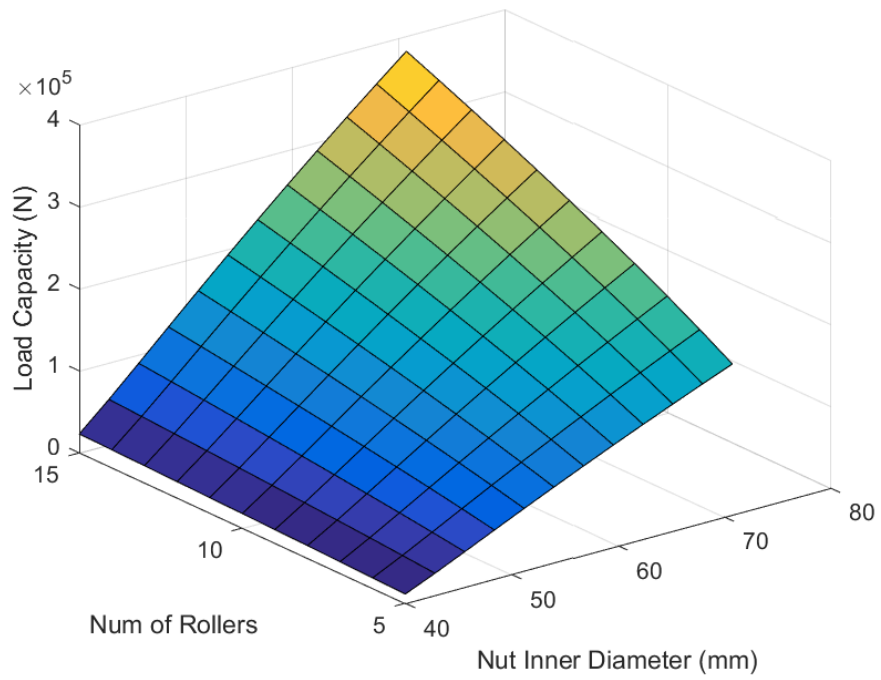


Figure 5.2 Load Capacity ( $d_n$  as dominant parameter)



(b) Length



(c) Number of Rollers

Figure 5.2 Continued

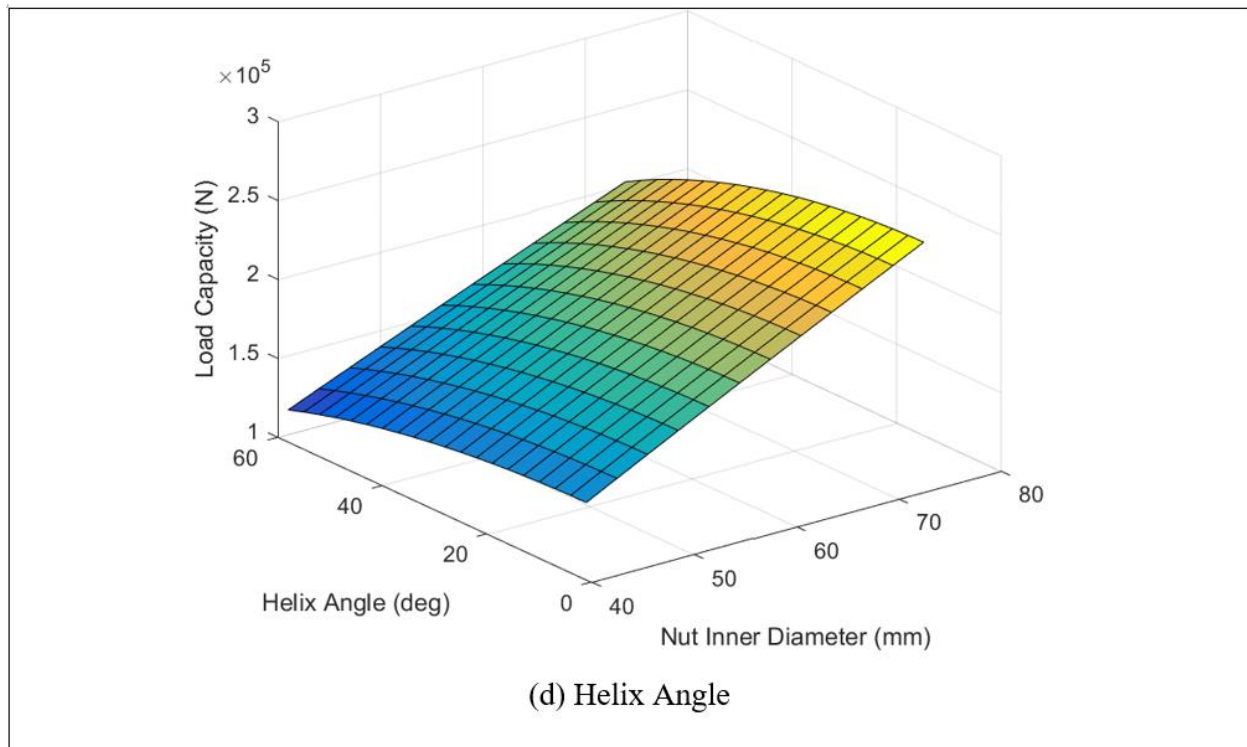


Figure 5.2 Continued

Figure 5.2 shows the results of a combination between the nut inner diameter and other parameters. In this case, the nut inner diameter is set as the dominant parameter where the other parameters need as secondary parameters to figure out the effect of each parameter. The screw diameter and the roller diameter are related parameters to each other. Thus, the nut inner diameter and screw diameter combination is investigated as a representative sample between the nut inner diameter and screw diameter case. The nut inner diameter and roller diameter case when nut inner diameter as Figure 5.2 (a) is the result of the load capacity where nut inner diameter and screw diameter change. As nut inner diameter increases, load capacity increases because nut inner diameter increase makes a larger inner space in the PRS. The inner space increase causes the screw diameter and roller diameter to increase. On the contrary, with a screw diameter increase the load capacity decreases if the nut inner diameter is fixed. This is caused by the roller diameter decrease because of the inner geometry constraints. When the inner diameter increases, the total inner space increases. Thus, screw diameter and roller diameter must increase simultaneously. However, the

screw diameter increase causes the roller diameter to decrease and therefore the load capacity decreases where the nut inner diameter is fixed. Even though the screw diameter increase may decrease the load capacity, the nut inner diameter increase can compensate for the load capacity decrease because the nut inner diameter is given more inner space. But the nut inner diameter needs to be limited in some cases. In other words, it is important to find the proper point of the screw diameter and roller diameter under limited inner space where nut inner diameter is fixed. Because of this, building the correct design process is critical and this will be discussed more in the chapter of combined parameter analysis. The case (b) is the result for load capacity when the nut inner diameter and the pitch change. The result indicates that nut inner diameter is dominant because load capacity increases when nut inner diameter increases. Pitch also causes load capacity increase. The interesting part of pitch change is that pitch results in a “curved” map. This shape change is bigger as the pitch is smaller and the nut inner diameter is larger. In other words, the larger pitch can carry more load. Overall, the pitch has a large effect on load capacity and needs to be considered as a dominant parameter. The case (c) shows the load capacity change when the nut inner diameter and length change. As proven, the nut inner diameter increase results in a load capacity increase. Length also brings load capacity increase. Even though load capacity value difference is not large when nut inner diameter is smaller, difference becomes bigger when nut inner diameter increases. In other words, effect of length to load capacity needs to be considered as another dominant parameter to get higher load capacity. The case (d) presents the result of the number of rollers’ effect on the load capacity. Increase of roller number means increase of contacts. This increase of load capacity is proportional to the increase in contacts. Case (d) proves this expectation. As shown, the load capacity increases as number of the rollers increases. However, the increase in the number of rollers brings the opposite result in terms of weight and it may affect force density, which will be analyzed in Chapter 6. Weight and Force Density Analysis. Case (e) gives the result of load capacity related to helix angle. Helix angle change doesn’t have much effect relative to other parameters such as nut inner diameter, screw diameter, length, and pitch.

Even though there is a small change when the helix angle increases, the helix angle can't be considered as a dominant parameter because of its small effect on the load capacity.

5.2.2.2 Dominant Parameter: Screw Diameter ( $d_s$ )

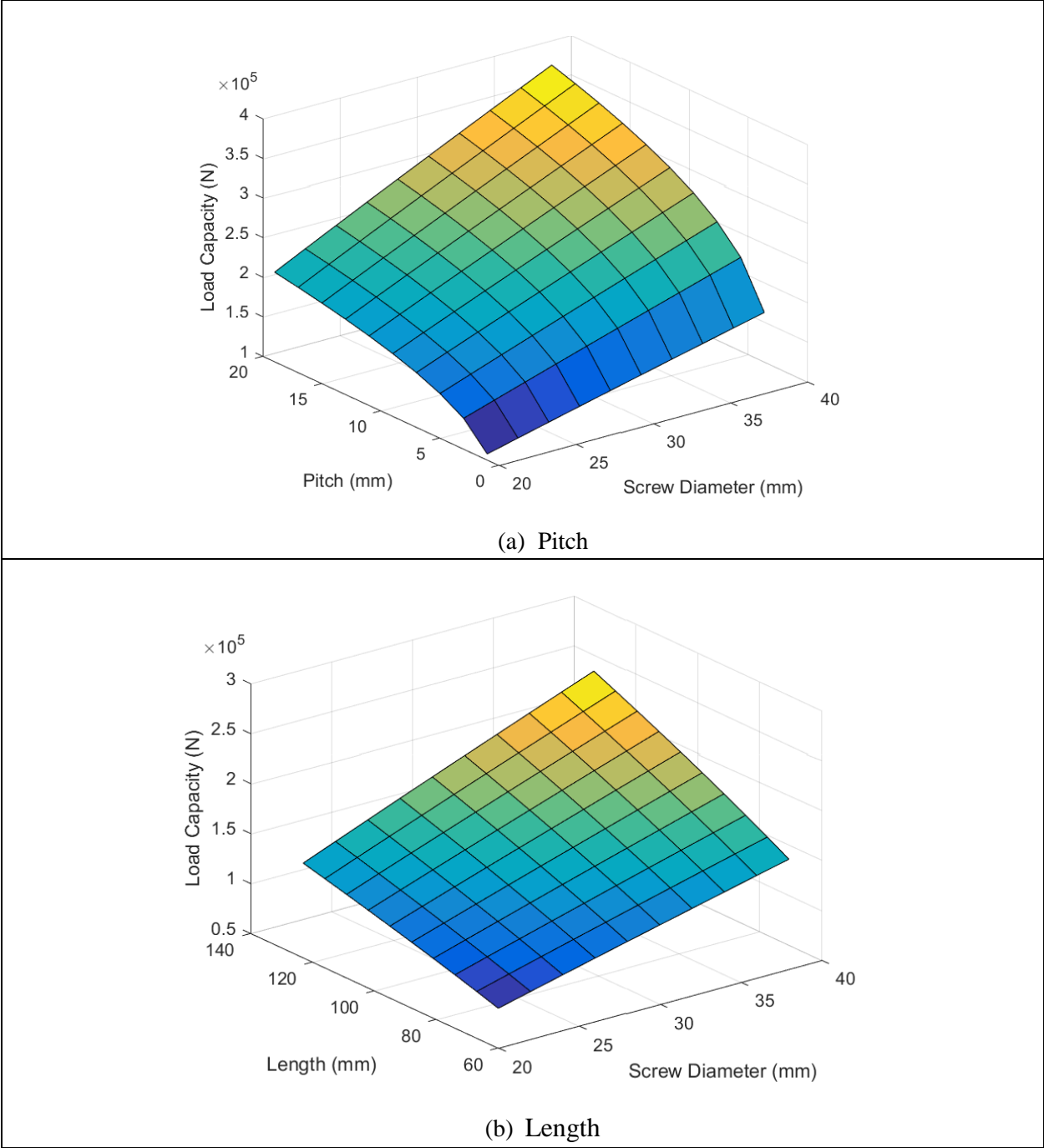
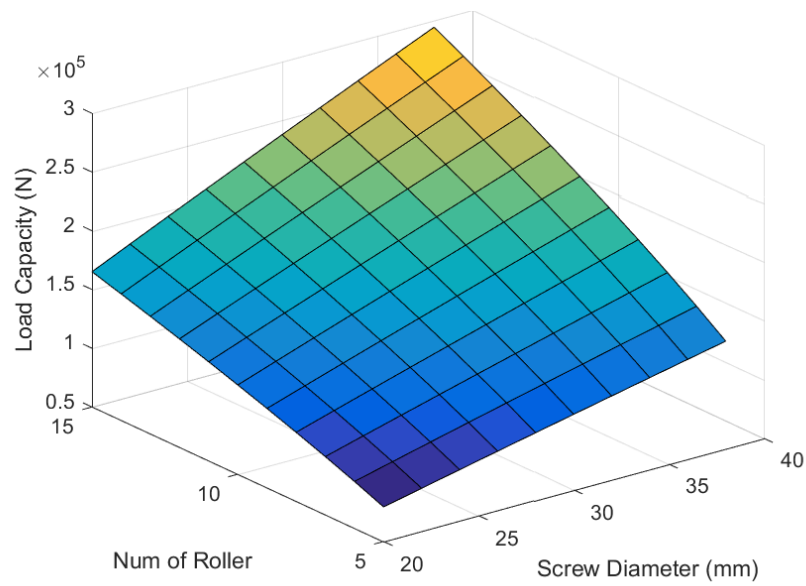
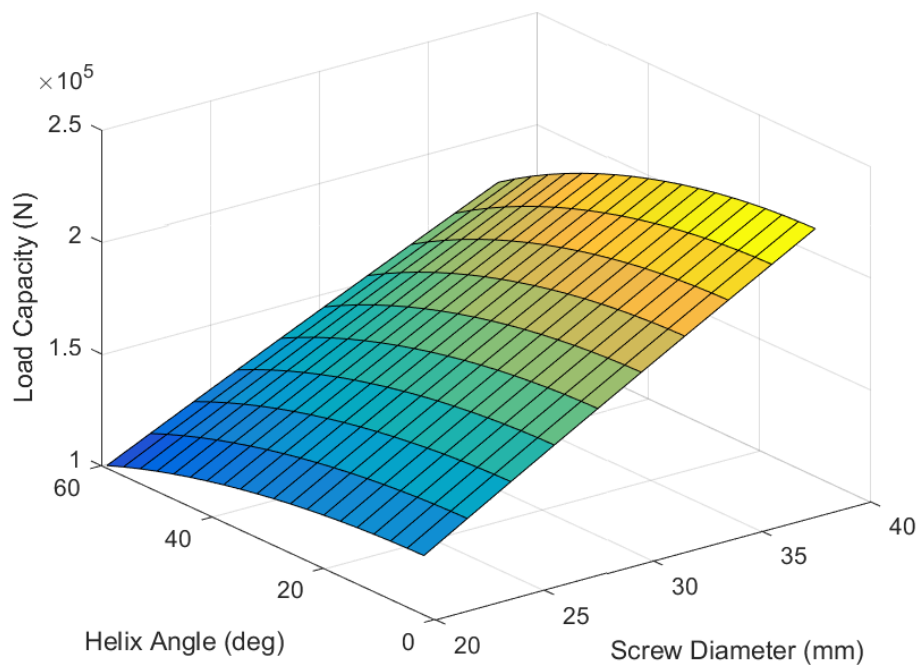


Figure 5.3 Load Capacity ( $d_s$  as dominant parameter)



(c) Number of Rollers



(d) Helix Angle

Figure 5.3 Continued

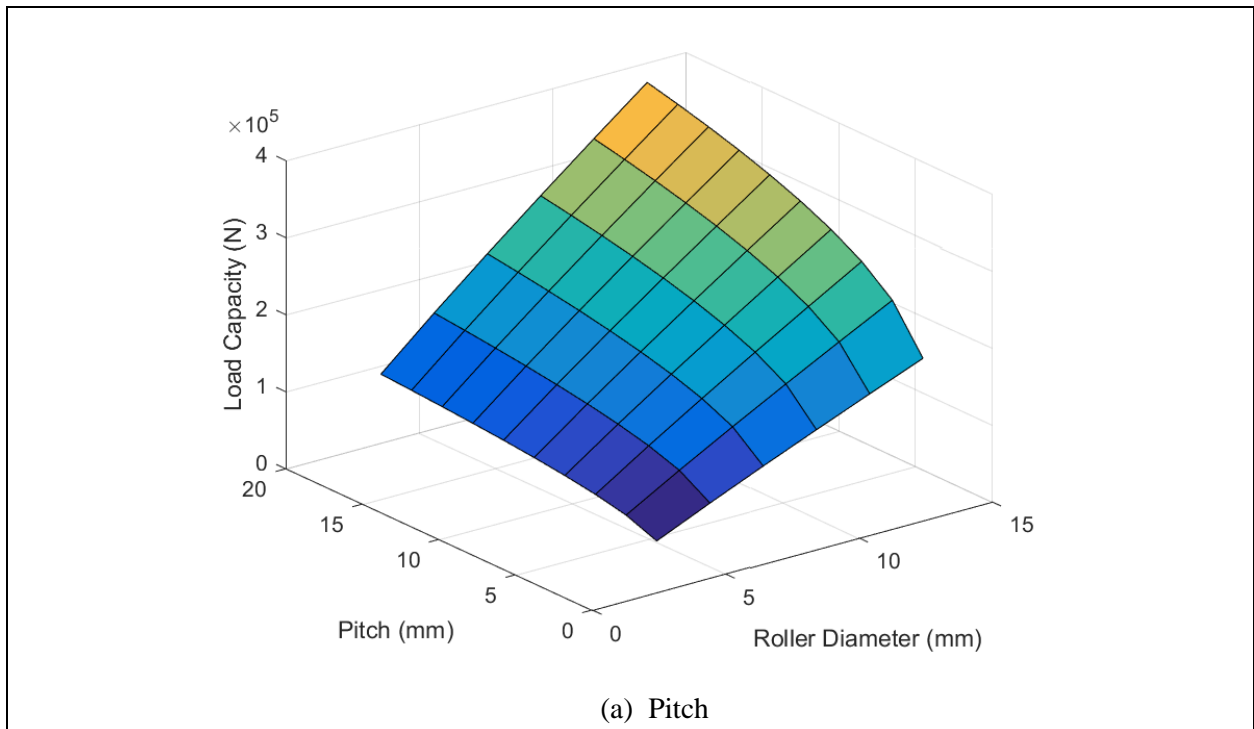


Figure 5.3 shows results of load capacity. The screw diameter is set as the dominant parameter and other parameters are used. Figure 5.3 (a) presents the effect of pitch to the load capacity when the screw diameter changes. Increase of load capacity due to screw diameter increase can be easily observed. Pitch also increases load capacity. Noticeable result for the pitch change is the curve's nonlinearity. Until pitch reaches until about 4 mm, load capacity difference is large and it gives steeper curve than large pitch condition. After this pitch point, load capacity curve becomes more linear. Like the previous two analyses, pitch can be considered as a dominant parameter. Figure 5.3 (b) is the result of the 3D plot of load capacity when screw diameter and length change. As shown, both the screw diameter and length increase load capacity. This means that length of PRS can deliver higher load and screw diameter also can carry more load in the system. Figure 5.3 (c) shows the load capacity change when the screw diameter and number of rollers change. The 3D plot presents a similar result with length change. However, the number of rollers increase creates a higher load capacity than the length increase. This is because there are more contacts in the case of numbers of roller change. Thus, the number of roller needs to be maximized in the allowable space. Figure 5.3 (d) presents the result of load capacity when screw diameter and helix angle change. As shown, the helix angle change doesn't give much change of load capacity even though it makes the map nonlinear. Therefore, the helix angle shouldn't be considered as a dominant parameter.

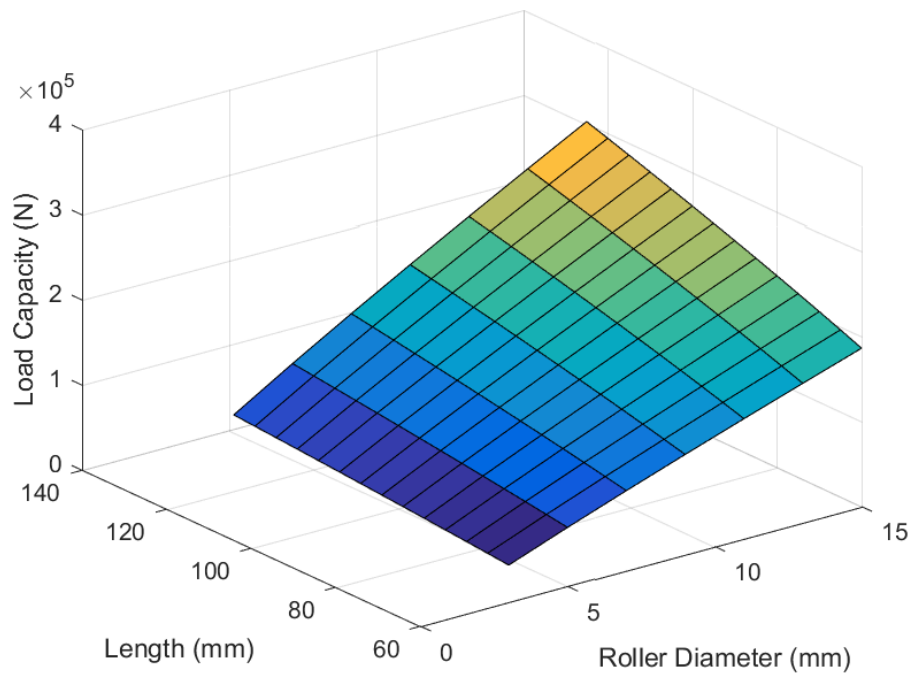
#### 5.2.2.3 Dominant Parameter: Roller Diameter ( $d_r$ )

Figure 5.4 shows the results of load capacity change when the roller diameter change is set as the dominant parameter and other parameters are used to investigate the effect on load capacity. Roller diameter is expected to increase load capacity and results prove this expectation. Figure 5.4 (a) shows the result of load capacity caused by roller diameter and pitch change. Like the earlier case (such as nut inner diameter and screw diameter), pitch increase also gives a rapid increase of load capacity when it is small. When pitch value is smaller than 5 mm in this case, the map nonlinearity

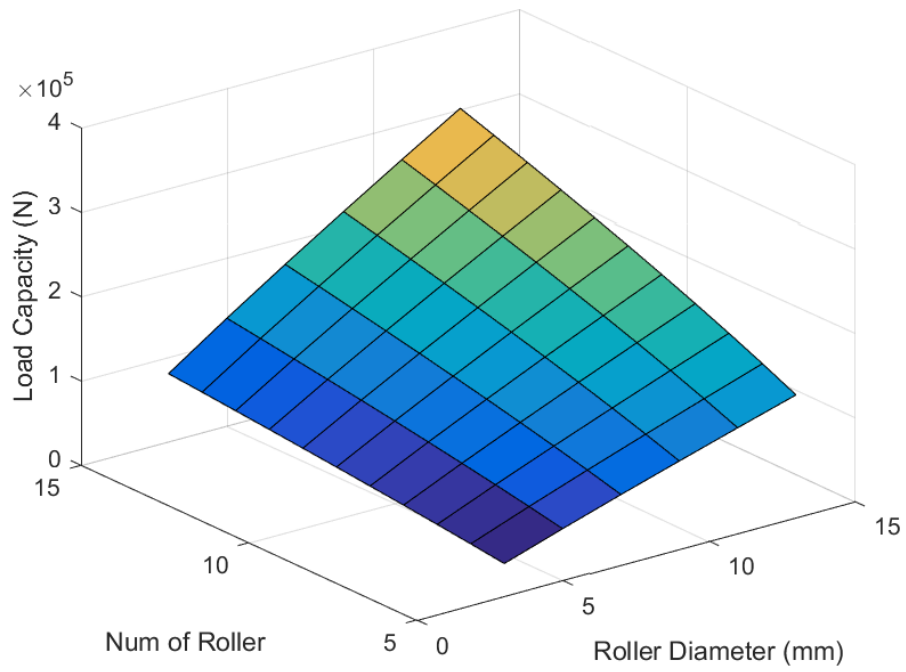
in load capacity is bigger. This indicates again that pitch needs to be considered as a dominant parameter to design the PRS such as load distribution, total deformation, and total stiffness results. Figure 5.4 (b) and (c) present the results of load capacity change when length of the PRS and the number of rollers change as secondary change parameters. Both cases linearly increase load capacity with roller diameter increase. However, the number of rollers change allows more load capability when the two cases (a) and (b) are compared. This is because of the same reason with the previous nut inner diameter and screw diameter change case where the number of rollers change increases the total number of contact points in the PRS system. Overall, the number of rollers and length are important factors to increase load capability. To be specific, the number of contact points is dominant to increase load capacity. Figure 5.4 (d) shows the load capacity change when the helix angle changes as a secondary parameter change. Figure 5.4 (d) also indicates that the helix angle change has a minor effect on load capacity like other cases, which are analyzed previously.



**Figure 5.4 Load Capacity ( $d_r$  as dominant parameter)**



(b) Length



(c) Number of Rollers

Figure 5.4 Continued

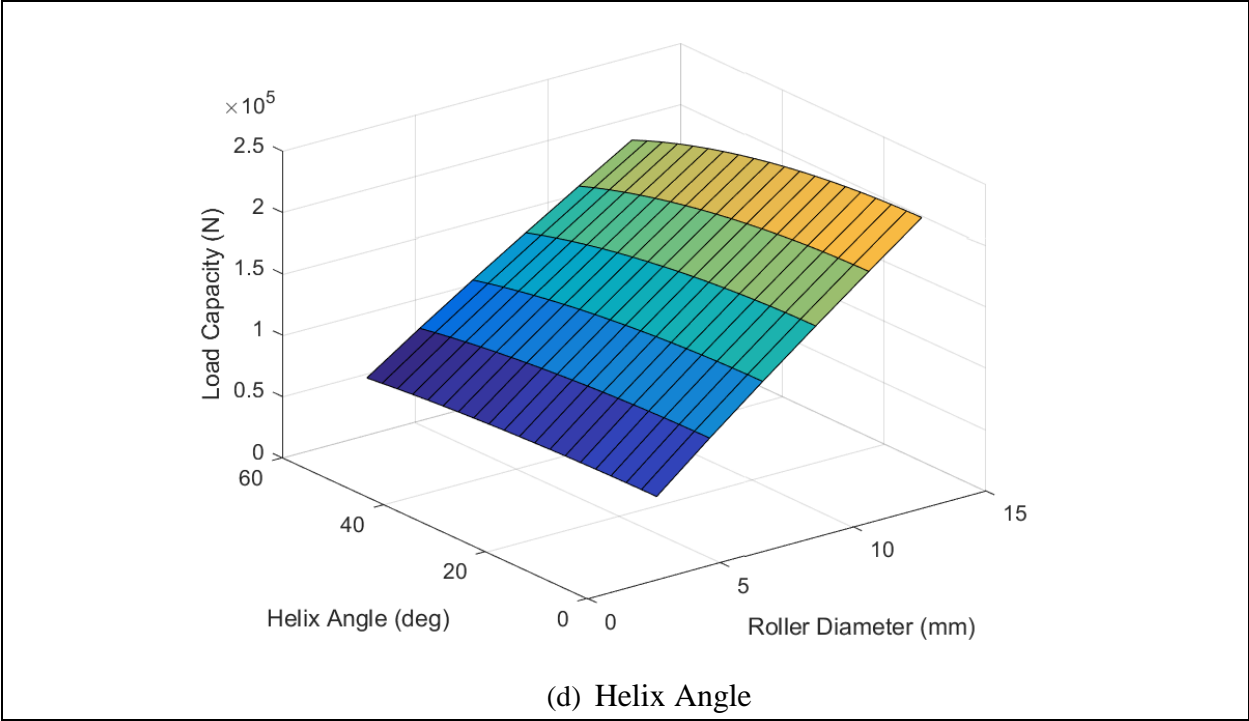


Figure 5.4 Continued

5.2.2.4 Dominant Parameter: Length (*L*)

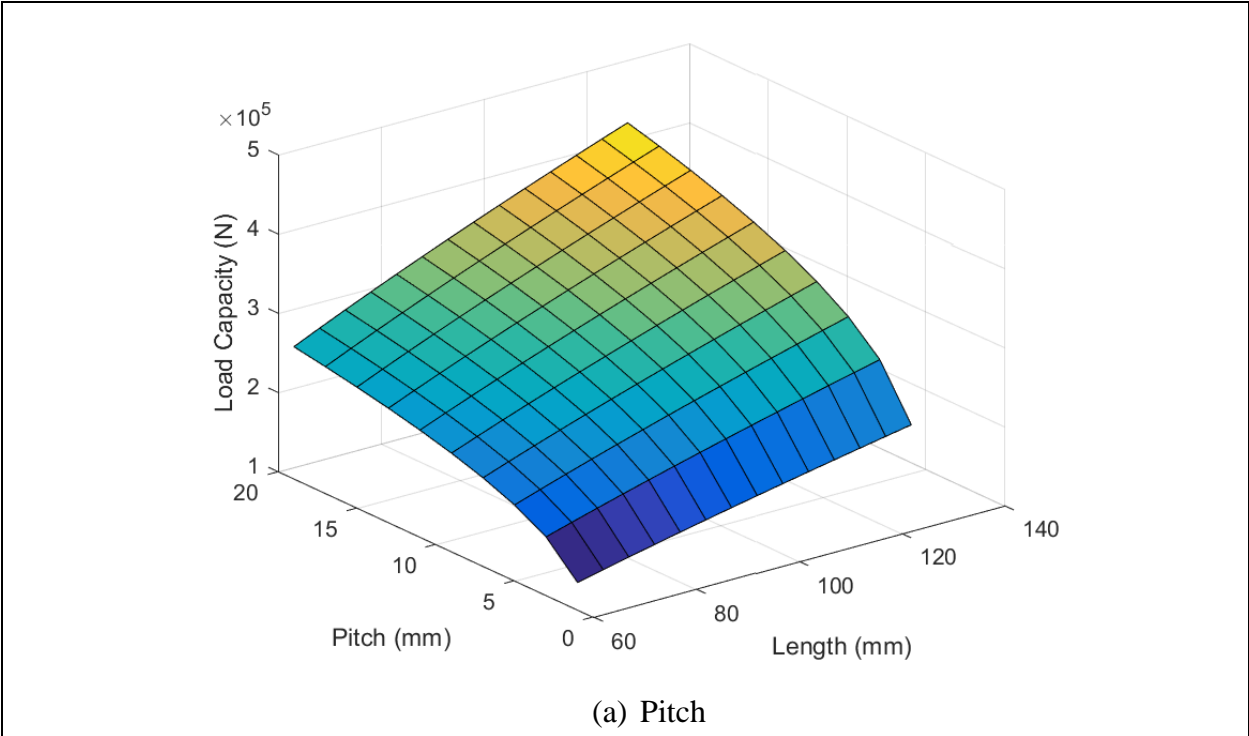


Figure 5.5 Load Capacity (*L* as dominant parameter)

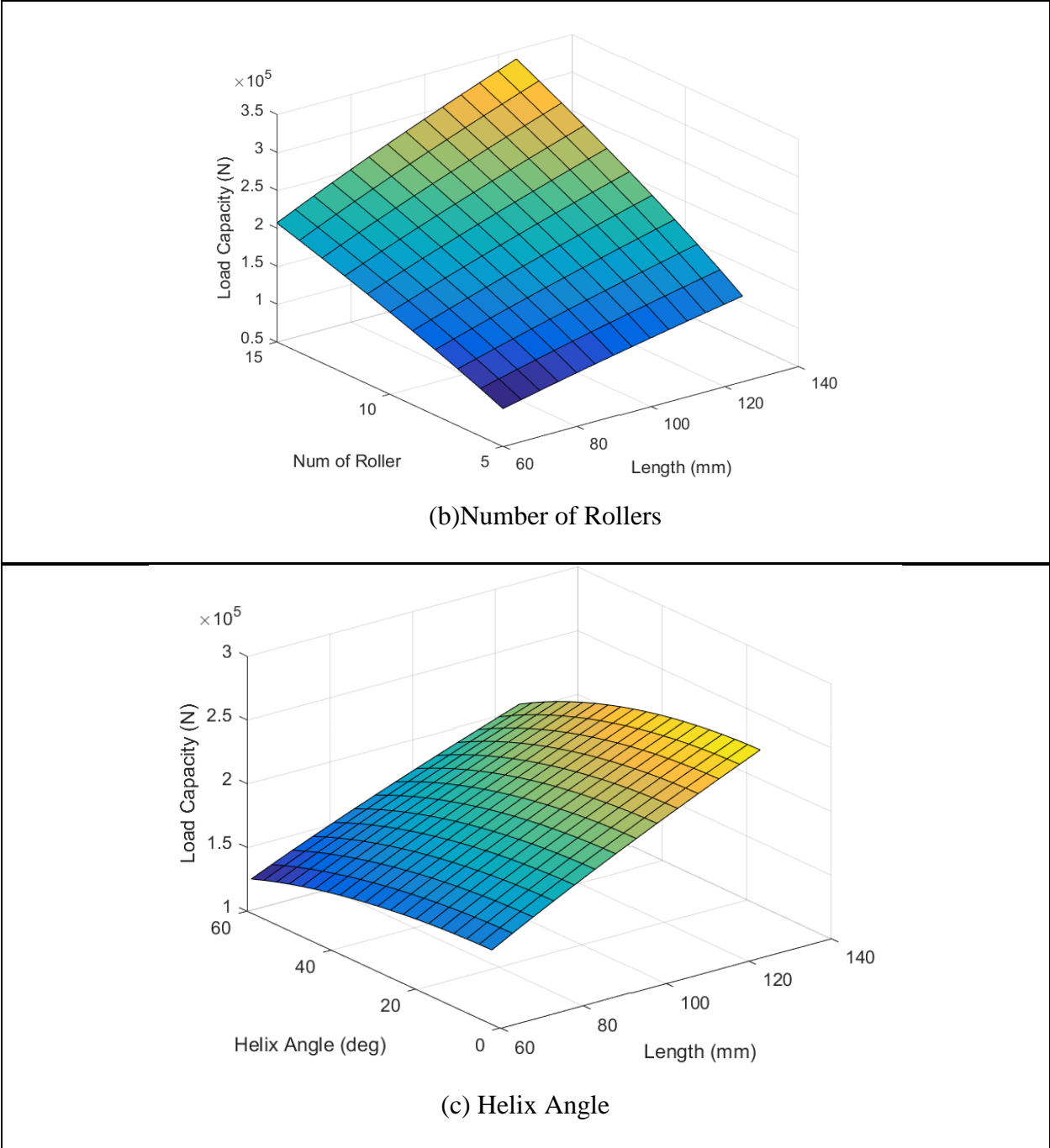


Figure 5.5 Continued

Figure 5.5 shows the results of load capacity change when we set length as a dominant parameter and other parameters are set as secondary factors to investigate the effect on load capacity. Figure 5.5 (a) is the result of load capacity when length and pitch change. Similar to the results of other diameter change cases, pitch change also gives a nonlinear curve compared to other 3D maps. This

proves again that the effect of pitch causes dynamic change when the value is small. It emphasizes the major role of pitch to the load distribution and indicates that pitch needs to be dealt carefully. The number of rollers and length has a linear effect on the load distribution change as shown in plot Figure 5.5 (b). Helix angle also has a minor impact with length change case and is presented in Figure 5.5 (c).

5.2.2.5 Dominant Parameter: Pitch ( $p$ )

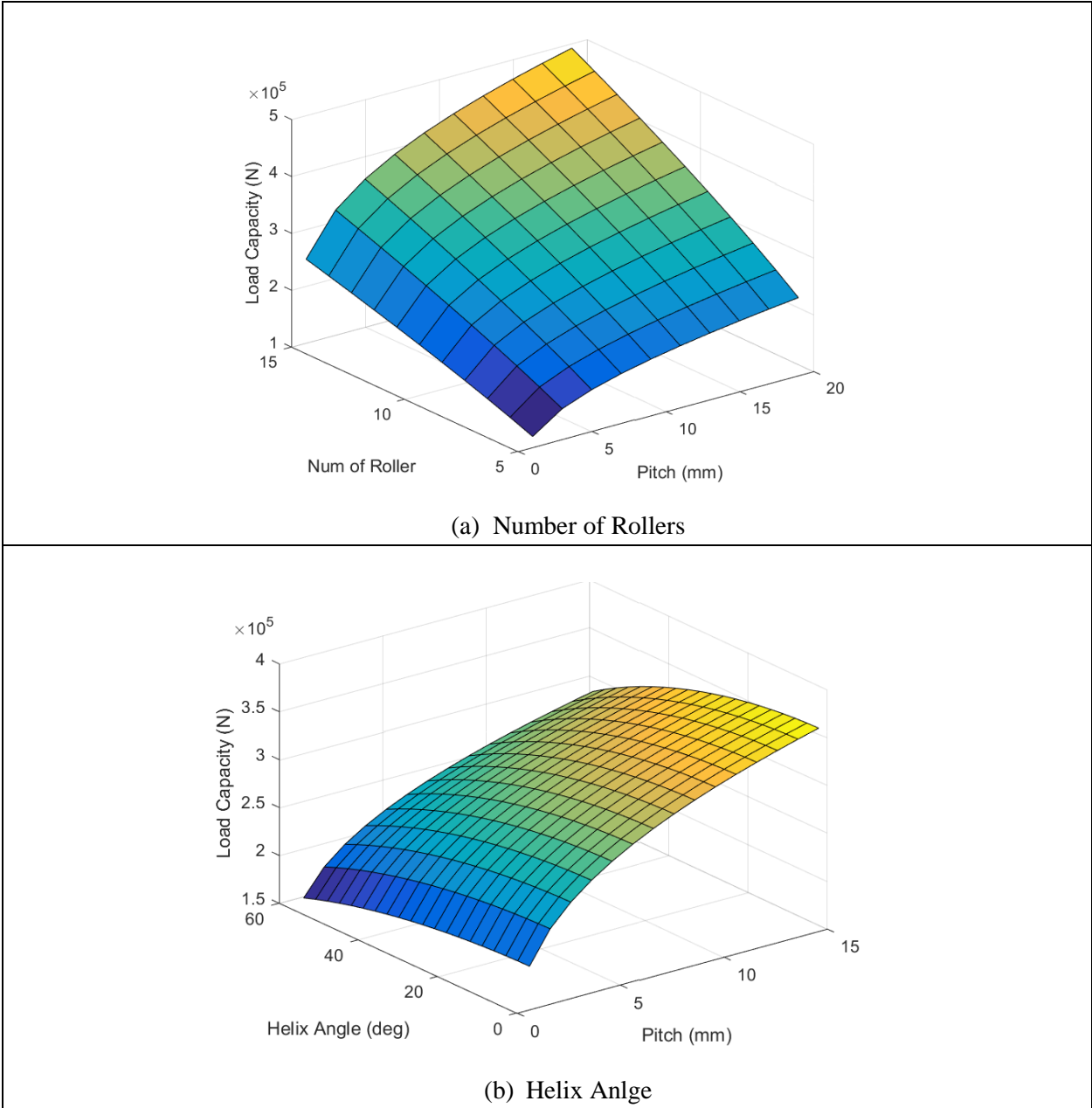


Figure 5.6 Load Capacity ( $p$  as dominant parameter)

Figure 5.6 gives two plots when pitch is set as the dominant parameter and the secondary parameters are the number of rollers and the helix angle. Figure 5.6 (a) is the result when the pitch and number of rollers change. As analyzed previously, the number of rollers makes a large increase in load capacity. Pitch shows its nonlinear characteristic. This proves again that pitch is very important parameter to decide optimal design of the PRS. This result indicates that building envelopes to compare result from other categories such as load distribution, total deformation and total stiffness is necessary. Because of this systemic and parametric demand, parameter envelopes will be built and discussed in later chapter. Figure 5.6 (b) presents the load distribution with change of the helix angle and pitch. As discussed above, pitch gives nonlinear curve. However, the helix angle doesn't give much change to load capacity (i.e., it is basically linear).

5.2.2.6 Dominant Parameter: Number of Rollers

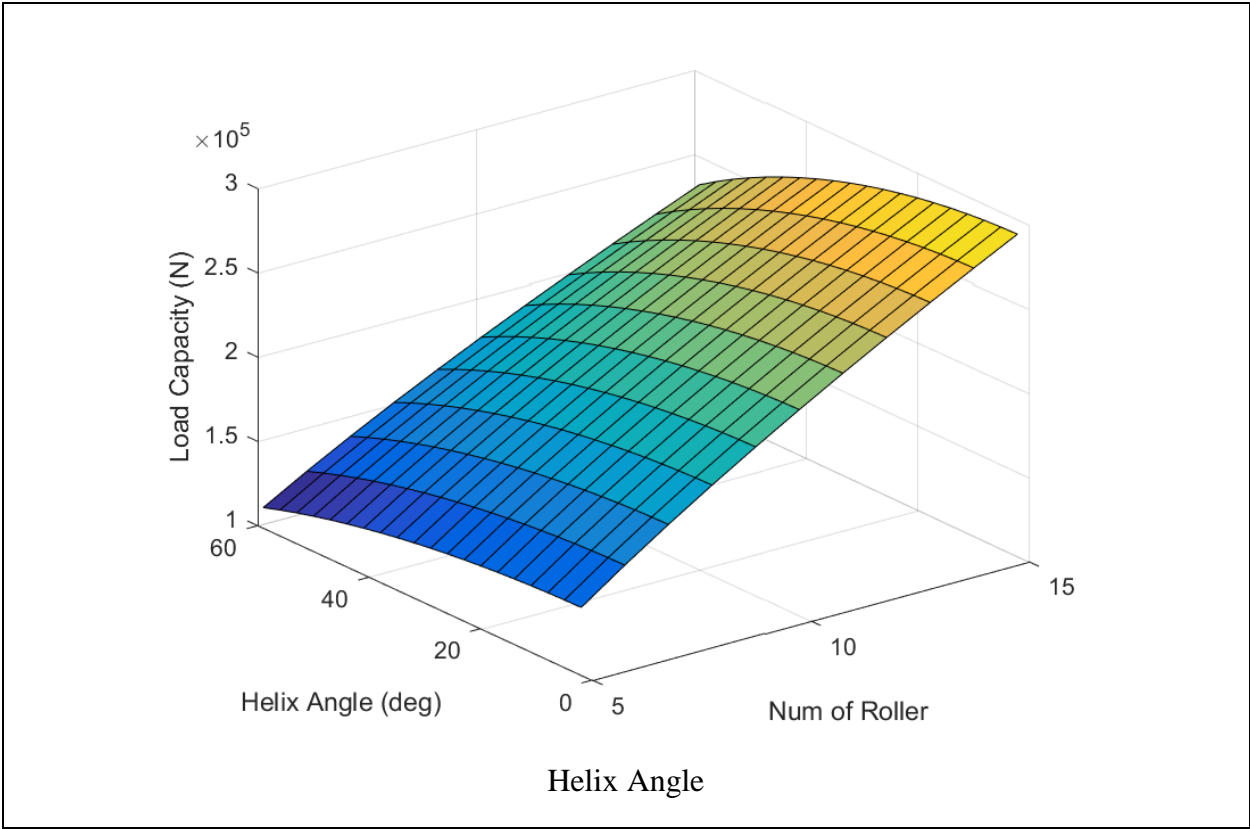


Figure 5.7 Load Capacity ( $N_r$  as dominant parameter)

Figure 5.7 shows the load capacity change when number of rollers and helix angle change. The helix angle doesn't have a major effect on load capacity. Only the number of rollers has a major effect on load capacity.

### 5.3 Chapter Conclusion

This chapter has analyzed load capacity with regard to several key parameters. Load capacity results come with combining two chosen parameters. As analyzed in each section, diameters such as nut inner diameter, screw diameter, and roller diameter are dominant parameters that increase load capability. However, we need to be careful to select appropriate screw diameter and roller diameter under the fixed nut inner diameter condition. The screw diameter increase can make higher load capacity as shown in Figure 5.3. In addition, roller diameter increase also can cause higher load transferring capability. In other words, both diameters have the capability to increase load capacity when they increase (without inner space limitation). However, inner geometry is restricted by the inner space such that the screw diameter and roller diameter are dependent each other. In other words, roller diameter decreases as screw diameter increases, or vice versa. Because of this, the interaction between screw diameter and roller diameter needs to be dealt with carefully. There is no doubt that pitch is a dominant parameter in terms of load capacity. In this chapter, results shows that a small pitch value causes lower load capacity in every case. Sudden load capacity increase occurs when pitch is small. Especially, this steep value change occurs in the range from 1 mm to 5 mm and then the map becomes linear after this range. Large pitch values are beneficial to achieve higher load capacity. Thus, choosing the proper value of pitch is important and this will be discussed about its exact role for the PRS design in the combination categories' analysis chapter. The number of rollers has a huge impact on the load distribution because it is affected by the number of total contact points. The increase of the number of rollers means an increase of the total contact points in the PRS. Then, it is necessary to discuss the effect of the number of rollers when all categories are combined in a later chapter. Length is related to the number of contact points because the number of total contact points increases when



length increases. However, length only makes a linear change and pitch and the number of threads is defined by the length of the PRS. Then, length will be fixed as constant when combined results are analyzed. As proved in all cases, helix angle doesn't have much impact on load capacity.

Overall, effect of each parameter on load capacity can be arranged as:

Parameter	Effect
Nut Inner Diameter $d_n$	It affects the inner space of the PRS and thickness of the nut. It makes a somewhat non-linear curve as it changes. When it has a high value, the load capacity is high because it increases the inner space of the PRS.
Screw Diameter $d_s$	It affects the roller diameter and nut inner diameter. It makes a linear increase for load capacity. As it increases, load capacity becomes higher based on the condition of enough inner space. However, it affects the roller diameter. The screw diameter change can cause a decrease of load distribution under the condition of a fixed nut inner diameter.
Roller Diameter $d_r$	It affects the inner space of the PRS and provides a somewhat non-linear curve for the load capacity. Because its increase is not larger than screw diameter, it provides higher load capacity when it increases.
Length $L$	It affects the number of total contact points in the PRS and gives a linear curve as it changes. Longer length provides more contact points in the PRS. Increase of length causes a higher load capacity.
Number of Rollers $N_r$	It affects the number of total contact points in the PRS. Then, it gives a higher load capacity as it increases.
Pitch $p$	It affects the lead of the PRS movement. And it gives a non-linear curve. The curve slope is steeper when its value is low. Because pitch is related the lead of the PRS, large pitch provides has higher load capacity.
Helix Angle $\beta_0$	It has a low effect on load capacity.

**Table 5.3 Parameter Effect on PRS for Load Capacity**

And each parameter can be classified as:

Primary Parameters	Support Parameters	Fixed Parameters
$d_n$ : Nut Inner Diameter $d_s$ : Screw Diameter $d_r$ : Roller Diameter $p$ : Pitch $N_r$ : Number of Rollers $L$ : Length	$\beta_0$ : Helix angle	$D_n$ : Nut Outer Diameter $\alpha_0$ : Contact Angle $N_s$ : Number of starts $f_c$ : Dimensionless Geometric Factor $N_c$ : Number of Contact Points

**Table 5.4 Parameter Classification for Load Capacity**

## CHAPTER 6. WEIGHT AND FORCE DENSITY ANALYSIS

This chapter investigates weight and force characteristics of the PRS, which is one of the most important elements for the design of the PRS. As an important element of the PRS, calculating weight and force density and analysis of the related parameters are essential. That is because weight and force density have a large impact on actuator design concern and can limit actuator performance in a limited space. For example, it is preferred to use light weight and high force density actuators in aircraft control surfaces because it can limit aircraft's surface control movement or maneuverability. In addition, it is also related to cost of the actuator. Thus, weight and force density should be considered as a main element for design process with other consideration such as load distribution, load capacity, deformation and stiffness. Especially, force density will be dealt mainly in this chapter because it is related to the load capacity and weight in the same time. In order to calculate the PRS weight and force density, theoretical nominal weight method is used. This nominal method is the longest method to calculate weight and is generally used. Steel Market Update [27] explains well about concept of the theoretical nominal weight and Timken Steel [28] suggests how each PRS component can be calculated. Screw parts are excluded for the weight calculation because screw length is not clear in the PRS mechanism. Rollers and nut are calculated separately because of their different shape. An important part of calculation is that portion of each component to calculate the PRS weight. Then, force density is calculated based on weight.

### 6.1 Weight of Rollers

As mentioned above, rollers and nut must be calculated separately because of their different shapes. Rollers are considered as a circular bar and coefficient [26] of circular bar for weight calculation is 0.006165 for the International System of Unit (kg). As explained in the Steel Market Update [27], steel density (weight per cubic inch) is  $0.2904 \frac{\text{lbs}}{\text{in}^3}$  and can be converted to 8038.272

$\frac{\text{kg}}{\text{m}^3}$ . Density is converted to a given coefficient based on the length. For the weight of the rollers, formula is presented as [28]:

$$W_r = 0.006165 d_r^2 N_r L_r \text{ (kg)} \quad (5.1)$$

where,

$W_r$  = Weight of Rollers

$d_r$  = Effective Diameter of Roller

$N_r$  = Number of Roller

$L_r$  = Length of Roller (meter)

## 6.2 Weight of Nut

As mentioned above, the nut weight calculation formula is different from the roller weight calculation formula. The nut is considered as a circular tube and coefficient [26] of circular tube for weight calculation is 0.02466 for International System of Unit (kg). Density of the nut is also  $8038.272 \frac{\text{kg}}{\text{m}^3}$  and density is converted to calculate nut weight. Nut weight calculation formula can be expressed as [28]:

$$W_n = 0.02466(D_n - T_n)T_n L_n \text{ (kg)} \quad (5.2)$$

where,

$W_n$  = Weight of Nut

$D_n$  = Nut Outer Diameter

$T_n$  = Thickness of the Nut

$L_n$  = Length of Nut (meter)

### 6.3 Total Weight

PRS total weight is summation of rollers weight and nut weight. Total weight formula can be expressed as:

$$W_t = 0.006165 d_r^2 N_r L_r + 0.02466(D_n - T_n)T_n L_n \text{ (kg)} \quad (5.3)$$

where  $L_n$  and  $L_r$  are assumed equal; then those two values can be expressed as  $L$ . Then, total weight formula can be expressed as:

$$W_t = 0.006165 d_r^2 N_r L + 0.02466(D_n - T_n)T_n L \text{ (kg)} \quad (5.4)$$

### 6.4 Force Density

Force density is an important indicator to determine the efficiency of dynamic load capacity per unit weight and dominant factor for deciding the effect of weight on the PRS design. The two dominant factors for calculation of force density are the dynamic load capacity and weight. The dynamic load capacity and weight have their own related parameters. Some parameters exist in both factors such as nut effective inner diameter ( $d_n$ ), effective screw diameter ( $d_s$ ), effective roller diameter ( $d_r$ ), number of roller ( $N_r$ ), and length ( $L$ ). Other parameter such as helix angle ( $\beta_0$ ), nut outer diameter ( $D_n$ ) and pitch ( $p$ ) are included in only one side. Even though, pitch is included only in the calculation of dynamic load capacity formula, pitch is also considered to calculate force density because pitch is one of the factors that is related to length. In this section, all the parameters mentioned above are used to analyze force density and two parameter are chosen to make maps. Recall that dynamic load capacity is calculated following Lemor [9] as:

$$C_a = f_c (\cos(\alpha_0))^{0.86} N_c^{\frac{2}{3}} D_c^{1.8} \tan(\alpha_0) (\cos(\beta_0))^{\frac{1}{3}} \quad (5.5)$$

where,

$C_a$  = Dynamic Load Capacity

$f_c$  = Geometric Factor of PRS System

$\alpha_0$  = Contact Angle between Contact bodies ( $45^\circ$ )

$N_c$  = Total Number of Contact Point

$D_c$  = Diameter of Rolling Element at the Contact Point

$\beta_0$  = Helix Angle of the Thread

and weight can be calculated by equation (5.1) – (5.4). Then, force density can be expressed as:

$$F_D = \frac{C_a}{W_t} \quad (5.5)$$

## 6.5 Force Density Analysis

### 6.5.1 Parameters

Primary Parameters	Fixed Parameters
$d_n$ : Effective Nut Inner Diameter	$D_n$ : Nut Outer Diameter
$d_s$ : Effective Screw Diameter	$f_c$ : Dimensionless Geometric Factor
$d_r$ : Effective Roller Diameter	$\alpha_0$ : Contact Angle
$N_r$ : Number of Rollers	$N_s$ : Number of Start
$L$ : Length	$C_{eff}$ : Weight Coefficient
$p$ : Pitch	
$\beta_0$ : Helix angle	

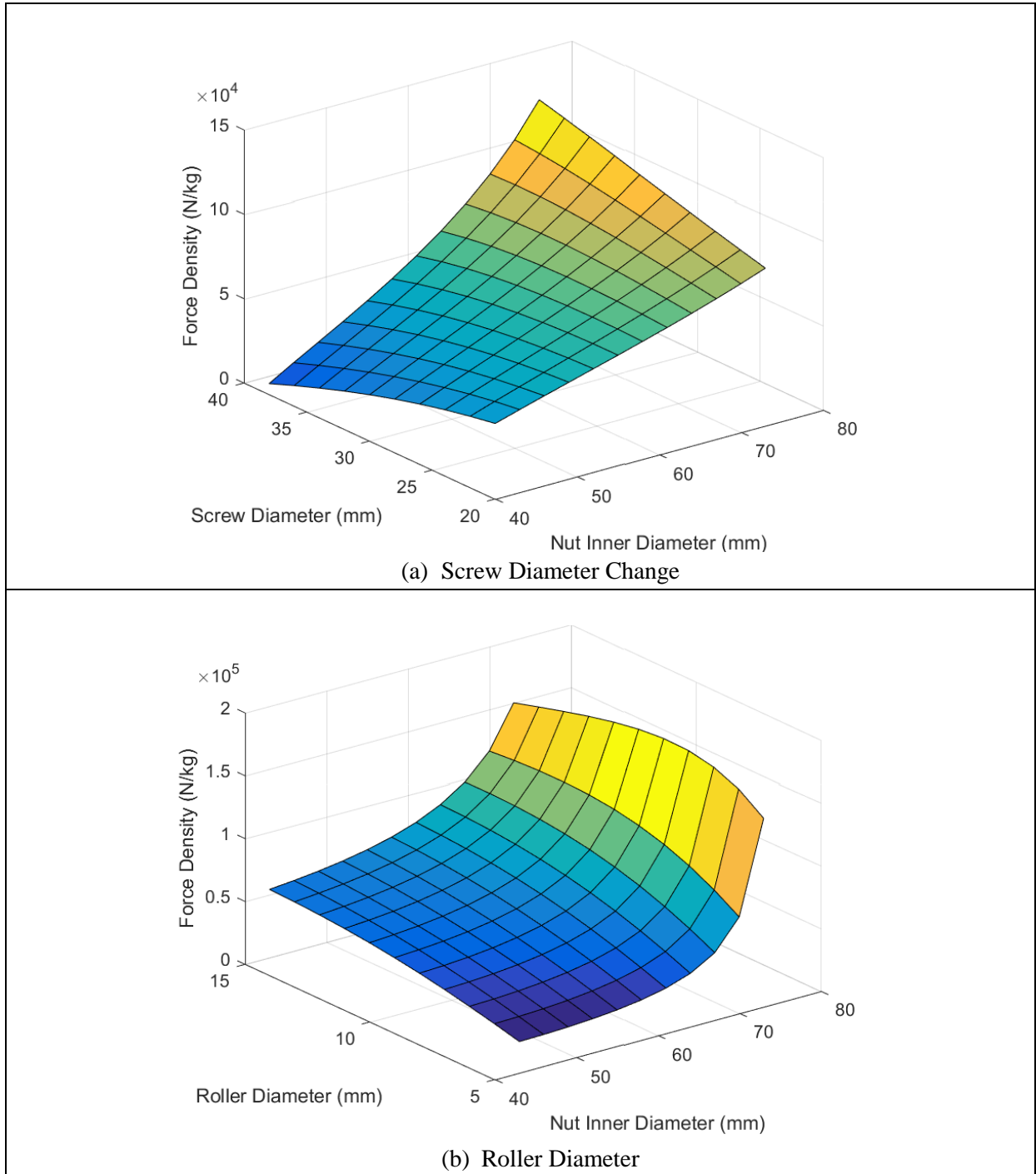
**Table 6.1 Parameters**

As shown above, there are 12 parameters that decide force density. Seven of them are variables such as nut inner diameter, screw diameter, roller diameter, number of rollers, length, pitch, and

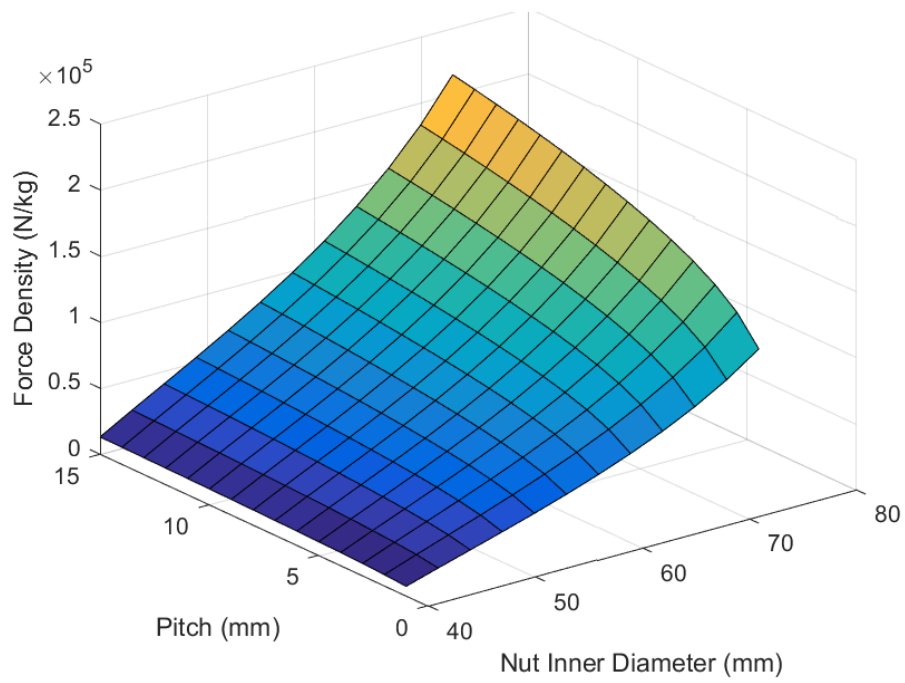
helix angle and the other five parameters are fixed. In order to examine the effect of each parameter on force density, two parameters are chosen and used to build maps.

### 6.5.2 Resulting Maps and Analysis

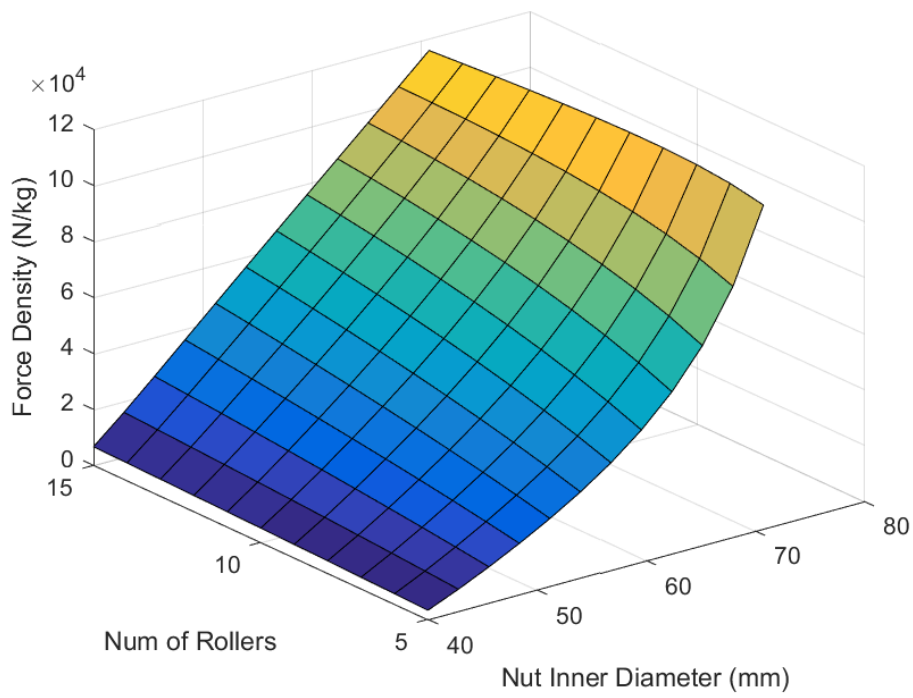
#### 6.5.2.1 Dominant Parameter: Nut Inner Diameter ( $d_n$ )



**Figure 6.1 Force Density ( $d_n$  as dominant parameter)**



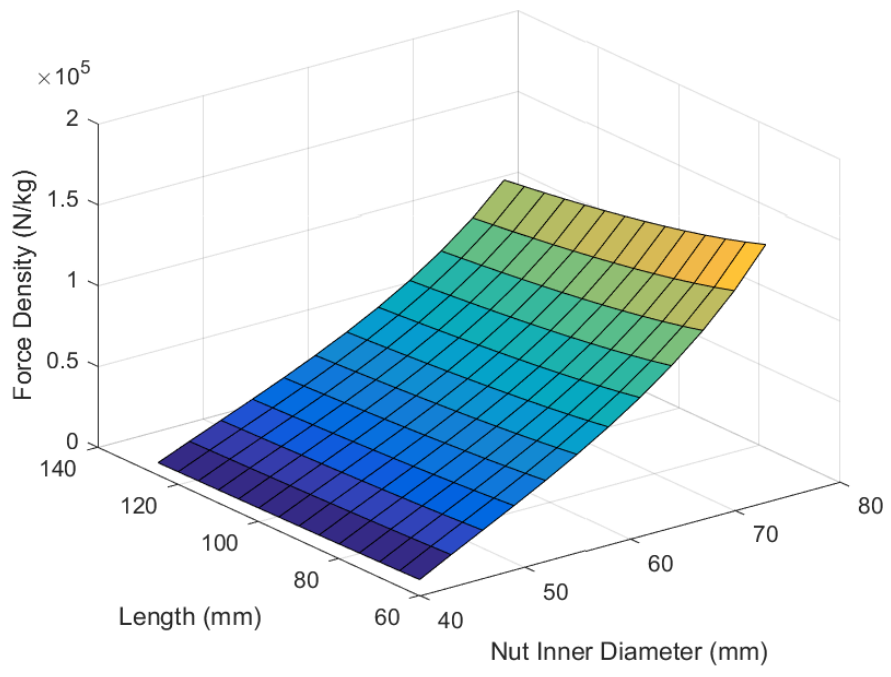
(c) Pitch



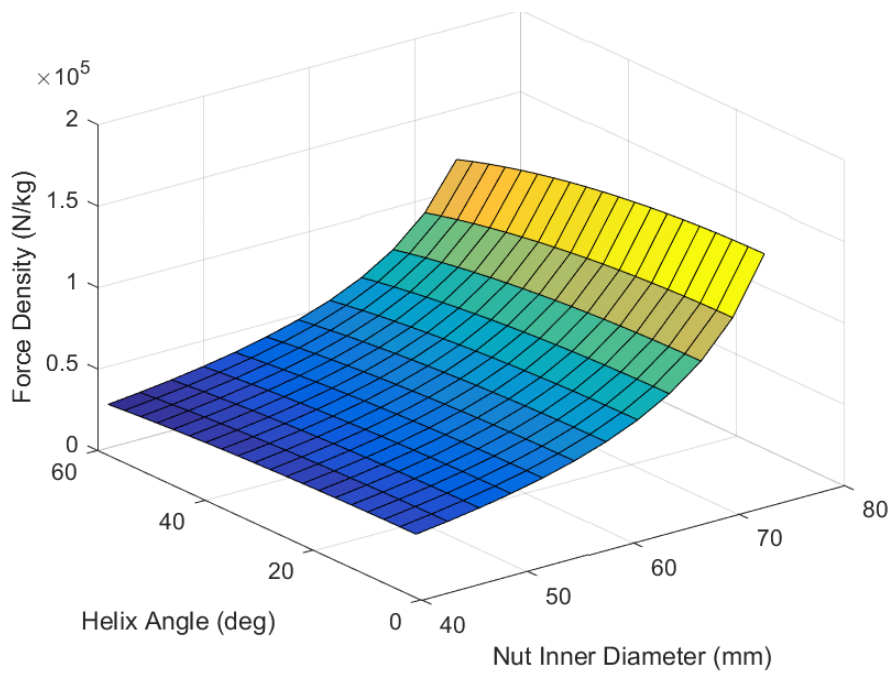
(d) Number of Rollers

Figure 6.1 Continued





(e) Length



(f) Helix Angle

Figure 6.1 Continued

Figure 6.1 shows the results of force density when the nut inner diameter is set as the primary parameter. Other parameters are chosen to combine with the nut inner diameter to achieve 3D maps. Figure 6.1 (a) presents the result of force density when screw diameter and nut inner diameter change. Because of the screw diameter and roller diameter interaction in the inner space of the PRS, force density decreases even as the screw diameter increases where nut inner diameter is fixed. This phenomenon continues until the nut inner diameter becomes about 65 mm. After this nut inner diameter point, force density increases when screw diameter increases. This is because the inner space is enough to accept the screw diameter increase. In other words, nut inner diameter increase compensates for the effect of screw diameter increase. Moreover, the map shows that load capacity passes the effect of the weight at this point. It is important to find useful value for the nut inner diameter, which covers the loss from screw diameter increase or roller diameter increase. Figure 6.1 (b) proves that nut inner diameter is the dominant parameter and roller diameter brings small amount of force density increase even roller diameter increases. When results are compared between Figure 6.1 (a) and Figure 6.1 (b), the screw diameter and roller diameter need to be adjusted to find optimal force density. Figure 6.1 (c) and Figure 6.1 (d) give similar 3D plots; however, pitch causes a higher force density value because the number of rollers increases weight. An interesting part from both cases is that the effect of each parameter brings nonlinear value change where the nut inner diameter is large. This point begins at about 65 mm. Force density value change is much steeper in the case of pitch increase. This means pitch and the number of rollers should be considered as dominant parameters in the process of PRS design. Figure 6.1 (e) and Figure 6.1 (f) are the results when length and helix angle change based on the nut inner diameter change. Results indicate that the length and helix angle have minor effect in the perspective of force density. Especially, length change causes load capacity increase, however, it also increases weight. These characteristics make balance of two different value changes to cancel each other. Overall, three diameter factors such as nut inner diameter, screw diameter, and roller diameter verify that those parameters have major effect on force density. In addition, pitch and the number of rollers are also verified that those parameters have some effect on force density

following the result in Figure 6.1. However, the last two cases such as length and helix angle doesn't seem to have a major impact in terms of force density under the condition of nut inner diameter change.

6.5.2.2 Dominant Parameter: Screw Diameter ( $d_s$ )

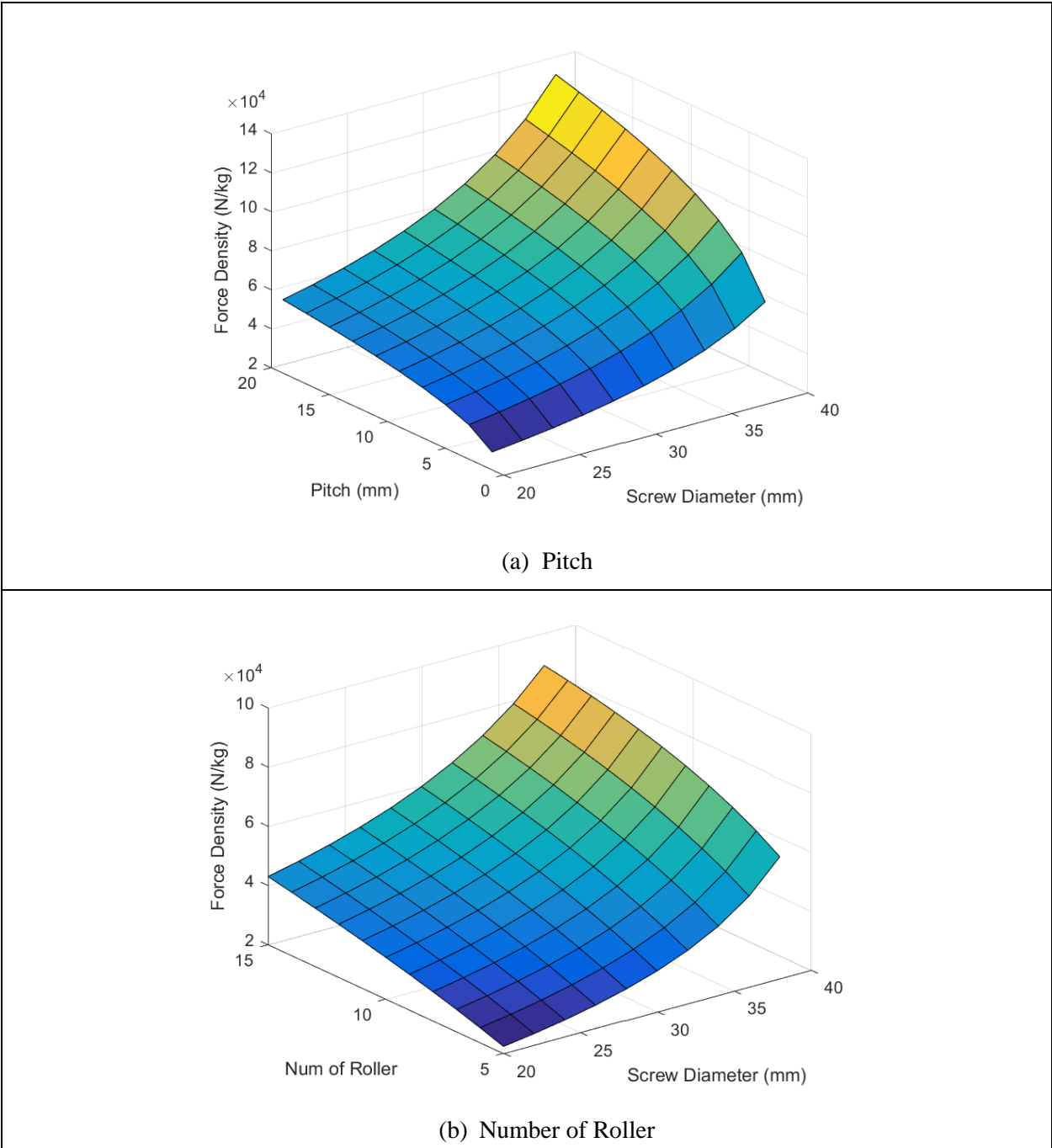
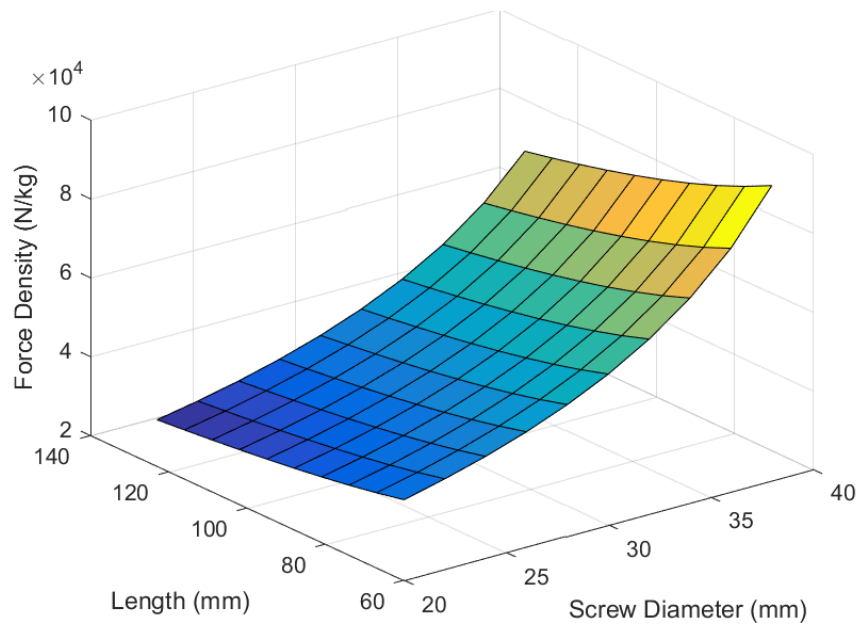
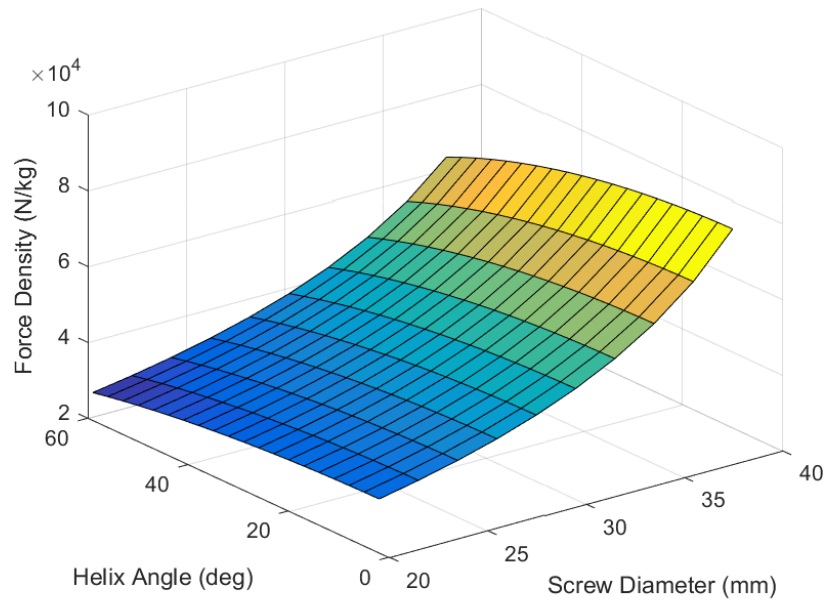


Figure 6.2 Force Density ( $d_s$  as dominant parameter)



(c) Length



(d) Helix Angle

Figure 6.2 Continued

Figure 6.2 shows the result of force density based on related parameter changes. In this case, the nut inner diameter is set to change its value in keeping with screw diameter change. The ratio is

suggested as  $\frac{5}{3}d_s$  following the general experience rule. Figure 6.1 (a) shows the result when screw diameter changes under the condition of fixed nut inner diameter. Then, unfixed nut inner diameter condition needs to be analyzed. All the results of Figure 6.2 shows that force density increases when the screw diameter increases. This proves that more inner space can result in higher force density. Interesting part from result Figure 6.2 (a) is that the effect of pitch increases as screw diameter increases. The force density map of each pitch value becomes more nonlinear from about 35 mm screw diameter. In addition, this result suggests that a larger pitch value is needed to achieve higher force density. The result shows that force density is extremely low under 2 mm. Figure 6.2 (b) and (c) present opposite results in terms of secondary parameter change. As mentioned, the number of rollers causes weight and load capacity increase. And length increase also increases weight and load. However, effect of length increase is much bigger than the number of rollers increase on the weight. This means that length increase can cause negative effect in terms of force density. On the contrary, the result shows that more rollers gives higher force density and it brings higher load capacity. Figure 6.2 (d) is the result of force density when the screw diameter and helix angle change. This proves that helix angle doesn't have much effect on force density. Overall, pitch and the number of rollers demonstrate a major role in force density and we need to be careful to choose length of PRS because of its influence as shown in Figure 6.2 (c).

### 6.5.2.3 Dominant Parameter: Roller Diameter ( $d_r$ )

Figure 6.3 is the result when related parameters change under the condition of roller diameter variable as the primary parameter. Results gives similar maps compared to Figure 6.2. The difference is the major change when roller diameter increases. The roller diameter change does not cause heavy weight change compared to the nut diameter change or length change. However, it does give a higher load capacity change when it increases. Figure 6.3 (b) shows this comparison. In the roller diameter side, a high force density increase as the roller diameter increases. Force density doesn't change much due to the length increase. Pitch change also gives dynamic value

increase when it is small. Force density rapidly increases about the 2 mm pitch value. When the roller diameter and number of rollers are combined, force density doesn't increase much when using small values for them.

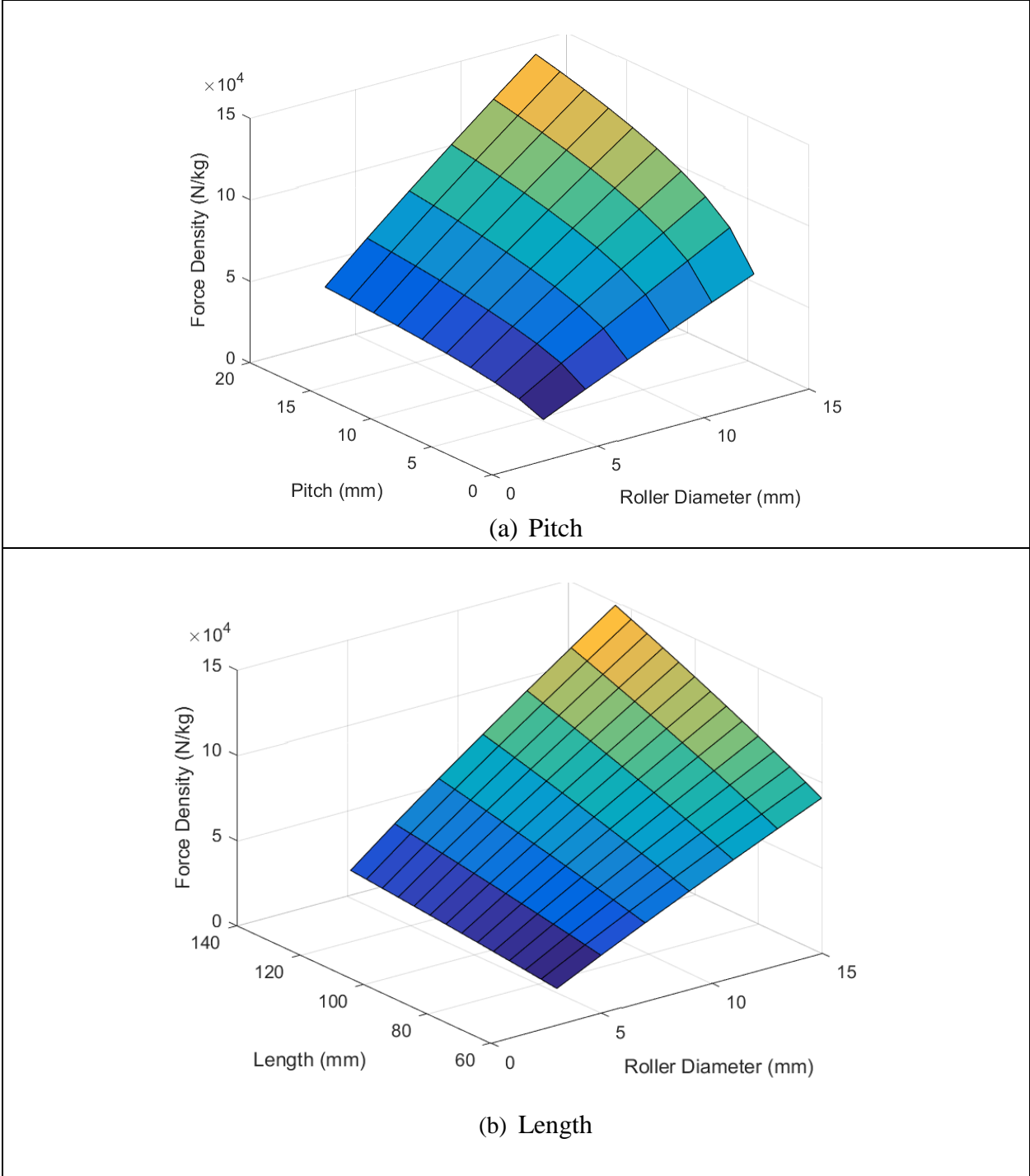
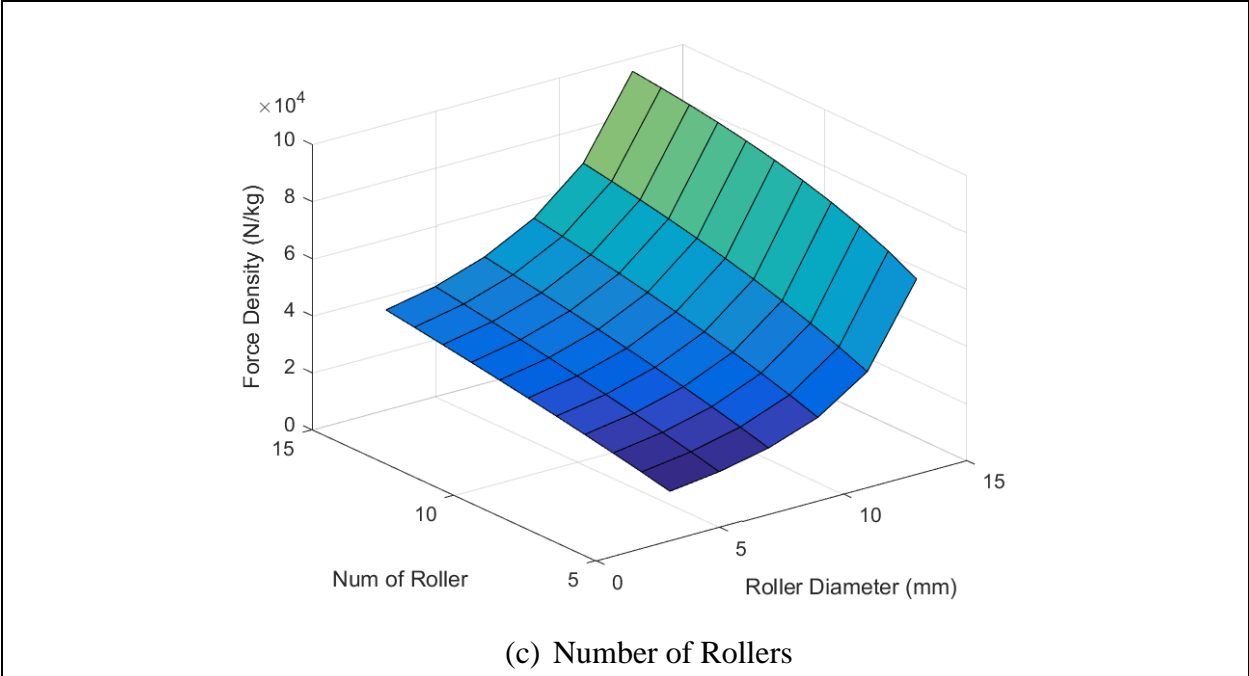
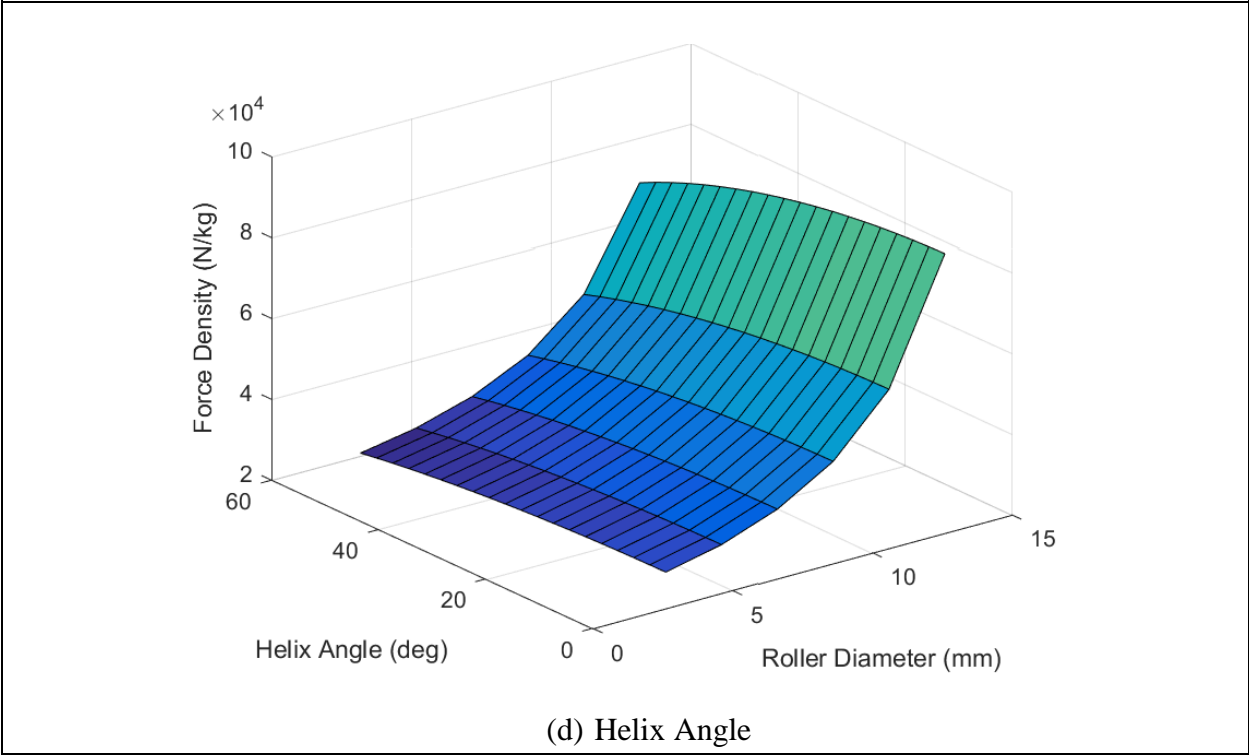


Figure 6.3 Force Density ( $d_r$  as dominant parameter)



(c) Number of Rollers



(d) Helix Angle

Figure 6.3 Continued

These two factors increase weight of rollers and cause total weight increase. Even though both of them are closely related to load capacity increase, weight increase is more effective in terms of force density when both parameters' value is low. However, the maps show that an increase of

the two parameters to achieve higher force density. Thus, higher values of roller diameter and number of rollers are important under the allowed inner space and weight condition. The helix angle has minor effect in this result.

6.5.2.4 Dominant Parameter: Length (L)

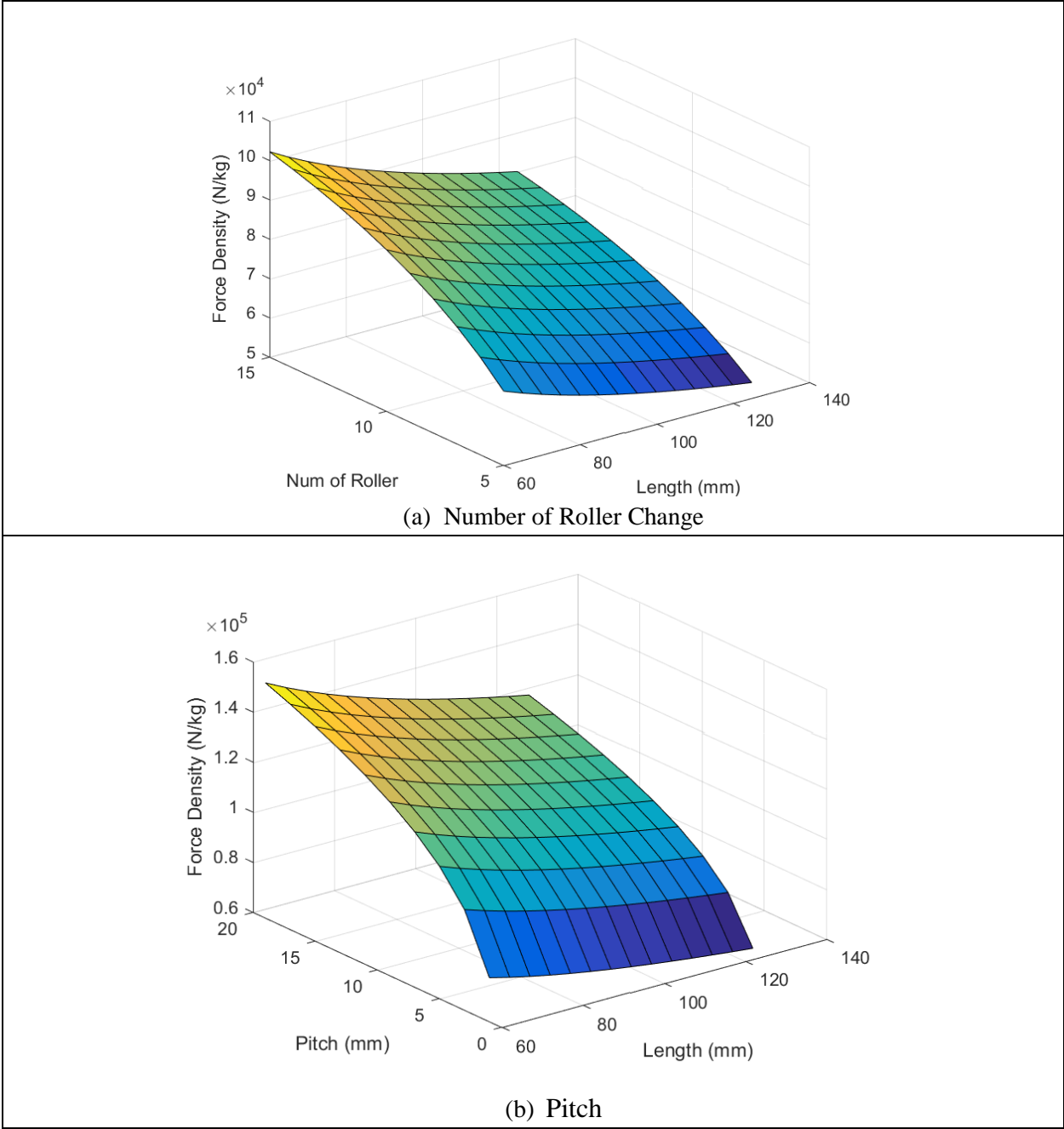


Figure 6.4 Force Density (L as dominant parameter)



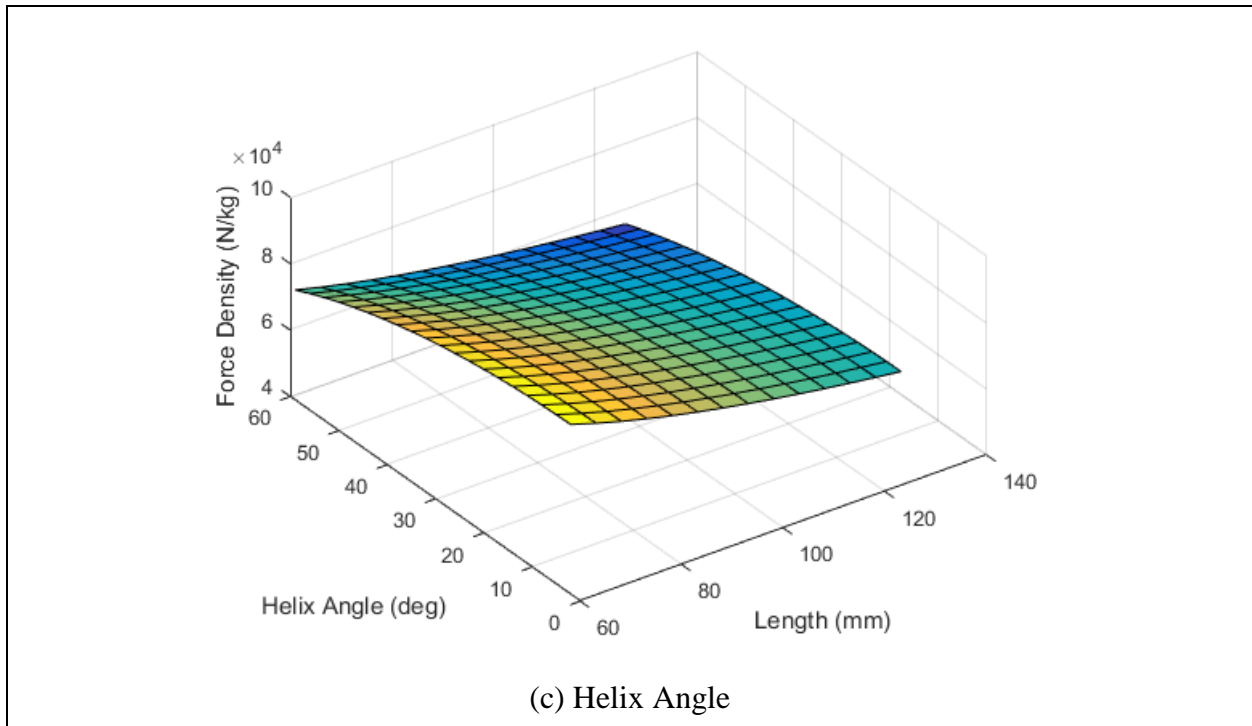


Figure 6.4 Continued

Figure 6.4 presents the results of force density when length is set as the dominant parameter. Under this condition, other related parameters are combined with length to find the effect on force density.

As shown, length doesn't have a major effect on force density because of the associated weight increase. However, Figure 6.4 (a) and (b) show the growth effect of the number of rollers and pitch. The number of rollers increases the total weight and force density increase is smaller than the pitch change case. The case of helix angle change give less change for force density. Overall, number of rollers and pitch have a major role for force density. And the length of the PRS can lower force density because of the associated weight increase and its effect on the force density.

#### 6.5.2.5 Dominant Parameter: Pitch ( $p$ )

Pitch is set as a primary parameter in Figure 6.5. Other parameters are number of rollers and helix angle. The number of rollers have a significant effect on the force density. Figure 6.5 (a) shows the result when pitch and the number of rollers vary. Pitch shows a rapid change when its value is

small. That change occurs near 2 mm. After this point, force density caused by pitch increases almost linearly.

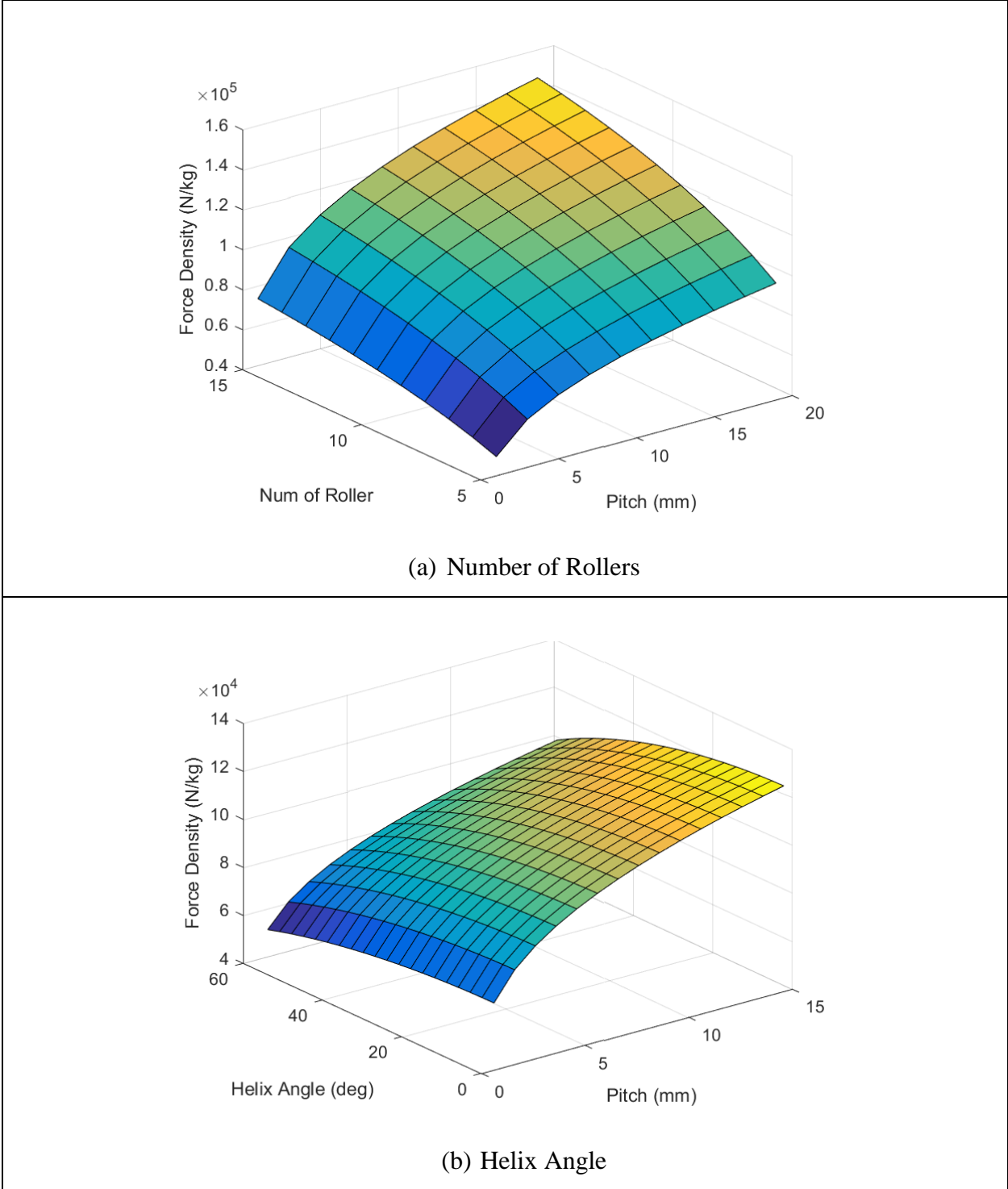
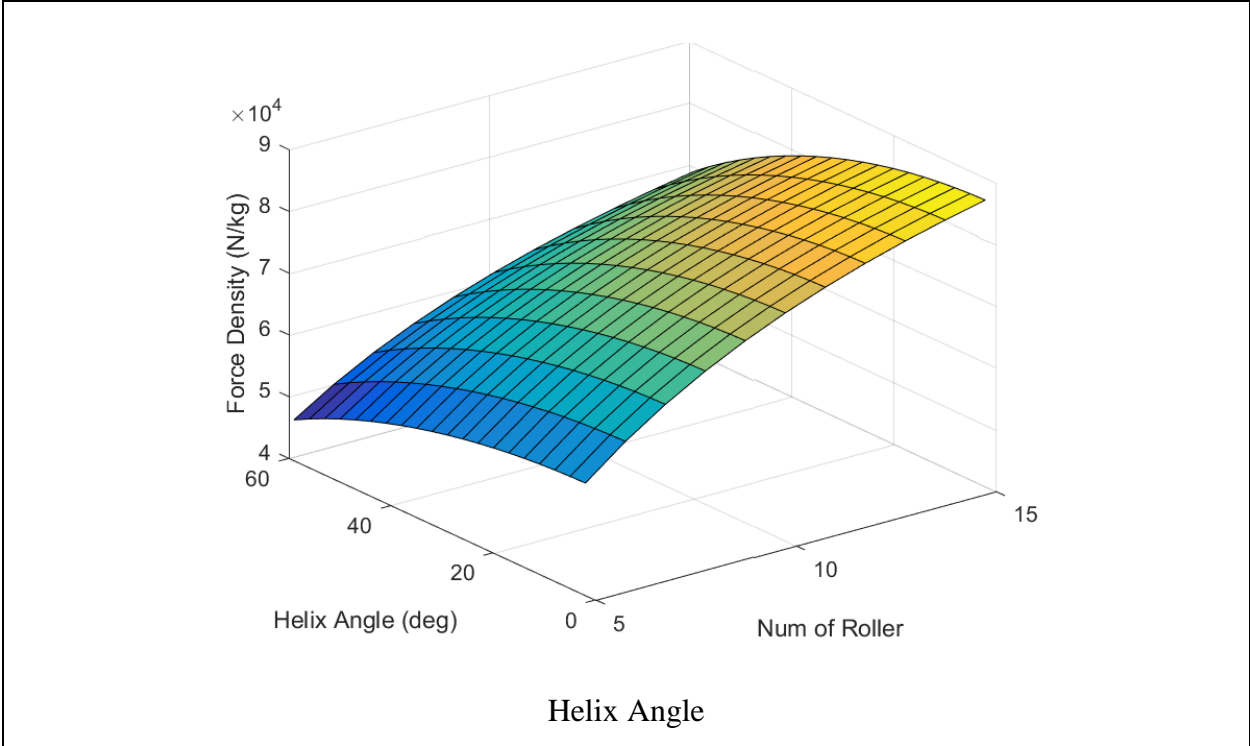


Figure 6.5 Force Density (*p* as dominant parameter)

The number of rollers increases force density. Even though the number of rollers increases total weight, the relative increase of load capacity is more than the weight increase. This indicates that more rollers gives higher force density. Then, if feasible, it is important to add more rollers in the PRS system under the allowable constraint of inner space. On the contrary, the helix angle doesn't have significant impact on force density. Overall, pitch and the number of rollers are dominant parameters in terms of force density and those parameters need to be further discussed in the chapter of combined categories later.

6.5.2.6 Dominant Parameter: Number of Rollers ( $N_r$ )



**Figure 6.6 Force Density ( $N_r$  as dominant parameter)**

Figure 6.6 shows the result of force density when the number of rollers is set as a dominant parameter. Helix angle is set as the secondary parameter in this case. Helix angle change makes a small difference as it increases. It can't be considered as a dominant parameter.

## 6.6 Chapter Conclusion

Force density is the concept of load capacity per unit weight and is a non-dimensional value. Force density suggests how effective load capacity is when it is compared to total weight. First of all, helix angle is considered as less important because it gives little force density changes in all cases. The number of rollers and roller diameter have a major effect on force density. However, the effect of these parameters becomes less significant when they both increase at the same time even though the value of force density still increases. Because of this, setting appropriate the roller diameter and the number of rollers is important keeping in mind the constraints of limited weight and inner space. As shown, nut inner diameter is a most dominant parameter relative to force density because it is the main factor to decide inner geometry. In other words, nut inner diameter allows enough space for roller and screw to achieve higher value of force density. This is the reason that those three diameters are dominant parameters for the PRS design and the results prove their effect on force density. Pitch is a significant parameter that also has a large effect on force density. Pitch is already considered as important parameter in Chapter 5. Load Capacity because of its effect on load capacity. Pitch increase causes a load capacity increase yet it doesn't add to weight. Thus, pitch is a good factor to achieve higher force density value. However, pitch value needs to be limited because it gives the opposite result in terms of total deformation and total stiffness of threads. Overall, pitch is a critical factor to design the PRS. Like the number of rollers, length increases total weight and load capacity in the same time. As shown, the 3D plot of length change doesn't give an outstanding change of force density. This is because weight increase caused by the PRS length increase is significant relative to its linear increase of load capacity. Then, if there is a weight limitation, it is recommended that other parameters to be changed that do not affect weight.

Overall, effect of each parameter on load capacity can be arranged as:

Parameter	Effect
Nut Inner Diameter $d_n$	It affects the inner space of the PRS and the thickness of the nut. It makes a non-linear curve as it changes. When it has a high value, the force density is high because it increases the inner space of the PRS and decrease the weight of the nut under the condition of fixed nut thickness.
Screw Diameter $d_s$	It affects the roller diameter and the nut inner diameter. It makes a non-linear increase of load capacity. Roller diameter decreases with a screw diameter increase. However, it also decreases weight of the rollers and nut. This provides a high force density when screw diameter increases.
Roller Diameter $d_r$	It affects the inner space of the PRS and provides a non-linear curve in terms of the force density. Because its increase is not larger than the screw diameter or nut inner diameter, it provides a modest increase in the load capacity when it increases compared to other diameters change.
Length $L$	It affects the weight and number of total contact points in the PRS and gives a somewhat non-linear curve as it changes. Longer length provides lower force density because of the effect of weight.
Number of Rollers $N_r$	It affects the weight and number of total contact points in the PRS. It gives higher load capacity as it increases; however, the value change is not high because it also increases weight.
Pitch $p$	It affects the lead of the PRS movement. And it gives a non-linear curve. Pitch increase provides a load capacity increase.
Helix Angle $\beta_0$	It has almost no effect on force density.

**Table 6.2 Parameter Effect on PRS for Force Density**

And each parameter can be classified as:

Primary Parameters	Support Parameters	Fixed Parameters
$d_n$ : Nut Inner Diameter $d_s$ : Screw Diameter $d_r$ : Roller Diameter $p$ : Pitch $N_r$ : Number of Rollers	$\beta_0$ : Helix angle	$D_n$ : Nut Outer Diameter $\alpha_0$ : Contact Angle $N_s$ : Number of starts $f_c$ : Dimensionless Geometric Factor $L$ : Length

**Table 6.3 Parameter Classification for Force Density**

## **CHAPTER 7. MAP / ENVELOPE DESIGN PROCESS:**

### **Part 1 – Groundwork Formulation for a Planetary Roller Screw**

For several decades, the planetary roller screw (PRS) has been under development since it was invented in 1954 by Strandgren [1] in his patent when the PRS is considered as a key component of linear electro-mechanical actuators (EMA). Recently, the electro-mechanical actuator (EMA) has received more attention as a significant component for future intelligent mechanical devices because of its advantages compared to traditional pneumatic or hydraulic actuators and the equivalent mechanical ball screw. These PRS based EMAs provide better performance by integrated design, extended durability and easy set up and installation. In addition, EMAs also excel in terms of perspective of precision and efficiency because EMA's produce more accurate motion control and reduce maintenance, operational cost, and energy consumption. The most important advantage is that there are no leaks, which is the weakest characteristic of hydraulic systems. Because of these, EMAs are considered to replace hydraulic and pneumatic actuators and are targeted for key applications such as aircraft surface control [2] and modern ship operation [3].

As the EMA becomes more important, the study of the PRS is also expanded for good design to enhance the EMA's efficiency and performance. The PRS is a mechanical device with low friction and high precision which is also called the planetary roller screw mechanism (PRSM). This mechanism converts rotational motion into linear motion or vice versa. The principle of the planetary roller is similar to the ball screw. The difference is that the PRS uses threaded rollers to transfer the load between the nut and the screw. The PRS is typically composed of three main components. The main components are the nut, the screw shaft, and the timed planetary rollers. As the screw shaft turns, its helical raceway meshes with the rollers that radially surround the screw shaft. During this operation, the rollers engage with threads on both the screw shaft and the nut. As will be mentioned and provided, the PRS is receiving considerable interest in both the research community and in industry to expand its application to areas such as medical, machine tools, aircraft, and military platforms. As mentioned above, the planetary roller screw (PRS) is a

mechanical transmission device, which converts rotary motion to linear motion. Many benefits exist relative to conventional transmission devices and it is becoming more widely used. These benefits relative to the ball screw are larger load carrying capability ( $\approx 3x$ ), better durability ( $\approx 30x$ ), less vibration, and higher precision in working conditions. Because of these advantages, the PRS is now being applied to many areas such as aerospace, precision machines, robotics, and modern ships. Previous work on the PRS focused on its kinematics and related applications. Otsuka et al. [5] investigate operating principles and provide angular factor relationships and structural configuration factor relationships such as the number of thread starts and each component diameter. Research on kinematics of the PRS was done by Velinsky et al. [6]. They focus on the relationship of each component's angular motion analysis and linear motion velocity. Jones et al. [7] derive the nature of the contact kinematics between the load carrying surfaces and provide several geometric relationships. Jones [8] discusses the kinematics of the PRS and develops a new approach to calculate stiffness and thread load distribution based on a direct stiffness method. In addition, he analyzes each component's stiffness and provides a stiffness matrix as a result. He does some parameter study; however, it does not utilize all parameters of the PRS. Lemor [9] discusses efficiency of the planetary roller screw and analyzes its advantages in terms of load capacity, life time, and efficiency. A formula is proposed to calculate the dynamic load carrying capacity of the PRS compared to conventional ball screws. However, he doesn't focus on parameter relationships and each parameter's effect on the PRS system. Otsuka et al. [10] examines theoretical load capacity and displacement results in comparison with experimental values. First, they compare the load distribution between the planetary roller screw and the ball screw. Zhang et al. [11] analyze Hertzian contact deformation and thread deformation and provide related formulas to calculate both based on contact mechanics. However, they provide limited analysis of parameter relationships and the effect of those parameters, which are an important part of the PRS design. Yang et al. [12] develop a load distribution formula. This equation is used for further research as developed by Ma et al. [13]. They analyze the rolling condition of the PRS and



expand previous research conditions and formulas. In addition, they investigate deformations on the thread and the load distribution is calculated based on the effective ball concept of contact points. They conduct several cases of parameter relationship analysis; however, the cases are limited. Recently, Zhang et al. [14] discuss stiffness based on the assumption that considers contact points as springs and suggests an improved approach to load distribution by adjusting thread related factors. In addition, they provide formulas to calculate thread stiffness, which is an important element for total screw thread stiffness. However, they don't provide fundamental relationships among the design parameters and their impact on the PRS. Lisowski et al. [15] investigate a computational model of the load distribution on the threads of the PRS. They consider the deformation of the component of the PRS as deformation in terms of rectangular volumes and verify the result with a finite element model. They provide results for comparison between the analytical model and numerical results; however, they focus less on the design process, which is a critical part of PRS development as pursued herein.

Overall, the listed literature does investigate numerous detailed topics to analyze the planetary roller screw. However, most of these do not focus on parameter effects on the PRS overall design. Even though several papers investigate formulas such as thread stiffness and load distribution - Ma [13] and Zhang [14] - and provide formulas for dynamic load capacity - Lemor [9]; however, there is not much analysis on parameter relationships and the effect of those parameters on the design of the PRS. For better understanding of the PRS analysis and real world applications, it is important to investigate how many related parameters exist for the PRS design and to determine the effect of these parameters relative to each other. In addition, it is also critical to analyze the parameter effect on the PRS. The intent in this work is to extend the previous work to further understand the impact of the controlling parameters and develop a useful design process.

This paper investigates the PRS parameter effect on four performance measures by combining the maps into envelopes. This process makes it easy to monitor the parameter's role in

all combinations. There are several parameters that are dominant for the PRS such as nut outer diameter, nut inner diameter, screw diameter, roller diameter, and pitch. Three of these parameters are related with nut thickness. Then, the role of nut thickness  $T_n$  (which is dependent on nut outer diameter, roller diameter, and screw diameter) since it then is not an independent design parameter. Note that nut thickness has an important effect on the PRS. In order to analyze the role of the nut thickness in the PRS, its volume is calculated, which is fundamental to all performance measures. Then volume is compared to the effects on the three measures derived by choosing nut outer diameter, screw diameter, and roller diameter. Load distribution is excluded in this comparison process, which will be discussed in detail later in this paper. After that, choosing a dominant design parameter is necessary to build 3D maps to investigate other effective parameters. Here we choose pitch ( $p$ ) as the dominant parameter because it gives the most non-linear results to all four performance measures. In other words, pitch needs to be dealt with carefully. There are four other key parameters to make 3D maps. These are nut outer diameter, screw diameter, roller diameter, and the dependent nut thickness. Then, there will be 12 individual maps before combining into envelopes. As known, load distribution represents how much load is applied on each thread when total axial load is applied on the PRS. In other words, one axis ( $x$ ) in the 3D map is fixed as the pitch for threads of the PRS components and the other axis ( $y$ ) represents each of the other three parameters in sequence. Load distribution is excluded here. Instead of using curved load distribution on each thread, the average axial thread load is used for the stiffness calculation. Three measures are combined to analyze parameter effect on the performance measures of the PRS. As mentioned above, the average thread load is used for the map combining process in order to analyze the effect on all three measures in the form of envelopes. The average load can be obtained by dividing the total axial load with the number of rollers and the number of threads. In terms of the method of combining these measures, there are two distinct methods. One is adding each performance map value. The other method is multiplication of each map. We need to compare these two methods and choose the one that best expresses each measure's characteristics as the

design parameter varies. Note that each map must be normalized by dividing map all values by the RMS for the map before comparative review on combining into envelopes is possible.

## 7.1 Volume and Measures Comparison Analysis

PRS volume is calculated by using cross-sectional area and length. Volume is included as a factor in supporting formulas of measures. And this volume consists of two individual volumes. One is nut volume and the other is roller volume. In terms of the nut volume, nut outer diameter is the main factor. And nut outer diameter is also related to nut thickness ( $t_n$ ), which is an important factor for weight. Nut thickness is dependent on three independent parameters. Those factors are nut outer diameter, screw diameter, and roller diameter. Clearly, thickness is an important factor to determine load distribution on threads, weight, and force density. A small thickness can cause poor load distribution in the PRS and it can harm total system load capacity. On the other hand, thickness provides low force density when it is large. Because of this, thickness needs to be carefully analyzed in detail. The formula to calculate nut thickness can be expressed as:

$$T_n = D_n - d_n = D_n - d_s - 2d_r \quad (7.1)$$

where,

$T_n$  = Nut Thickness

$D_n$  = Nut Outer Diameter

$d_s$  = Nut Inner Diameter

$d_s$  = Screw Diameter

$d_r$  = Roller Diameter

Then, the formula for the total volume can be expressed as:

$$V_{total} = \pi \{(D_n^2 - d_n^2) + N_r d_r^2\} L = \pi \{(D_n - d_n)(D_n + d_n) + N_r d_r^2\} L \quad (7.2)$$

As shown, total volume includes nut volume and roller volume where nut thickness is implicit. In order to compare values between volume and other resulting values of performance measures, formulas are needed. First, total stiffness can be established by adding Hertzian and thread deformation based on contact theory [21], Harris [22], and Yamamoto's analysis [20]. Total deformation is expressed as adding these deformations [13]:

$$\delta_{total} = \delta_{hn} + \delta_{hs} + \delta_{tn} + \delta_{ts} \quad (7.3)$$

where,

$\delta_{total}$  = Total Deformation

$\delta_{hn}$  = Hertzian Deformation Nut Side

$\delta_{hs}$  = Hertzian Deformation Screw Side

$\delta_{tn}$  = Thread Deformation Nut Side

$\delta_{ts}$  = Thread Deformation Screw Side

Then, total stiffness can be expressed as:

$$k_{total} = \frac{F_{axial}}{\delta_{total}} \quad (7.4)$$

where,

$k_{total}$  = Total Stiffness

$F_{axial}$  = Axial Load on Thread

$\delta_{total}$  = Total Deformation

Second, load capacity is expressed by Lemor [9] as:

$$C_a = f_c (\cos(\alpha_0))^{0.86} N_c^{\frac{2}{3}} D_c^{1.8} \tan(\alpha_0) (\cos(\beta_0))^{\frac{1}{3}} \quad (7.5)$$

where,

$C_a$  = Dynamic Load Capacity

$f_c$  = Geometric Factor of PRS System

$\alpha_0$  = Contact Angle between Contact bodies ( $45^\circ$ )

$N_c$  = Total Number of Contact Point

$D_c$  = Diameter of Rolling Element at the Contact Point

$\beta_0$  = Helix Angle of the Thread

The diameter of the rolling element at the contact point is defined by Lemor [9] as:

$$D_c = \left( (2.5p) d_r 2^{\frac{1}{2}} \right)^{\frac{1}{2}} \quad (7.6)$$

Last, weight is presented by Timken Steel [28] as:

$$W_t = 0.006165 d_r^2 N_r L + 0.02466(D_n - T_n)T_n L \text{ (kg)} \quad (7.7)$$

where,

$W_t$  = Total Weight

$D_n$  = Nut Outer Diameter

$d_r$  = Effective Diameter of Roller

$N_r$  = Number of Roller

$T_n$  = Thickness of the Nut

$L$  = Length (meter)

With equation (7.1) – (7.7), volume and three performance measures can be calculated and compared. In order to analyze the relationship among them, parameter changes and tables can be established in terms of the nut outer diameter ( $D_n$ ), screw diameter ( $d_s$ ), roller diameter ( $d_r$ ).

First, the nut outer diameter range is set as 54 – 81 mm and screw diameter range is set as half of the nut outer diameter. Proportions of the screw diameter comes from CMC's catalog [17]. Then, the roller diameter is set as two ranges to investigate the role of nut thickness, which is a major factor for volume. Roller diameter increases at 1 mm increment in the first case. This provides the case where nut thickness decreases. Then, the roller diameter is set as  $\frac{1}{3}$  of the screw diameter following a general rule of thumb, which is introduced in the patent by Strandgren [1]. Based on these two cases, we suggest 10 values for each case. The table for the first case is presented as:

Nut Outer Diameter (mm)	Screw Diameter (mm)	Roller Diameter (mm)	Nut Thickness (mm)	Volume (m <sup>3</sup> )	Stiffness ( $\frac{N}{mm}$ )	Load Capacity (kN)	Weight (kg)	Force Density ( $\frac{kN}{kg}$ )
54	27	9	9	0.763	10672.1	165.082	1.498	110.194
57	28.5	10	8.5	0.851	9353.2	182.095	1.633	111.502
60	30	11	8	0.944	8170.23	198.900	1.772	112.257
63	31.5	12	7.5	1.043	7112.49	215.518	1.914	112.587
66	33	13	7	1.148	6168.84	231.969	2.060	112.588
69	34.5	14	6.5	1.258	5328.19	248.268	2.210	112.331
72	36	15	6	1.374	4579.96	264.429	2.364	111.873
75	37.5	16	5.5	1.496	3914.25	280.464	2.521	111.257
78	39	17	5	1.623	3321.97	296.382	2.682	110.517
81	40.5	18	4.5	1.756	2794.88	312.192	2.846	109.680

**Table 7.1 1<sup>st</sup> Case of Volume and Values of Measures Comparison**

Table 7.1 shows the results between volume and other values for the three performance measures. The volume increases even though nut thickness decreases because of the roller diameter increase. When the volume increases, total stiffness on the thread decreases. This is because the nut thickness decreases. On the other hand, weight and load capacity increase when volume increases. This comparison result is presented in Figure 7.1.

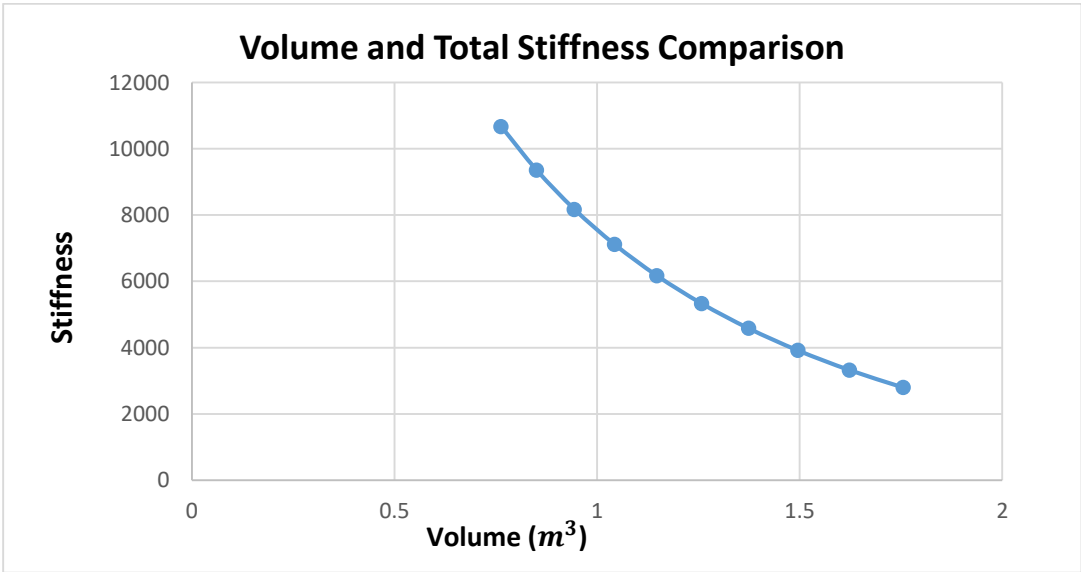


**Figure 7.1 1<sup>st</sup> Case of Volume and Total Thread Stiffness Comparison**

As mentioned above, volume and the total thread stiffness comparison provides an opposite proportional graph like Figure 7.1. This can be expressed as:

$$y = -1669.084733 x^5 + 13080.12347 x^4 - 42831.63605 x^3 + 75804.59582 x^2 - 77647.75201 x + 40816.78204 \quad (7.8)$$

where,

$x = \text{Volume}$

$y = \text{Total Thread Stiffness}$

A second useful comparison occurs when volume and load capacity (Figure 7.2) are compared to each other. This shows a different result compared to Figure 7.1.

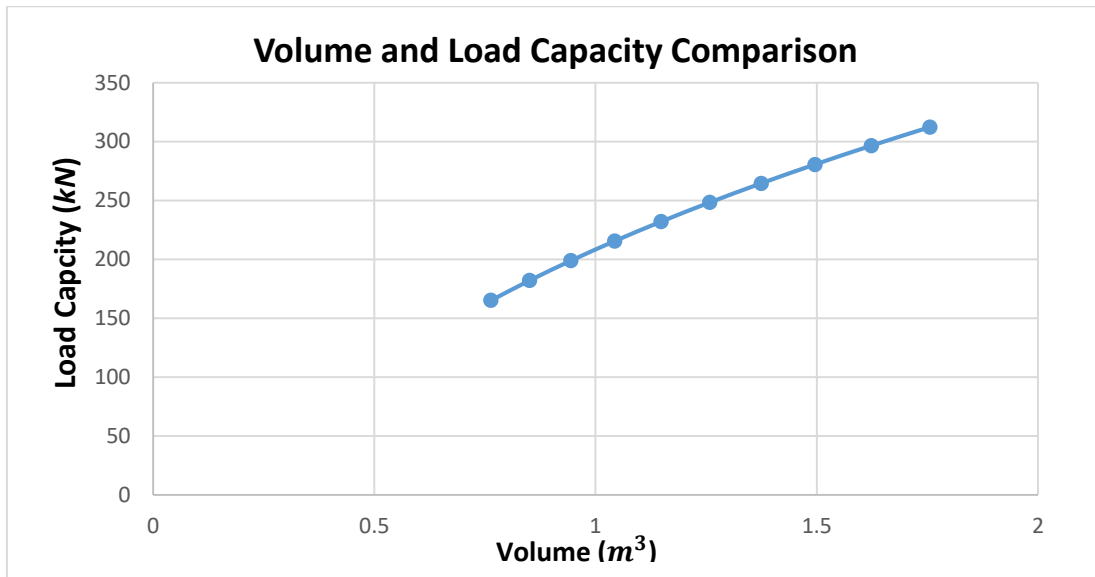


**Figure 7.2 1<sup>st</sup> Case of Volume and Load Capacity Comparison**

There a volume and total thread stiffness comparison provides a proportional increase graph. When volume increases, load capacity also increases. This relationship can be expressed as:



$$y = 8.803919974 x^5 - 67.96418356 x^4 + 220.2269572 x^3 - 397.9952443 x^2 + 530.2832892 x - 84.9710269 \quad (7.9)$$

where,

$x = \text{Volume}$

$y = \text{Load Capacity}$

Finally, volume and weight are compared to each other (Figure 7.3). This also as expected, provides proportional increase graph similar to Figure 7.2.

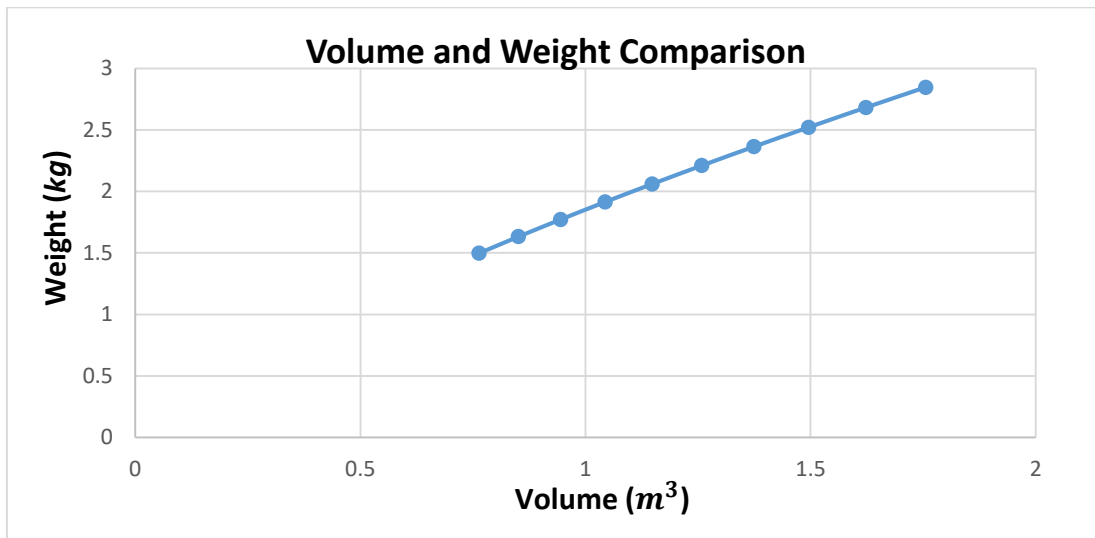


**Figure 7.3 1<sup>st</sup> Case of Volume and Weight Comparison**

Figure 7.3 shows the result of a comparison between volume and weight. Weight is an important factor in PRS design and it increases when volume increases. This relationship can be expressed as:

$$y = 2.901147059 \cdot 10^{-2} x^5 - 2.262064181 \cdot 10^{-1} x^4 + 7.453980657 \cdot 10^{-1} x^3 - 1.394046858 x^2 + 2.747646594 x - 4.936226644 \cdot 10^{-2} \quad (7.10)$$

where,

$$x = \text{Volume}$$

$$y = \text{Weight}$$

For the next case, roller diameter is set as  $\frac{1}{3}$  of the screw diameter as mentioned previously. In addition, screw diameter is set as half the value of the nut outer diameter. Then, the key parameter is the roller diameter. Overall, this causes the nut thickness to increase. And it provides some interesting results. The comparison table among volume and the other measures is presented in Table 7.2.

Nut Outer Diameter (mm)	Screw Diameter (mm)	Roller Diameter (mm)	Nut Thickness (mm)	Volume ( $m^3$ )	Stiffness ( $\frac{N}{mm}$ )	Load Capacity (kN)	Weight (kg)	Force Density ( $\frac{kN}{kg}$ )
54	27	9	9	0.763	10672.066	165.082	1.498	110.194
57	28.5	9.5	9.5	0.851	10263.574	173.313	1.669	109.093
60	30	10	10	0.942	9885.200	181.501	1.850	107.542
63	31.5	10.5	10.5	1.039	9533.732	189.649	2.039	105.694
66	33	11	11	1.140	9206.398	197.758	2.238	103.655
69	34.5	11.5	11.5	1.246	8900.796	205.830	2.446	101.501
72	36	12	12	1.357	8614.830	213.867	2.663	99.287
75	37.5	12.5	12.5	1.473	8346.667	221.870	2.890	97.052
78	39	13	13	1.593	8094.695	229.842	3.126	94.822
81	40.5	13.5	13.5	1.718	7857.490	237.783	3.371	92.619

**Table 7.2 2<sup>nd</sup> Case of Volume and Values of Measures Comparison**

Table 7.2 shows a second comparison case of volume and values of three performance measures. The difference between Table 7.1 and Table 7.2 is the roller diameter and nut thickness. In Table 7.1, roller diameter increases 1 mm for each set. Roller diameter increases by its dependence on the screw diameter in Table 7.2. Even though both cases increase roller diameter, changing the reference is the key. This difference governs the nut thickness for each case. In the first case, nut thickness decreases. However, nut thickness increases in the second case. In the second case,

volume increase causes stiffness to decrease but the value change is much smaller than in the first case. This is because of the nut thickness decreases. Even though nut outer diameter and screw diameter increase causes a total thread stiffness decrease, the nut thickness compensates for the total thread stiffness decrease. Volume increase also causes a high increase in the load capacity and weight compared to Table 7.1. However, the load capacity increase is not high even though volume increases. This is because roller diameter changes does not increase much compared to the first case. And Table 7.2 proves that nut thickness increase causes higher weight compared to Table 7.1. This phenomenon results in a lower force density. Overall comparison results among volume and the values of the other three performance measures are presented in Figure 7.4

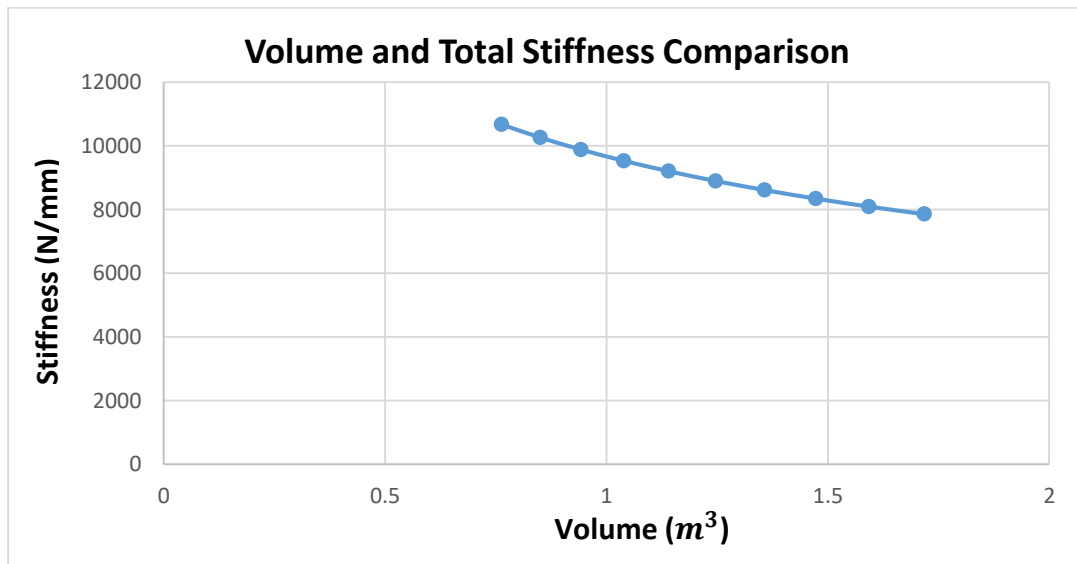


**Figure 7.4 2<sup>nd</sup> Case of Volume and Total Thread Stiffness Comparison**

Figure 7.4 shows the volume and total stiffness on the threads relationship when the nut thickness increases. Overall, the volume increase cause a stiffness decrease, which is shown in both cases in Figure 7.1 and Figure 7.2. However, nut thickness compensates for this stiffness decrease as presented in Figure 7.4. In other words, a thicker nut provides a higher stiffness on the threads and decreases total deformation. The relationship between volume and total stiffness can be expressed as:

$$y = -37.50696641 x^5 + 748.1918886 x^4 - 4059.119313 x^3 + 10326.7345 x^2 - 14885.44204 x + 17577.19917 \quad (7.11)$$

where,

x = Volume

y = Load Capacity

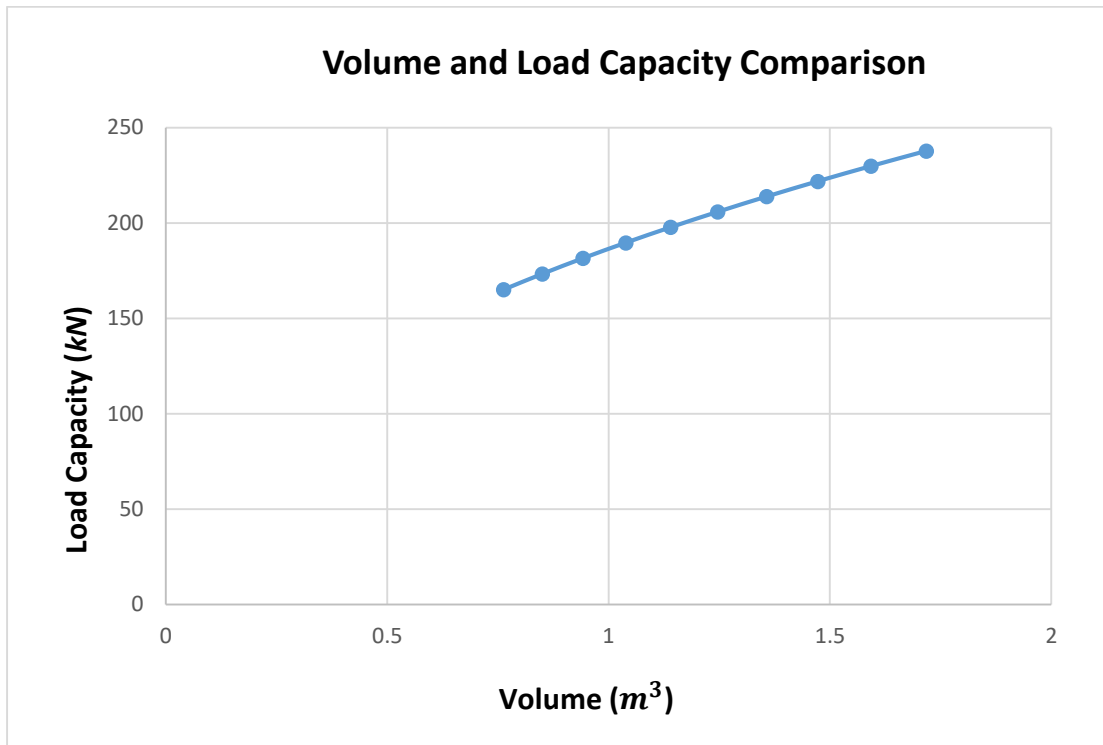


**Figure 7.5 2<sup>nd</sup> Case of Volume and Load Capacity Comparison**

Figure 7.5 shows the relationship between volume and load capacity. Load capacity increases when volume increases. However, it provides a lower load capacity when compared to Figure 7.2. This is because of the influence of the roller diameter. Even though nut thickness increases in this case, Figure 7.5 shows that the smaller roller diameter can cause a lower load capacity.

$$y = -5.762218356 x^5 + 34.06775475 x^4 - 71.12572861 x^3 + 43.03709984 x^2 + 103.9963808 x + 82.20940208 \quad (7.12)$$

where,

x = Volume

y = Load Capacity

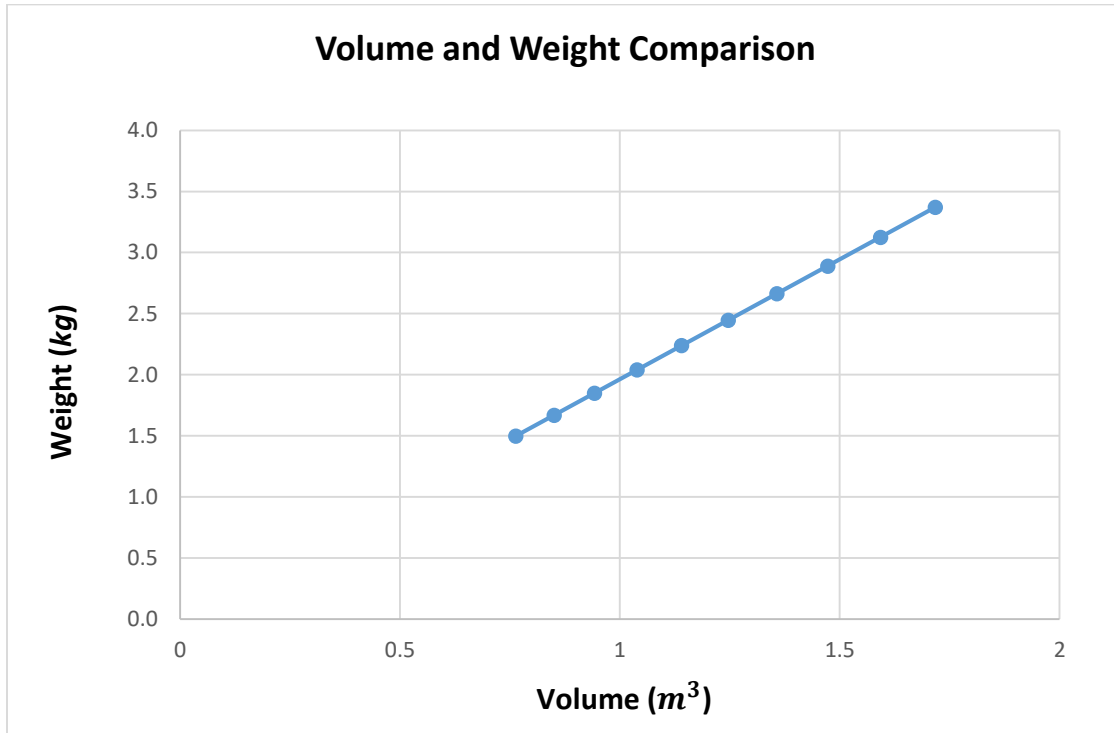


**Figure 7.6 2<sup>nd</sup> Case of Volume and Weight Comparison**

Figure 7.6 presents the result of relationship between volume and weight. This case provides heavier PRS weight compared to Figure 7.3. This means that an increase of nut thickness makes for a heavier weight of the PRS compared to the roller diameter increase case. Then, this can cause lower force density because this case provides heavier weight and lower load capacity compared to the first case as presented in Table 7.1 and Table 7.2.

$$y = -2.310565803 \cdot 10^{-1} x^5 + 1.470807143 x^4 - 3.669795483 x^3 + 4.476872057 x^2 - 7.035043836 \cdot 10^{-1} x + 6.196821555 \cdot 10^{-1} \quad (7.13)$$

where,

x = Volume

y = Load Capacity

Overall, volume has an important meaning to the PRS as shown analytically above. Volume increase can cause large changes in terms of the three principle measures. As known, volume depends on nut thickness, roller diameter, and length. Results from the first and second cases show how the nut thickness and roller diameter affect the PRS' stiffness depending on nut thread, load capacity, weight, and force density. Nut thickness provides higher stiffness on the threads; however, it causes a roller diameter decrease and total weight increase. And this inner geometry change affect results in a decrease of load capacity and force density. Overall, adjusting volume and parametric factors of the volume is a major issue for PRS design.

## 7.2 Dominant Parameter Relationship Analysis

Based on above analysis and previous analysis, there are 5 commonly used parameters that have a large effect on the PRS. Those parameters are nut outer diameter, nut inner diameter, screw diameter, roller diameter, and pitch. Pitch gives the most non-linear results in all four performance measures compared to the other parameters. Thus, we set pitch as the x-axis and set the other four parameters at the y-axis in this section where the z-axis becomes the performance of interest measure. In order to analyze the effect of nut thickness, we vary nut outer diameter for two cases and fix the nut outer diameter for the other two cases, say screw and roller diameter change. And root mean square is plotted to determine where the effect gives large PRS performance measures. The root mean square is expressed as  $M_{ts}$ ,  $M_{lc}$ ,  $M_{fd}$  each for total stiffness, load capacity, and force density. Because there are four maps for each performance measure, the number is attached next to symbol to distinguish each case.

### 7.2.1 Total Stiffness on Thread

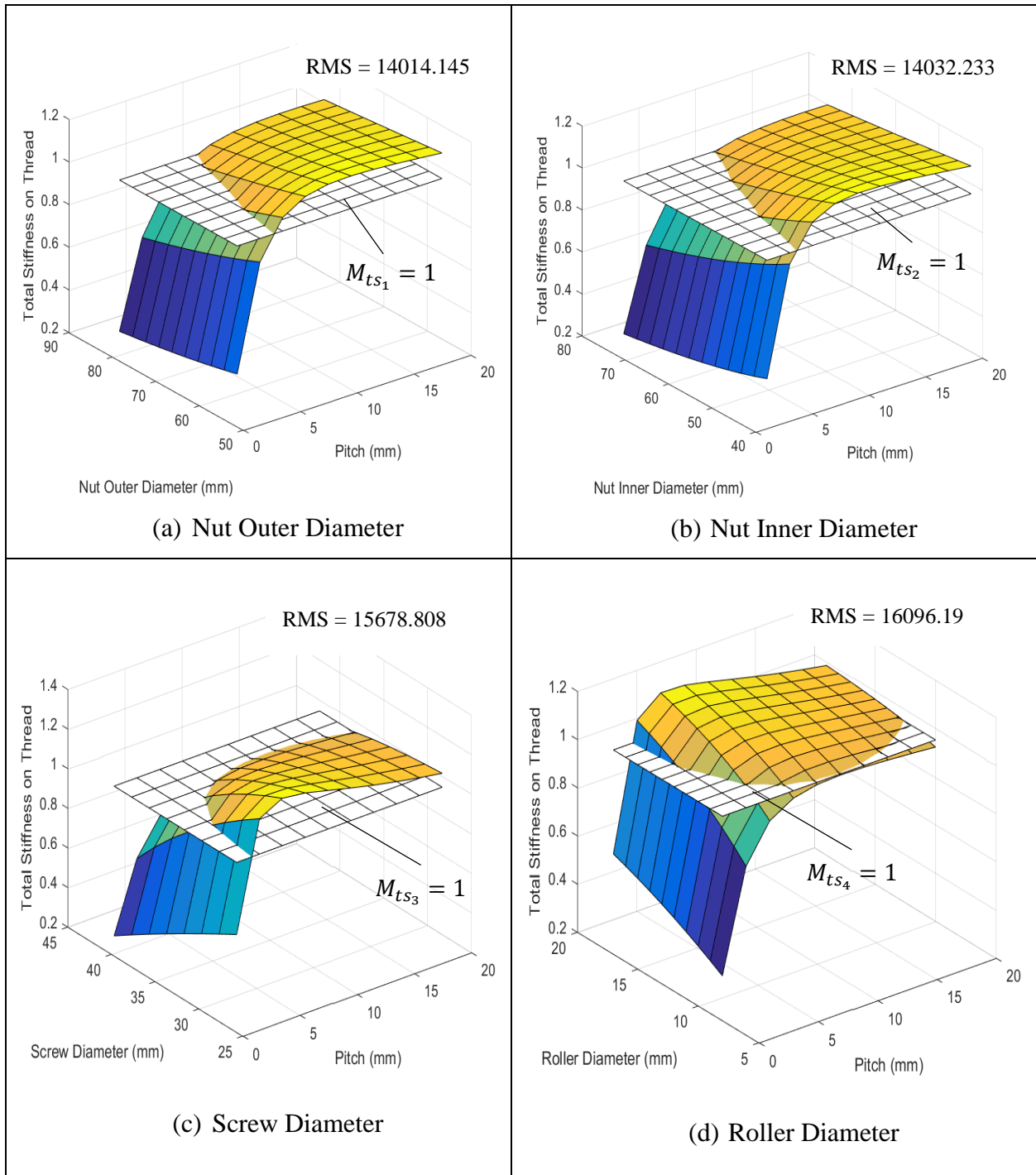


**Figure 7.7 Comparison of Total Stiffness on Thread**

Figure 7.7 shows map results of total stiffness on the threads when the pitch is set as the primary parameter. The other four parameters, the nut outer diameter, nut inner diameter, screw diameter, and roller diameter are set as secondary parameters. As mentioned, the root mean square is plotted

as  $M_{ts}$  to recognize the more useful parameter range for the PRS design. And each root mean square is distinguished as  $M_{ts1}$ ,  $M_{ts2}$ ,  $M_{ts3}$ , and  $M_{ts4}$  for the different parameter cases. In terms of total stiffness on the threads, there are decreases of total stiffness when the nut outer diameter, nut inner diameter, and screw diameter increase. However, the decreased value is not large. This is because the nut thickness is large enough to compensate for the total stiffness decrease as shown before. Even though the screw diameter increase causes a decrease of total stiffness when it is combined with pitch, this is because the nut thickness is a little smaller than the other two cases. On the contrary, total stiffness on the threads increases when roller diameter is combined with pitch. It increases the total stiffness up to a specific point and then it stops. Increase in the roller diameter also causes the nut thickness to decrease like the other inner geometric diameters. However, this result indicates that sufficient roller diameter is needed to achieve higher total stiffness on the threads. In terms of pitch variation, it does not need to be large in value. In this analysis, pitch only needs to reach a normalized value of 6 mm to achieve the maximum total PRS stiffness. Overall, achieving sufficient roller diameter is important while maintaining sufficient nut thickness in terms of the total stiffness on threads.

### 7.2.2 Load Capacity

Figure 7.8 presents the load capacity comparison when the pitch is set as the primary parameter. All four of the other parameters provide an increase of the load capacity with pitch increase. Root mean square values are drawn and expressed as  $M_{lc1}$  to  $M_{lc4}$  for each parameter case. These results indicate that nut thickness and sufficient roller diameter are needed to achieve higher load capacity. Figure 7.8 (a) and (b) vary the nut thickness and provide higher load capacity values than Figure 7.8 (c). Figure 7.8 (c) provides lower load capacity because of smaller nut thickness. On the contrary, Figure 7.8 (d) provides the highest load capacity value as the roller diameter increases. Even though roller diameter decreases the nut thickness, it proves again that the larger roller diameter is necessary to achieve higher load capacity. These different parameter



effects on the principal performance measures provide a key reason to utilize envelopes for more rapid and clearer understanding.

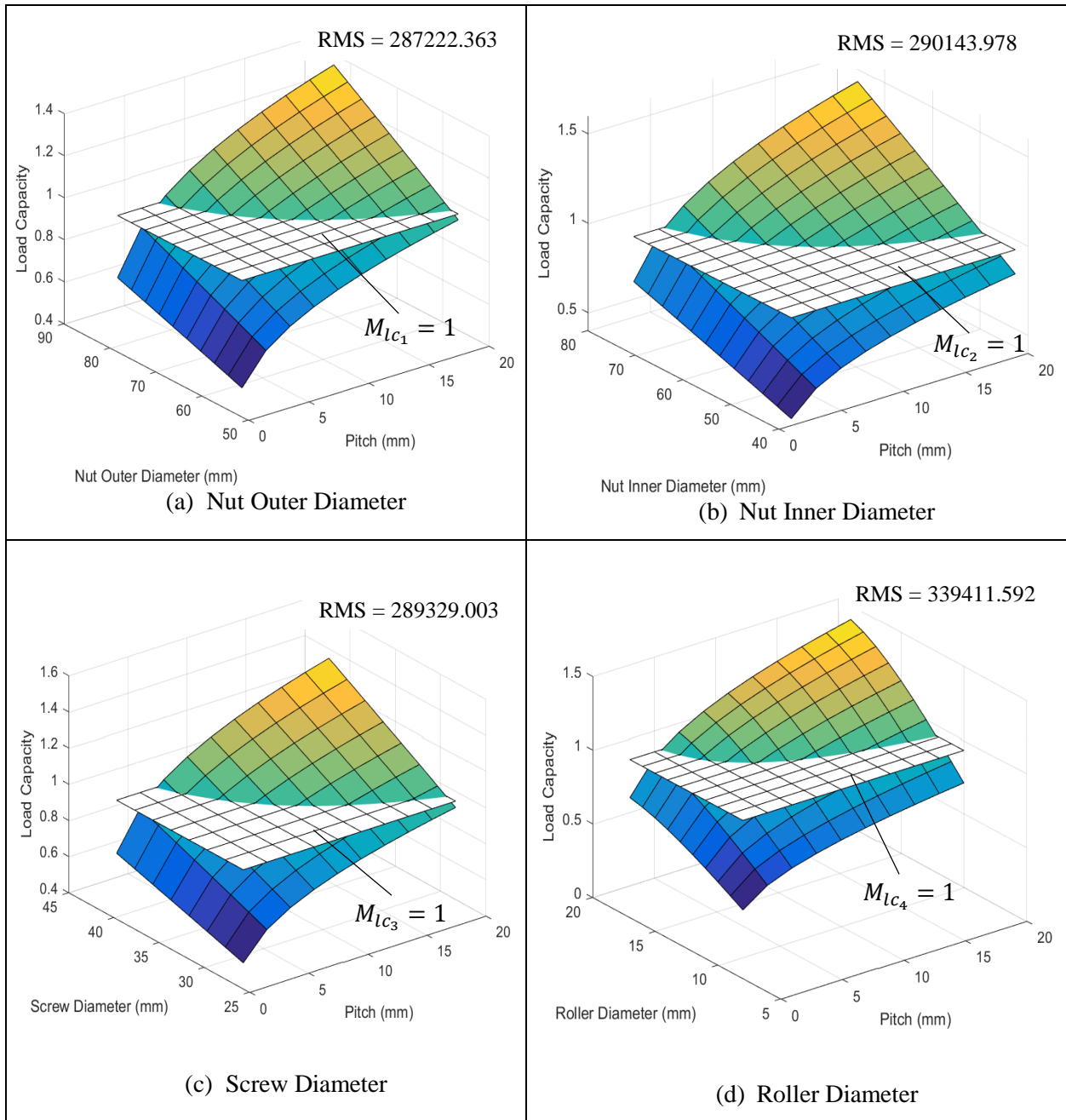


**Figure 7.8 Comparison of Load Capacity**

### 7.2.3 Force Density

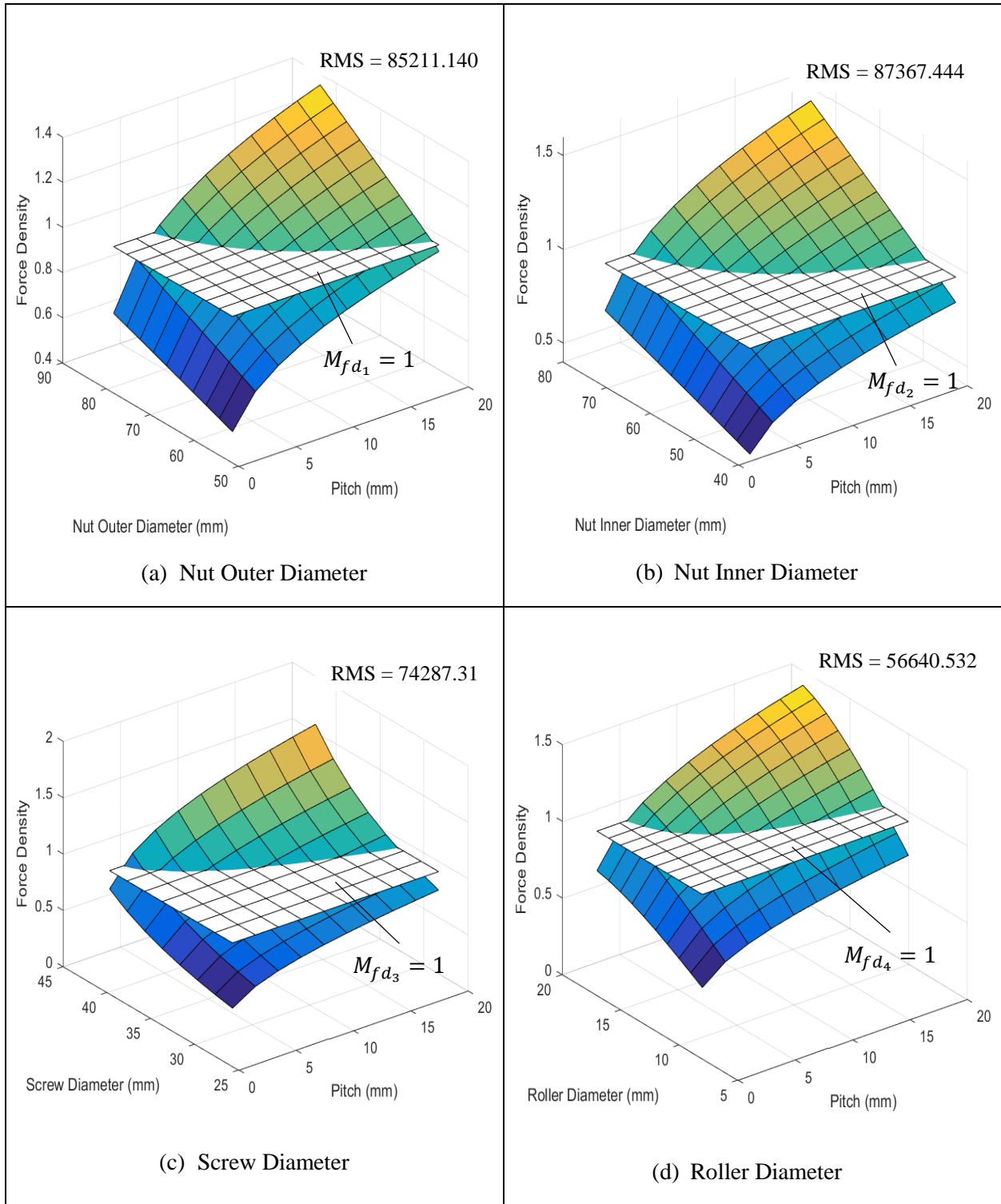


**Figure 7.9 Comparison of Force Density**

Figure 7.9 shows the force density comparison when pitch and the other diameters change. Figure 7.9 (a) to (d) show that the nut thickness and roller diameter have a large effect on force density because of weight sensitivity. Root mean square values are presented from  $M_{fd_1}$  to  $M_{fd_4}$  for each parameter case. Force density is clearly sensitive to weight. For example, the screw diameter increase causes nut thickness to decrease and it results in a large increase of load capacity as shown in Figure 7.9 (c). Figure 7.9 (d) presents different results when compared to Figure 7.9 (c). Force density increases as roller diameter increases. However, too large a roller diameter decreases force density because of the roller weight increase. These different results caused by different parameter changes requires a combination measure analysis and envelopes, which will be discussed in the next section. .

### 7.3 Combined Measures Analysis

In Section 7.2, we discussed the requirement of combined measures analysis for building envelopes. In this section, three measures are combined in one 3D map using methods to result in one envelope to contain all characteristics of each performance measure. In order to separate good PRS design dimensions for parameters, in all cases of root mean square is added or multiplied for each method. In other words, values of the root mean square are added for the method of adding performance measures and are multiplied for the method of multiplying performance measures. The added root mean square value is expressed as  $M_A^*$  and the multiplied root mean square value is written as  $M_M^*$ .

#### 7.3.1 Adding Measure Values

Figure 7.10 shows the results of adding performance measures to form envelopes when pitch and other key parameters vary. All four cases provide somewhat non-linear maps. In particular, the pitch change results in rapid envelope change (i.e. small threads are uniformly unattractive) when pitch is small.

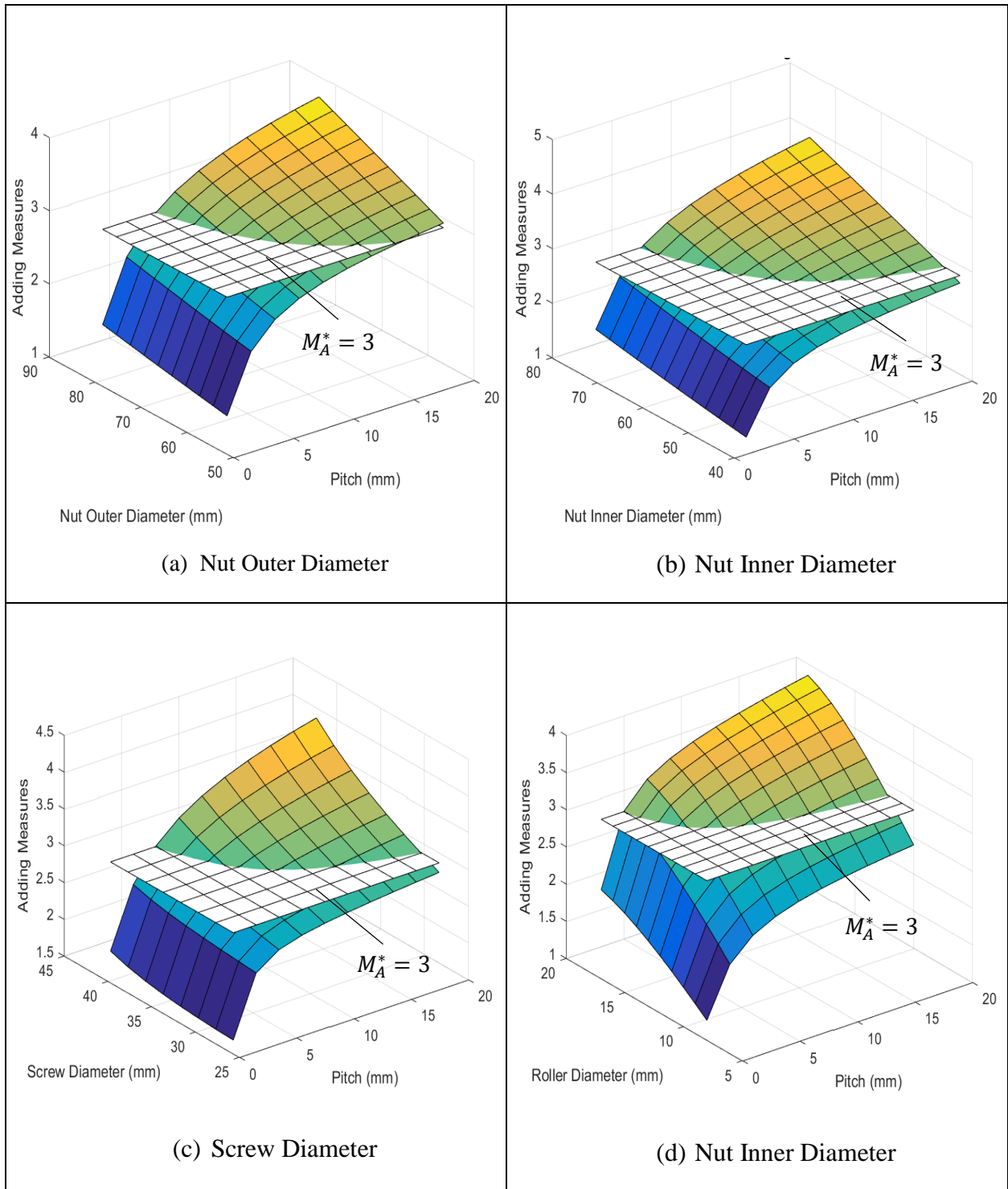


**Figure 7.10 Adding Measures**

As shown, all added values are the normalized value of 5. All four normalized 3D maps represent one performance measure. In addition, these maps show each performance map's change properties. Even though each parameter case has a unit scale when normalized, the adding performance measure method gives higher values ( $\approx 4x$ ). This helps to interpret the effect of parameter change for performance measures of the PRS. Adding all values of performance measures provides a larger range to easily monitor changes.

### 7.3.2 Multiplying Measure Values

In this section, the method of multiplying performance measures is introduced. Figure 7.11 presents four combinations when pitch and the other four parameters change. Pitch still has the dominant effect on the multiplying measures results. All four 3D maps are non-linear and have steeper slopes compared to the adding performance measure method. Each original map's maximum normalized value is under 2. The multiplying performance measures method provides more non-linear maps illustrating more clearly the effect of the changing design parameters. This means that the multiplying performance measure method can show even small effects of parameter variation on the PRS performance measures. For example, the nut outer diameter and the screw diameter provides large changes when the two parameters becomes large as in Figure 7.11 (a) and (c). This is because nut thickness significantly affects load capacity as shown in Figure 7.11 (a). As shown, the screw diameter change case is different compared to the nut outer diameter change case. As the screw diameter increases, it decreases both nut thickness and weight. This provides a major effect on the PRS performance. However, a thin nut can cause lower values as presented in Figure 7.11 (b). The nut inner diameter increase brings an overall performance value decrease even though the nut outer diameter increases. But the proportion of the increase of the nut outer diameter is smaller than the nut inner diameter increase. Then, note that the nut thickness decreases when the nut inner diameter increases. Figure 7.11 (d) proves the key importance of the roller diameter to illustrate its fundamental meaning for design. Overall, the method of multiplying performance

measure maps to create envelopes is better than the adding because it best represents the relative meaning of each measure's characteristics and the overall effect of the governing parameters on the PRS.

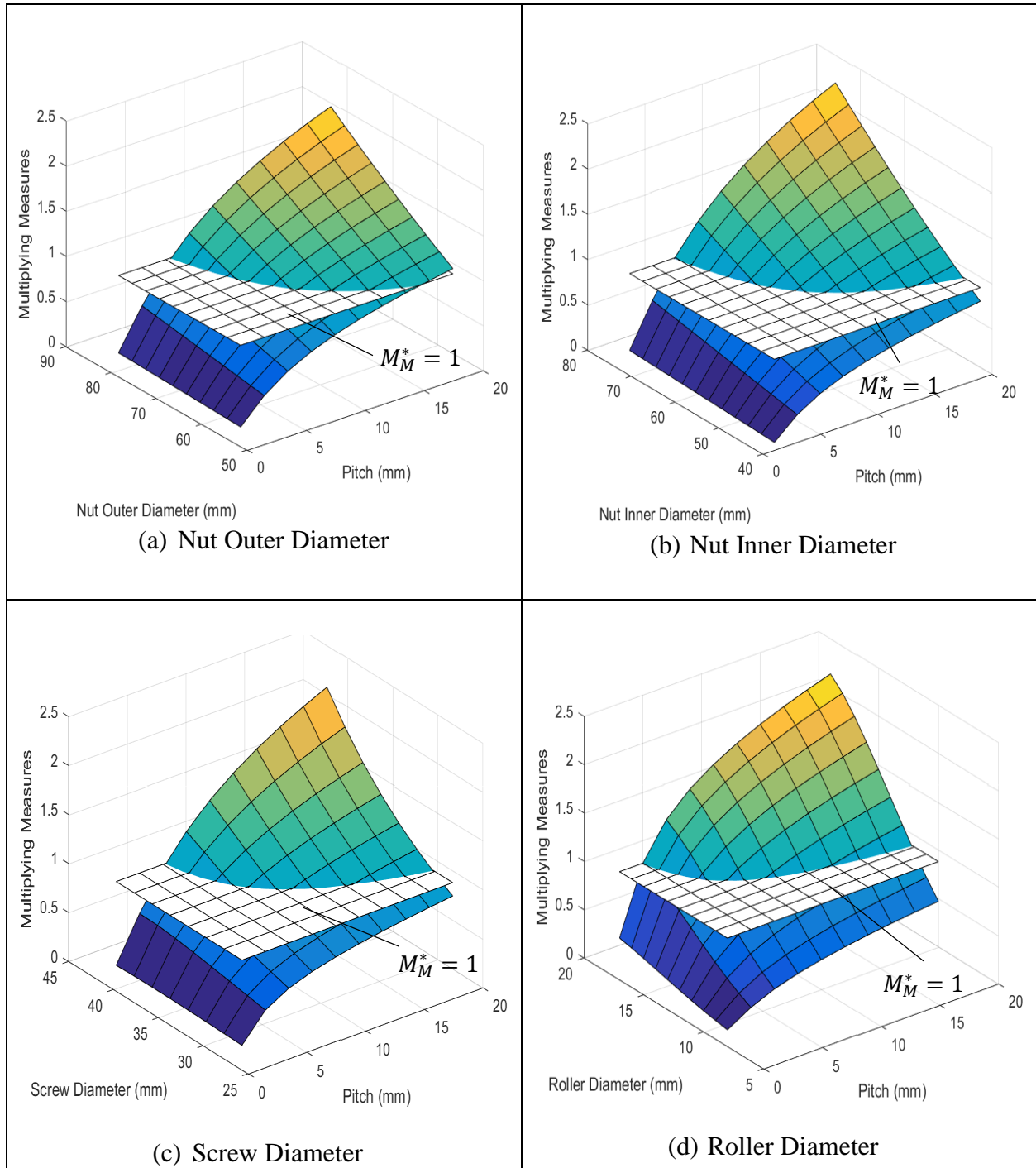


Figure 7.11 Multiplying Measures

## 7.4 Chapter Conclusion

In this paper, the dominant parameters on the PRS are arranged and analyzed in detail. In addition, a method is discussed for combining different properties of the measures. As investigated, nut thickness and roller diameter are key factors to determine optimal design of the PRS. Nut thickness is dependent on nut outer diameter, screw diameter, and roller diameter. Because nut thickness is dependent and has a large effect on performance measures for the PRS, it needs to be dealt with carefully. In addition, it is clearly related to volume. Volume increase generally increases load capacity and keeps the total stiffness decrease smaller when the length is fixed. However, it also increases weight and this causes a drop in force density. This means that an increase of nut thickness has two opposite effects on the PRS capability. In terms of roller diameter, it also needs to be dealt with carefully in the design process because of its importance as shown in the resulting envelopes. A large roller diameter helps to improve PRS capability such as total stiffness, load capacity, and force density. However, those capabilities start to decrease after a specific roller diameter value (i.e., the envelope growth levels off). Roller diameter is a key factor, which decreases nut thickness. Even though the roller diameter increase provides higher values of the performance measures, nut thickness decrease lowers that capability of the PRS as a result. In other words, it is very important to find a correct combination between nut thickness and roller diameter within a given geometry and a given volume.

In order to determine the effect of all parameters on all measures of the PRS, two methods are conducted (adding / multiplying maps to form envelopes). The method of multiplying performance measures is recommended because of its useful non-linearity (i.e., increased parametric sensitivity). Here we provide a table that compares the adding method and the multiplying method. The resulting values of both the adding method and the multiplying method are presented. This scale adjustment process makes it easy to watch the effect of parametric changes in terms of the performance measures for both methods. Note that white reference surfaces represent the added and multiplied RMS values for all normalized performance measures (both added and multiplied).

	Adding Method	Multiplying Method
Nut Outer Diameter		
<p>Note: There is a scale difference between the adding and the multiplying methods. The multiplying method has a larger range scale. The multiplying method provides a more non-linear map than the adding method. This helps the designer to better visualize the results caused by parametric change. In addition, the multiplying method is more sensitive to even small changes and shows clearer value change than the adding method.</p>		
Nut Inner Diameter		
<p>Note: Scale difference is shown between the adding and the multiplying method. The multiplying method has a larger range of scale. The multiplying method shows more non-linearity as the parameter values increase. As shown, there are larger value changes below and above the RMS reference surface. In addition, the multiplying method is more sensitive to parametric changes and shows clearer differences.</p>		

**Table 7.3 Adding /Multiplying Method Comparison**



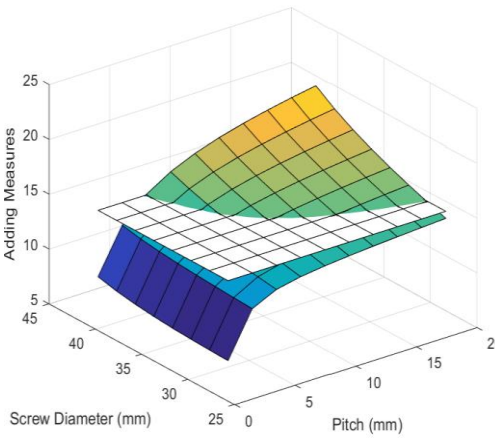
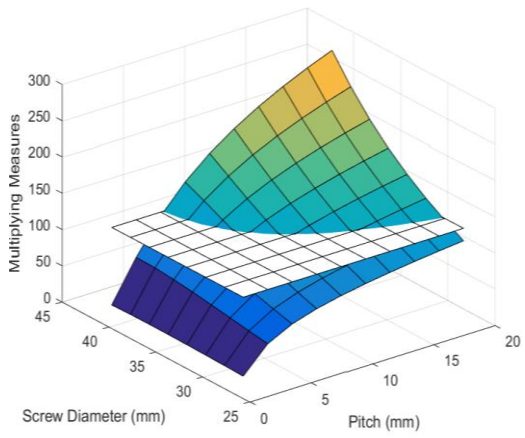
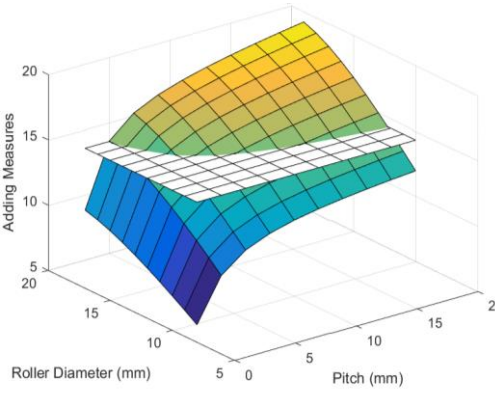
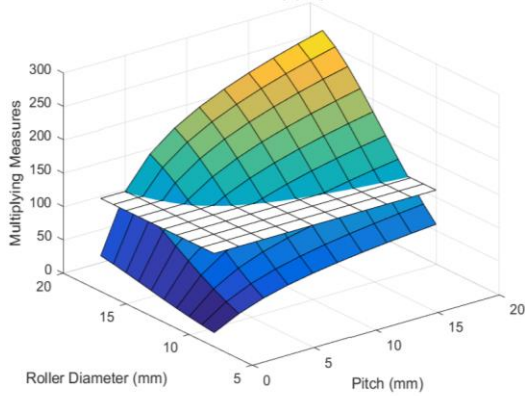
<p style="text-align: center;">Screw Diameter</p>		
	<p>Note: The multiplying method has a larger range of scale. The multiplying method provides more a non-linear map. This multiplying case also shows that there are larger value changes below and above the RMS reference surface. This gives a clearer understanding of the effects caused by parametric change.</p>	
<p style="text-align: center;">Roller Diameter</p>		
	<p>Note: The multiplying method has a larger range of scale. As shown, the multiplying method provides larger value changes and is more non-linear. This makes it easy to monitor the effects caused by parameter change and provides clearer results.</p>	

Table 7.3 Continued

Table 7.3 gives a brief comparison of the adding and multiplying methods for each performance measure envelope. Even though a scale adjustment process is needed for easy monitoring of the

parametric effect on the PRS performance measures, this multiplying approach contains a clearer representation of each measure caused by parameter as change compared to the adding method. With the multiplying method, it is easy for the designer to visualize these changes of the performance measures and determine the effect of the basic parameters on the PRS overall design.

## **CHAPTER 8. MAP / ENVELOPE DESIGN PROCESS:**

### **Part 2 – Parametric Management Using Combined Measure Envelopes**

For several decades, the planetary roller screw (PRS) has been under development since it was invented in 1954 by Strandgren [1] in his patent when the PRS is considered as a key component of electro-mechanical linear actuators (EMA). Recently, the electro-mechanical actuator (EMA) is receiving more attention as a significant component for future intelligent mechanical devices because of its advantages compared to traditional pneumatic or hydraulic actuators and the equivalent mechanical ball screw. These PRS based EMAs provide better performance by integrated design, extended durability and easy set up and installation. In addition, EMAs are also profitable in the perspective of precision and efficiency because EMA's produce more accurate motion control and reduce maintenance, operational cost, and energy consumption. The most important advantage is that there are no leaks, which is the weakest characteristic of hydraulic systems. Because of these, EMAs are considered to be able to replace hydraulic and pneumatic actuators and are targeted for key applications. As the EMA becomes more important, the study of the PRS is also expanded for good design to enhance the EMA's efficiency and performance. Previous work on the PRS focused on its kinematics and related applications. Very useful research on kinematics of the PRS was done by Velinsky et al. [6]. They focus on the relationship of each component's angular motion analysis and linear motion velocity. Jones et al. [7] derive the nature of the contact kinematics between the load carrying surfaces and provide several geometric relationships. Jones [8] discusses the kinematics of the PRS and develops a new approach to calculate stiffness and thread load distribution based on a direct stiffness method in his dissertation. In addition, he analyzes each component's stiffness and provides a stiffness matrix as a result. He does some parameter study; however, it does not utilize all parameters of the PRS. Lemor [9] discusses efficiency of the planetary roller screw and analyzes its advantages in terms of load capacity, life time, and efficiency. A formula is proposed to calculate the dynamic load carrying capacity of the PRS compared to conventional ball screws. Yang et al. [12] develop a

load distribution formula. This equation is used for further research as developed by Ma et al. [13]. They analyze the rolling condition of the PRS and expand previous research conditions and formulas. In addition, Ma et al. [29] analyze frictional heat model of the PRS in terms of load distribution. The work by Ma [13], [29] resulted in a finite number of useful design rules of value in the design process:

1. PRS stiffness increases somewhat with load
2. Friction increase is parabolic with load
3. Normal contact force and axial deformation drop by 2x when the thread groove angle goes down from 130 to 80°, while friction forces drop by 3x
4. Small helix angle ( $\approx 10^\circ$ ) has a small effect on friction and axial deformation
5. Friction is independent of the number  $n$  of thread contacts but axial deformation inversely correlates with the number of threads (drops by 3x when  $n$  goes from 10 to 40).

Ashok and Tesar [30] does research about a visualization framework for real time decision making in a multi-input and multi-output system such as battlefield operations, complex system design, and human support systems. They build decision surfaces to aid the decision making process, and they show the value of using performance maps to visualize real world problems. In addition, Ashok and Tesar [31] discuss why performance maps and envelopes are needed for the decision making process. Most of the systems that exist are highly non-linear and complex. Human input is always necessary for the decision making process to control and operate these systems. In order to make systems work properly, performance maps and envelopes are necessary. Bandaru and Tesar [32] design and analyze multi stage gear systems using performance maps. They look at several cases of the gear train geometry and make maps and envelopes that help designers make rapid design decisions. Budynas et al. [33] describes fundamental mechanical device design knowledge and the related design process. In addition, they provide several useful tables, which are used many times for precise design.

This chapter provides several envelopes to help designers to achieve a high capability PRS design. The PRS is an evolutionary device in terms of performance measures such as load distribution, total stiffness on the thread mesh, load capacity, and force density. Prior research on the PRS generally focused on specific application requirements or limited design parameter analysis. In order to maximize the capability of the PRS, an effective design process is necessary where the parameter effect analysis is a fundamental factor in this design process. There are many performance measures that affect PRS capability. Each design parameter has its characteristic effect on the PRS. The most influential parameters on the PRS are pitch, nut outer diameter, nut inner diameter, screw diameter, and roller diameter. Those parameters have different effects on each performance measure. These different effects need to be combined and normalized for easy understanding of the required parameter value to meet desired PRS capabilities. This need can be met by using envelopes that present how the design point on the envelope surface moves as the dominant design parameters change. These envelopes provide a better understanding of the PRS mechanism and simplify the design effort of the PRS by enhancing the designer's judgment by means of visualization.

### 8.1 Envelopes of PRS Performance Measures

This section discusses four envelopes such as total stiffness on the thread mesh, load capacity, force density, and weight and how to use the combined envelopes for design. Three of the normalized measures have a relatively small range. Scales of all envelopes are adjusted by multiplication of all envelopes to provide a larger range of scale. In order to combine all four maps, the four design parameters are normalized by their root mean square values. These normalized scales and the original scale will be provided with the envelope. We choose several design points on the combined envelope such as a starting point A and design result points (B1, B2, and B3). Each point provides its design parameter values for each performance measure envelope. This enables the designer to directly obtain design parameters for a chosen design point (B3).

### 8.1.1 Envelope of Total Stiffness on Thread

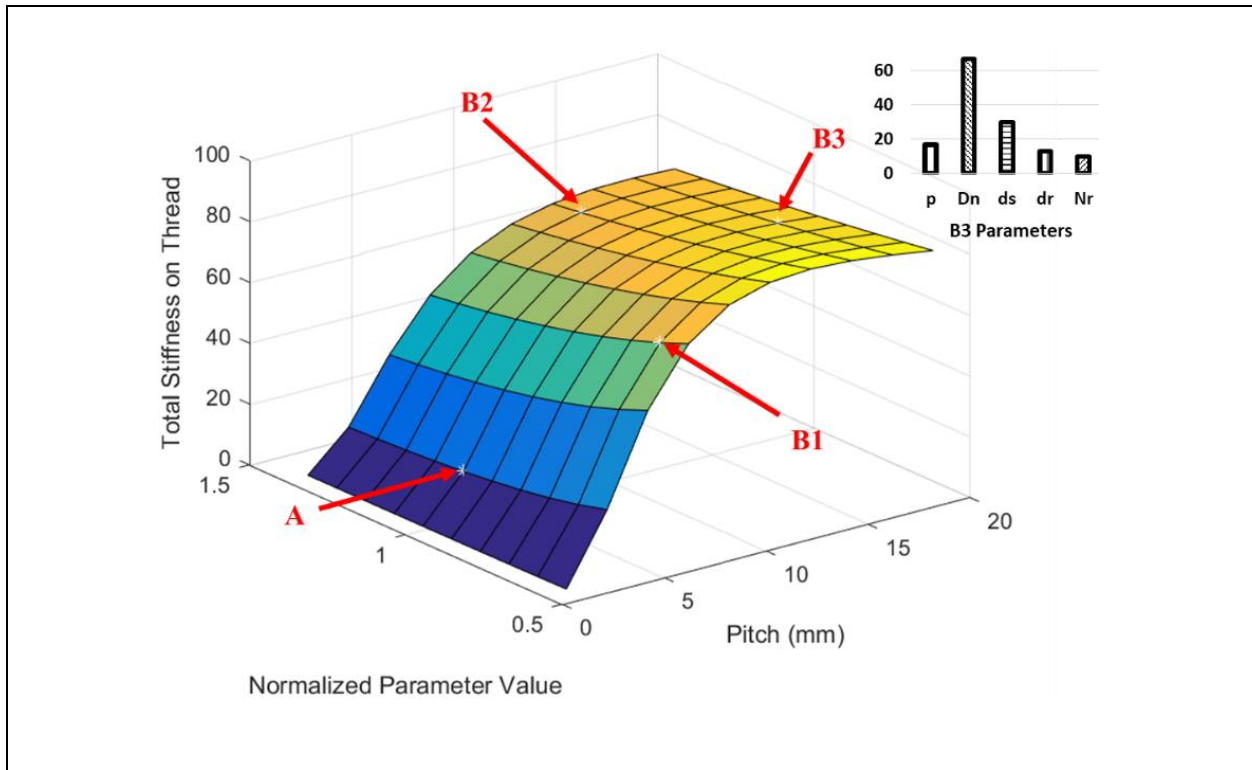


**Figure 8.1 Normalized Total Stiffness Envelope**

Normalized Scale	$N_r$	$d_r$ (mm)	$d_s$ (mm)	$D_n$ (mm)
0.55104921	6	7.8	18	40
0.642936666	7	9.1	21	46.67
0.734824122	8	10.4	24	53.34
0.826711577	9	11.7	27	60.01
0.918599033	10	13	30	66.68
1.010486489	11	14.3	33	73.35
1.102373945	12	15.6	36	80.02
1.1942614	13	16.9	39	86.69
1.286148856	14	18.2	42	93.36
1.378036312	15	19.5	45	100.03

**Table 8.1 Scale Range Chart Comparison Chart**

Figure 8.1 is the normalized total stiffness for the thread mesh envelope, which combines four performance related maps including the nut outer diameter, screw diameter, roller diameter, and number of rollers. As shown, pitch is set as the primary parameter and placed at the x-axis. The y-axis represents the normalized design parameters. All four parameters are normalized for the same range on the y-axis. Then, any given point on the envelope provides its basic design parameters such as nut outer diameter, screw diameter, roller diameter, and number of rollers including pitch. All normalized parameter values can be found in Table 8.1. This then, is the start of the design process. There are four points that represent one design starting point (A) and three chosen design result points (B1, B2, and B3) on the envelope. First, A is about 14.98 on the envelope and the relative (x, y) coordinates are (3, 1.01). That means pitch is 3 mm and normalized y-axis value is 1.01. This y-axis value can be found in Table 8.1. When we see this value 1.01 on the vertical line, Table 8.1 provides all four design parameter values. In terms of design starting point (A), the parameter value represents the nut outer diameter 73.35 mm , screw diameter 33 mm, roller diameter 14.3 mm, and the number of rollers is 11. As mentioned, there are three selected design result points and these points also provide design parameter values in the same manner as for design starting point (A). In Figure 8.1, a set of bars for the three design parameters would automatically change magnitude as the designer moved the design location on the envelope surface.

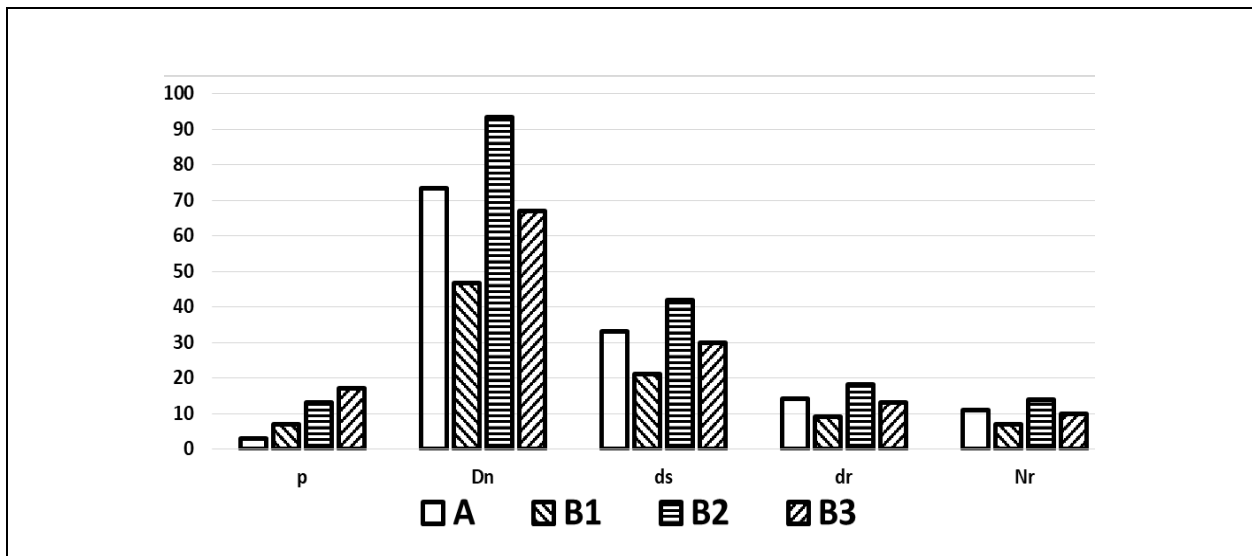


Figure 8.2 Parameter Comparison Chart for Total Stiffness on Thread

	<b>A</b>	<b>B1</b>	<b>B2</b>	<b>B3</b>
$p$ (mm)	3	7	13	17
$D_n$ (mm)	73.35	46.67	93.36	66.88
$d_s$ (mm)	33	21	42	30
$d_r$ (mm)	14.3	9.1	18.2	13
$N_r$	11	7	14	10

**Table 8.2 Parameter Comparison Table for Total Stiffness on Thread**

Figure 8.2 and Table 8.2 present design parameters given by each point on the envelope. As shown, any point on the envelope can be expressed directly in terms of design parameter values. Among the three resulting design points, B2 has the highest stiffness value even though it has the smallest parameter values of nut outer diameter ( $D_n$ ), screw diameter ( $d_s$ ), roller diameter ( $d_r$ ), and number of rollers ( $N_r$ ) but sufficient pitch ( $p$ ) value. This shows the importance of the combined envelope to be the basis for a new form of the design process. Overall, we can visually monitor the parameter values when the design point moves. The total stiffness on the thread mesh indicates that some parameter value increase causes a small decrease of the total stiffness but an increase in the pitch provides the opposite result.

### 8.1.2 Envelope of Load Capacity

Figure 8.3 presents a figure related to load capacity. Figure 8.3 indicates that large pitch and diameters of the PRS components provide a much higher load carrying capability. Design point A is the starting point of design with relative parameters of nut outer diameter 60.01 mm, screw diameter 27 mm, roller diameter 11.7 mm, number of rollers 9, and pitch 3 mm. For other design points, we move A to three locations at B1, B2, and B3. These three design points provide three different parameter sets. As shown, load capacity increases when pitch and the other parameters



increase and we can see that larger diameters of the PRS have a much better load carrying capability.

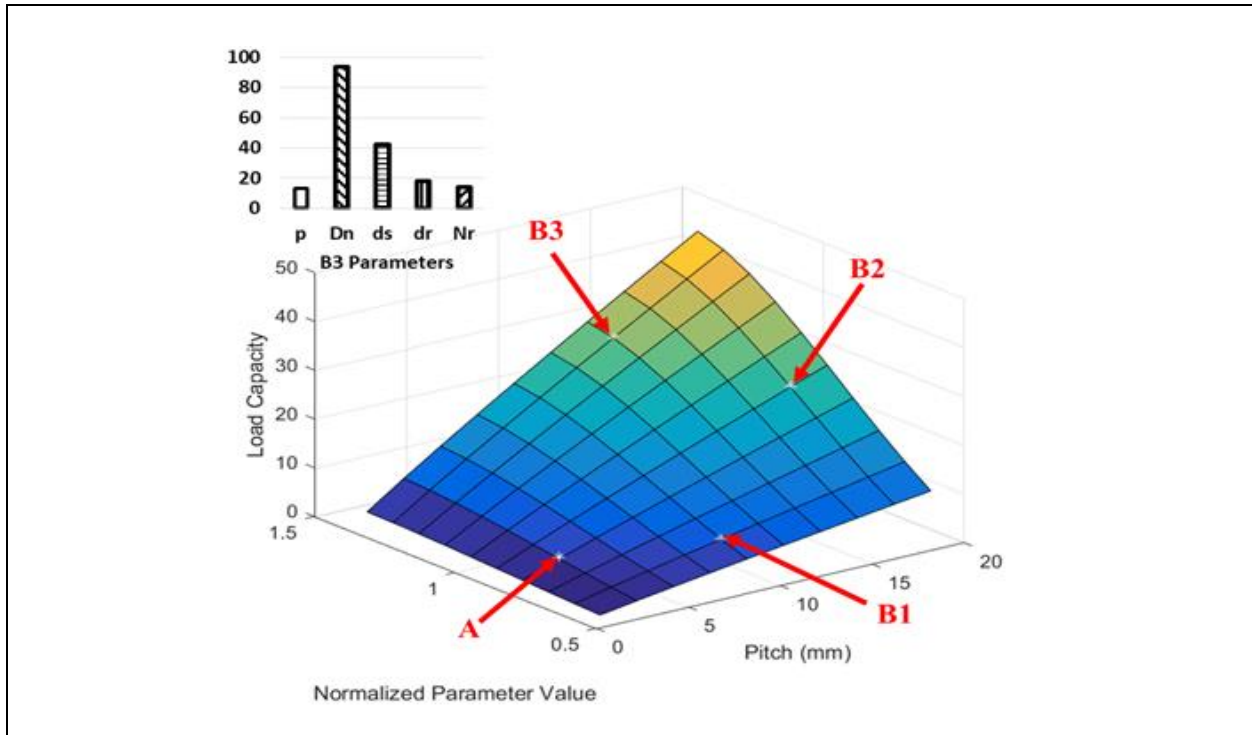


Figure 8.3 Normalized Load Capacity Envelope

	A	B1	B2	B3
$p$ (mm)	3	7	17	13
$D_n$ (mm)	60.01	46.67	66.68	93.36
$d_s$ (mm)	27	21	30	42
$d_r$ (mm)	11.7	9.1	13	18.2
$N_r$	9	7	10	14

Table 8.3 Parameter Comparison Table for Load Capacity

The parameter sets of the three design points (B1, B2, and B3) are shown in Table 8.3 as a comparison chart of each parameter in the set including design starting point A. This shows that large dimensions of the PRS components and pitch provide increased load capacity. However, one direction of design towards B1 does not provide higher load carrying capacity where some of the

design parameter values are small. Even though the result value of B2 on the envelope is relatively high with large pitch, it is not large compared to B3 on the same envelope. In other words, proper combining of pitch and other design parameters can provide better load carrying capability as shown. If increase between pitch and the other design parameters are compared in terms of load capacity, increase of other design parameter values of the PRS have a somewhat higher impact than pitch.

### 8.1.3 Envelope of Force Density

Figure 8.4 shows the resulting envelope for force density. We again start at point A and three design points (B1, B2, and B3). The design at starting point A gives parameters for nut outer diameter of 80 mm, screw diameter 36 mm, roller diameter 15.6 mm, and number of rollers 12 including pitch 3 mm. This design starting point only gives a low value of 3.4925 on the envelope, which has 40.3686 as a maximum value. Because of this initial low design result, we move the design point to three different locations to achieve a higher value on the envelope.

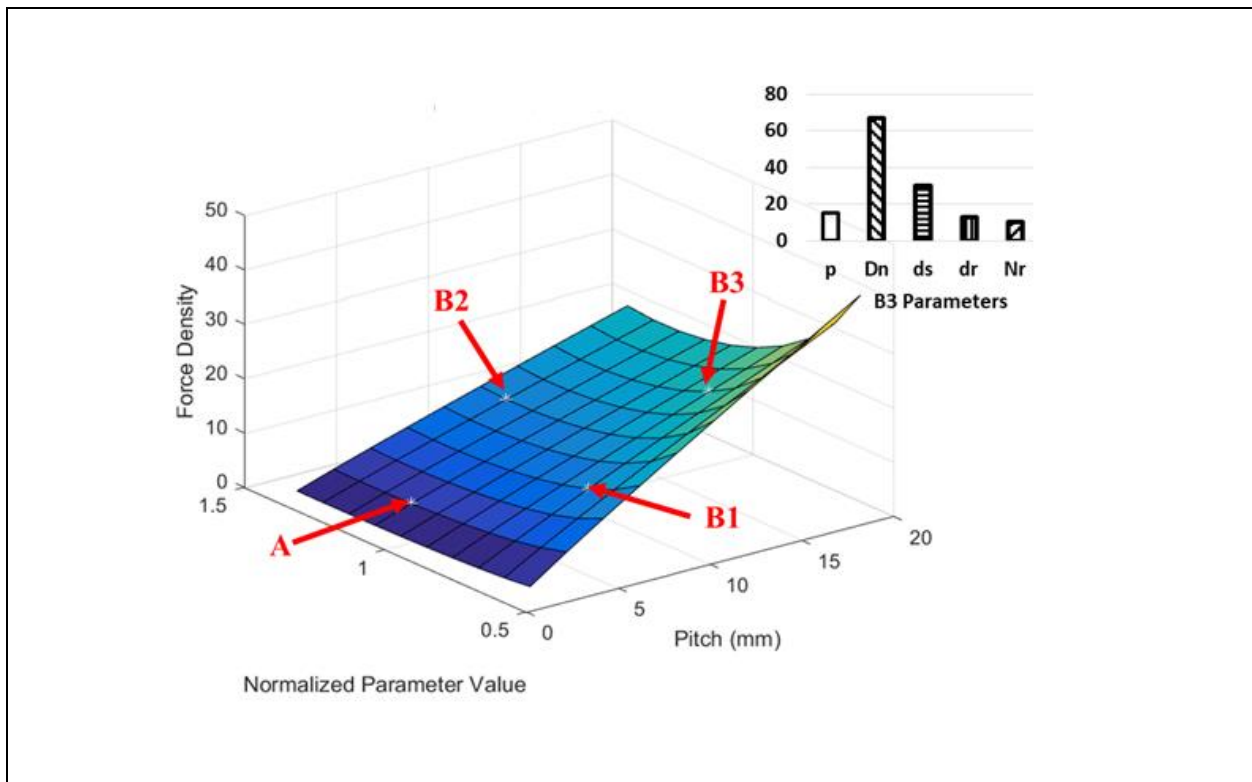


**Figure 8.4 Normalized Force Density Envelope**

As shown, B3 has the highest value among the three points with large pitch and small dimensions because of the envelope's monotonic increase. Each design point provides parameter values of nut outer diameter, screw diameter, roller diameter, and number of rollers. The resulting design parameters are presented in Table 8.4. When the pitch value increases, force density also increases. Force density somewhat decreases when the other parameters increase. This is because dimensional increase causes total weight increase. When diameters and the number of rollers are small, the effect of parameter change is not large. However, larger parameter values cause a decrease of force density because of the effect of the increased weight. This indicates the importance of the geometric parameters such of nut outer diameter, screw diameter, and roller diameter, and the number of rollers.

	<b>A</b>	<b>B1</b>	<b>B2</b>	<b>B3</b>
$p$ (mm)	3	7	11	15
$D_n$ (mm)	80.02	53.34	93.36	66.68
$d_s$ (mm)	36	24	42	30
$d_r$ (mm)	15.6	10.4	18.2	13
$N_r$	12	8	14	10

**Table 8.4 Parameter Comparison Table for Force Density**

As mentioned, design points B3 gives the highest value of force density among the three design points. Table 8.4 presents the relative parameter values for these four designs. This process helps designer to visualize the performance measure change relative to the corresponding change in the governing design parameters.

#### 8.1.4 Envelope of Total Weight

Figure 8.5 presents the envelope of total weight. Pitch has almost no effect on weight. As shown, weight increases gradually when PRS inner geometric parameters increase. The weight

envelope provides a relatively simple envelope compared to the other three envelopes. Where design starting point A moves to three different locations, all design points also provide their parameter sets. Those parameter sets are presented in Table 8.5.

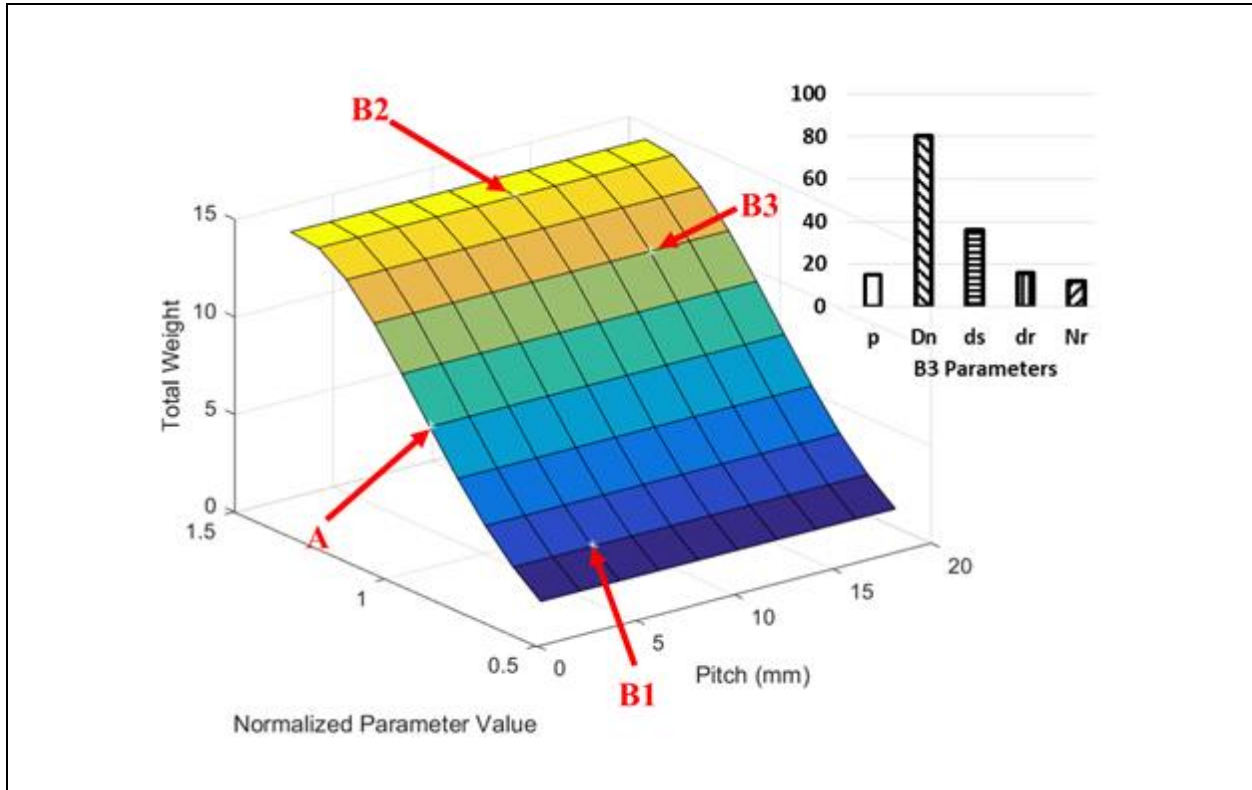


Figure 8.5 Normalized Total Weight Envelope

	<b>A</b>	<b>B1</b>	<b>B2</b>	<b>B3</b>
$p$ (mm)	3	5	11	15
$D_n$ (mm)	66.68	46.67	93.36	80.02
$d_s$ (mm)	30	21	42	36
$d_r$ (mm)	13	9.1	18.2	15.6
$N_r$	10	7	14	12

Table 8.5 Parameter Comparison Table for Total Weight

As mentioned, Table 8.5 presents each design point’s parameter set. Because total weight is not related to pitch change, design point B2 has the highest total weight among the three design points in Figure 8.5. Table 8.5 shows that B2 has the largest dimensions. This again shows how the visual display of the performance envelopes makes for a rapid approach to achieve useful dimensions of the PRS.

### 8.2 Design Process Analysis by Combined Envelopes

In this section, all envelopes are combined into one total envelope including weight (even though force density contains weight) so that all four measures are normalized. Then, multiplying weight does not cancel out force density. We compare adding and multiplying envelopes and discuss which type of envelope is more useful and sensitive to change of the design parameter values.

#### 8.2.1 Comparison between Adding and Multiplying Envelopes

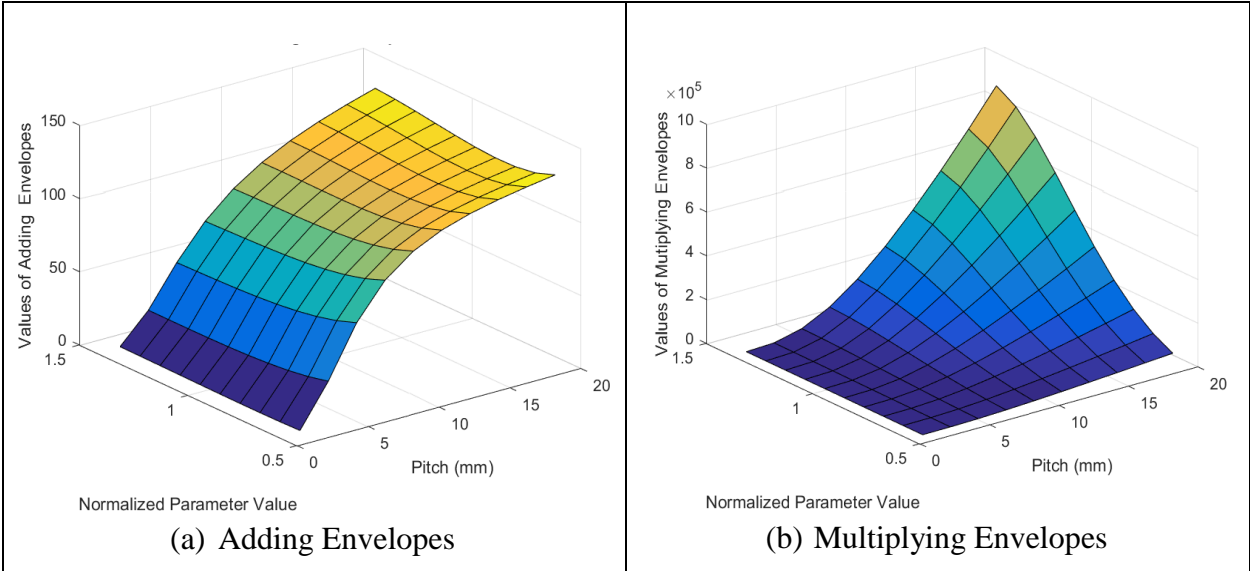


**Figure 8.6 Comparison of Adding and Multiplying Envelopes**

Figure 8.6 shows the different shapes of the combined envelopes. Figure 8.6 (a) is the added envelope result and Figure 8.6 (b) is the multiplied envelope result. Figure 8.6 (a) is similar to the

total stiffness envelope because the total stiffness envelope has the highest value among the four envelopes. On the other hand, Figure 8.6 (b) provides the most useful combined result based on the four envelopes. From this comparison, multiplying envelopes gives a visually more useful envelope. Multiplying envelopes will be analyzed in more detail for the design process in the next section.

### 8.2.2 Design Process Analysis of Combined Envelope

Here, one envelope is introduced, which combines all envelopes such as total stiffness on the thread mesh, load capacity, and force density. This final envelope does include weight even though force density contains weight because all four measures are normalized. The designer can track every individual value of each measure and parameter values, which are considered to build these combined envelopes.

Figure 8.7 shows one envelope, two comparison charts, and two supporting value comparison tables. Figure 8.7 (a) is the final combined envelope with four design points on the envelope surface. A is the design starting point with three other points (B1, B2, and B3) distinct from the design starting point A. Each resulting design point has its own values for the combined performance measure and the design parameter values.

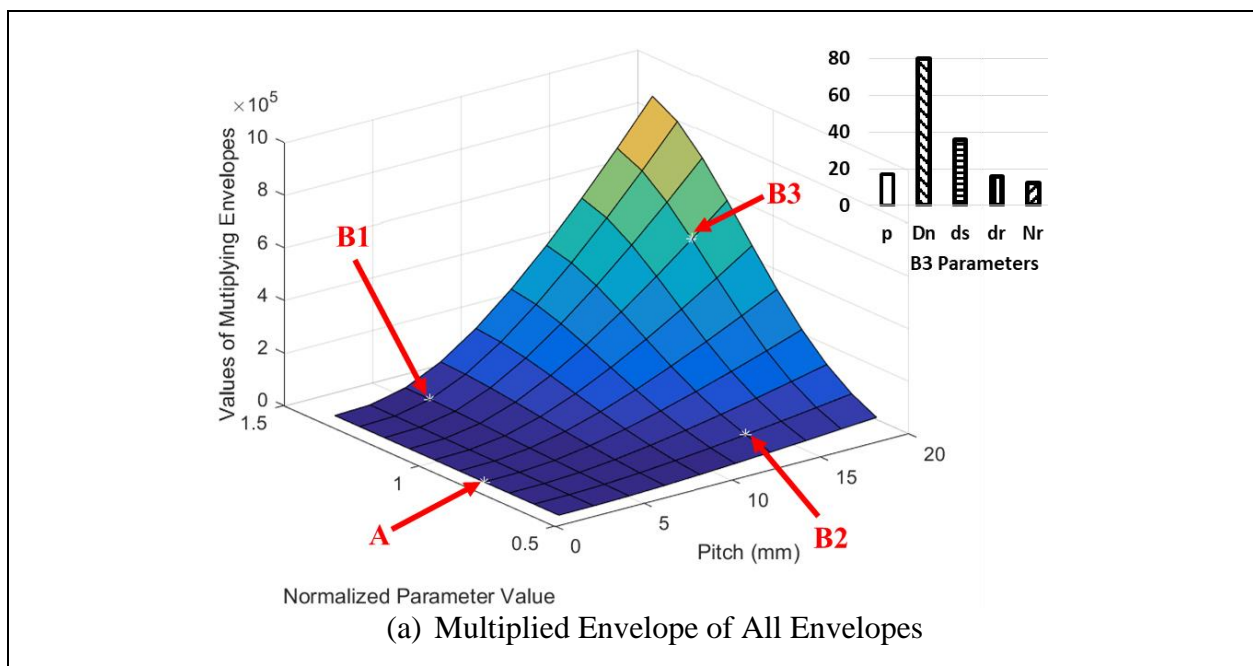


**Figure 8.7 Measure and Parameter Analysis on Final Envelope**

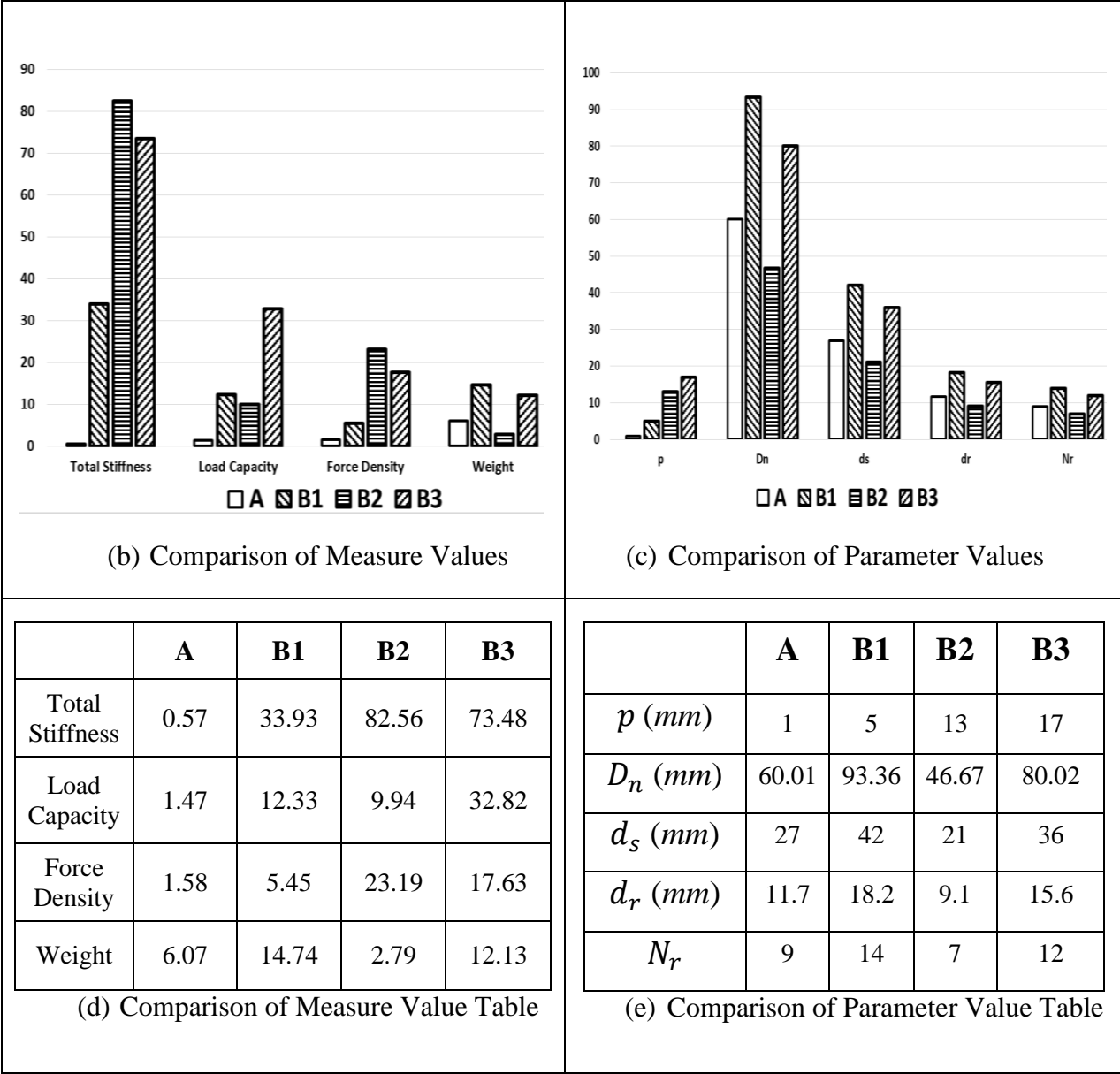
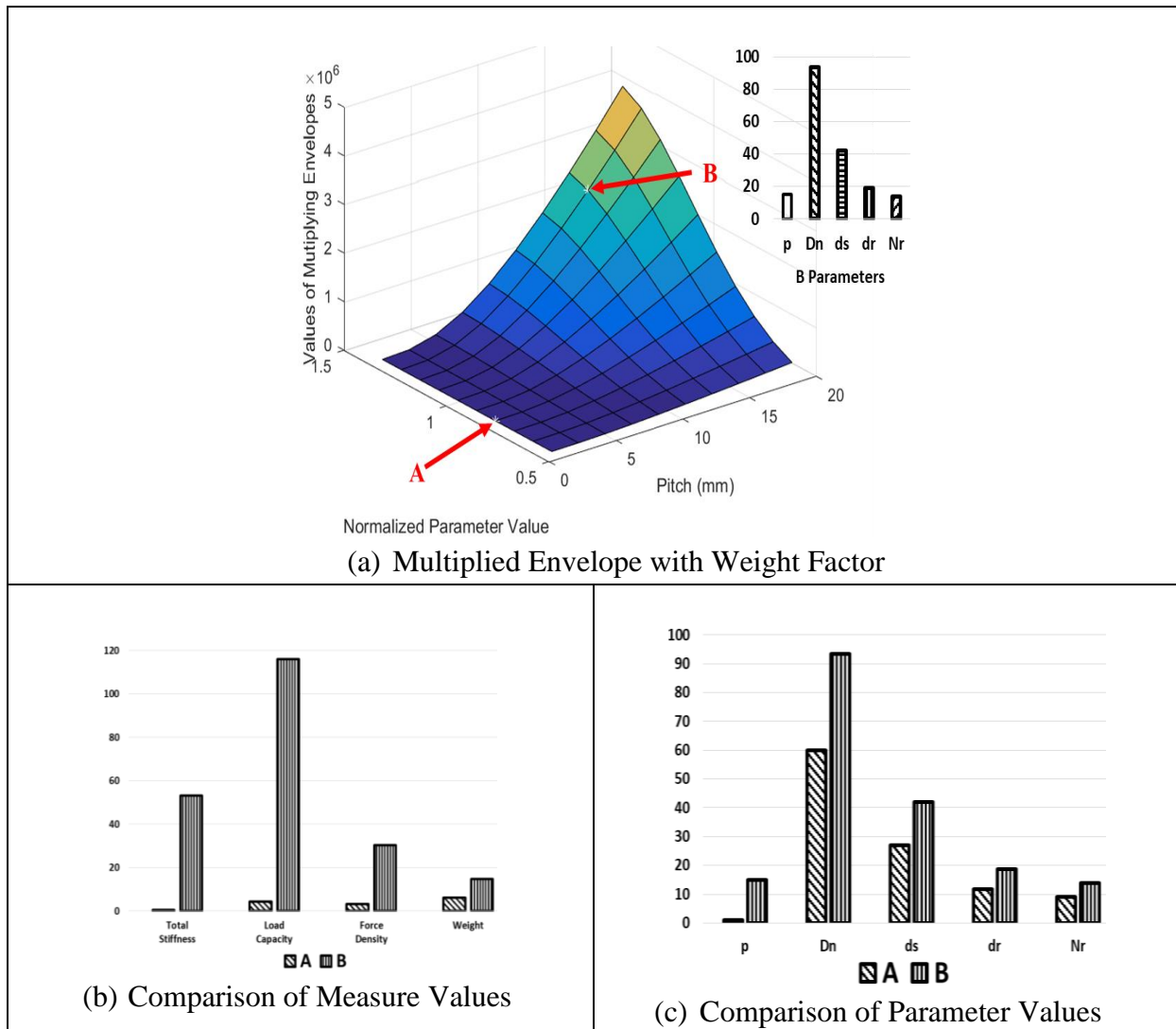


Figure 8.7 Continued

The overall performance and resulting parameter values are presented in Figure 8.7 (b) and (c). These values are tracked from Figure 7. (a) as the final combined envelope. This process helps the designer to visually monitor change of the overall performance and parameter values.

### 8.3 Design Process Using weighted Combined Envelopes

The previous single performance measure envelopes were based the multiplication of individual maps each depending on a different design parameter ( $D_n, d_s, d_r, N_r$ ) along the y-axis with the dominant parameter pitch ( $p$ ) along the x-axis. Here, we wish to expand the designer's overall design capacity by combining several of these performance measure envelopes into one envelope where a weighting factor ( $w_1, w_2, w_3$ , and  $w_4$ ) is used to govern their relative importance as determined by the designer for a given application. The basic performance measures are stiffness of the thread mesh, load capacity, force density, and weight.



**Figure 8.8 Measure and Parameter Analysis on Final Envelope Using Weight Factor**



	Performance Measure Values				Parameter Values				
	Total Stiffness	Load Capacity	Force Density	Weight	$p$ (mm)	$D_n$ (mm)	$d_s$ (mm)	$d_r$ (mm)	$N_r$
<b>A</b>	0.43	4.42	3.16	6.07	1	60.01	27	11.7	9
<b>B</b>	53.28	115.9	30.39	14.74	15	93.36	42	18.82	14

(d) Value Comparison Table

Figure 8.8 Continued

Figure 8.8 shows the combined envelope, comparison chart, and numerical value table. The envelope on Figure 8.8 (a) provides combined values of all envelopes by multiplication with weight factors ( $w_1, w_2, w_3,$  and  $w_4$ ). We choose representative weight factors such as  $w_1 = 0.75,$   $w_2 = 3, w_3 = 2,$  and  $w_4 = 1$ . All weight factor values represent the related importance of each performance measure. From this envelope, the designer can track every individual value of each measure and each design parameter value. For example, A is the design starting point and B is the final design result point distinct from the design starting point A. The resulting design point has its own values for the measure and the design parameter values (Figure 8.8 (d)). These performance measures and parameter values are presented in Figure 8.8 (b) and (c). These values can be tracked on Figure 8.8 (a) as the final combined envelope. This process helps the designer to monitor changing values of the combined performance measures and design parameter values and to prioritize each performance measure for a given application.

#### 8.4 Analysis of Other Significant Performance Measures

In this section, we present formulas of six additional performance measures such as thread contact pressure (stress), load distribution, efficiency, life rating (durability), inertia, and velocity

reduction ratio. Each related formula contains several design parameters including those described before such as nut outer diameter, screw diameter, roller diameter, number of rollers, and pitch.

#### 8.4.1 Contact Pressure

Contact pressure formula by based on contact mechanics [21] and Lisowski's analysis [24].

It can be expressed using equation (8.1) as:

$$p_c = 3 \frac{F_{normal}}{2\pi ab} \quad (8.1)$$

where,

$F_{normal}$  = Normal Load on the Thread (contact point)

$a, b$  = Semi-axis of the Ellipse of Contact

Semi-axis of the ellipse of contacts  $a$  and  $b$  are determined by depending on the radii of curvatures as obtained by Ma et al [13].

$$a = m_a \left( \frac{3F_{normal}Y^*}{2 \Sigma \rho} \right)^{\frac{1}{3}} \quad (8.2)$$

and

$$b = m_b \left( \frac{3F_{normal}Y^*}{2 \Sigma \rho} \right)^{\frac{1}{3}} \quad (8.3)$$

where,

$m_a, m_b$  = Hertz Coefficient

$Y^*$  = Effective Young's Modulus =  $\frac{1-\nu_s^2}{Y_s} + \frac{1-\nu_n^2}{Y_n}$

$\Sigma\rho$  = Sum of Curvature

According to the Hertz theory, the nut side radii of curvature and screw side radii of curvature are expressed as  $R_{r11}$ ,  $R_{r12}$ ,  $R_{n21}$ ,  $R_{n22}$  for the nut side and  $R_{r11}$ ,  $R_{r12}$ ,  $R_{s21}$ ,  $R_{s22}$  for the screw side.

$R_{r11}$  and  $R_{r12}$  are the radius of effective ball for both nut and screw side contact curvatures and,

$R_{n21}$ ,  $R_{n22}$ ,  $R_{s21}$ ,  $R_{s22}$  are the radii of nut and screw contact thread surface curvature in detail.

Firstly, radii of curvature in the nut side are listed as:

$$R_{r11} = \frac{d_r}{2 \sin(\alpha_0)} = R \quad (8.4)$$

$$R_{r12} = \frac{d_r}{2 \sin(\alpha_0)} = R \quad (8.5)$$

$$R_{n21} = \infty \quad (8.6)$$

$$R_{n22} = \frac{d_r + d_s + 2R \cos(\alpha_0)}{-2 \cos(\alpha_0)} \quad (8.7)$$

Then, principal curvatures are expressed as:

$$\rho_{r11} = \frac{2 \sin(\alpha_0)}{d_r} = \frac{1}{R} \quad (8.8)$$

$$\rho_{r12} = \frac{2 \sin(\alpha_0)}{d_r} = \frac{1}{R} \quad (8.9)$$

$$\rho_{n21} = \frac{1}{\infty} = 0 \quad (8.10)$$

$$\rho_{n22} = \frac{-2 \cos(\alpha_0)}{d_r + d_s + 2R \cos(\alpha_0)} \quad (8.11)$$

Next, the radii of curvature in the screw side can be expressed as:

$$R_{r11} = \frac{d_r}{2 \sin(\alpha_0)} = R \quad (8.12)$$

$$R_{r12} = \frac{d_r}{2 \sin(\alpha_0)} = R \quad (8.13)$$

$$R_{s21} = \infty \quad (8.14)$$

$$R_{s22} = \frac{d_r + d_s - 2R \cos(\alpha_0)}{2 \cos(\alpha_0)} \quad (8.15)$$

Then, principal curvatures can be expressed as:

$$\rho_{r11} = \frac{2 \sin(\alpha_0)}{d_r} = \frac{1}{R} \quad (8.16)$$

$$\rho_{r12} = \frac{2 \sin(\alpha_0)}{d_r} = \frac{1}{R} \quad (8.17)$$

$$\rho_{s21} = \frac{1}{\infty} = 0 \quad (8.18)$$

$$\rho_{s22} = \frac{2 \cos(\alpha_0)}{d_r + d_s - 2R \cos(\alpha_0)} \quad (8.19)$$

where,

$$R \text{ is } \frac{d_r}{2 \sin(\alpha_0)}$$

$d_r$  = Roller diameter

$\alpha_0$  = Contact Angle (45°)

As shown above, contact pressure formula contains several parameters such as screw diameter, roller diameter, and Hertz coefficient for each side of contact. Especially, curvature values of the contact surface is important factor in terms of contact pressure. Load on contact point can be a parameter to determine contact pressure when load distribution on each thread is calculated; however, the average axial load can be used for one contact point to calculate contact pressure. As known, pitch and length are dominant parameters to determine total number of contacts in the PRS and these two also can be parameters to obtain contact pressure when axial load is applied on the PRS. Then, we can build more complex (but easy to monitor) envelopes for designers. As noted by Ma [13] the angle between the thread surfaces also strongly affects this stress value and the PRS load capacity.

#### 8.4.2 Load Distribution

Load distribution formula is given by Yang's [12] as:

$$F_{load\ i} = F_{load\ i-1} - \frac{Nr\ l}{4(H_n + H_s)} \left( \frac{1}{Y_n A_n} + \frac{1}{Y_s A_s} \right) \sum_{k=1}^n F_{axial\ j} \sin(\alpha_0) \cos(\beta_0) \quad (8.20)$$

where,

$F_{load}$  = Load on each thread in the axial direction

$H_n$  = Elastic modulus of elliptical contact points in the nut side

$H_s$  = Elastic modulus of elliptical contact points in the screw side

$N_r$  = Number of Roller

$l$  = Lead of the screw and the nut

$Y_n$  = Young's modulus of the nut

$Y_s$  = Young's modulus of the screw

$A_n$  = Effective cross section area of the nut

$A_s$  = Effective cross section area of the screw

$\alpha_0$  = Contact angle

$\beta_0$  = Helix angle

Here,  $H_n$  and  $H_s$  are the functions of contact bodies' curvature formula and the elastic modulus such that  $H_n$  and  $H_s$  can be defined as the elastic modulus of the nut and the screw where there is an elliptical contact point, respectively. These can be expressed following Yang's analysis [12] as:

$$H_n = \delta^* \left( \frac{3}{2Y_n^* \Sigma \rho_n} \right)^{\frac{2}{3}} \left( \frac{\Sigma \rho_n}{2} \right) \quad (8.21)$$

and

$$H_s = \delta^* \left( \frac{3}{2Y_s^* \Sigma \rho_s} \right)^{\frac{2}{3}} \left( \frac{\Sigma \rho_s}{2} \right) \quad (8.22)$$

where,

$\delta^*$  = Function of the contact surface curvature function  $F(\rho)$

$\delta^*$  is determined by function  $F(\rho)$  and it can be expressed by the curvature functions:

$$F_n(\rho) = \frac{|(\rho_{r11} - \rho_{r12}) + (\rho_{n21} - \rho_{n22})|}{\Sigma \rho_n} \quad (8.23)$$

and

$$F_s(\rho) = \frac{|(\rho_{r11} - \rho_{r12}) + (\rho_{s21} - \rho_{s22})|}{\Sigma \rho_s} \quad (8.24)$$

The relationship between  $\delta^*$  and  $F(\rho)$  is given by Harris [22] and presented in Appendix A. As shown, load distribution has many dominant parameters such as the number of rollers, lead of the PRS, nut outer diameter, nut inner diameter, screw diameter, and roller diameter. Lead of the screw has two factors. Those are pitch and number of starts. Because lead is dependent on pitch and the number of starts in the load distribution calculation, pitch and the number of starts can be considered as independent parameters. Note that load distribution is the calculation of load on each thread when axial load is applied on the PRS. Then, the x-axis should be fixed as the number of threads. In other words, all parameters must be combined in the design process (including number of threads) in terms of load distribution. Then, the designer can monitor the distributed load on each thread when the parameters change.

#### 8.4.3 Theoretical Life of PRS

Theoretical life is expressed as  $L_{10}$  and it represents the operating time with  $10^6$  revolutions. One is load capacity ( $C_a$ ) and the other is cubic mean load ( $F_{mc}$ ). Creative Motion Control (CMC) catalog [17] provides formulas to calculate the life of the PRS.

$$L_{10} = \left( \frac{C_a}{F_{mc}} \right)^3 \quad (8.25)$$

Lemor [9] provides the dynamic load capacity formula as:

$$C_a = f_c (\cos(\alpha_0))^{0.86} N_c^{\frac{2}{3}} D_c^{1.8} \tan(\alpha_0) (\cos(\beta_0))^{\frac{1}{3}} \quad (8.26)$$

where,

$C_a$  = Dynamic Load Capacity

$f_c$  = Geometric Factor of PRS System

$\alpha_0$  = Contact Angle between Contact bodies ( $45^\circ$ )

$N_c$  = Total Number of Contact Point

$D_c$  = Diameter of Rolling Element at the Contact Point

$\beta_0$  = Helix Angle

The diameter of the rolling element at the contact point is defined by Lemor [9] as:

$$D_c = \left( (2.5p) d_r 2^{\frac{1}{2}} \right)^{\frac{1}{2}} \quad (8.27)$$

where  $p$  is the pitch of the thread and  $d_r$  is the effective roller diameter. Equivalent cubic mean load can be obtained in the CMC catalog [17] as:

$$F_{mc} = \frac{(F_{s1}^3 L_1 + F_{s2}^3 L_2 + F_{s3}^3 L_3 + \dots)^{\frac{1}{3}}}{(L_{s1} + L_{s2} + L_{s3} + \dots)^{\frac{1}{3}}} \quad (8.28)$$

where,

$F_{s1}, F_{s2}, F_{s3}$  = Stroke Force Component

$L_{s1}, L_{s2}, L_{s3}$  = Each Stroke Related to Each Load

Life rating of the PRS design uses several design parameters such as the number of contact points, nut outer diameter, nut inner diameter, screw diameter, and pitch. The number of contact points consists of the number of rollers and length divided by pitch. There are some additional parameters that determine the envelope for the life rating calculation. If we know the stroke and applied force on the PRS, these also can be parameters used for the life rating. Based on all the parameters related to life rating, we can build design performance maps and this would be shown as an additional performance envelope to expand the design process.



#### 8.4.4 Efficiency

Efficiency of the PRS is dependent on parameters such as friction, lead, and screw diameter. CMC [17] provides an efficiency formula.

$$\eta = \frac{1}{1 + \frac{\pi d_s \mu}{l}} \quad (8.29)$$

where,

$\eta$  = Theoretical Efficiency

$l$  = Lead of Screw

$d_s$  = Screw diameter

$\mu$  = Friction Coefficient

In terms of friction, Ma et al. [29] and Yang et al. [34] focus on rolling friction of the components. They investigate frictional moments of the PRS under several conditions. Clearly, friction of the PRS is dependent on many factors and conditions.

#### 8.4.5 Velocity Ratio of the PRS

In order to design a PRS transmission as part of an electro-mechanical actuator (EMA), it is necessary to calculate the velocity ratio (reduction ratio) between the prime mover ((rotation of the input linear screw) and translation (linear motion) of the nut. The planetary roller and the nut have the same linear velocity  $V_n = V_r$ . Considering the lead as the roller-screw mesh ( $N_s$  – number of starts,  $p$  - number of inches per thread), the diameters ( $d_s, d_r$ ) of the roller and the screw, then the reduction ratio  $R_{PRS}$  is

$$R_{PRS} = \frac{N_s p d_s}{d_r} \quad (8.30)$$

This algebraic result would become a very simple map in terms of four elementary design parameters. Nonetheless, its importance requires that it be used as a map component in all combinations of maps in the performance envelopes. Note that given an output load  $F_n$  on the nut then the input torque  $T_s$  on the screw would be

$$T_s = F_n R_{PRS} \quad (8.31)$$

#### 8.4.6 Equivalent Inertia of the PRS

Given the PRS as a transmission in a linear EMA, it also becomes necessary to describe total equivalent inertia. The nut and the roller have the same linear velocity  $V_n = V_r$  with masses  $M_N, M_r$ . Then, the equivalent linear inertia would be

$$\bar{I}_{n,r} = (M_N + M_r) \left( \frac{N_s p d_s}{d_r} \right)^2 \quad (8.32)$$

The inertia content of the  $N_r$  rotating rollers would be

$$\bar{I}_r = N_r \left( \frac{d_s}{2d_n} \right)^2 I_r \quad (8.33)$$

where  $I_r$  is the single roller rotating inertia. Finally, the rotary inertia of the screw is  $I_s = \bar{I}_s$  such that the total PRS equivalent inertia is

$$\bar{I}_{PRS} = (M_N + M_r) \left( \frac{N_s p d_s}{d_r} \right)^2 + N_r \left( \frac{d_s}{2d_n} \right)^2 I_r + I_s \quad (8.34)$$

Since the design parameters are squared, the combination as a map will be a complex parabolic surface. Note that  $M_N, M_r, I_r, I_s$  can be expressed as formulas in terms of component weights, lengths, and diameters.

## 8.5 Chapter Conclusion

The planetary roller screw (PRS) is a high end rotary to linear transmission. As described in Section 8.4, it can be represented by 10 or more performance measures (see Table 8.6) and 10 or more design parameters (see Table 8.7). This matrix of choices is indeed complex. Yet the unit must be designed to meet a set of given task requirements. Clearly, if the design of a prime mover is added to the PRS to make an EMA to respond to command, this complexity increases.

Performance Measures	Symbol
Total Stiffness on Thread	$k_{total}$
Load Capacity	$C_a$
Force Density	$F_D$
Total Weight	$W_t$
Contact Pressure (Stress)	$p_c$
Load Distribution	$F_{load\ i}$
Theoretical Life (Durability)	$L_{10}$
Efficiency	$\eta$
Velocity Ratio of the PRS	$R_{PRS}$
Equivalent Inertia of the PRS	$\bar{I}_{PRS}$

**Table 8.6 Performance Measures**

Here, it is clear that starting with the process of the PRS design alone is quite demanding. The normal approach is to choose a few representative values for each of the design parameters of all the performance measures. Suppose that each parameter is represented by an open set of 10 numbers (there are 10 design parameters) and 10 performance measures. Given one millisecond per design set, this would represent  $(10)^{10}$  numbers of combinations or  $10^7$  seconds, which is one

year's time. Hence, brute force parameter based calculation (the forward decision process) is far too cumbersome not only because of the time consumed but also because the designer's judgment can't be of assistance.

Design Parameters	Symbol
Nut Outer Diameter	$D_n$
Nut Inner Diameter	$d_n$
Screw Diameter	$d_s$
Roller Diameter	$d_r$
Number of Rollers	$N_r$
Number of Starts	$N_s$
Thread Pitch	$p$
Length of System	$L$
Number of Contact Points	$N_c$
Roller Angular Velocity Ratio ( $\omega_r/\omega_s$ )	$\omega_{r\text{ratio}}$

**Table 8.7 Design Parameters**

Here, we present the design process in terms of parametrically based performance maps. These maps have highly visual content (usually monotonic) and the designer can move towards points on the map surface that closely meets the needed performance requirements. While doing so, a set of parameter bars would increase / decrease to let the designer judge, if these values are suitable for the designer's application. This is what is called the inverse design approach. The designer visually chooses the output performance values (on the maps), which best meets the application requirements and the design parameters are simply read out from the coordinate axes values for that design point on the envelope surface. Hence, the inverse is direct (using the designer's judgment) and the forward is indirect (leading to considerable uncertainty and computational complexity). Given the performance maps (10 are listed here), they can be

combined into envelopes by using normalized values (say root mean square – RMS) to either add or multiply maps. Thus far, the experience is that multiplication is the best in that it increases sensitivity due to changes in the design parameters therefore augmenting the designer's judgment.

It is true that map based envelopes are in themselves complex. It appears that one principal design parameter can be combined with four or five secondary normalized (in range) parameters to form an envelope based on four or five maps. Hence, the whole process may require several envelopes combining different sets of maps. Each map may be weighted in importance for a given application to further refine the clarity of the resulting performance measures. This weighting process would be intuitive and would depend on the level of experience that the designer has in each application domain.

It is clear, however, that the inverse process (choose the desired performance and calculate the required design parameters) is superior to the standard forward approach. This comparative choice also applies to the forward / inverse problem of motion programming in serial robot manipulation.

Given an active system of 200 distinct configurations and perhaps 20 highly coupled non-linear independent inputs under human command, the same question still arises. Do we guess at the inputs or choose the outputs to directly calculate the inputs to enable very fast decision making for system control. This then generalizes to the decision question: is it parallel, serial or some combination? Do we want the operator / designer in command to enhance human judgment (driving a car, doing robot surgery, designing a 20 parameter actuator, operating a complex 2000 configuration battlefield platforms, etc.)?. Clearly, the map / envelope process provides a standard numerical "look-up table" to dramatically reduce computational time and uncertainty while responding directly to human command (judgment).

The process has been developed here for the 10 map / 10 parameter planetary roller screw (PRS). It can be applied in all such domains where performance and parametric clarity exists. In

real time control, the performance measure clarity will be less with uncertainty bounds due to limitations in human command. This uncertainty can be managed by archiving performance data and reducing the uncertainty bounds (say for efficiency, responsiveness, temperature, noise, wear, etc.) Over time, the maps / envelopes will change (degrade) such that the difference with the built certificate maps / envelopes can be used to predict remaining useful life (condition based maintenance –CBM). This archiving can also be used to improve repetitive duty cycles (home to work for automobile operation) by adjusting all essential performance maps / envelopes. This requires a sophisticated use of deep learning techniques.

Overall, this revolution in the decision process will enable remarkable progress in the design and operation of our highly coupled non-linear systems (cars, trucks, trains, buses, aircraft, orthotics, surgery, construction machinery, etc.) representing at least a \$1.5 trillion / year economic sector in the U.S. The simplified decision methods of the past (brute force design parameter selection, classical control theory, virtual human judgment) must now be discarded in favor of computational intelligence (high speed computation) based on a combination of mechanical performance measures and AI's deep learning.

## CHAPTER 9. CONCLUSIONS AND RECOMMENDATIONS

The objective of this report is to revolutionize the design process for highly non-linear and complex mechanical components in terms of a number of performance measures to formally obtain the design parameters by the inverse design process. This was done by using performance measure maps and their combination as envelopes for a parametrically dense mechanical linear transmission, the planetary roller screw (PRS).

For Chapter 1, we discuss the advantage of the planetary roller screw and analyze its motion. In order to prove the PRS' value compared to conventional linear transmission device, we consider the design of the PRS in terms of parametric effect on the whole PRS system and introduce four performance measures. These four measures are used to understand how many parameters are involved in the design objective of the PRS mechanism. The four measures are load distribution, total thread deformation and stiffness, dynamic load capacity, and force density.

Chapter 2 describes the kinematic geometry of the PRS in order to explore what parameters exist and to understand parameter relationships among the PRS components. In this chapter, the fundamental PRS structure and terminology are presented. In addition, the angular and axial motion of the PRS is analyzed. The nut, screw, and roller have their rules of relationships for design of the PRS. Figure 2.6 is very useful to construct the inner space of the PRS when we investigate parameter effects such as nut inner diameter, screw diameter, and roller diameter. Based on this chapter's analysis, parameter relationships and their effect on load distribution, thread deformation, thread stiffness, load capacity, and force density can be further investigated and analyzed in the next chapters.

Chapter 3 investigates the effect of each parameter to the total deformation and total stiffness of the planetary roller screw thread and classifies the dominant parameters and supporting parameters. Parameters are nut outer diameter, nut inner diameter, screw diameter, roller diameter, number of rollers, pitch, number of start, and helix angle. Especially, the nut outer diameter and

nut inner diameter show a great influence on the total deformation and total stiffness. This means that nut thickness is basic factor in terms of total deformation and total stiffness when we design the planetary roller screw. Other parameters also have significant effect on PRS such as screw diameter, roller diameter, and pitch. On the other hand, helix angle has a minor effect on the total deformation and total stiffness. The work here is the first step to classify dominant parameters. This is important to understand and decide which parameters have a significant effect on planetary roller screw design.

For Chapter 4, we investigate load distribution characteristics of the PRS. When the load is applied to the PRS, each thread of each component has its own amount of distributed load. The feature of the load on each thread is that the first several threads support more load and load on the following threads decreases. A parameter effect analysis is done for all parameters. Several parameters have a major effect on load distribution. Those parameters are considered as dominant design parameters such as the nut outer diameter, nut inner diameter, screw diameter, roller diameter, pitch, and number of starts. The number of rollers and helix angle don't have much impact on the load distribution. Both the screw diameter and roller diameter condition and pitch and number of starts condition have different results in terms of total deformation and total stiffness. Those two cases cause completely opposite results between load distribution analysis, total deformation, and total stiffness analysis. This result demonstrate that the usefulness of combined maps and envelopes.

Chapter 5 analyzes dynamic load capacity that is a dominant factor for the PRS design process. Dynamic load capacity is a value that is expressed as a force unit. The general meaning of the dynamic load capacity is the load that provides a life of one million revolutions of the inner nut race. We investigate the effect of each parameter on dynamic load capacity and the results show that diameters such as nut inner diameter, screw diameter, roller diameter, and pitch are dominant parameters that increase load capability. The number of rollers also have large effect on



load capacity because it affects the number of total contact points in the PRS. Moreover, this analysis demonstrates the importance of careful design of the inner geometry factors such as screw diameter and roller diameter. Both parameters have the capability to increase load capacity. However, inner geometry is restricted by the inner space such that the screw diameter and roller diameter are dependent each other. Because of this, the interaction between screw diameter and roller diameter needs to be dealt with carefully.

Chapter 6 investigates force density based on dynamic load capacity and weight. As an important element of the PRS, calculating weight and force density and analysis of the related parameters are essential because it is desired to use light weight and high force density actuators. Parameter analysis provides results that nut inner diameter, screw diameter, roller diameter, number of rollers, pitch, and length have large effects on force density. However, those parameters need to be dealt with carefully because each parameter change is related to weight change except for pitch. Then, the resulting value of force density would be lowered due to weight increase. A representative parameter is length and the number of rollers. These two parameters increase load capacity, however, they also increase total weight of the PRS and the effect of this weight increase is significant. Moreover, results provide that the relationship among the inner geometry parameters are also important for the same reason given for the number of rollers and length. These results indicate that the whole PRS system is complex when all parameters and measures are considered at the same time. This reality confirms the need for maps and envelopes for the design of the PRS.

Chapter 7 arranges the dominant parameters for the PRS and provides analysis in detail. In order to achieve the detailed analysis, methods of combining different characteristics of the measures are introduced and discussed. This chapter also investigates the effect of the volume, which is related to nut thickness, roller diameter, and the number of rollers. These parameters are related to both weight and load capacity. Then, these affect to PRS performance in terms of performance measure maps and combined envelopes. The results prove again the importance of

proper choice of inner geometry factors. Then, it is important to find a correct combination within a given geometry. Two methods are conducted (adding / multiplying maps to form envelopes) in order to determine the effect of all parameters on all measures of the PRS. The multiplying method is recommended because of its useful visual non-linearity and sensitivity. All performance maps are normalized and adjusted to scale for better monitoring of result values on the maps since some normalized values are small. After comparison between the two methods of performance measure maps, the multiplying approach contains a clearer representation of variation in each measure caused by design parameter change as compared to the adding method. This is because it is to recognize small changes of envelope values and makes it easy for the designer to visualize these changes of the performance measures and determine the effect of the basic parameters on the PRS overall design.

In Chapter 8, we discuss the design process. An effective design process is necessary in order to maximize the capability of the PRS, since the parameter effect analysis is a fundamental factor in this design process. Each design parameter has its characteristic effect on the PRS. These different effects need to be combined and normalized for rapid understanding of the required parameter value to meet desired PRS capabilities. This need can be achieved by using envelopes that present how the design point on the envelope moves as the dominant design parameters change. In addition, when designer has chosen values on the envelopes, the analytics also provide an inverse approach to find design parameter values. Chapter 8 shows how the parameter and performance values change when the design point moves from starting point to resulting point on the envelopes. These envelopes provide a better understanding of the PRS mechanism and simplify the design effort of the PRS by enhancing the designer's judgment by means of visualization. This chapter introduces six more performance measures with related formulas and references, which are important for total PRS design like the other four measures of total stiffness on the thread mesh, load capacity, force density, and weight. Finally, we present 10 representative performance

measures and 10 design parameters. This matrix of choices is indeed complex. Yet the unit must be designed to meet a set of given task requirements.

In general, the design process benefits from accurately defined measures with low uncertainty. Going to the operation of a 200 configuration highly coupled system (each configuration needs its own measures) by having meaningful performance maps / envelopes to makes decisions in milliseconds is possible. Actual data needed to confirm where the system is on the reference maps / envelopes will depend on excess low cost sensor information. Given “learned” maps, performance will go up (efficiency, response, durability, temperature, noise, etc.). Say, a repeat duty cycle occurs (home to work), then how do we refine those maps and envelopes? Do we make these envelopes visible to the operator so he / she can best use his / her judgment to match real conditions (bad traffic, poor weather, high winds, icy road surfaces, etc. for driving or for similar conditions for surgery, or for construction machines, or for battlefield systems to best meet emerging threats, etc.)? The same applies to condition-based maintenance (CBM) of these systems – i.e. deep learning must now be involved. Overall, building performance maps and envelopes is fundamental for design process and provides major benefits for optimal design, easy monitoring, rapid decision, and fast response for designer / operator.

## APPENDIX A. DIMENSIONLESS CONTACT PARAMETERS TABLE

As mentioned in Chapter 3, dimensionless contact quantity ( $\delta^*$ ) is the function of  $F(\rho)$ . Values are presented in Figure A.1 – A.3 and summarized in Table A.1

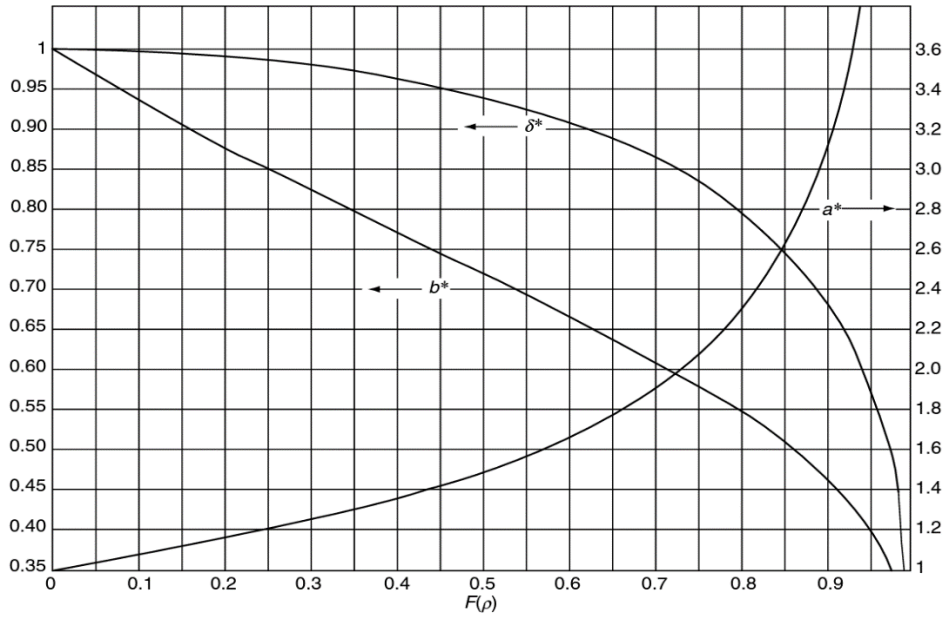


Figure A.1 Function of  $F(\rho)$  and  $a^*, b^*, \delta^*$  Graph 1 (Extracted from Harris (2006))

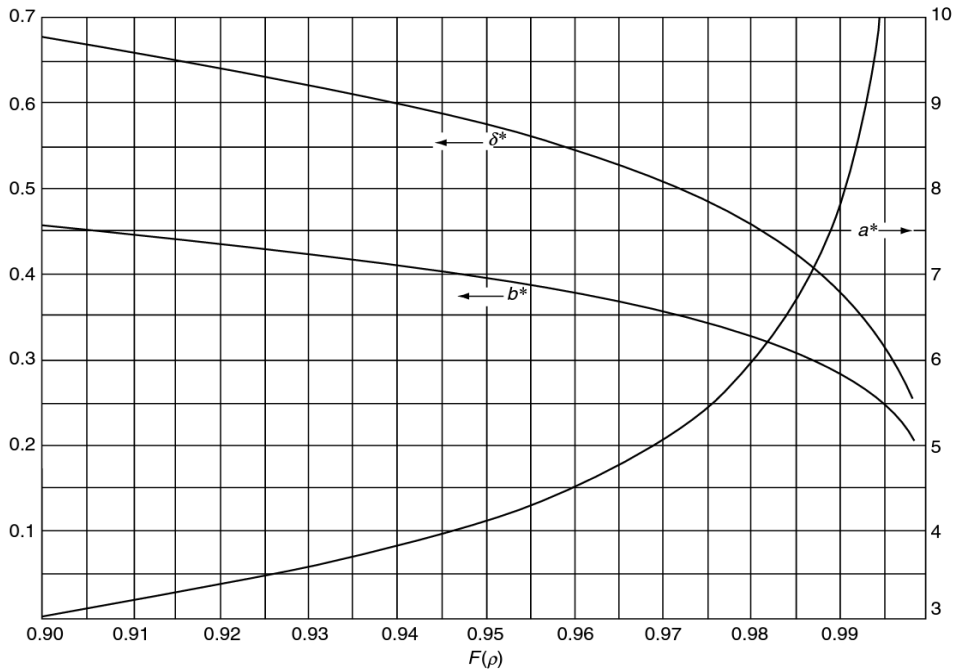
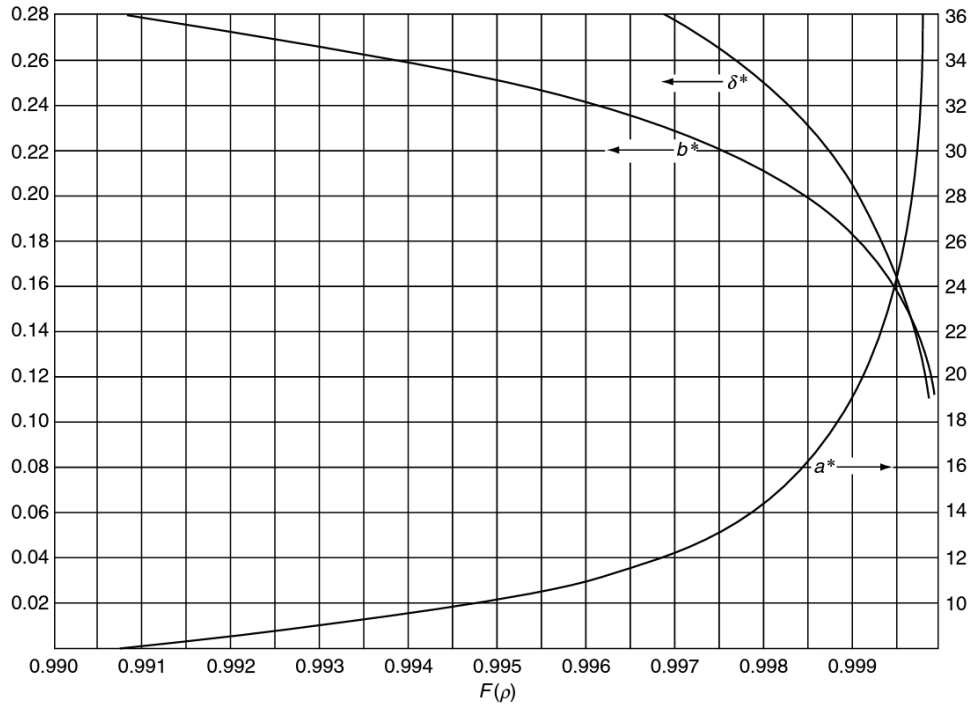


Figure A.2 Function of  $F(\rho)$  and  $a^*, b^*, \delta^*$  Graph 2 (Extracted from Harris (2006))



**Figure A.3 Function of  $F(\rho)$  and  $a^*$ ,  $b^*$ ,  $\delta^*$  Graph 3 (Extracted from Harris (2006))**

**Dimensionless Contact Parameters**

$F(\rho)$	$a^*$	$b^*$	$\delta^*$
0	1	1	1
0.1075	1.0760	0.9318	0.9974
0.3204	1.2623	0.8114	0.9761
0.4795	1.4556	0.7278	0.9429
0.5916	1.6440	0.6687	0.9077
0.6716	1.8258	0.6245	0.8733
0.7332	2.011	0.5881	0.8394
0.7948	2.265	0.5480	0.7961
0.83495	2.494	0.5186	0.7602
0.87366	2.800	0.4863	0.7169
0.90999	3.233	0.4499	0.6636
0.93657	3.738	0.4166	0.6112
0.95738	4.395	0.3830	0.5551
0.97290	5.267	0.3490	0.4960
0.983797	6.448	0.3150	0.4352
0.990902	8.062	0.2814	0.3745
0.995112	10.222	0.2497	0.3176
0.997300	12.789	0.2232	0.2705
0.9981847	14.839	0.2072	0.2427
0.9989156	17.974	0.18822	0.2106
0.9994785	23.55	0.16442	0.17167
0.9998527	37.38	0.13050	0.11995
1	$\infty$	0	0

**Table A1. Dimensionless Contact Parameters (Extracted from Harris (2006))**

## REFERENCES

- [1] Strandgren, C., 1954, “Screw-Threaded Mechanism”, U.S. Patent 2,683,379.
- [2] Koran, L., 2007, “Duty Cycle Analysis for Aircraft Control Surface Actuation,” M.S. thesis, Mechanical Engineering, University of Texas at Austin.
- [3] Tesar, D and Krishnamoorthy, G., 2008, “Intelligent electromechanical actuators to modernize ship operations,” *Naval Engineers Journal*, 120(3), pp. 77–88.
- [4] Ma, S., Zhang, T., Liu, G., Tong, R. and Fu, X., 2015, “Kinematics of Planetary Roller Screw Mechanism considering Helical Directions of Screw and Roller Threads,” *Mathematical Problems in Engineering*, 2015, pp. 1-11.
- [5] Otsuka, J., Fukada, S. and Osawa, T. 1987, “Fundamental Study of Planetary Screw: Structure and Coefficient of Friction,” *Bulletin of the Japan Society of Precision Engineering*, 21(1), pp. 43-48.
- [6] Velinsky, S., Chu, B. and Lasky, T., 2009, “Kinematics and Efficiency Analysis of the Planetary Roller Screw Mechanism,” *Journal of Mechanical Design*, 131(1), pp. 11-16.
- [7] Jones, M. and Velinsky, S., 2012, “Contact Kinematics in the Roller Screw Mechanism,” *Journal of Mechanical Design*, 135, pp. 051003-1-10.
- [8] Jones, M., 2013, “Mechanics Based Design of the Planetary Roller Screw Mechanism,” Ph.D. dissertation, Mechanical and Aeronautical Engineering, University of California at Davis.
- [9] Lemor, P., 1996, “An Efficient and Reliable Mechanical Component of Electro-Mechanical Actuators,” *Proceedings of the 31<sup>st</sup> Intersociety Energy Conversion Engineering Conference*, IECEC, Washington, DC, 1, pp. 215-220.
- [10] Otsuka, J., Osawa, T. and Fukada, S., 1989, “A Study on the Planetary Roller Screw: Comparison of Static Stiffness and Vibration Characteristics with Those of the Ball Screw,” *Bulletin of the Japan Society of Precision Engineering*, 23(3), pp. 217-223.
- [11] Zhang, Z. and Li, M., 2011, “Analysis on the accuracy of the electric cylinder-with planetary roller screw,” *Manufacture Information Engineering of China*, 40(19), pp. 72-74

- [12] Yang, J., Zhenxing, W., Jisheng, Z. and Wei, D., 2011, "Calculation of the Load Distribution of a Planetary Roller Screw for Static Rigidity," *Journal of Huazhong University of Science and Technology (Natural Science Edition)*, 39(4), pp. 1-4.
- [13] Ma, S., Liu, G., Tong, R. and Zhang, X., 2012, "A New Study on the Parameter Relationship of Planetary Roller Screw," *Mathematical Problems in Engineering*, 2012, pp. 1-29.
- [14] Zhang, W., Liu, G., Tong, R. and Ma, S., 2015, "Load distribution of planetary roller screw mechanism and its improvement approach," *Journal of Mechanical Engineering Science*, 230(18), pp. 3304-3318.
- [15] Lisowski, F., 2014, "The Analysis of Displacements and the Load Distribution between Elements in a Planetary Roller Screw," *Applied Mechanics and Materials*, 680(2014), pp. 326-329.
- [16] Exlar., "Advantages of Roller Screw Technology," Exlar Corporation, n.d from <http://exlar.com/why-exlar/many-advantages-roller-screw/>
- [17] CMC., "Creative Motion Control Planetary Roller Screws: Delivering Innovative Linear Motion Solutions," CMC Corporation, n.d, Product Catalog, pp. 1-24.
- [18] "Screw Thread," Wikipedia, 16 Mar. 2017, from [https://en.wikipedia.org/wiki/Screw\\_thread/](https://en.wikipedia.org/wiki/Screw_thread/)
- [19] "Roller Screw," Wikipedia, 15 Mar. 2017, from [https://en.wikipedia.org/wiki/Roller\\_screw/](https://en.wikipedia.org/wiki/Roller_screw/)
- [20] Yamamoto, S., 1984, "Theory and Calculation of Screw Thread connection," Shanghai Science and Technology Literature Press, pp. 45-49.
- [21] Johnson, K., 2003, *Contact Mechanics*, 9<sup>th</sup> ed., Cambridge University Press, Cambridge, U.K., pp. 84-106
- [22] Harris, T. and Kotzalas, M., 2006, *Essential concepts of bearing technology*, 5<sup>th</sup> ed., CRC Press, Boca Raton, FL, pp. 108-114.
- [23] "Contact Mechanics," Wikipedia, 15 Mar. 2017, from [https://en.wikipedia.org/wiki/Contact\\_mechanics#Assumptions\\_in\\_Hertzian\\_theory](https://en.wikipedia.org/wiki/Contact_mechanics#Assumptions_in_Hertzian_theory)
- [24] Lisowski, F., 2015, "Numerical Computation of Stress and Deformation in the Planetary

- Roller Screw Components,” Technical Transaction Mechanics, pp. 141-148.
- [25] Brandlein, J., Eschmann, P., Hasbargen, L. and Weigand, K., 1999, *Ball and Roller Bearing: Theory, Design, and Application*, 3<sup>rd</sup> ed., John Wiley & Sons, Chichester, U.K.
- [26] “Calculation of the Theoretical Weight of Steel Chart,” Donghao Stainless Steel, n.d, from <http://tubingchina.com/Calculation-of-theoretical-weight-of-steel.htm>
- [27] “Theoretical Nominal Weight,” Steel Market Update, n.d, from <https://www.steelmarketupdate.com/resources-mobile/steel-buyers-basics?showall=&start=11>
- [28] Timken Steel, “Theoretical Footweight Calculator,” Timken Steel Corporation, n.d, from <http://www.timkensteel.com/what-we-know/theoretical-footweight-calculator>
- [29] Ma, S., Liu, G., Tong, R., and Fu, X., 2015, “A Frictional Heat Model of Planetary Roller Screw Mechanism Considering Load Distribution,” *Mechanics Based Design of Structure and Machines*, 43, pp.164-182
- [30] Ashok, P. and Tesar, D., 2008, “A Visualization Framework for Real Time Decision Making in a Multi-Input Multi-Output System,” *IEEE Systems Journal*, 2(1), pp. 129-145
- [31] Ashok, P. and Tesar, D., 2013, “The Need for a Performance Map Based Decision Theory,” *IEEE Systems Journal* 7(4), pp. 616-631
- [32] Bandaru, N., 2011, “Map Based Visual Design Process for Multi-Stage Gear Drives,” M.S. thesis, Mechanical Engineering, University of Texas at Austin.
- [33] Budynas, R. G. and Nisbett, J. K., 2015, *Mechanical Engineering Design*, 10<sup>th</sup> ed., McGraw- Hill, New York, NY.
- [34] Yang, J., Yang, Z., Zhu, S. and Du, W., 2011, “Effect of preload on axial deformation and friction of planetary roller screw,” *Journal of Mechanical Transmission* 35(12), pp.16–22



## VITA

Hyunho Jung was born in Wolgang, Haenam, Republic of Korea, the son of Sungim Kang and Youngmin Jung. After completing his work at Changpyeong High School, Changpyeong, Damyang, in 2003, he entered the Republic of Korea Air Force Academy in Cheongju, Chungcheong. He received his Bachelor of Science degree in Mechanical Engineering for the Republic of Korea Air Force Academy in March 2007 and was commissioned an officer in the Republic of Korea Air Force as F-15K Fighter Jet Co-Pilot. He entered The Graduate School at The University of Texas at Austin in August of 2015.

E-mail: jung.hyunho@utexas.edu

This thesis was typed by the author.